THERMAL CHARACTERIZATION OF COMPOSITES OF POLYAMIDE-6 AND POLYPROPYLENE INVOLVING BORON COMPOUNDS VIA DIRECT PYROLYSIS MASS SPECTROMETRY

A THESIS SUBMITTED TO
THE GRADUATE SCHOOL OF NATURAL AND APPLIED SCIENCES
OF
MIDDLE EAST TECHNICAL UNIVERSITY

BY

GÜLLÜ CEYDA İŞBAŞAR AFACAN

IN PARTIAL FULFILLMENT OF THE REQUIREMENTS FOR
THE DEGREE OF DOCTOR OF PHILOSOPHY

IN

POLYMER SCIENCE AND TECHNOLOGY

SEPTEMBER 2013

Approval of the thesis:

THERMAL CHARACTERIZATION OF COMPOSITES OF POLYAMIDE-6 AND POLYPROPYLENE INVOLVING BORON COMPOUNDS VIA DIRECT PYROLYSIS MASS SPECTROMETRY

submitted by **GÜLLÜ CEYDA İŞBAŞAR AFACAN** in partial fulfillment of the requirements for the degree of **Doctor of Philosophy in Polymer Science and Technology Department, Middle East Technical University** by,

Prof. Dr. Canan Özgen
Dean, Graduate School of **Natural and Applied Sciences** _____

Prof. Dr. Teoman Tinçer
Head of Department, **Polymer Science and Technology** _____

Prof. Dr. Jale Hacaloğlu
Supervisor, **Chemistry Dept., METU** _____

Prof. Dr. Ülkü Yılmazer
Co-Supervisor, **Chemical Engineering Dept., METU** _____

Examining Committee Members:

Prof. Dr. Erdal Bayramlı
Chemistry Dept., METU _____

Prof. Dr. Jale Hacaloğlu
Chemistry Dept., METU _____

Prof. Dr. Nursel Dilsiz
Chemical Engineering Dept., Gazi University _____

Prof. Dr. Göknur Bayram
Chemical Engineering Dept., METU _____

Assist. Prof. Dr. İrem Erel
Chemistry Dept., METU _____

Date: **03/09/2013**

I hereby declare that all information in this document has been obtained and presented in accordance with academic rules and ethical conduct. I also declare that, as required by these rules and conduct, I have fully cited and referenced all material and results that are not original to this work.

Name, Last Name: Güllü Ceyda İŞBAŞAR AFACAN

Signature:

ABSTRACT

THERMAL CHARACTERIZATION OF COMPOSITES OF POLYAMIDE-6 AND POLYPROPYLENE INVOLVING BORON COMPOUNDS VIA DIRECT PYROLYSIS MASS SPECTROMETRY

İşbaşar Afacan, Güllü Ceyda
Ph.D., Department of Polymer Science and Technology
Supervisor : Prof. Dr. Jale Hacaloğlu
Co-Supervisor: Prof. Dr. Ülkü Yılmazer

September 2013, 189 pages

In this work, the effects of addition of boron compounds, boron phosphate (BPO_4), zinc borate (ZnB), borosilicate (BSi) and lanthanum borate (LaB), on thermal degradation characteristics of composites of polyamide 6 (PA6) and polypropylene (PP) are analyzed via Direct Pyrolysis Mass Spectrometry (DP-MS) technique. The composites of PA6 involve nitrogen containing flame retardants, melamine (Me) or melamine cyanurate (MC); or phosphorus containing flame retardant, aluminum diethylphosphinate (AlPi), with or without organically modified clay. Composites of PP involve intumescent flame retardants (IFR) with or without maleic anhydride grafted polypropylene (PP-g-MA) and organically modified clay.

The presence of Me or MC does not affect thermal stability of PA6, but due to the strong interactions between Me, MC or isocyanic acid and PA6, generation of new fragments occurs and loss of Me or MC is shifted to high temperatures. Presence of boron compounds results in significant changes in loss of Me and MC and thermal degradation products of the PA6.

The presence of AlPi decreases thermal stability of PA6 noticeably. Addition of boron compounds or organically modified clay, improves the thermal stability of PA6/AlPi composite, most probably due to the weakening of the interactions between AlPi and PA6.

Addition of boron containing compounds to PP involving IFR, improves the thermal stability of PP; yet, no significant differences in the thermal degradation pathways of PP are observed. Moreover, decrease in the relative intensities of PP based fragments with high mass and in those of both pentaerythritol (PER) and ammonium polyphosphate (APP) based fragments are recorded.

Upon addition of Cloisite 15A, the thermal stability of PP is decreased. Inclusion of IFR to this composite improves the thermal stability. Inclusion of all boron compounds (especially ZnB) affects the thermal stability of the composite.

Keywords: Polyamide 6, polypropylene, boron compounds, pyrolysis mass spectrometry, thermal degradation

ÖZ

BORON BİLEŞİKLERİ İÇEREN POLİAMİD-6 VE POLİPROPİLEN KOMPOZİTLERİNİN DİREKT PİROLİZ KÜTLE SPEKTROMETRESİ İLE ISIL NİTELENDİRİLMESİ

İşbaşar Afacan, Güllü Ceyda
Doktora, Polimer Bilimi ve Teknolojisi Bölümü
Tez Yöneticisi : Prof. Dr. Jale Hacaloğlu
Ortak Tez Yöneticisi: Prof. Dr. Ülkü Yılmazer

Eylül 2013, 189 sayfa

Bu çalışmada, boron fosfat (BPO_4), çinko borat (ZnB), borosilikat (BSi) ve lantan borat (LaB) gibi boron bileşiklerinin eklenmesinin, poliamid 6 (PA6) ve polipropilen (PP) kompozitlerinin ısıl bozunma karakterlerine etkisi, Direkt Piroliz Kütle Spektrometresi tekniği kullanılarak incelenmiştir. PA6 kompozitleri, melamin (Me) veya melamin siyanürat (MC) gibi azot içeren alev geciktiricileri yahut organik olarak modifiye edilmiş killi veya kilsiz alüminyum dietilfosfinat (AlPi) gibi fosfor içeren alev geciktiricileri içerir. PP kompozitleri, maleik anhidrit aşılı polipropilen (PP-g-MA) ve organik olarak modifiye edilmiş kil ihtiva eden veya etmeyen kabaran alev geciktiricileri (IFR) içerir.

PA6'nın ısıl kararlılığı Me veya MC'nin varlığından etkilenmediği halde; Me, MC veya izosiyanik asit ile PA6 arasındaki güçlü etkileşimler sonucunda yeni parçacıklar oluşur ve Me veya MC salınımı yüksek sıcaklıklara kayar. Boron bileşiklerinin varlığı, Me ile MC salınımında ve PA6'nın ısıl bozunma ürünlerinde belirgin değişikliklere sebep olur.

AlPi varlığında, polimerin ısıl kararlılığı belirgin ölçüde azalır. Boron bileşikleri veya organik olarak modifiye edilmiş kil eklenmesi, büyük olasılıkla AlPi ile PA6 arasındaki etkileşimin zayıflamasından dolayı, PA6/AlPi kompozitinin ısıl kararlılığını geliştirir.

IFR içeren PP'ye boron içeren bileşiklerin eklenmesi, PP'nin ısıl kararlılığını geliştirir; fakat PP'nin ısıl bozunma yollarında kayda değer fark gözlenmez. Ayrıca, PP temelli yüksek kütleli parçacıklar ile PER ve APP temelli parçacıkların göreli yoğunluklarında azalma kaydedilir.

Cloisite 15A eklenmesi üzerine PP'nin ısıl kararlılığı azalır. Bu kompozite IFR eklenmesi, ısıl kararlılığı geliştirir. Tüm boron bileşiklerinin (özellikle ZnB) eklenmesi, kompozitin ısıl kararlılığını etkiler.

Anahtar Kelimeler: Poliamid 6, polipropilen, boron bileşikleri, piroliz kütle spektrometresi, ısıl bozunma

ACKNOWLEDGEMENTS

I would like to express my gratitude to my supervisor Prof. Dr. Jale Hacaloğlu, for her guidance, support, understanding and tolerance throughout my entire thesis study.

I would like to express my appreciation to my co-supervisor Prof. Dr. Ülkü Yılmazer, who has shown great patience and understanding, especially throughout the beginning period of my thesis study.

I am also grateful for Prof. Dr. Erdal Bayramlı and his former Ph.D. student Assist. Prof. Dr. Mehmet Doğan, for helping me to obtain the composite materials which were analyzed within this study.

I also wish to thank all my Ph.D. thesis committee members for their invaluable comments and contributions.

I wish to tender my thanks to my labmates for their collaboration on my experimental studies in Mass Spectrometry Laboratory, Chemistry Department, METU.

I would sincerely thank my managers employed in Türkiye İlaç ve Tıbbi Cihaz Kurumu, for encouraging me to complete my thesis study.

Finally, I am indebted to my parents, my sister and my husband, who never let me lose my motivation and energy, regardless of any circumstance.

TABLE OF CONTENTS

LIST OF FIGURES

FIGURES

LIST OF SCHEMES

SCHEMES

LIST OF TABLES

TABLES

LIST OF ABBREVIATIONS

2M2HT	Dimethyl, Dihydrogenatedtallow, Quaternary Ammonium
AlPi	Aluminum Diethylphosphinate
APP	Ammonium Polyphosphate
BC	Burn to Clamp
BPO4	Boron Phosphate
BSi	Borosilicate
CFA	Charring and Foaming Agent
Da	Dalton
DP-MS	Direct Pyrolysis Mass Spectrometry
DSC	Differential Scanning Calorimetry
EI	Electron Impact
eV	Electron Volt
FD/MS	Field Desorption Mass Spectrometry
FTIR	Fourier Transform Infrared Spectrometry
GC	Gas Chromatography
HRR	Heat Release Rate
IFR	Intumescent Flame Retardant
kW/m^2	Kilowatts per Square Meters
LaB	Lanthanum Borate
LC	Liquid Chromatography
LOI	Limit of Oxygen Index
m/z	Mass to Charge Ratio
MC	Melamine Cyanurate
Me	Melamine
MMT	Modifier for Montmorillonite
MPP	Melamine Pyrophosphate
MS	Mass Spectrometry
MT2EtOH	Methyl, Tallow, Bis-2-Hydroxyethyl, Quaternary Ammonium
NIST	National Institute of Standards and Technology
PA6	Polyamide 6
PA66	Polyamide 66
PEPA	1-oxo-4-hydroxymethyl-2,6,7-trioxa-1-phosphabicyclo[2.2.2]octane
PER	Pentaerythritol
PMMA	Poly(methyl methacrylate)

PP	Polypropylene
PP-g-MA	Maleic Anhydride Grafted Polypropylene
PST	Polymer Science and Technologies
Py	Pyrolysis
RI	Relative Intensity
SEM	Scanning Electron Microscopy
TEM	Transmission Electron Microscopy
TGA	Thermal Gravimetric Analysis
TIC	Total Ion Current
UL	Underwriters Laboratory
XRD	X-Ray Diffraction
ZnB	Zinc Borate

CHAPTER 1

INTRODUCTION

In the last few decades, polymers have become indispensible materials which can be seen everywhere in daily life, such as personal care products, textiles, house furniture, electronic devices, automotive industry, etc. Therefore, polymers are under great interest of scientists and industrialists. In order to increase their usability and reliability, polymers are required to be manufactured chemically more stable and physically more durable. To be able to improve these properties of polymers, various studies are done by the scientists throughout the world. The knowledge of thermal degradation characteristics and mechanism and effects of additives on thermal degradation behavior is of crucial importance, especially in high temperature applications. Other related important issues are flammability of polymers and improvement of fire retardancy.

1.1. Thermal Degradation of Polymers

As mentioned above, polymers find place almost everywhere in our daily life. When risk of fire and fire protection comes into mind, a very critical issue called "fire retardancy of polymers" needs to be mentioned. Therefore, many studies about improving fire retardancy of polymers are done by scientists. One of the main ways of achieving this goal is to determine the thermal degradation mechanisms of polymers.

Thermal degradation of polymers can be explained as the chemical changes which occur without including any reagent or any other chemical, at significantly high temperatures [**1**]. When a polymer is treated by heat, bonds in the main chain and side groups/chains, the main chain linkages, substituted atoms or groups and side chains, are affected separately [**2**].

Generally, free radicals are formed as a result of the main chain scissions which can occur at either any linkage or the weakest link in the chain. Moreover, thermal degradation can easily be initiated by the labile structures of chain ends with double bond. Also depolymerization can occur due to the continuous reactions of the formed macro radicals. Additionally, at moderate temperatures macro radicals can undergo intermolecular or intramolecular transfer. As a result of this transfer, molecular weight drops. Double bonds present in the chain can cause crosslinking that may result in a network structure [**2**].

1.1.1. Mechanisms of Thermal Degradation

Throughout the heat treatment of polymers, due to the fracture of a chemical bond and the formation of free radicals, molecule degradation takes place, where a molecule is broken

into fragments. The stability of the resulting smaller molecules and the chemical bond types included have effect on the characteristic properties of the fragments formed [**3**].

Monomers come together and form polymers as a result of polymerization reactions. The resulting polymers have long carbon chains. Since all the bonds in the chain are very similar to each other, breakdown of these chains may occur randomly along the main chain. Fragments with different lengths, some of which are large molecules (such as oligomers) and some of which are small ones, are generated. Small molecules may show similar chemical properties as the monomer, whereas large molecules may have similar chemical properties with the polymer [**3**].

Heat treatment, having a great effect on all parts of a polymer (bonds along the main chain and side groups/chains), forces the polymer to undergo thermal degradation. Thermal degradation can occur through side group eliminations, main chain scissions or depolymerization.

1.1.1.1. Side Group Elimination

Throughout the heat treatment of polymers involving side groups, degradation of the main chain may occur after side group eliminations or reactions. Elimination of side groups may occur first, if the side groups have weak bonds. After the elimination of side groups, unsaturated polymer chains, which may undergo further reactions to generate aromatic molecules, are generated. For instance, evolution of HCl from a polymer with a side atom Cl, such as polyvinyl chloride, is considered as side group elimination and is followed by production of characteristic aromatics. Additionally, release of H_2O or CO_2 molecules is also classified as side group elimination [**1, 3, 4**].

1.1.1.2. Chain Scission

Bond cleavages of a polymer that occur under heat treatment can be a random scission, which can cause the evolution of oligomers with different chain lengths. Random scission can continue undergoing further reactions [**4**].

Bond cleavages occur not only by elimination reactions but also by free radical mechanisms [**4**]. Scheme 1-1 summarizes the free radical mechanism, where “P” and “R” refer to polymer and polymeric radical, respectively and “n”, “r” and “s” indicate the number of monomer units [**5**].

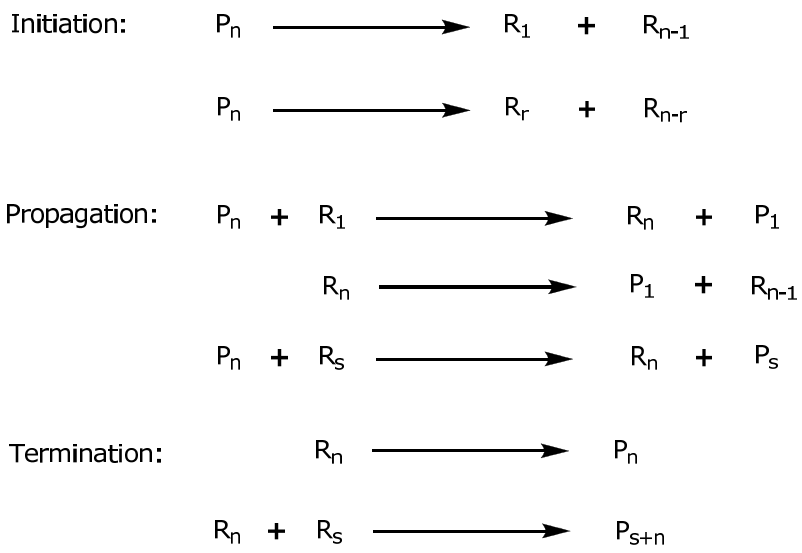

Scheme 1-1 Simple free radical mechanism [**5**]

1.1.1.3. Depolymerization

When a chain scission occurs not randomly but in a regular manner, where monomer units of the corresponding polymer are generated, such thermal degradations are called depolymerization [**4**]. Depolymerization is a free radical mechanism which is exactly the reverse reaction mechanism of the polymerization [**1**]. There are several polymers which can depolymerize. For instance, if poly(methyl methacrylate) (PMMA) is heated to elevated temperatures, the major degradation product is its monomer (methyl methacrylate). The reaction occurs in the following manner:

Firstly, as a result of the initiation step, which takes place on the backbone of the polymer, two macroradicals are formed. Next, beta scission arises where monomer unit is generated. Along the macroradical, beta scissions take place one after another, until the last monomer is formed. Such a sequence of scissions is called *unzipping* [**3**].

1.1.2. Techniques Used to Investigate Thermal Degradation Characteristics

Thermal stability of polymers is under interest of most scientists. The knowledge of thermal degradation characteristics of polymers is crucial for improvements of polymers for various applications and for environmental concerns. Thermal degradation characteristics of polymers are investigated by various techniques, such as Thermogravimetric Analysis (TGA), Differential Scanning Calorimetry (DSC) and Pyrolysis (Py).

In Thermogravimetric Analysis (TGA), the change in mass of a polymer, which goes under temperature controlled heating process, is measured [**1**]. As a result a thermal curve is obtained which is plotted as weight percent (or weight) versus temperature (or time).

Mainly, the temperature at which weight loss begins and the temperature at which maximum rate of weight loss occurs are determined by the interpretation of the curve.

Differential Scanning Calorimetry (DSC) measures the rate of heat flow into a sample and a reference, as a function of temperature, which is automatically controlled by the test equipment. The output of this process is heat flux versus temperature curve. By interpretation of this curve; transitions of amorphous and crystalline polymers (which are glass transition), crystallization from the melt during cooling (cold transition and melting), can be observed [**6**].

1.1.2.1. Pyrolysis

Chemical degradation occurring in the presence of heat is called pyrolysis. In order a chemical degradation to be called pyrolysis, it is supposed to take place at significantly higher temperatures as compared to ambient temperature [**4**].

Pyrolysis is an analytical technique by which either behavior of the molecule during pyrolysis or investigation of resulting fragments of molecule can be studied. Therefore, nature and identity of the parent molecule can be revealed. The production of smaller fragments from larger molecules throughout the pyrolysis, leads the use of pyrolysis as a sample preparation technique for other analytical instruments, such as gas chromatography (Py-GC), gas chromatography-mass spectrometry (Py-GC/MS), mass spectrometry (Py-MS) and Fourier-transform infrared spectrometry (Py-FTIR) [**3**].

In pyrolysis-gas chromatography (Py-GC), pyrolyzates are brought into the GC column, where they are separated, by a flow of inert gas, such as N_2 or He. Along with other GC detectors, mass spectrometry (MS) is also used as a detector in qualitative and quantitative analysis of polymers. In this case, the instrument used is called as pyrolysis-gas chromatography-mass spectrometer (Py-GC/MS). MS reflects the complex pattern of the parent polymer via mass spectrum regarding each peak in the GC; hence, the polymer characterization, the identification of contaminants and additives in polymeric samples and the determination of polymer degradation mechanisms can be done. This property makes Py-GC/MS an advantageous pyrolysis technique [**7**].

1.1.2.1.1. Pyrolysis-Mass Spectrometry

Researches on thermal properties of a sample, such as thermal stability, degradation products and degradation mechanisms, can be carried out by the application of pyrolysis. When a mass spectrometer is coupled with an analytical instrument, it gains the ability to separate the components according to their volatilities and their thermal stabilities.

Mass spectrometers can be coupled with a solid probe inlet port. The presence of this probe, which is kept under vacuum, makes the insertion and analysis of solid samples possible. Thus, a solid sample located in a heatable probe can be placed directly into the ion source of the mass spectrometer. Heating the solid sample in the probe first makes the

sample volatilize or desorb compounds, and then the resulting species ionize. Pyrolysis probes are somewhat similar to solid probes, however pyrolysis probes consist of a filament which can be heated up to higher temperature levels (approximately 1000°C), as compared to solid probes. The heating profile of the filament can be programmed and controlled by computer software. Via using pyrolysis probes, the sample can be pyrolyzed and directed into the ion source. As a result of the programmable heating profile in the pyrolysis probe, the degradation mechanism of the sample can be understood [**3**]. In other words, degradation of the sample takes place by heating up in the pyrolysis probe, and this is followed by the fragmentation of the pyrolyzates which occurs during the ionization in the mass spectrometer. The detection of all ionic fragments finally yields the mass spectrum, which is a complex spectrum called *pyrogram*. The interpretation of this spectrum requires an advanced knowledge, in order to understand the degradation mechanism of the sample [**4**].

Mass Spectrometry

An analytical technique which measures the molecular masses of molecules and atoms separately and accurately by transforming them into charged ions is called mass spectrometry (denoted as "MS"). Mass spectrometry allows gain of quantitative information of an analyte about its structure specificity and sensitivity. Moreover, mass spectrometry facilitates to survey the reaction dynamics and chemistry of ions. Additionally, data related to physical properties like ionization energy, enthalpy of a reaction, proton and ion affinities can be obtained via mass spectrometry. Mass spectral data can also be used to authenticate theoretical predictions which are based on molecular orbital calculation. As a result, in addition to these excellent properties, being a highly precise and sensitive analytical technique makes mass spectrometry a preferred technique among chemistry, medicinal chemistry, biology, pharmaceutical science, forensic science, material science, etc. [**8**].

Main Parts of Mass Spectrometry

Main parts of mass spectrometers (shown in Figure 1-1) are *the ion source*, where the molecules enter the mass spectrometer and are transformed into gas phase ionic; *the mass analyzer*, where the formed ions are grouped in terms of their mass to charge ratios by the help of applied electromagnetic fields; and *the ion detector*, on which the passed ions generate electrical current that is amplified and detected [**8**, **9**].

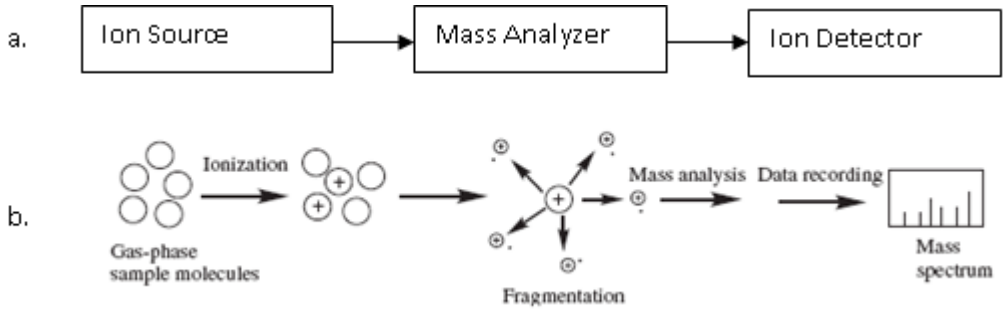

Figure 1-1 a) Main parts of mass spectrometers b) Main processes in mass spectrometers

First two parts of mass spectrometer (ion source and mass analyzer) are always kept under vacuum for two main reasons. The first one is to avoid any chemical reaction, which may occur through collision of ions with gaseous particles present in the compartments and may cause the formation of new species. The second one is to let the ions move freely [**8**, **9**].

There are several ionization techniques, some of which are ionization of volatile materials, desorption/ionization methods and spray ionization methods. These techniques also have their sub-classifications [**10**].

Mass analyzers can be divided into two basic groups, namely scanning and non-scanning mass analyzers. Magnetic and electric sectors, quadrupole mass filter and quadrupole ion trap can be labeled under scanning mass analyzers. Time of flight and Fourier transform ion cyclotron resonance can be classified as non-scanning mass analyzers [**10**].

Various types of ion detectors are available. Electron multipliers and related devices, and photon multipliers are the main detector types of mass spectrometers [**10**].

Polymers and Mass Spectrometry

Polymers have complicated molecular structures, i.e. there are linear and branched polymers, homopolymers, heteroatomic polymers and copolymers (alternating, block or graft). Moreover, intermolecular and intramolecular interactions show variations among polymers. The length of polymer chains differs from one chain to another. Therefore, characterization of polymers is very sophisticated and various analytical techniques are required in order to obtain physical, mechanical and thermal properties of polymers.

Mass spectrometry is a widely used analytical technique in which various ion sources and mass analyzers can be assembled and which can be coupled with another analytical technique, such as headspace-GC/MS, GC/MS, LC-MSMS, Py-GC/MS, DP-MS, etc. Depending on the purpose of the analysis, the most appropriate mass spectrometer system should be selected [**11**].

When polymers are under concern, various mass spectrometry systems are also available. One of those systems is the direct pyrolysis mass spectrometry, abbreviated as DP-MS. DP-MS turns out to be a reasonable method for determining the thermal degradation mechanisms of polymers. Filament pyrolyzers in DP-MS are placed very close to the ion source, so that formed pyrolysates are immediately transported (by high vacuum) to the ion source and they are ionized. This prevents secondary reactions and condensation reactions. Therefore, detection of even unstable thermal degradation products becomes possible. However, dissociation of thermal degradation products continues in the ion source compartment of the DP-MS. The resultant spectrum obtained is very complex and difficult to interpret [**11**].

Furthermore, information about thermal stability, composition, microstructure and additives can also be obtained by DP-MS [**11**].

1.2. Flame Retardancy

A material is said to have flame retardancy behavior; if it slows down the flame growth and flame propagation when it is subjected to a fire. Similarly, a flame retardant material slows down the growth and propagation of any flames which is caused by the material itself, when it catches fire. A material with flame retardancy property does burn but not easily or rapidly. It can either self-extinguish when the source of flame is removed after ignition, or stay lighted when it is ignited, and it burns relatively slowly [**12**].

Flame retardants are either additives which makes a polymer burn slowly, or polymers which have the ability to retard the flame growth after ignition.

1.2.1. Main Ways Flame Retardants Act

Flame retardant materials reveal their flame retardancy property physically, chemically or in both ways.

Flame retardants act physically in three distinct ways: cooling, forming a protective layer and dilution. Firstly, flame retardants can cool the sample via endothermic reactions. Secondly, they can prevent heat and O_2 from reaching to the sample and any flammable compound from reaching to vapor phase. Thirdly, dilution of radicals in flame can be done by release of H_2O and CO_2 [**13**].

Chemical action of flame retardants can be examined in two ways where the phase of reaction (i.e. gas or solid phase) gains importance. During the reaction in the gas phase, flame retardants prevent formation of radical reactions within the flame. This phenomenon reduces the concentration of radicals which results in extinguishment of flame. By this way, heat releasing processes gradually decay and the system cools down. Unfortunately, these reactions yield release of toxic and irritant semi-burnt products, such as CO. Thus, toxicity of the flame gases may increase. Throughout reaction in the solid phase, fire retardants function as cleaving the polymer; therefore, polymer melts and starts to drop

away from the flame. Better solid phase retardants cause formation of carbonaceous char which covers polymer surface as a layer. As a result of char formation, evolution of smoke and semi-burnt products decreases. Synergistic effect of blowing agents results in swelling between polymer and char, which offers better insulation [**13**].

1.2.2. Types of Flame Retardants

There are various types of flame retardants which are commonly used; such as halogenated compounds, phosphorus based compounds, intumescent flame retardants, boron containing compounds, etc.

1.2.2.1. Halogens

Halogen containing compounds are the most effective fire retardants whose action mechanism is based on the carbon-halogen bond scission [**12**]. High efficiency of halogens makes them much more preferable and widely used. Additionally, small dosages of halogens are enough to reach successive flame retardancy [**14**]. The stability order of carbon-halogen bond is: F>Cl>Br>I. Fluorine compounds are the most stable ones; however, they are preferred for their synergistic effects. Generally brominated and chlorinated compounds are used to make the polymer gain flame retardancy property in two ways: Firstly, brominated or chlorinated organic compound can be added to the polymer. Secondly, halogenated molecules can be embedded into the polymer chain via copolymerization. Besides these advantages, having the disadvantages of formation of toxic products and large amount of smoke during the combustion, makes halogen usage restricted and much less preferable [**12**].

1.2.2.2. Phosphorus Containing Flame Retardants

Phosphorus containing flame retardants, such as red phosphorus, ammonium polyphosphates, organophosphates and phosphinates, are commonly used within many polymers [**15**].

Phosphorus containing flame retardants indicate their flame retardancy property in either condensed or vapor phase, or in both phases. During condensed phase, phosphorus is oxidized to phosphoric acid which causes carbonaceous char formation and causes a layer formation covering the polymer surface. This layer prevents liberation of volatile species from polymer during combustion. This process lowers the smoke emission in case of a fire. Furthermore, evolved volatile species form a vapor barrier, which is less combustible, and evolution of these species cools down the polymer. During gas phase, reactive phosphorus based species (PO*, P* and HPO), which are able to draw away free radicals (which participate in the combustion mechanism), are formed [**15**].

Aluminum Diethylphosphinate (AlPi, OP1230)

Aluminum diethylphosphinate (AlPi) (Figure 1-2) is a kind of dialkylphosphinate salt which is a phosphorus based and additive type flame retardant. This organic phosphinate has an advantage that, no liberation of toxic and harmful compounds is observed after burning of AlPi containing sample [**16**, **17**]. Furthermore, its excellent mechanical and electrical properties, its stability against heat and chemicals make the usage of AlPi much more preferable [**18**]. Phosphorus shows its functionality in gaseous or condensed phases. In gaseous phase, flame retardation is achieved due to radical trapping property of phosphorus; in condensed phase, phosphorus leads to carbon char formation [**17**].

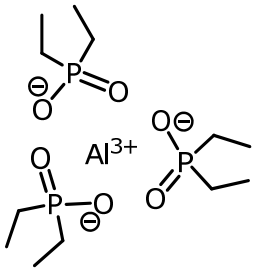

Figure 1-2 Chemical structure of Aluminum Diethylphosphinate

1.2.2.3. Nitrogen Containing Flame Retardants

Nitrogen containing flame retardants are less toxic compared to halogen containing ones; thus they are environmentally friendly. Moreover, they do not form dioxin, halogen acids; but they generate little amount of smoke during burning. Materials depending on nitrogen containing flame retardant have a major advantage that they are recyclable. Melamine and its derivatives are the most well known and preferred nitrogen containing flame retardants [**19**].

Melamine (Me) and Melamine Cyanurate (MC)

The usage of melamine (Me) (Figure 1-3 a) and its derivatives as flame retardant draws great interest due to the lack of release of toxic moieties which are formed as a result of burning. Melamine acts on burning process in three main ways:

- Me behaves like a heat sink by absorbing the heat during sublimation; thus it cools the matrix.
- Me behaves as an inert gas and when sublimated, it dilutes the oxygen and fuel gases present.
- Me causes increase in dripping of the polymer [**20**].

Melamine cyanurate (MC) (Figure 1-3 b) is a derivative of melamine, which is composed of melamine and cyanuric acid. MC is also used as a flame retardant. MC decomposes into Me and cyanuric acid through an endothermic process. This endothermic process indicates the effect of heat sink, thus it exhibits flame retardancy. The flame retardancy procedure of liberated Me has been mentioned above.

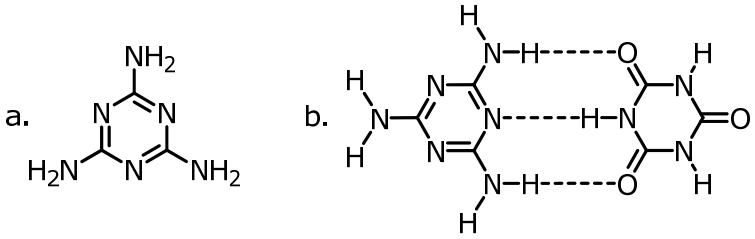

Figure 1-3 Chemical structure of a) Melamine b) Melamine Cyanurate

1.2.2.4. Intumescent Flame Retardants (IFR)

During burning process, intumescent systems have the ability to generate charred layer, which acts as a physical barrier that reduces the rate of heat and mass transfer occurring between the gas and condensed phases. In other words, the formation of char is followed by foaming of the exterior layer of burning substrate. Foaming prevents the substrate from the heat flux or the flame [**21**, **22**].

Intumescent flame retardants are composed of three components:

- **i.** An acid source (decomposes and generates mineral acid, then participates in the dehydration of the carbonific compound in order to form carbon char)
- **ii.** A carbonific (polyhydric) (char forming) compound
- **iii.** A spumific (blowing) agent (degrades to release gaseous molecules which result in the swelling of the char) [**21**, **22**]

Decomposition of acid source starts the intumescent process which is summarized in Figure 1-4, schematically. The temperature at which decomposition takes place must be lower than the pyrolysis temperature of the polymer. The decomposed acid source participates in decomposition of the carbonific compound during which carbonaceous char is formed. The hot and viscous char is ready to be swollen by the spumific agent. The key point in swelling of the char is that, the temperature of both decomposition of carbonific compound and spumific agent must be same; if not, intumescence process will fail [**23**].

One of the IFR systems is the ammonium polyphosphate, (APP) and pentaerythritol, (PER) system, in which APP (Figure 1-5 a) functions as both an acid source and the spumific agent (because of the formation of ammonia gas as a result the APP heating) and PER (Figure 1-5 b) functions as carbonific compound [**21**, **22**].

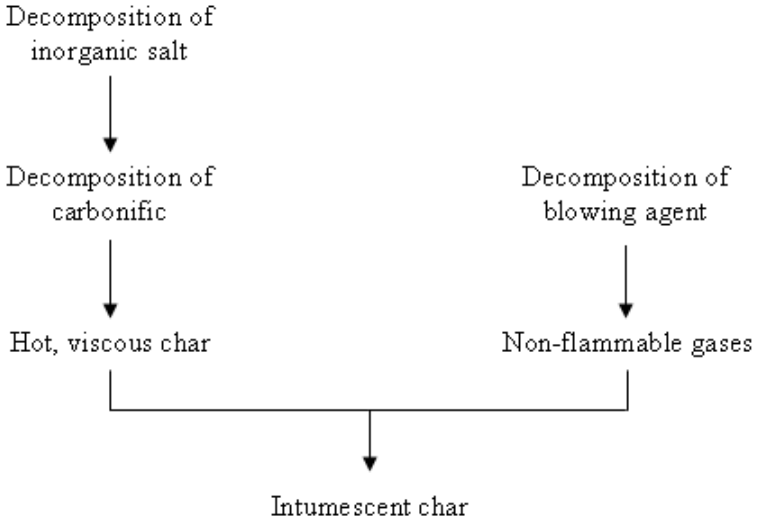

Figure 1-4 Schematic summary of the intumescent process

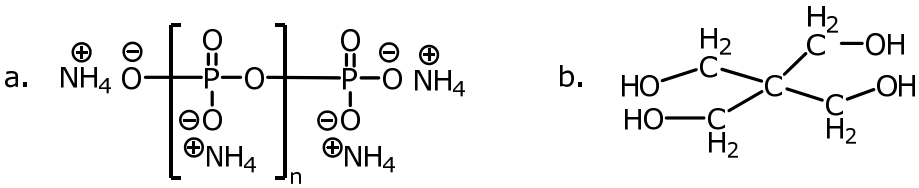

Figure 1-5 Chemical structure of a) APP and b) PER

1.2.2.5. Boron Containing Flame Retardants

Boron containing flame retardants, such as borates and boric acid, which function in the condensed phase, lead to redirection of the degradation process. Therefore, carbon is preferably formed instead of CO and CO_2. A protective char formation, which causes flame retardancy, occurs and results in a protective barrier so that O_2 cannot reach and oxidize the char [**19**]. Other boron-containing flame retardants are boron phosphate BPO_4, zinc borate, ZnB, borosilicate, (BSi) and lanthanum borate (LaB).

Boron Phosphate (BPO_4)

Boron phosphate (BPO_4) has an inorganic polymeric structure (Figure 1-6 a). If phosphoric acid and boric acid (Figure 1-6 b) are warmed together up to calcining temperature, BPO_4 is obtained. It is a white solid that is infusible and remains without decomposition up to 1450-1462°C, where it starts to vaporize [**12**].

a.

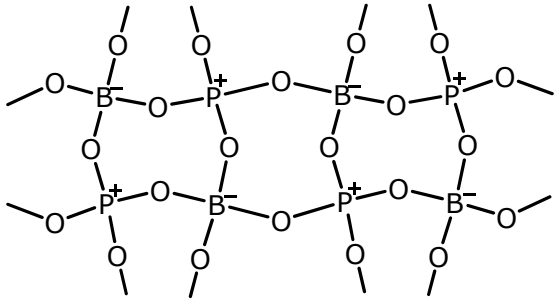

b.

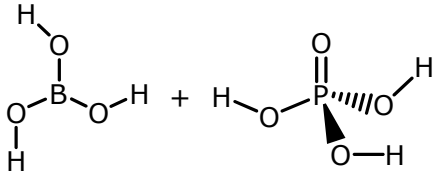

Figure 1-6 Chemical structure of a) boron phosphate and b) phosphoric acid plus boric acid

Zinc Borate (ZnB)

Zinc borate (ZnB), which is one of the boron-containing flame retardants, has the general formula of $xZnO.yB_2O_3.zH_2O$. There are various formulations of ZnB, depending on the reaction conditions. Some of the common formulations are shown in Table 1-1. $2ZnO.3B_2O_3.3.5H_2O$, $2ZnO.3B_2O_3$ and $4ZnO.B_2O_3.H_2O$ remain stable up to 290-300°C, to at least 500°C and to higher than 415°C, respectively [**12**].

Table 1-1 Common ZnB Formulations

Formula	Trade Name
$2ZnO.3B_2O_3.7H_2O$	ZB-237
$2ZnO.2B_2O_3.3H_2O$	ZB-223
$2ZnO.3B_2O_3.3.5H_2O$	Firebrake ZB
$2ZnO.3B_2O_3$	Firebrake 500
$4ZnO.B_2O_3.H_2O$	Firebrake 415

Zinc borates act as flame retardant in various ways. For instance, zinc borates lead to formations of char, decrease the rate of heat release, and suppress the emission of smoke, formation of carbon monoxide and afterglow combustion. Furthermore, they have synergistic effect in the presence of metal hydroxides [**12**].

$2ZnO.3B_2O_3.3.5H_2O$ is obtained as the result of either the reaction between boric acid and zinc oxide (Scheme 1-2 a) or the reaction between borax pentahydrate and zinc sulfate (Scheme 1-2 b). It had been found by single crystal x-ray crystallography that, this particular ZnB has the structure of $Zn[B_3O_4(OH)_3]$ (Scheme 1-2 c). Furthermore, it is used as a flame retardant, and it suppresses the smoke evolution and afterglow combustion. Moreover, it acts as an anti-arcing agent [**12**].

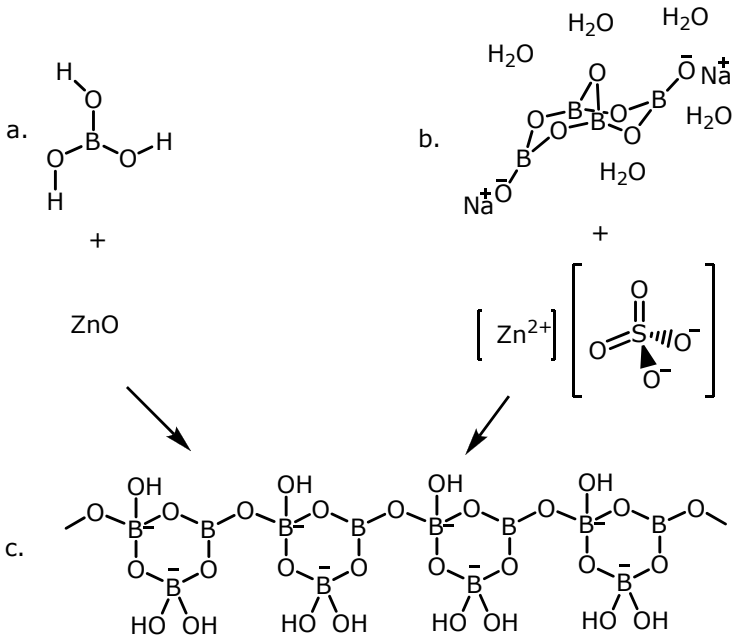

Scheme 1-2 Reaction between a) boric acid and zinc oxide, b) borax pentahydrate and zinc sulfate and the chemical structure of c) $Zn[B_3O_4(OH)_3]$ where the Zn^{2+} are not shown

Borosilicate (BSi)

Borosilicate glass includes glasses dependent on boric acid, silica and a metal oxide. It exhibits outstanding resistance against heat and chemicals [**12**]. Boron and silicon containing preceramic oligomers can be prepared by condensation of boric acid with vinyltriethoxysilane at around 150°C. The possible molecular structure was given in Figure 1-7 [**24**].

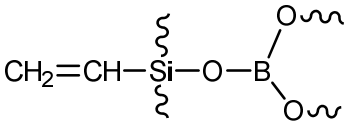

Figure 1-7 The possible molecular structure of boron and silicon containing preceramic oligomers

Lanthanum borate, (LaB)

LaB was used as a synergy agent on the flame retardant properties of intumescent PP composites recently. It is synthesized by microwave irradiation of urea and 1:2 molar ratio of La_2O_3 and H_3BO_3 at 1000 W at ambient conditions followed by further heating at 950°C and characterized by XRD, TGA and SEM methods and found to have orthorhombic structure [**25**].

1.2.2.6. Silicon Containing Flame Retardants

Silicon containing flame retardants, which make considerable improvements in flame retardancy properties of polymers, act in either condensed or vapor phase, or in both. In condensed phase, they yield char formation. In vapor phase, they trap the active radicals. Silicon containing flame retardants are considered as one of the environmentally friendly flame retardants due to reduction in toxic residue formation [**12**]. Silicone is a widely used flame retardant which is regarded as being environmentally friendly. Various silicone based materials exist; such as silicones, silanes, silsesquioxanes, silica and silicates [**12**]. Borosilicate is also regarded as a silicon containing flame retardant.

1.2.2.7. Nanocomposite Flame Retardants

A composite is called nanocomposite when at least one of its components is in the range of nanoscale (usually smaller than 100nm). Layered silicates, which have two dimensions in micrometers, one dimension in nanometers, are used to prepare nanocomposites [**26**]. Flame retardant mechanism of nanocomposites is based on the formation of high performance carbonaceous silicate char, which covers the surface during the combustion. This carbonaceous silicate char is an insulation layer which decreases the mass loss of degradation products [**27**].

Cloisite 30B and Cloisite 15A

Cloisite 30B and Cloisite 15A are modified natural montmorillonites which are, as mentioned above, layered silicates. The modifiers of the Cloisite 30B and 15A are methyl, tallow, bis-2-hydroxyethyl, quaternary ammonium (MT2EtOH) (Figure 1-8 a) and dimethyl, dehydrogenated tallow, quaternary ammonium (2M2HT) (Figure 1-8 b), respectively [**28**, **29**].

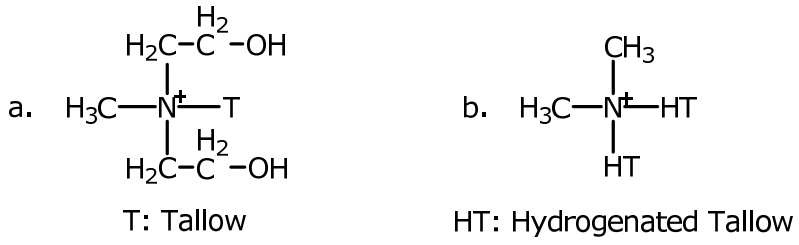

Figure 1-8 Chemical structure of a) MT2EtOH and b) 2M2HT

1.3. Polyamide 6 (PA6)

Polyamide 6 (PA6) (Figure 1-9 a), which is found out by Schlack in 1938, is formed by the addition polymerization reaction of ε-caprolactam (Figure 1-9 b) in the presence of water [**30**, **31**]. In literature, it is stated that the first production of PA6 was started in Germany in 1940. The first application areas of PA6 were for military, during World War 2. Afterwards, the production of PA6 for other purposes became widespread in many countries [**30**]. The number "6" refers to six carbon atoms in the monomer structure. PA6 shows similar properties as PA66. PA6 has a remarkable mechanical properties, toughness, chemical, oil, heat (between 80-150°C) and abrasion resistance, gas barrier properties and low gasoline permeability. It absorbs water at a high rate. PA6 is also known as self-extinguishing. Moreover, according to the Underwriters Laboratory UL-94 Test (UL-94) the flammability of PA66 is rated as V0 [**32**].

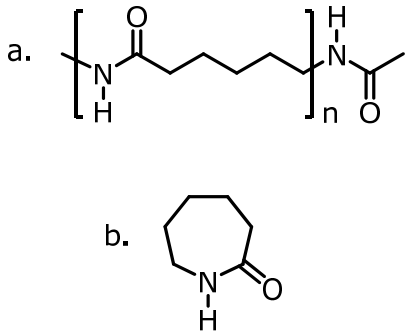

Figure 1-9 Chemical structure of a) Polyamide 6 and b) ε-caprolactam

1.3.1. Thermal Degradation of PA6

Many studies have been done on thermal degradation of PA6. As a general fact; if PA6 is treated with heat, ε-caprolactam will be generated as the main degradation product [**5**, **30**]. Some other structures such as acetonitrile, HCN, NH_3, acrylonitrile, 3-cyanopropene, 4-

cyanobutudiene, 4-pentenal, linear dimer and etc. also form as a result of heat treatment [**5**].

As mentioned in [**30**]; firstly, scission takes place at the weakest C—N bonds. Then, random or almost random scission occurs during the thermal degradation of PA6. The peptide bonds (CO—NH) along the chain undergo hydrolytic scission which is then followed by the decomposition of the acid groups formed; therefore increase in the concentration of CO_2 is observed [**30**].

According to Levchik et al.; two kinds of reactions, primary and secondary reactions, have an important role in thermal degradation of PA6. While the former one occurs at temperatures lower than 300°C, the latter one takes place at temperatures higher than 300°C. It is mentioned that homolytic scission of peptide bond (CO—NH) is the starting point of the thermal degradation of PA6. As a consequence of this reaction; primary amide, nitrile, vinyl, isocyanate and alkyl chain ends form (Scheme 1-3) [**30**].

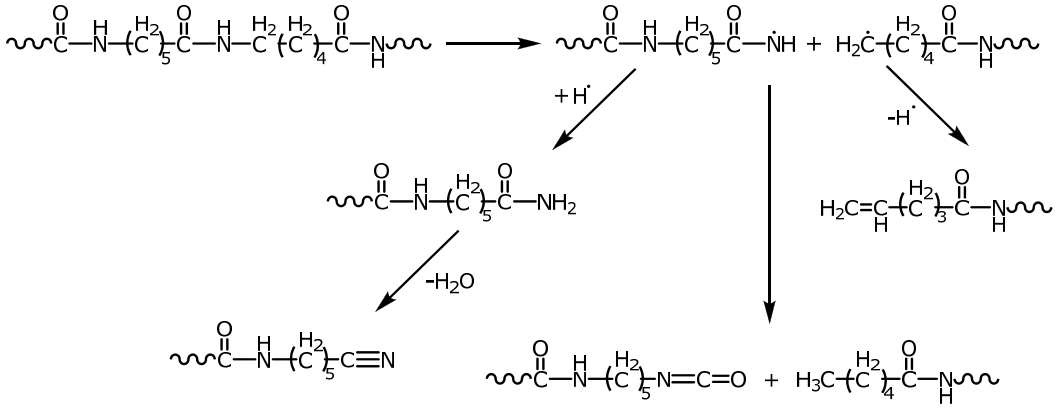

Scheme 1-3 Formation of primary amide, nitrile, vinyl, isocyanate and alkyl chains through homolytic scission of peptide bond

Amines, amides and nitriles are found to be the characteristic fragments of thermal degradation of PA6, as a result of pyrolysis analyses of PA6 via field ion mass spectrometer at 530-800°C. It is proposed that homolytic scission of nitrogen-carbonyl bonds occur during the pyrolysis of PA6 (Scheme 1-4) [**30**].

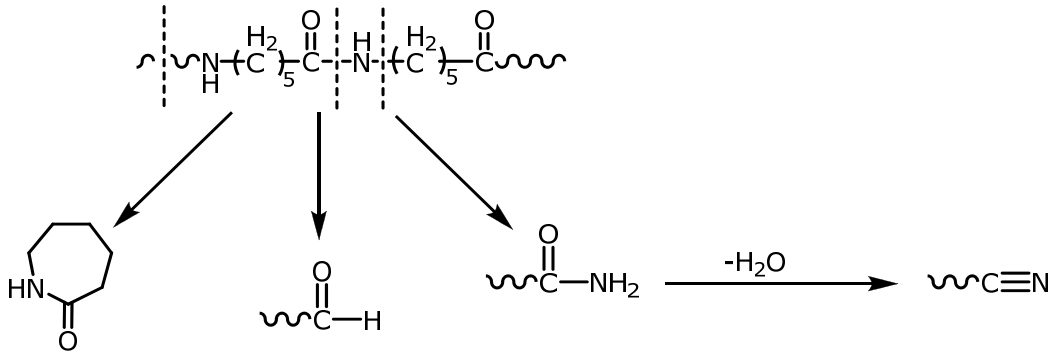

Scheme 1-4 Homolytic scission of nitrogen-carbonyl bonds

Levchik et al. state that; caprolactam is determined as the principal volatile product of PA6 pyrolysis. The secondary product is nitrile in pyrolysis gas chromatography at 550°C, whereas the secondary products are hydrocarbons and acrylonitrile in pyrolysis at 510°C, 610°C and 770°C [**30**].

It is mentioned in the review that; the dominant degradation mechanism of PA6 is based on the experimental conditions. In the presence of H_2O, hydrolysis of peptide bonds is predominant (Scheme 1-5). However, N-alkylamide bond scission (Scheme 1-6) or CH_2—CH_2 bond scission (which is at the β-position to carbonyl group) (Scheme 1-7) become dominant at high temperature. Various low molecular weight hydrocarbon species are formed as a result of further decomposition of the degradation products by random chain scission [**30**].

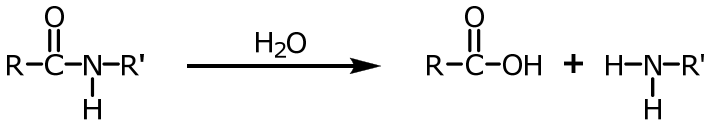

Scheme 1-5 Hydrolysis of peptide bonds in the presence of H_2O

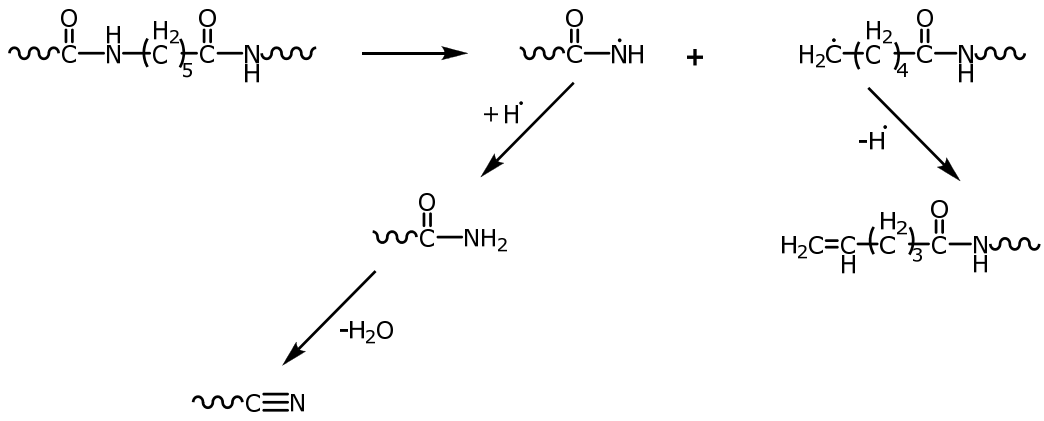

Scheme 1-6 N-alkylamide bond scission at high temperatures

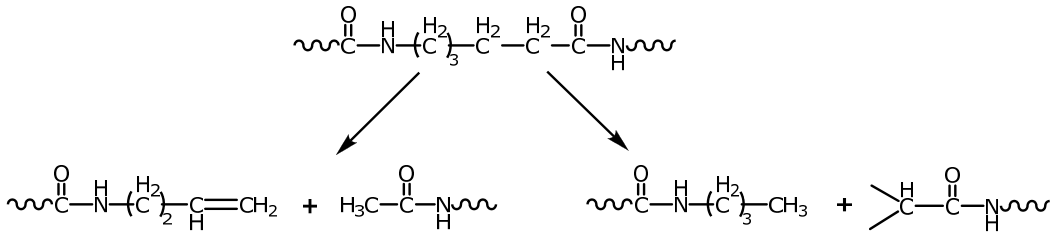

Scheme 1-7 CH_2—CH_2 bond scission at the β-position at high temperatures

According to the review; the thermal degradation of PA6, which is pyrolyzed directly in the ion source, starts with the formation of cyclic oligomers of caprolactam at temperature above 390°C. Cis-elimination occurs through H-shift in a six-membered intermediate which causes the scission of the NH—CH_2 bond (Scheme 1-8). Soft ionization, which occurs by using field desorption mass spectrometry (FD/MS), generates larger ionized fragments of polymer. In the degradation of PA6, fragments are grouped under four series; xM_n-14, xM_n-18, xM_n-44 and xM_n-62, where 14, 18, 44 and 62 refer to the loss of methylene group (cleavage of CH_2—CH_2, CH_2—NH or CH_2—CO bonds), H_2O (in order to generate mononitrile after cis-elimination), $CONH_2$ (which evolves as a result of C—CO amide bond breakage) and H_2O + $CONH_2$, respectively [**30**].

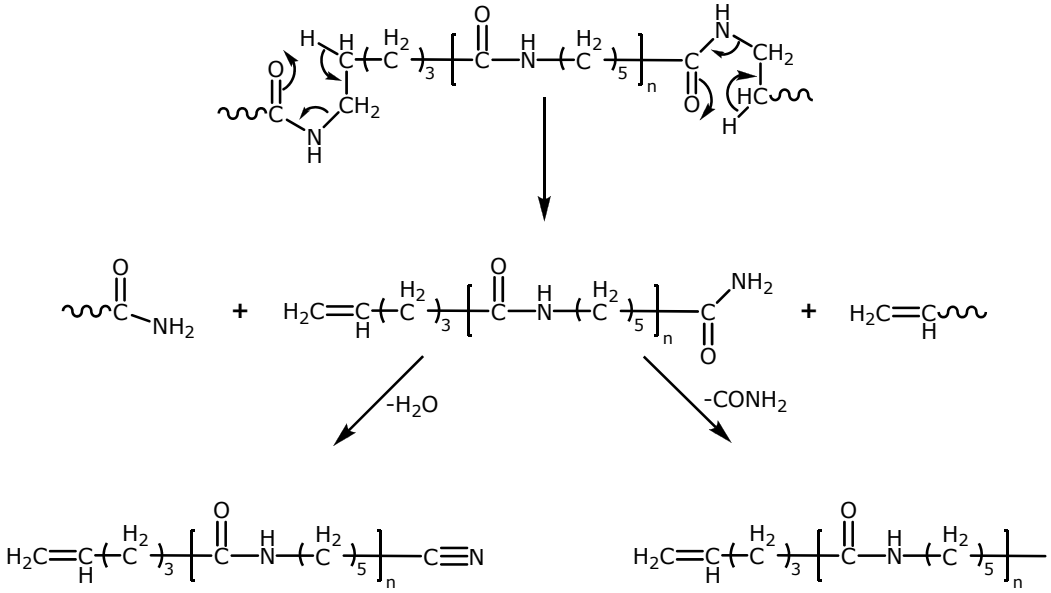

Scheme 1-8 Cis-elimination via H-shift through a 6 membered ring intermediate

As stated by the reviewer; the presence of H_2O initiates a series of reaction, which are hydrolysis (occurs at terminal amide group, resultant product is ε-aminocaproic acid) and cyclization of acid (generates caprolactam or cyclic oligomers of caprolactam and H_2O). Besides, aminolysis and acidolysis reactions are also possible. Both of the reactions can take place either intermolecularly or intramolecularly as shown in Scheme 1-9, Scheme 1-10, Scheme 1-11 and Scheme 1-12. The more amino end groups exist, the higher amount of generation of caprolactam occurs. In addition, if the number of free amino end groups is low, the rate of caprolactam formation is slow. On the other hand, the presence of carboxyl end groups, instead of amino end groups, makes the formation of cyclic oligomers with higher size occur more rapidly [**30**].

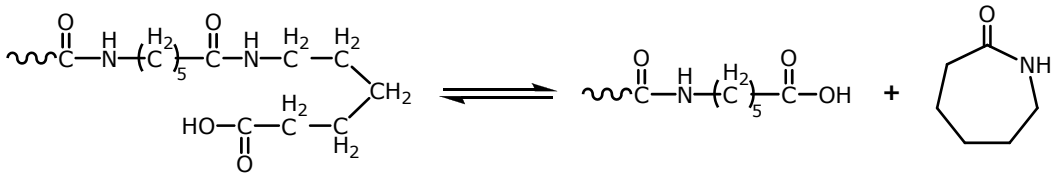

Scheme 1-9 Intramolecular acidolysis reaction

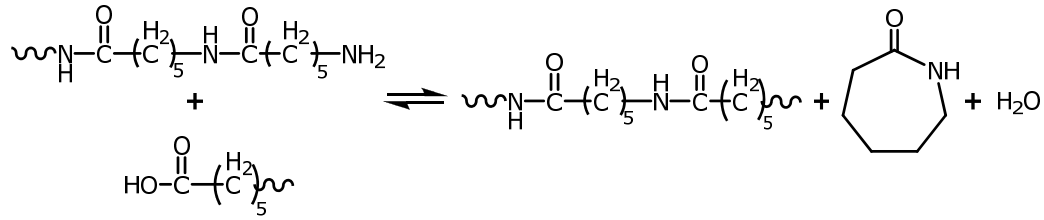

Scheme 1-10 Intermolecular acidolysis reaction

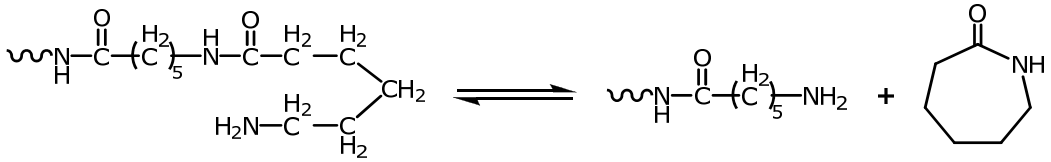

Scheme 1-11 Intramolecular aminolysis reaction

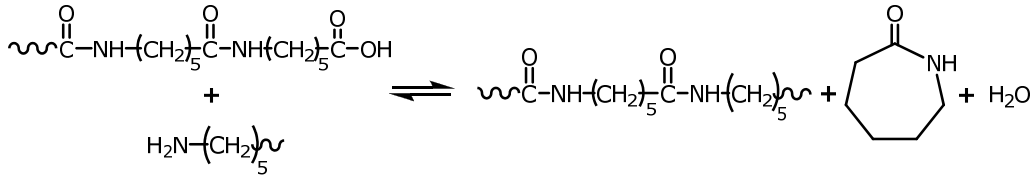

Scheme 1-12 Intermolecular aminolysis reaction

Another investigation mentioned in the review is about cyclic amide production. For all the unmodified polylactams, production of cyclic amides is the main thermal degradation route via intramolecular amide exchange, which includes exchange process (back biting) (Scheme 1-13 a) and aminolysis (end biting) (Scheme 1-13 b) [**30**].

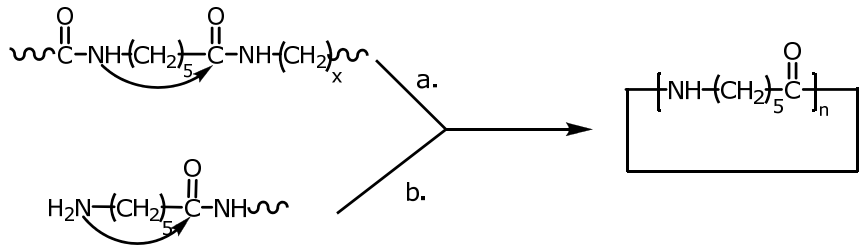

Scheme 1-13 a) Intramolecular amide exchange reaction (back biting) b) Aminolysis reaction (end biting)

Secondary reactions, which are also mentioned in the review, are liable for formation of network structures in the aliphatic polyamides. Hydrolysis of the peptide bond (CO—NH) by H_2O is followed both by the condensation reaction of carboxyl end groups to give CO_2 and H_2O, and by the condensation of the amino end groups to give ammonia (Scheme 1-14). Carbonyl and secondary amine groups, which are located in the chain, are possible active sites for the formation of branched structures (Scheme 1-15). Occurrence of these reactions leads to the generation of crosslinked structure; thus results in gel formation [**30**].

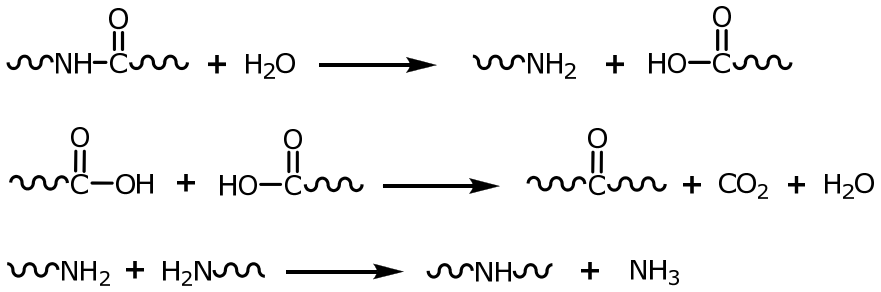

Scheme 1-14 Hydrolysis of peptide bond followed by condensation of both carboxylic end groups and amino end groups

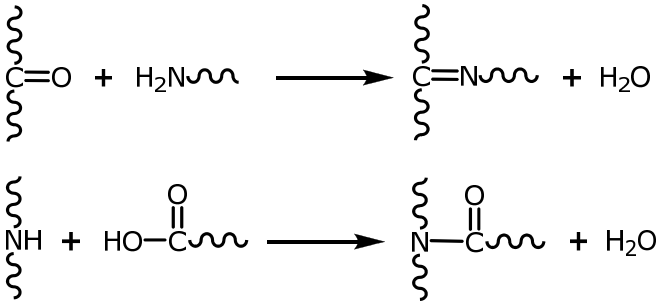

Scheme 1-15 Formation of branched structures

Reviewer also mentions that, during heating process the concentration of amino end groups does not decrease despite the generation of NH_3. Expectedly, the mechanism does not occur through interaction between two amino end groups (Scheme 1-16). Similarly, evolution of CO_2 does not take place via elimination of carboxylic chain ends. H_2O is eliminated through the reaction between ε-caprolactam and acid end group, forming an intermediate which then undergoes either decarboxylation or isomerization (Scheme 1-17). The intermediate can also be formed as a result of a reaction between acid end group and adjacent amide group. But, if this reaction takes place between acid end group and amide group of another chain, branched structures will result (Scheme 1-18) [**30**].

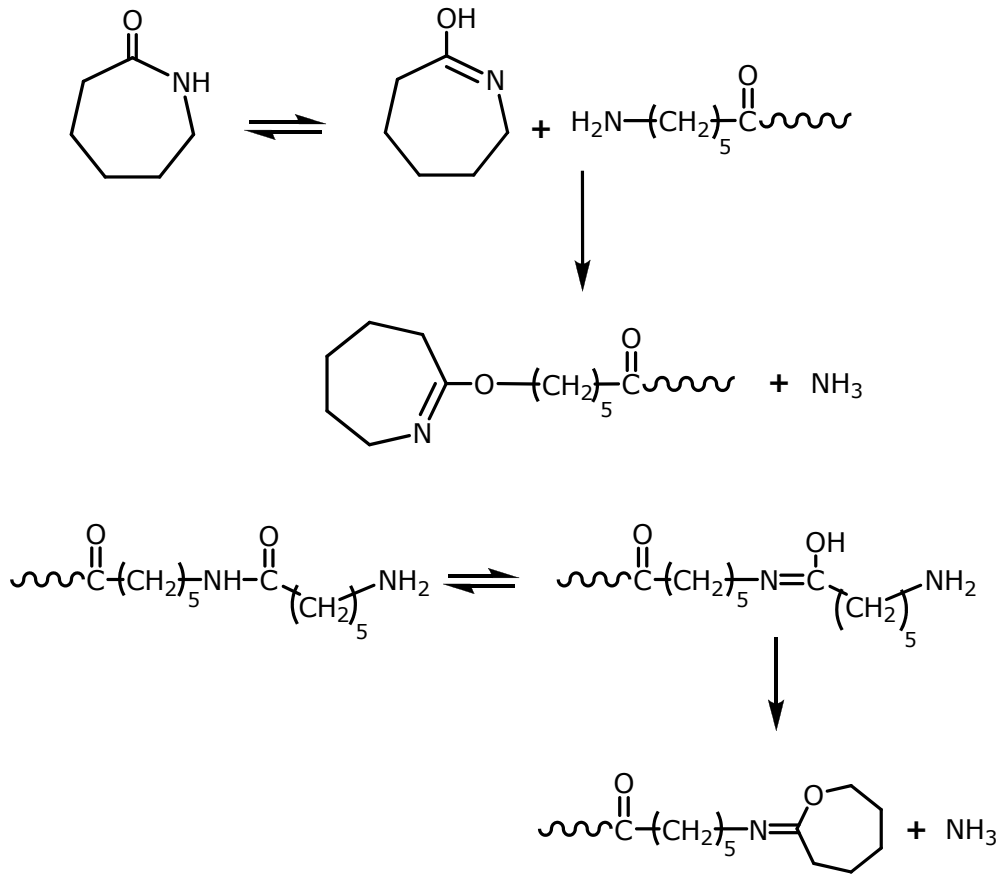

Scheme 1-16 Generation of NH_3

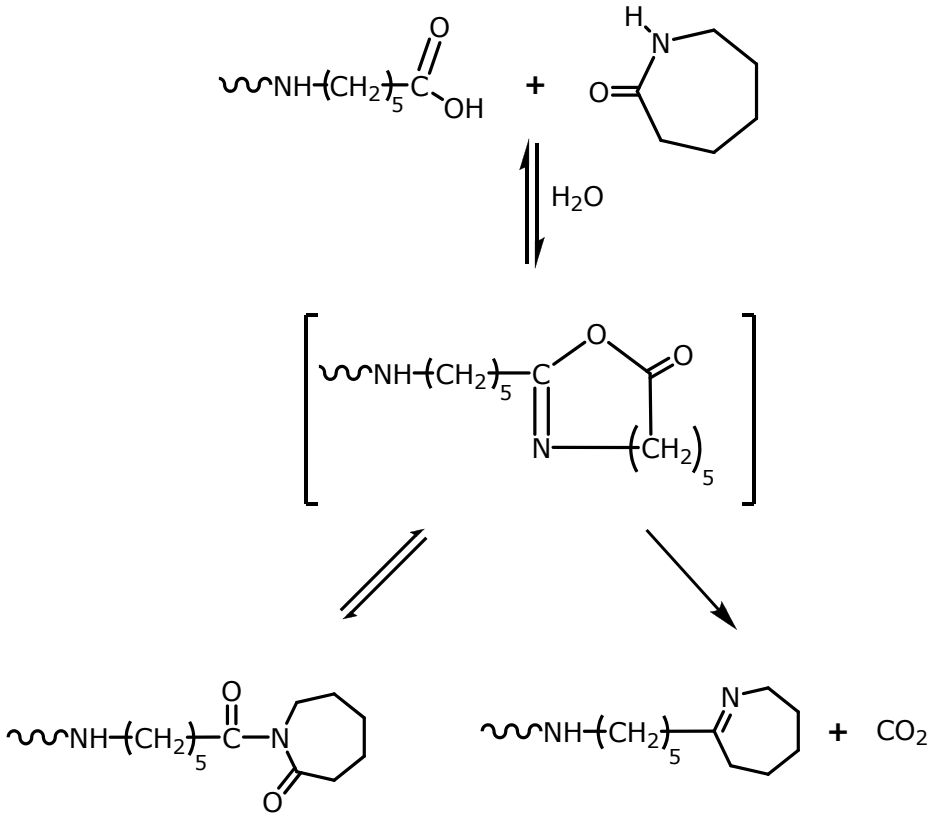

Scheme 1-17 Reaction between ε-caprolactam and acid end group resulting in either decarboxylation or isomerization of the intermediate

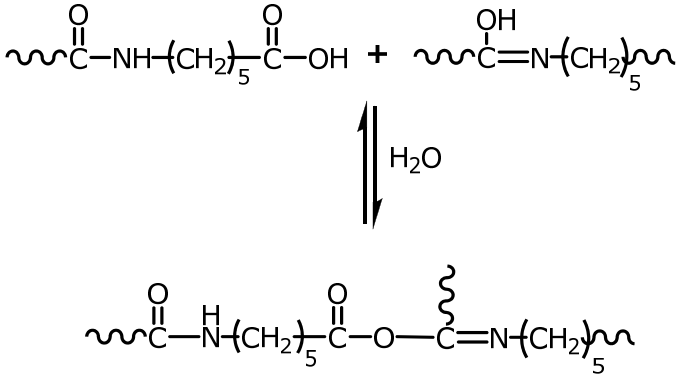

Scheme 1-18 Formation of branched structure through the reaction between acid end group and amide group of another chain

According to the review, thermal degradation occurring through linear heating under inert atmosphere can cause weight loss via three steps: The volatilization of residual H_2O and low molecular weight oligomers are considered as the first step. In the second step, primary degradation of PA takes place which can result in the volatilization of most of the material and the formation of crosslinked structure. Moreover, in the third step the crosslinked structure can degrade upon further heating and form thermally stable char [**30**].

Liu and Wang proposed two degradation pathways for PA6 according to the analysis via Py-GC-MS. In the first one, degradation of PA6 occurs through oxidative degradation (Scheme 1-19) whereas in the second one, it occurs through weak bond cleavage (Scheme 1-20). It was mentioned that main products of oxidative degradation of PA6 were caprolactam and cyclopentanone. On the other hand, in addition to caprolactam, long chain fragments were formed mainly in the degradation of PA6 through weak bond cleavage [**33**].

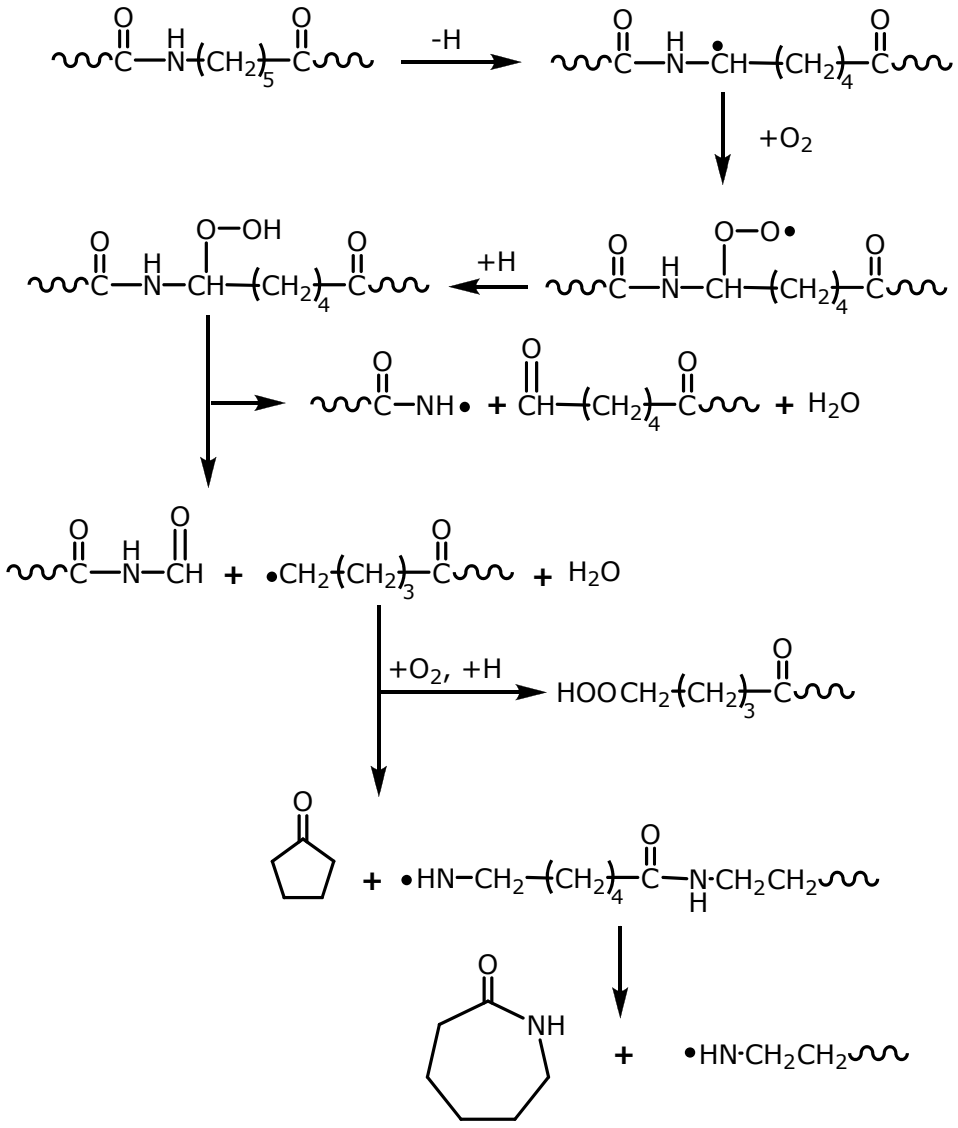

Scheme 1-19 Oxidative degradation of PA6

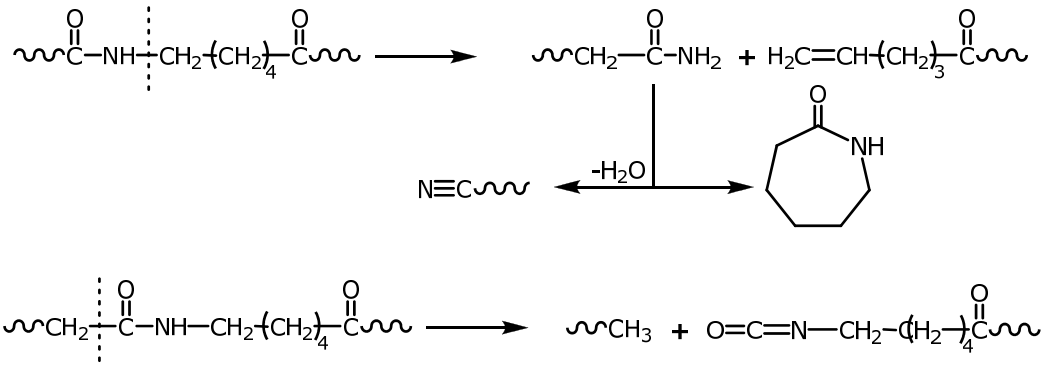

Scheme 1-20 PA6 degradation mechanism through weak bond cleavage

Steenbakkers et al. investigated the effect of melamine cyanurate on thermal degradation products of PA6. It was concluded that evolution of NH_3 from degradation of both MC and PA6 could be the reason of ineffectiveness of MC addition on degradation product distribution of PA6. Main degradation products of PA6 with and without MC were caprolactam, alkylcyanides and NH_3. The presence of MC had a slight influence on the residual amount of crosslinked degradation product formation [**34**].

1.3.2. Flame Retardancy of PA6

Polyamide 6 is used as engineering plastic in certain application areas, such as textile, electronics, due to its chemical stability, outstanding electrical and mechanical properties. On the other hand, PA6 is not preferred in as many application areas as expected because of its low limiting oxygen index and inflammability. Therefore, it is significantly important to produce PA6 with improved flame retardancy [**35**, **38**]. For this reason, various kinds of flame retardants are used, such as halogen, phosphorus, nitrogen, boron and silicon containing additives. They can be used either separately or as binary-ternary combinations of flame retardants due to their synergistic effects [**38**]. Despite being very effective, halogen containing flame retardants are not preferred, because of the evolution of toxic and corrosive gases and black smoke during their combustion [**36**]. Therefore, halogen-free flame retardants, which are environmentally friendly, are used instead of halogen containing ones. For instance; melamine and its derivatives are used to improve the flame retardancy of PA6 [**37**]. PA6 is destabilized by melamine, and dripping of PA6 is increased. Thus, removal of fuel source from the burning area is achieved [**38**]. Boron compounds, such as zinc borate, are also environmentally friendly flame retardants. They are generally used together with other flame retardants because they act as synergist [**37**].

Liu and Wang investigated the flame retardancy mechanism of melamine cyanurate flame retardant PA6. It was concluded that the presence of MC had essential effect on the degradation of PA6 after the analyses of melt-drip phase, condensed phase and gaseous phase. It was determined that MC leads the PA6 to degrade through weak bond cleavage as a result of the interaction of amide groups of PA6 with melamine or cyanurate. In

addition, oligomers were formed. According to their study, these oligomers could result in increase in rate of formation of melt drips, by which combustion heat and latent fuel were removed and amount of volatile flammable constituents were reduced. Furthermore, these oligomers could undergo self-condensation reactions; therefore stable crosslinked structures were produced. Crosslinked structures yielded improvement on condensed phase and could cause increase in generation of char layer which acted as a barrier and prevented the exchange of heat, volatile degradation products and oxygen. They also indicated that degradation of pristine PA6 occurred via oxidation degradation; as a consequence of this kind of degradation, small molecular products were formed [**33**].

Bourbigot et al. investigated the flammability of PA6/clay hybrid nanocomposite textiles. It was aimed to find new pathways in order to obtain flame retardant textiles with durability, without losing their mechanical properties and also basic properties of the textile. For this purpose, an exfoliated structure of PA6/clay hybrid nanocomposite was obtained by counter-rotating twin-screw extruder in which PA6 was melted and mixed with the clay. In order to get multifilament yarns of PA6/clay hybrid nanocomposite, melt spinning process was performed. In this study, it was determined that PA6/clay hybrid nanocomposite had 40% lower heat release rate as compared to pure PA6 [**39**].

Dahiya et al. studied thermal behavior of PA6/bentonite/ammonium polyphosphate composites. They determined via XRD (X-Ray Diffraction) peaks and TEM (Transmission Electron Microscopy) images of PA6/org-bentonite nanocomposites that, PA6/bentonite/ammonium polyphosphate composites showed both ordered exfoliation and slightly ordered intercalation. Furthermore, it was found that the presence of organically modified bentonite increased thermal degradation temperature of PA6 by about 17°C (from 456°C to 473°C). On the other hand, addition of APP into PA6/org-bentonite nanoclay decreased the thermal degradation temperature by about 100°C. However, addition of APP increased the char yield of PA6/org-bentonite nanoclay by about 20%. Studies based on different particle size of APP showed similar effects on thermal stability and char yield. Thus, it was concluded that org-bentonite/APP would be a preferred nanoclay flame retardant system for PA6 [**40**].

The flame retardancy and physical properties of PA6, melt processed in the presence of various amounts of melamine polyphosphate and layered silicates, were investigated by Kiliaris et al. It was determined through XRD (X-Ray Diffraction) analyses that the resultant PA6/silicate/Me polyphosphate nanocomposite had exfoliated structure. Molecular weight of PA6 reduced because of degradation of polymer during the preparation of thePA6/silicate nanocomposite. Addition of Me polyphosphate increased the reduction of molecular weight. Crystallinity of polymer was decreased in the presence of both silicate and Me polyphosphate. Tensile strength and tensile modulus of PA6 were enhanced, while loss of ductility of PA6 was observed. Flammability of PA6 was improved in the presence of silicate and Me polyphosphate. Pristine PA6 failed in the UL-94 test. Kiliaris et al. mentioned that layered silicates and Me polyphosphate acted together in flame retardancy mechanism of PA6 by forming an impermeable barrier on the surface of PA6. Polyphosphoric acid, generated by the decomposition of Me polyphosphate, reacted with PA6, producing phosphoric esters, which caused degradation

to unsaturated species and further degradation to char. Acting as a catalyst of acidic sites also led to formation of char on the surface of the silicates as a result of the Hoffman elimination of clay modifier. Enlargement of char occurred during the volatilization of NH_3, formed by the degradation of Me and PA6. Thus, an intumescent protective barrier was formed. Moreover, reassembling of silicates on the surface of the burning substance resulted in an additional barrier, while reaction of Me polyphosphate with silicate generated an aluminophosphate structure which protected the substrate. As a consequence, addition of silicate and Me polyphosphate to PA6 reduced the flammability of pure PA6 and resulted in V2 rating in UL-94 testing [**41**].

Fang et al. preferred to use melamine (Me) as a modifier for montmorillonite (MMT) instead of using a common modifier, i.e. organic modifier, because of combustibility property of organic modifier. Melamine pyrophosphate (MPP) was used as a complex of blowing agent and acid source to make an intumescent flame retardant system in combination with Me-MMT. PA6 was melt blended in the presence of Me-MMT and MPP in order to get intercalated and exfoliated structures of PA6/Me-MMT composites. According to their findings; noncombustible gas formed by Me expanded spacing between MMT layers. Furthermore, MMT particles were forced by the air flow generated by MPP, and MMT particles were moved from inner side toward outer surface of the matrix. This motion was followed by various degradation products which resulted in aggregation on the surface of char. The defects on the char layer were filled by the MMT particles, therefore the char layer became stronger to prevent heat and mass transfer and melt dripping. Moreover, PA6/Me-MMT composite got better results from LOI and UL-94 testing (35.0 and V0, respectively), than that of pure PA6 (21.0 and V2, respectively) [**42**].

Zhang et al. studied flame retardancy of PA6 with melamine cyanurate and layered silicates. It was concluded that PA6 gained high degree of flame retardancy with the addition of 13 wt% of MC, whereas the addition of organically modified layered silicates more than 0.2 wt% influenced antagonistically. Melamine sublimation (an endothermic process) took place before combustion and during the pyrolysis of the polymer and diluted the flammable gases evolved throughout the pyrolysis. Moreover, interference of melamine to the H-bonding of PA6 resulted in decomposition of the polymer. Furthermore, generated cyanuric acid caused decomposition of the PA6. As a result, reduction in viscosity and thus increased in dripping was observed. Addition of layered silicates affected the flame retardancy conversely. Interaction between polymer chains and exfoliated layers of organically modified clays increased the melt viscosity. Thus, Me evolved much more slowly during the pyrolysis and dripping rate slowed down. Increase in melt viscosity during pyrolysis caused increase in the size and the mass of the drops. As a conclusion, the UL-94 rating for samples with more than 0.2 wt% layered silicates was determined as V2. On the other hand, samples with only MC got V0 rating from UL-94 test [**43**].

1.4. Polypropylene

Polypropylene (abbreviated as PP, shown in Figure 1-10 a) is produced by coordination catalyst polymerization of propylene (Figure 1-10 b) which is an addition polymerization in the presence of a special catalyst, named Ziegler-Natta. Generally, monomers are added to the chain in head to tail fashion. Moreover, PP has mainly three molecular configurations, isotactic, syndiotactic and atactic. Isotactic PP is a crystalline polymer due to its highly regular structure (stereoregularity). In other words, isotactic PP has a helical structure in which three monomer units form a repeating unit of the helix. Methyl groups are located around this structure, making close packing possible. This regular structure results in highly crystalline polymer [**5**, **44**]. In general, presence of crystalline structure has influence on the physical, mechanical and thermal properties, for instance being harder and thus more brittle, and more stable against heat. Additionally, due to the presence of tertiary carbon atoms in its structure, PP is susceptible to oxidative degradation at significantly high temperatures. When PP is exposed to heat, random chain scissions take place at the weakest linkages. Radicalic species are formed and they undergo additional reactions where small molecules and also macroradicals are formed. Propylene is also a thermal degradation product of the polymer. During the pyrolysis of PP, formation of dimer, trimer and tetramer fragments are also observed [**1**, **3**, **5**, **44**].

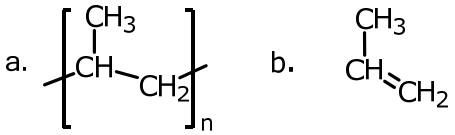

Figure 1-10 a) Polypropylene b) Propylene

1.4.1. Thermal Degradation of PP

Isotactic PP degrades oxidatively under heat treatment and sunlight. Degradation results in yellowing and worsening of mechanical properties. Mechanism of this degradation depends on free radical chain reaction which causes polymer chain scission. This radicalic degradation mechanism is a cyclic reaction and is called autoxidation. In order autoxidation to occur, existence of the radical species is essential. In the case of isotactic PP, which is a saturated hydrocarbon, generation of radical species is almost impossible under common degradation conditions. Therefore, in order to progress thermal oxidative degradation, an initiator is needed. For this purpose, low molecular weight compounds, such as dialkyl peroxides, hydroperoxides and macroradical species are used as initiators. On the other hand, when isotactic PP with unsaturated end group is of concern, initiator will be the unsaturated end group instead of allyl radical which has high resonance stability. Furthermore, double bond of unsaturated end group undergoes reaction with radicals which is resulted in inhibition of degradation [**45**].

Degradation of isotactic PP takes place through chain scission which results in shifting of the molecular weight distribution to lower molecular weight region. In investigation of thermal degradation of PP under isothermal condition at 190°C, it is concluded that a heterogeneous degradation occurs [**46**].

Abstraction of H atom from PP backbone by free radicals is the first step of the oxidative degradation. Peroxides can be used as radical initiators in the degradation of PP at high temperatures. In the presence of peroxides and heat, the degradation of PP under N_2 results in increase in molecular weight, instead of decrease; whereas, the degradation of PP under O_2 results in significant decrease in molecular weight. Molecular oxygen is selective for the abstraction of H atom from tertiary sites where tertiary radical species are formed. Furthermore, these tertiary radical species break into smaller chains [**47**].

1.4.2. Flame retardancy of PP

Intumescent flame retardants are used to make the PP thermally more stable. During burning process, IFR forms a char layer above PP which prevents PP from further thermal degradation. Thus, flame retardant properties of PP are said to be improved [**48**].

Both organic and inorganic phosphorus compounds, such as pyrophosphoric acid and alkyl-aryl phosphonates, are used as flame retardants for PP. Phosphorus compounds are not only used alone in PP but also used in the presence of halogen or nitrogen containing compounds. Especially ammonium polyphosphate (APP) is used in the presence of pentaerythritol (PER) as intumescent systems for PP. Furthermore, APP-PER intumescent systems can be used with borosiloxane in PP, which improves the fire retardancy. The use of silicotungistic acid for its synergist effect to IFR systems in PP causes the increase in the LOI value and the increase in the thermal stability at high temperatures [**44**].

Nanocompounds, such as organically modified montmorillonites, TiO_2, Sb_2O_3 and borosiloxanes, are also used as flame retardant in polypropylene. Due to its low price, montmorillonite is one of the mostly preferred nanocompounds. Complete dispersion of montmorillonite within organic polymer is an essential point. In order to achieve the most appropriate dispersion of montmorillonite within the polymer, modification of the montmorillonite by exchanging the sodium cations with the organophilic cations (which have long alkyl chains) should be done. Enhancement in the mechanical properties is obtained in exfoliated nanocomposites (in which the layers of the montmorillonite are completely delaminated). Yet, in the case of intercalated nanocomposites (in which polymer chain is intercalated into layers of the montmorillonite, but interlaminar contact between the layers is maintained), improvement of fire retardancy performance is achieved. Fire retardancy activity of montmorillonite nanocomposites is believed to be dependent on gasification and precipitation of montmorillonite. While polymer is gasified or burned away, montmorillonite precipitates at the surface, therefore a barrier is formed which prevents the diffusion of O_2 into polymer and the evolution of volatiles away from polymer. Moreover, aluminasilicate in the montmorillonite forms a highly concentrated layer on the surface of the burning polymer, which acts as a boundary between the

polymer surface and its surrounding. Hence prevention of mass and flame transfer from/to the polymer are achieved. Additionally, some flammability characteristics, such as ignition time, ignition temperature and heat release rate, are influenced by the formation of that boundary. Furthermore, substitution of Fe for Al or Si atoms results in trapping of radicals, thus combustion rate diminishes [**26**, **44**].

Zhang et al. investigated flame retardancy effect of melamine pyrophosphate (MPP) and 1-oxo-4-hydroxymethyl-2,6,7-trioxa-1-phosphabicyclo[2.2.2]octane (PEPA) on polypropylene. While the limiting oxygen index showed an increase by the addition of MPP or PEPA, the composites failed in UL-94 testing. On the other hand, improvement of both UL-94 test rating and LOI value was observed in ternary composite of PP / MPP / PEPA (70% : 15% : 15%). As a conclusion, it was stated that an intumescent protective layer, which led to a decrease in heat release rate, was generated through burning of ternary composites. Zhang et al. indicated that PEPA and MPP had synergistic effect on each other [**49**].

Xu and Li synthesized a new triazine polymer which acts a charring and foaming agent (CFA) in intumescent flame retardant (IFR) systems. The influence of CFA on flame retardancy and thermal degradation of polypropylene (PP) was investigated. An IFR system containing CFA, ammonium polyphosphate and Zeolite 4A (32% : 64% : 4%) was prepared. It was found that the IFR system had effective flame retardancy in PP. PP with 18 wt% of IFR passed the UL-94 test with V0 rating, furthermore the LOI value of this composite reached 30.2. Although no change was observed in UL-94 rating (V0), the LOI value increased to 37.0 by increasing the IFR loading to 25 wt%. Moreover, it was found that CFA could form char by itself and APP addition could improve char formation. According to the calculation made, it was concluded that IFR could affect the temperature, at which thermal degradation of PP took place, could shift the temperature to higher value and could lead to char formation in PP-IFR composite [**50**].

1.5. Aim of the Study

The aim of this study is to investigate the effects of boron containing flame retardants such as BPO_4, ZnB, BSi or LaB on thermal degradation characteristics of two industrially important polymers, polyamide 6, (PA6) and polypropylene, (PP) composites via direct pyrolysis mass spectrometry. The polyamide 6 composites involve nitrogen flame retardants such as melamine, (Me) or melamine cyanurate, (MC), or phosphorous flame retardant aluminum diethylphosphinate, (AlPi), with or without methyl, tallow, bis-2-hydroxyethyl, quaternary ammonium organically modified 1% Cloisite 30B. On the other hand, polypropylene composites involve intumescent flame retardant, (IFR) (ammonium polyphosphate-pentaerythritol, APP/PER system) with or without 5% maleic anhydride grafted polypropylene and dimethyl, dehydrogenated tallow, quaternary ammonium organically modified 2% Cloisite 15A. In order to investigate the effects of boron compounds on thermal degradation characteristics, thermal degradation behaviors of each component of the composites and pristine composites are also studied systematically and compared.

CHAPTER 2

EXPERIMENTAL

2.1. Materials

Materials analyzed in this study, polyamide 6 (PA6) and polypropylene (PP) composites involving boron compounds, have been prepared by Assist. Prof. Dr. Mehmet Doğan during his Ph.D. studies in the Department of Polymer Science and Technologies (PST) at METU [**51**]. The compositions of the composites and the data related to flame retardancy obtained from literature are summarized from Table 2-1 to Table 2-6 [**25**, **37**, **38**, **51**, **52**]. PA6, with a trade name Bergamid B65 Natur- TP was purchased from Polyone, PP, with a trade name Petoplen EH-251 was obtained from PETKİM A.Ş., and PP-g-MA, with a trade name Exxelor PO 1015 was received from ExxonMobil. The preparation of BPO_4, BSi and LaB samples were given in detail in the literature [**25**, **37**, **52**]. The other flame retardants used in the preparation of the samples were obtained from various suppliers that are summarized in Table 2-7 [**51**].

Table 2-1 PA6 based samples with a secondary component of Melamine

PA6 (%)	Melamine (%)	BPO_4 (%)	ZnB (%)	BSi (%)	UL-94 Rating	LOI Value	Char Yield (%)
100	-	-	-	-	V2	22.5	0.00
80	20	-	-	-	V0	31.0	0.00
80	17	3	-	-	V0	28.6	4.09
80	17	-	3	-	V2	25.6	3.29
80	17	-	-	3	V0	29.7	3.18

Table 2-2 PA6 based samples with a secondary component of Melamine Cyanurate

PA6 (%)	MC (%)	BPO_4 (%)	ZnB (%)	BSi (%)	UL-94 Rating	LOI Value	Char Yield (%)
100	-	-	-	-	V2	22.5	0.00
85	15	-	-	-	V0	31.8	0.60
85	12	3	-	-	V0	27.0	3.63
85	12	-	3	-	V2	24.4	3.34
85	12	-	-	3	V2	29.4	2.49

Table 2-3 PA6 based samples with a secondary component of Aluminum Diethylphosphinate without Cloisite 30B

PA6 (%)	AlPi (%)	BPO_4 (%)	ZnB (%)	UL-94 Rating	LOI Value	Peak HRR (kW/m^2)	Char Yield (%)
100	-	-	-	V2	22.5	975	0.00
85	15	-	-	V0	29.5	695	1.00
85	14	1	-	V0	29.0	755	1.50
85	14	-	1	V0	29.5	480	2.80

Table 2-4 PA6 based samples with a secondary component of Aluminum Diethylphosphinate with Cloisite 30B

PA6 (%)	AlPi (%)	Cloisite 30B (%)	BPO_4 (%)	ZnB (%)	UL-94 Rating	LOI Value	Peak HRR (kW/m^2)	Char Yield (%)
85	14	1	-	-	V0	29.5	575	1.50
85	13	1	1	-	V0	29.5	535	2.60
85	13	1	-	1	V0	31.0	380	4.30

Table 2-5 PP based samples with a secondary component of IFR

PP (%)	IFR (%)	BPO_4 (%)	BSi (%)	LaB (%)	UL-94 Rating	LOI Value	Peak HRR (kW/m^2)	Char Yield (%)
100	-	-	-	-	BC	17.5	920	0.00
80	19	1	-	-	V0	30.0	226	8.80
80	19	-	1	-	V0	25.5	255	7.20
80	19	-	-	1	V0	27.0	260	11.00

Table 2-6 PP based samples with secondary components of Cloisite 15A and IFR

PP (%)	PP-g-MA (%)	Cloisite 15A (%)	IFR (%)	BPO_4 (%)	ZnB (%)	BSi (%)	UL-94 Rating	LOI Value	Peak HRR (kW/m^2)	Char Yield (%)
93	5	2	-	-	-	-	BC	18.2	565	1.40
73	5	2	20	-	-	-	BC	23.5	199	8.80
73	5	2	15	5	-	-	V2	25.6	193	14.60
73	5	2	15	-	5	-	BC	24.6	334	15.30
73	5	2	15	-	-	5	V2	24.2	206	14.00

First four sets of samples (given in Table 2-1, Table 2-2, Table 2-3 and Table 2-4) are based on PA6 and a secondary component melamine, melamine cyanurate and AlPi, respectively. The polymer matrix of last two sets of samples (given in Table 2-5 and Table 2-6) is PP. For the samples shown in Table 2-5, the secondary component is IFR (IFR=APP:PER=3:1). For the last sample set given in Table 2-6, while Cloisite 15A and IFR are used as the secondary materials, PP-g-MA is used to disperse Cloisite 15A into the polymer more efficiently. Maleic anhydride-grafted-polypropylene (PP-g-MA) (Figure 2-1) is obtained by grafting maleic anhydride onto molten polypropylene in the presence of an organic peroxide. This grafting process attracts attention because it improves the compatibility, adhesion and reactivity of the polypropylene [**53**].

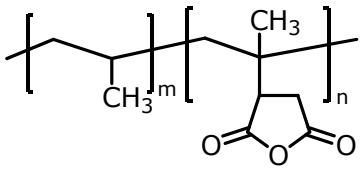

Figure 2-1 Chemical structure of maleic anhydride-grafted polypropylene (PP-g-MA)

PP-g-MA is generally used as a compatibilizing agent. It is difficult to get a thoroughly mixed polymer/clay (PP/clay) blend due to significant difference in polarities of the polymer and clay. PP-g-MA is used to overcome this handicap. It causes enhancement in polymer polarity, so that the adhesion and the miscibility between polymer and clay increase [**54-56**].

Table 2-7 Materials used in the preparation of samples and their suppliers

Material	Trade Name	Supplier
Melamine (Me)	Malefine	DSM
MC	Ciba® MELAPUR® MC25	Ciba
AlPi	OP1230	Clariant
ZnB	Firebrake ZB	Luzenac
APP	Exolit AP	Clariant
PER	Pentaerythritol	Merck
Cloisite 30B	Cloisite® 30B	Southern Clay Products Inc.
Cloisite 15A	Cloisite® 15A	Southern Clay Products Inc.

2.2. Direct Pyrolysis Mass Spectrometry

All the samples mentioned in the previous Section were pyrolyzed separately. DP-MS analyses were carried out by using *Waters Micromass Quattro Micro GC triple quadrupole Mass Spectrometer* with a mass range 10 – 1500 Da. EI (electron impact) ion source was coupled to a direct insertion probe. 70 eV EI mass spectra, at a rate of 1 scan/s, were continuously recorded during the pyrolysis. Deep capillary quartz tubes were used as sample containers. The temperature was raised to 50˚C at a rate of 5˚C/min, then was raised to 650˚C at a rate of 10˚C/min and was kept at that temperature for 5 minutes. The whole analysis lasted approximately 70 minutes. The pyrolysis mass spectrometry analyses were repeated several times to ensure reproducibility. At each identical analysis cycle, almost exactly same trends were observed.

2.3. Data Analysis

During the direct pyrolysis mass spectrometry analyses, thermal degradation products further dissociate during the ionization process. Thus, direct pyrolysis mass spectra of polymers are usually very complex. In order to control extent of fragmentation during ionization soft ionization techniques such as chemical ionization or low energy electron impact ionization can be used. However, each method has its own limitations. For the analyses of thermal behavior of the samples by direct pyrolysis mass spectrometry technique, the first step is to record variation of total ion yield as a function of temperature, total ion current, (TIC) curve. The mass spectra recorded at the maximum of the peaks in the TIC curves are then analyzed first and possible assignments for the characteristic and/or intense peaks are made. Another difficulty that increase complexity, arises from the fact that the fragments that are structural isomers and the products involving different combinations of C, H, O but with the same m/z values contribute to the intensity of the same m/z peak in the mass spectrum. Thus, what is important in pyrolysis MS analysis is not the detection of a peak, but the variation of its intensity as a function of temperature, which is called as single ion pyrogram or evolution profile. The trends in the evolution profiles are evaluated in order to categorize the fragments according to the similarities in their evolution profiles that can be used to determine the source of the related product, or the mechanism of thermal degradation.

Pyrolysis analysis of a polymer composite is even more complicated as expected. It is not possible to investigate all the processes taking place during the thermal degradation of a composite without the knowledge of the thermal degradation characteristics of each component present. Thus, systematic analyses involving investigation of thermal degradation characteristics of all components of the composite separately and samples involving mixtures of components have to be performed.

CHAPTER 3

RESULTS AND DISCUSSION

In this work, the effects of boron compounds, namely zinc borate (ZnB), boron phosphate (BPO_4), borosilicate (BSi) and lanthanum borate (LaB) on thermal degradation characteristics of polyamide 6 and polypropylene involving nitrogen or phosphorus containing flame retardants such as melamine (Me), melamine cyanurate (MC), aluminum diethylphosphinate (AlPi, OP1230) (with or without organically modified clay) or ammonium polyphosphate (APP)/pentaerythritol (PER) (with or without organically modified clay) are investigated by direct pyrolysis mass spectrometry (DP-MS) technique.

3.1. The Effects of Boron Compounds on Thermal Degradation Characteristics of PA6 Composites

In order to investigate the effects of boron compounds on thermal degradation characteristics of PA6 composites, thermal degradation behaviors of each component of the composites and pristine composites have to be known. Thus, DP-MS analyses of PA6, Me, MC and AlPi; PA6 involving 20% melamine, PA6 involving 15% melamine cyanurate, PA6 involving 15% aluminum diethylphosphinate (AlPi, OP1230) and PA6 involving 14% aluminum diethylphosphinate and 1% Cloisite 30B are performed and discussed for comparison.

3.1.1. PA6

In literature, many detailed investigations on thermal degradation of polyamide 6 can be found. It has been determined, also in our study, that the main thermal degradation product of PA6 is caprolactam [**5**, **30**]. The total ion current (TIC) curve, the variation of total ion yield as a function of temperature, indicates a single step thermal degradation mechanism for PA6 (Figure 3-1). The mass spectrum recorded at 465°C, at the maximum of the peak, present in the TIC curve, is also given in the figure. Intense peaks are due to the monomer (M, m/z=113 Da) and the protonated monomer (MH, m/z=114 Da) ions and the products with m/z values 96, 84, 69, 55, 45, 44, 30 and 18 Da, can be formed by dissociative ionization of the monomer and oligomers. The related assignments made are summarized in Table 3-1.

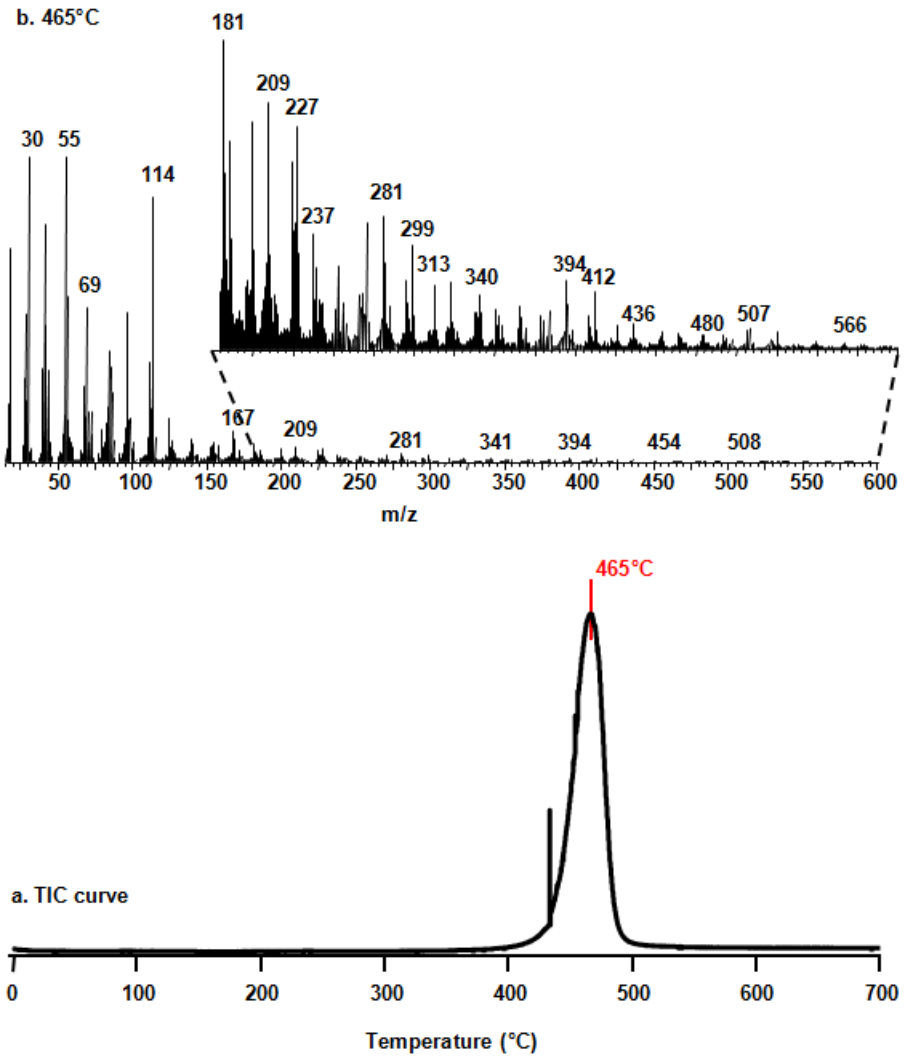

Figure 3-1 a) The TIC curve and b) the pyrolysis mass spectrum at 465°C of PA6

Table 3-1 Relative intensities, RI, of characteristic and/or intense peaks recorded in pyrolysis spectrum of PA6 at 465°C

m/z (Da)	RI	Assignment
18	703.6	H_2O
30	968.8	NH_2CH_2
44	304.7	$CONH_2$, $NH_2C_2H_4$ and/or CO_2
45	65.7	COOH
55	1000.0	C_4H_7
69	496.7	$(CH_2)_3C_2H_3$
84	362.4	$CO(CH_2)_4$
96	479.1	$(CH_2)_5CN$
111	335.1	$(CH_2)_5C{=}NHCH_2$
113	283.3	M
114	872.7	MH
130	13.0	$HN(CH_2)_5COOH$
139	78.6	MCN
167	97.0	$MC{=}NCH_2CH_2$
194	3.8	$C4H_8NC(NCO(CH_2)_5)$
221	4.0	$C_5H_9NC(NCO(CH_2)_5)CH_2$
298	3.4	$NCNH(CH_2)MC(OH)(NH_2)NHCH_2$
566	1.1	M_5H
591	0.5	M_5CN
620	0.7	$M_5H(CH_2)_5C{=}NCH_2CH_2$

Peaks due to protonated monomer and oligomers, M_xH (m/z= 114, 227, 340, 453 and 566 Da for x=1 to 5) are noticeably intense. Peaks due to M_xOH (m/z= 130, 243, 356, 469 and 582 Da for x=1 to 5), M_xCN (m/z= 139, 252, 365, 478 and 591 Da for x=1 to 5), M_xCONH_2 (m/z= 157, 270, 383, 496 and 609 Da for x=1 to 5), $M_xC{=}NCH_2CH_2$ (m/z= 167, 280, 393, 506 and 619 Da for x=1 to 5) and $M_xHC{=}NCH_2CH_2$ (m/z= 168, 281, 394, 507, 620 and 732 Da for x=1 to 6) are also detected, but their intensities are very weak.

Single ion evolution profiles of almost all products are identical; pointing out that the thermal degradation of the polymer follows energetically almost similar reaction pathways (Figure 3-2).

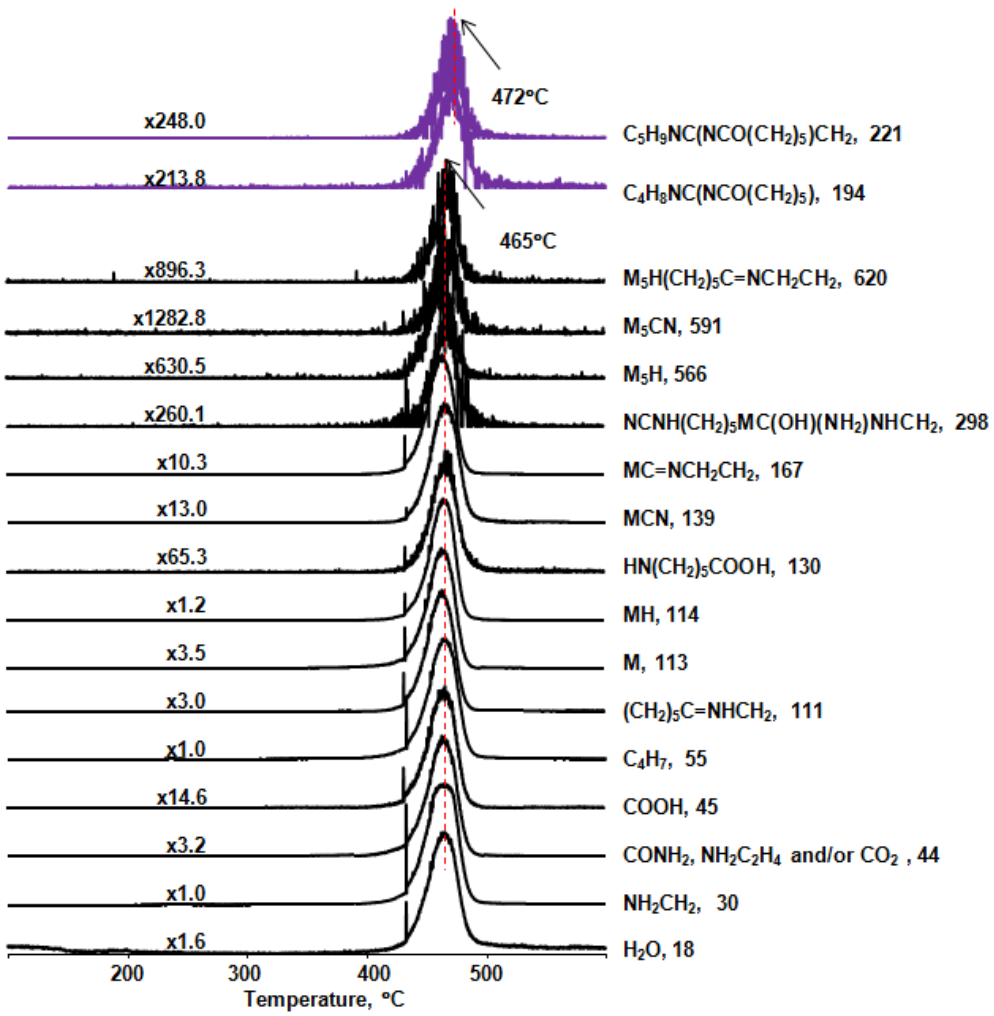

Figure 3-2 Single ion evolution profiles of some selected fragments recorded during pyrolysis of PA6

Caprolactam and cyclic oligomers are generated via various reaction pathways as indicated in Section 1.3.1 and review [**30**]. Evolution of NH_3, H_2O and CO_2 are also detected.

Throughout the pyrolysis and/or dissociative ionization processes, H-transfer to —NH group or McLafferty type rearrangement reactions may cause formation of protonated monomer and oligomers (Scheme 3-1) [**20**].

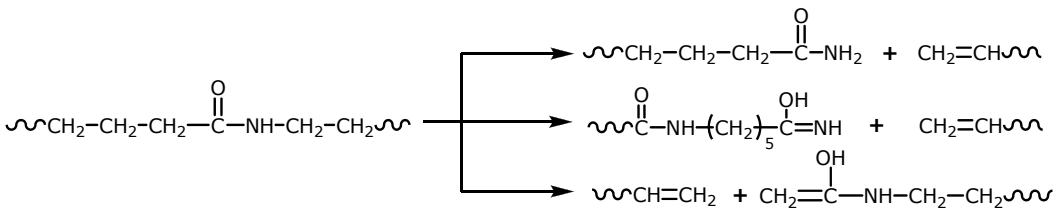

Scheme 3-1 Generation of protonated oligomers

By the elimination of H_2O from these products, as shown in Scheme 3-1, products with C=N linkage and —CN end groups can be formed (Scheme 3-2) [**20**].

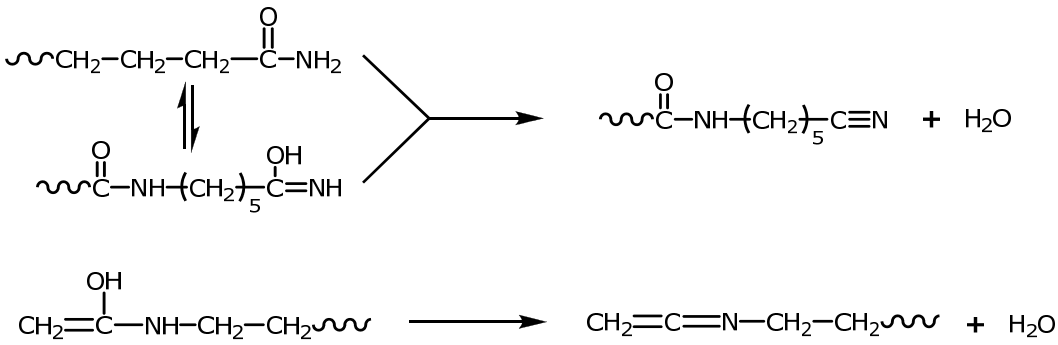

Scheme 3-2 Formation of products with C=N linkage and —CN end groups

There are several pathways by which elimination of H_2O may take place. For instance, as mentioned in Section 1.3.1, during the thermal degradation of PA6, intermolecular aminolysis reactions, condensation of carboxylic chain ends, in which CO_2 is also generated, dehydration of chains with primary amide end groups and reactions between caprolactam and acid end groups generate H_2O [**30**]. Moreover, another possible pathway for the elimination of H_2O may be due to interactions of carbonyl groups with ammonia. H_2O and cyanide end groups may be eliminated through H-transfer reactions; therefore

derivatives of imines may be generated (Scheme 3-3) [**20**]. This reaction pathway is supported by the detection of products, such as $NCNH(CH_2)_5MC(OH)(NH_2)NHCH_2$ (m/z= 298 Da) and $(CH_2)_5NHCN$ (m/z= 111 Da).

When carbonyl group of a chain reacts with the amine group of another chain, instead of NH_3 (intermolecular interactions), at high temperatures a crosslinked structure is formed (Scheme 3-4) [**20**]. The chains with crosslinked structure have higher thermal stability. Detection of $C_5H_9N=C(NCO(CH_2)_5)CH_2$ (m/z= 221 Da) and $C_3H_6N=C(NCO(CH_2)_5)CH_2$ (m/z= 194 Da) supports the occurrence of these intermolecular reactions. These two proposed mechanisms are thought to occur under high temperatures; otherwise such nucleophilic reactions need acidic catalyst to take place.

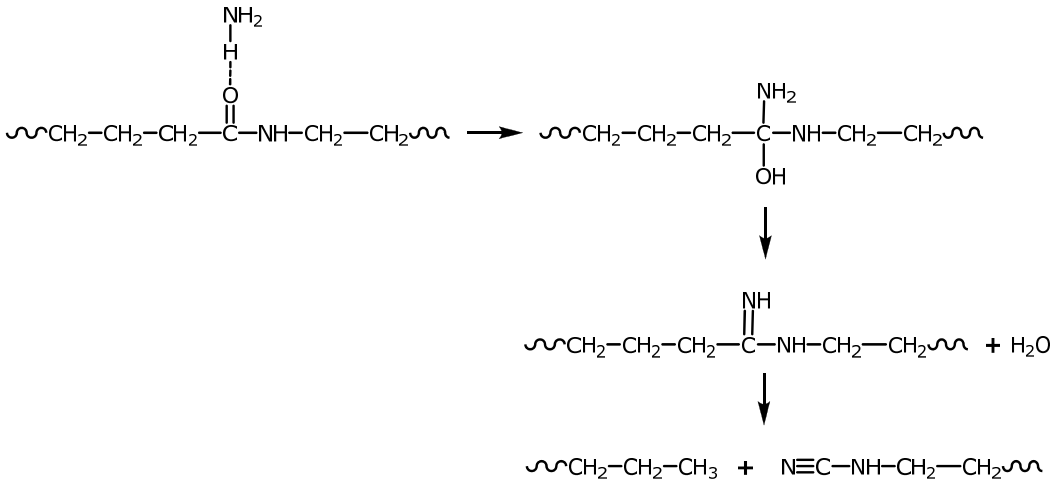

Scheme 3-3 Reaction of carbonyl group with NH_3

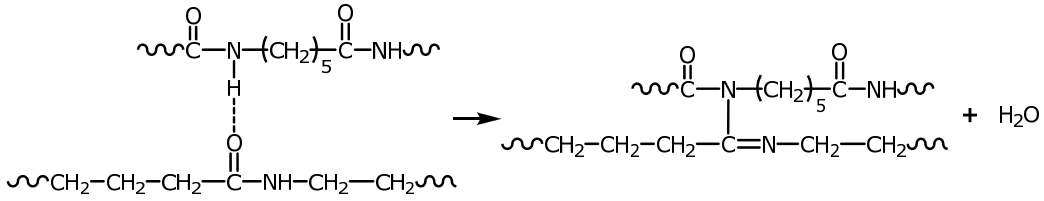

Scheme 3-4 Intermolecular reaction between amine group and carbonyl group of two different chains

In this study, evolution of OH fragment with high yield via during pyrolysis or dissociative ionization of H_2O makes differentiation of NH_3 (17 Da), impossible. The lack of observable NH_3 generation may also be due to the reactions between NH_3 and carbonyl group of PA6 [**20**].

3.1.2. Melamine (Me)

Melamine (Me) is analyzed by direct pyrolysis mass spectrometry (Py-MS) alone, in order to elucidate the effect of Me on thermal degradation mechanism of PA6. The TIC curve shows a single peak (Figure 3-3). Mass spectrum recorded at 212°C at the maximum of the peak, which is present in the TIC curve, is also given in the figure. The mass spectrum of Me obtained is almost identical to the mass spectrum of Me given in the MS-NIST library. This result supports the fact that Me undergoes sublimation instead of degradation [**20**].

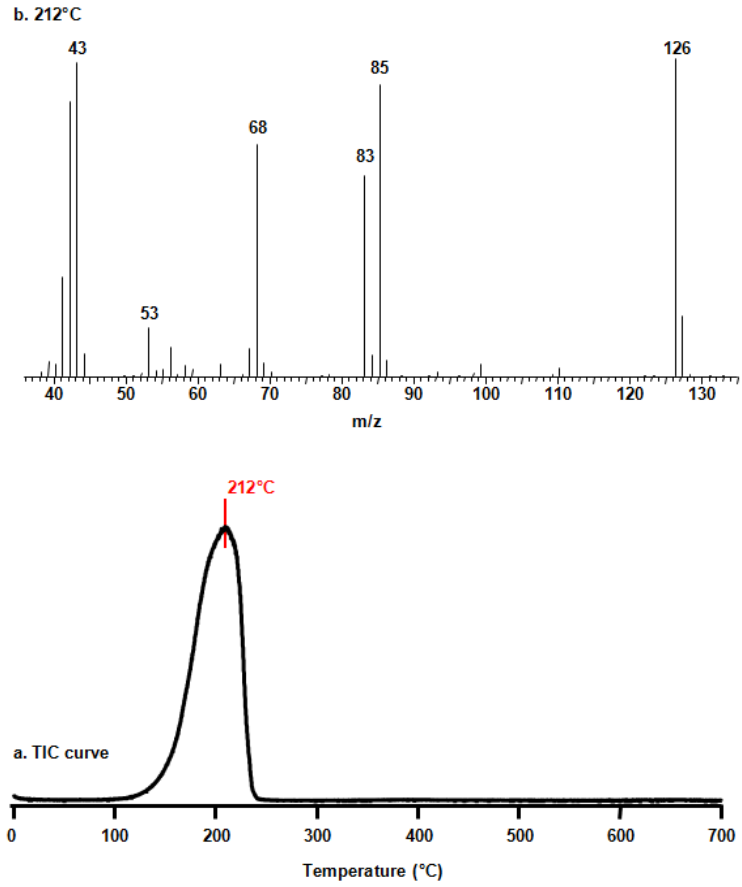

Figure 3-3 a) The TIC curve and b) the pyrolysis mass spectrum at 212°C of Me

Base peak in the pyrolysis mass spectrum of Me at 212°C is the molecular ion peak (m/z= 126 Da). Other dominant peaks, whose assignments are shown in Table 3-2, are at m/z= 85, 68, 43 and 42 Da [**20**].

Table 3-2 Relative intensities, RI, of characteristic and/or intense peaks recorded in pyrolysis spectrum of Me at 212°C

m/z (Da)	RI	Assignment
42	859.0	N_2CH_2
43	981.3	N_2CH_3
68	708.6	$N_3C_2H_2$
85	912.1	$N_4C_2H_5$
126	1000.0	$N_6C_3H_6$

Single ion evolution profiles of all products show identical trends, pointing out that sublimation of Me starts at about 150°C (Figure 3-4) [**20**].

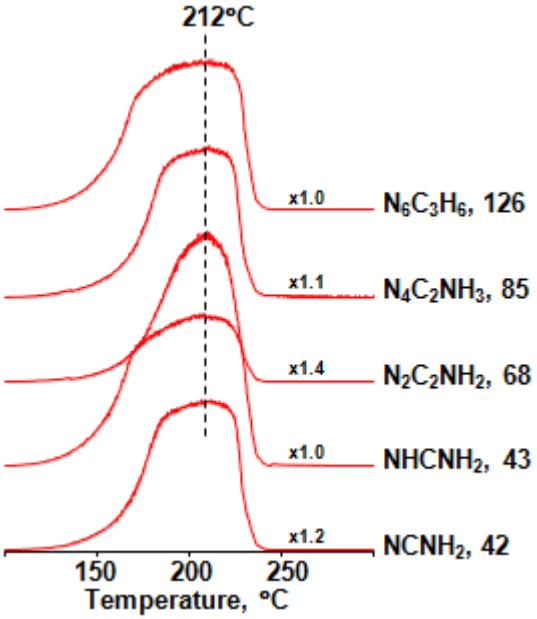

Figure 3-4 Single ion evolution profiles of some selected fragments recorded during pyrolysis of Me

3.1.3. Melamine Cyanurate (MC)

Melamine cyanurate (MC) is analyzed by direct pyrolysis mass spectrometry (DP-MS) alone, in order to determine the effect of MC on thermal degradation mechanism of PA6. The TIC curve shows a single peak (Figure 3-5). Mass spectrum recorded at 261°C at the

maximum of the peak present in the TIC curve, is also given in the figure. The distinctive mass spectrum of MC is the combination of mass spectra of Me and cyanuric acid [**20**].

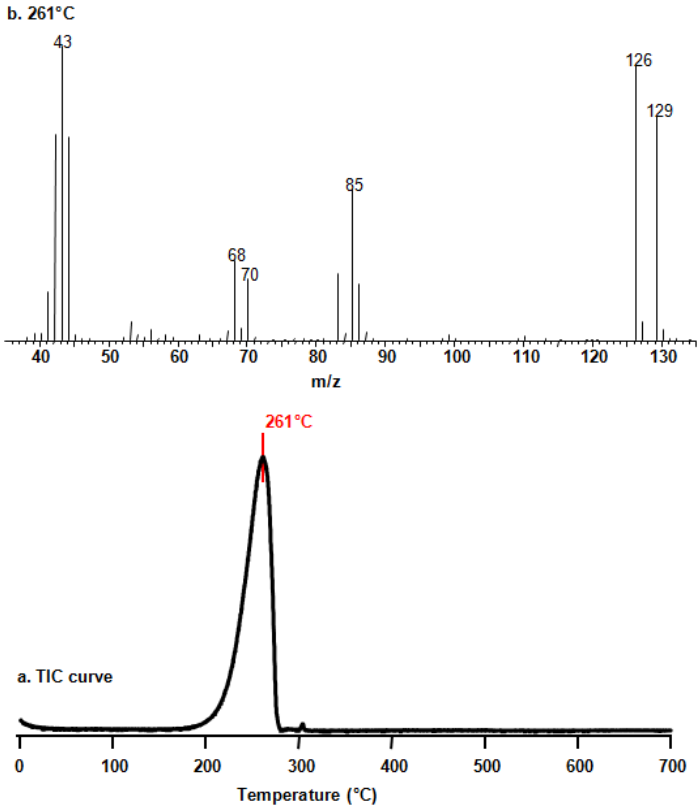

Figure 3-5 a) The TIC curve and b) the pyrolysis mass spectrum at 261°C of MC

Peaks, relative intensities of characteristic and/or intense peaks and the assignments made are summarized in Table 3-3.

Table 3-3 Relative intensities, RI, of characteristic and/or intense peaks recorded in pyrolysis spectrum of MC at 261°C

m/z (Da)	RI	Assignment
42	688.8	N_2CH_2, NCO
43	1000.0	N_2CH_3, NCOH
44	708.6	N_2CH_4, $CONH_2$
68	263.2	$N_3C_2H_2$
70	194.5	NC_2O_2
85	522.9	$N_4C_2H_5$
86	196.9	$N_2C_2O_2H_2$
126	915.1	$N_6C_3H_6$
129	751.7	$N_3C_3O_3H_3$

Single ion evolution profiles of all characteristic fragments are similar, indicating sublimation of Me and cyanuric acid before degradation (Figure 3-6) [**20**].

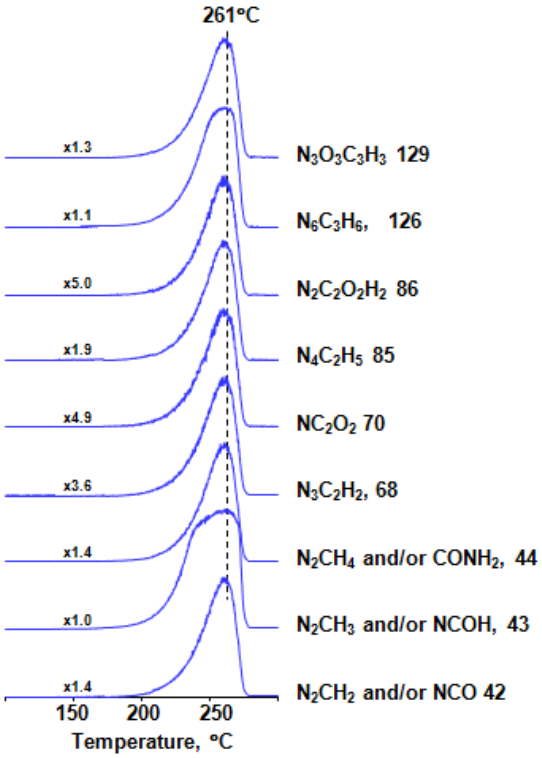

Figure 3-6 Single ion evolution profiles of some selected fragments recorded during pyrolysis of MC

3.1.4. Aluminum Diethylphosphinate (AlPi, OP1230)

Pure aluminum diethylphosphinate (AlPi, OP1230) is also analyzed by direct pyrolysis mass spectrometry (DP-MS), in order to differentiate the effect of AlPi on thermal degradation mechanism of PA6.

As mentioned in Section 1.2.2.2, phosphorus shows its functionality in gaseous or condensed phases. In gaseous phase, phosphorus inhibits the flame via radical trapping; in condensed phase, phosphorus promotes carbon char formation. Flame retardant used, chemical structure of the polymer and interaction with other additives determine the activity of phosphorus. In spite of the fact that vaporization of AlPi takes place, Lewis acid-base interaction is possible between α-carbon at the amide group (strong Lewis acid) and phosphinate (weak Lewis base) [**17**].

The TIC curve shows two peaks (Figure 3-7). The mass spectra recorded at 391°C and 423°C, at the maximum of the peaks present in the TIC curve are also presented in the figure.

Peaks due to fragments with Al—O—P linkages, are observed in the temperature range of 360°C to 460°C. Most of the aluminum phosphate and phosphinate compounds are known to be primarily four coordinate and dimeric [**57**, **58**]. Depending on the literature findings; assignments for the characteristic and/or intense peaks are summarized in Table 3-4. In addition, the relative intensities of these fragments are also given in the table [**59**].

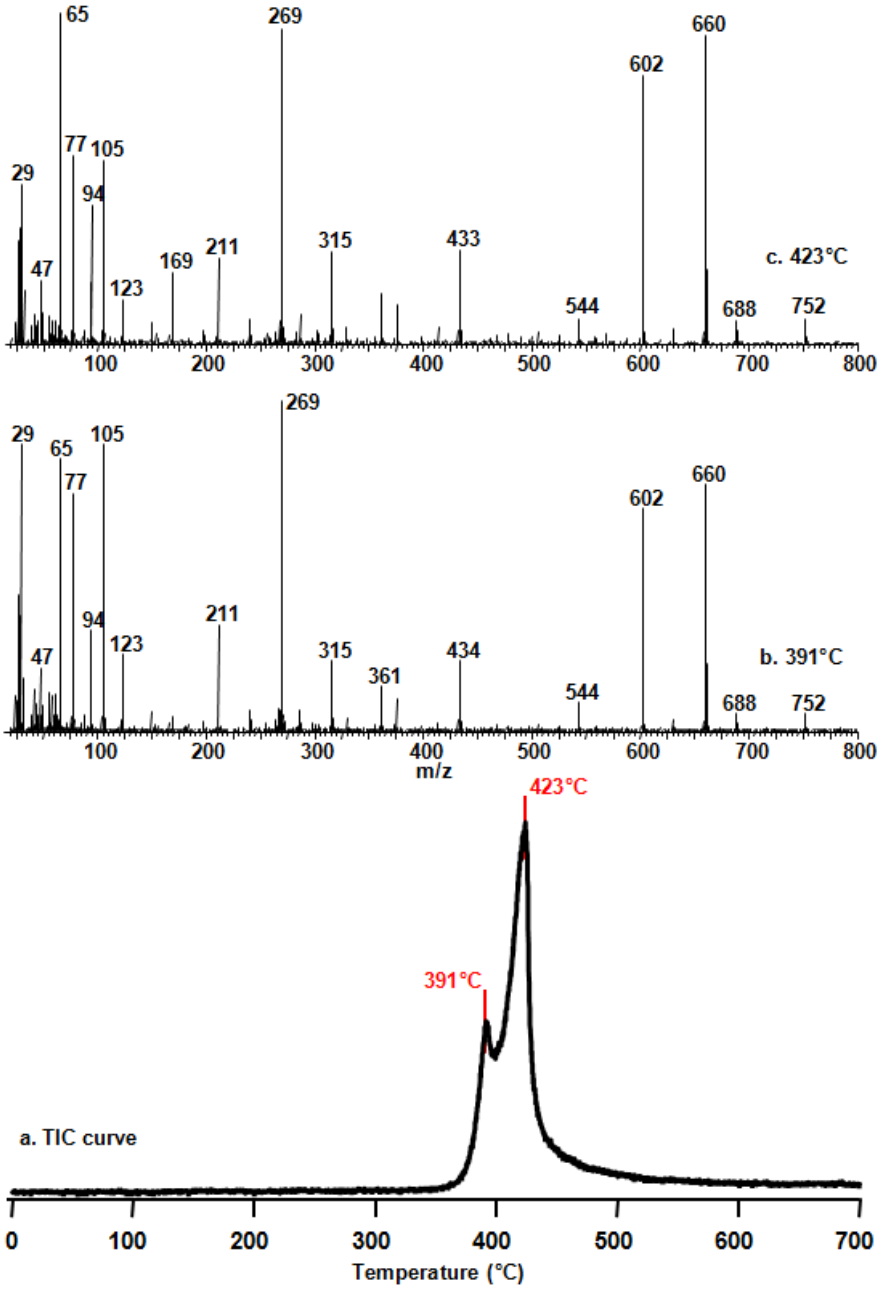

Figure 3-7 a) The TIC curve and the pyrolysis mass spectra at b) 391°C and c) 423°C of AlPi

Table 3-4 Relative intensities, RI, of characteristic and/or intense peaks recorded in the pyrolysis mass spectra of AlPi at 391°C and 423°C

m/z (Da)	RI		Assignment
	391°C	423°C	
29	762.8	490.4	AlH_2
47	199.5	182.8	PO
65	832.9	953.4	P_2H_3, HPO_2H
77	514.2	535.8	C_2H_5POH
94	286.3	393.6	$C_2H_5P(OH)_2$
105	790.2	617.8	$(C_2H_5)_2PO$
122	36.7	38.9	$(C_2H_5)_2PO_2H$
123	234.1	121.4	$(C_2H_5)_2P(OH)_2$
169	46.7	200.8	$(C_2H_5)_2PO_2PHO$
211	321.2	260.7	$((C_2H_5)_2PO)_2H$
269	1000.0	961.8	$(C_2H_5)_2PO_2AlO_2P(C_2H_5)_2$
315	179.7	231.6	$(C_2H_3)_2AlO_2(PO(C_2H_3)_2)_2$
361	119.6	124.7	$((C_2H_3)(H_2PO_2))AlO_2(PO(C_2H_5)_2)_2$
433	-	253.1	$(C_2H_5)_3(HPO)Al_2(O_2)_2(HP(C_2H_5)_2)_2$
434	180.1	-	$(C_2H_5)_3(H_2PO)Al_2(O_2)_2(HP(C_2H_5)_2)_2$
544	64.9	-	$(C_2H_5)_2(H_2PO)(PO(C_2H_5)_2)O_2H_2Al_2(O_2)_2(P(C_2H_5)_2)_2$
602	655.2	827.7	$H_2[(OP(C_2H_5))_2OPHOH](C_2H_5)[Al(C_2H_5)O_2P(C_2H_5)_2]_2$
660	724.2	1000.0	$(C_2H_5)(OP)AlO_2(P(C_2H_5)_2)_2O_2Al[(P(C_2H_5))_2O_2(P(C_2H_5))_2O]$
688	67.8	67.3	$(OPH)(C_2H_4)_2AlO_2(P(C_2H_5)_2)_2O_2Al[(P(C_2H_5))_2O_2(P(C_2H_5))_2O]$
752	51.7	67.5	$[(P(C_2H_5)O)_3AlO_2P(C_2H_5)_2]_2$

The possible structures of high mass fragments with Al—O—P linkages, predicted depending on literature findings [**59**], are shown in Figure 3-8.

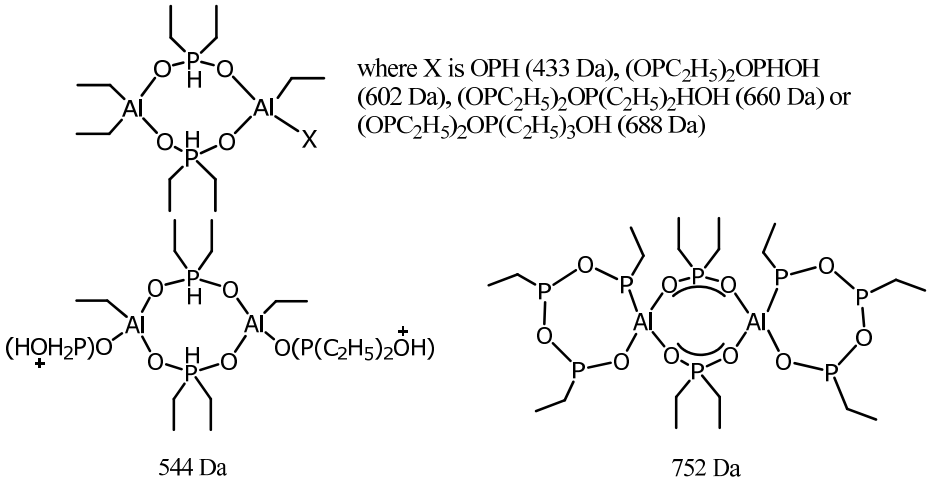

Figure 3-8 Possible structures of high mass fragments involving Al—O—P linkages

Single ion evolution profiles of almost all characteristic fragments present slight differences (Figure 3-9).

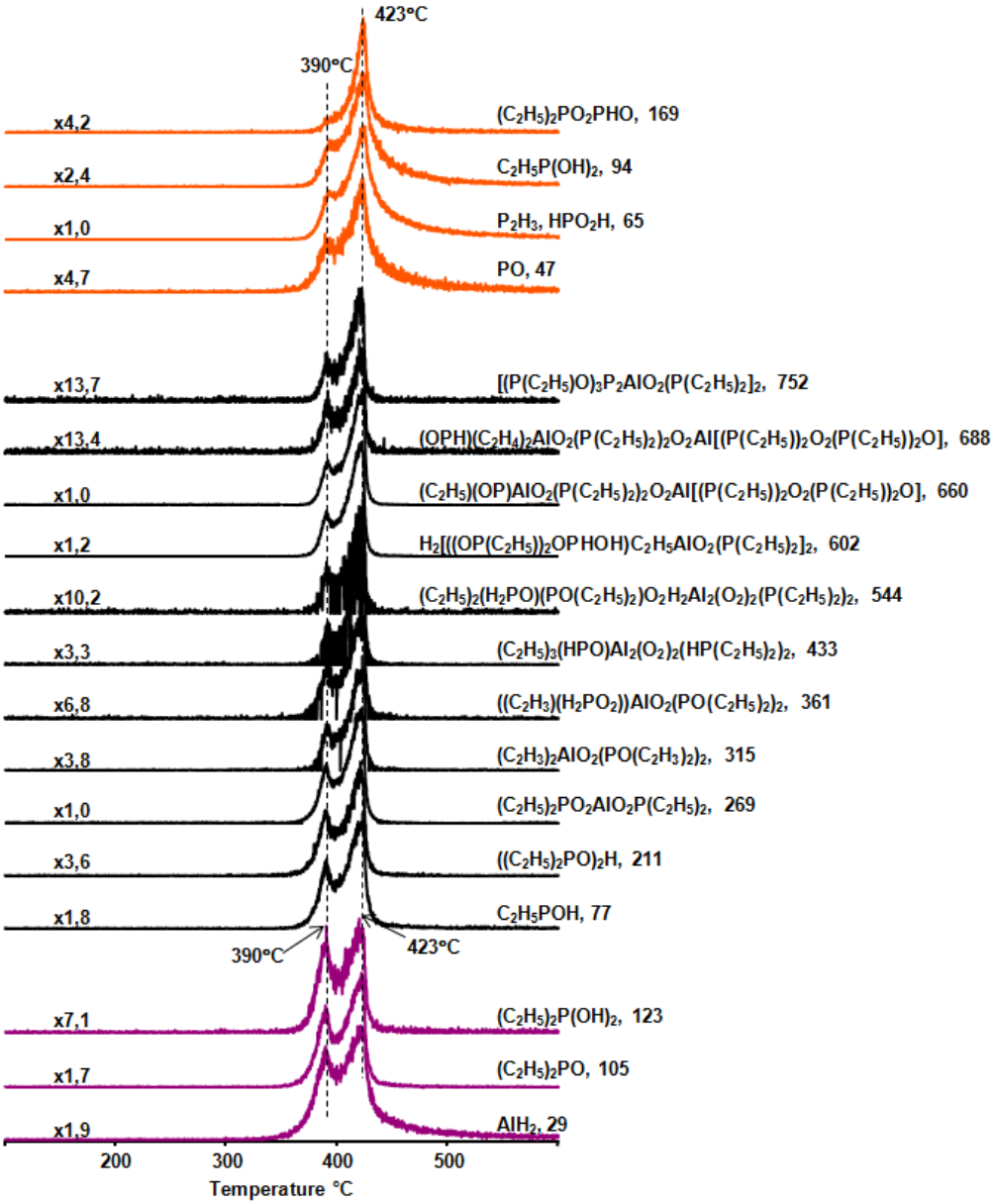

Figure 3-9 Single ion evolution profiles of some selected fragments recorded during the pyrolysis of AlPi

3.1.5. Cloisite 30B

The mass spectrum of Cloisite 30B recorded at 365.1°C is presented in Figure 3-10. The spectrum is dominated by peaks due to fragments such as CH_3NCH_2 (43 Da), $CH_3NHC_2H_4$ (58 Da), $CH_3NCH_2(C_2H_4)$ and/or C_5H_{11}(71 Da), $CH_3N(C_2H_3)_2$ and/or C_6H_{11} (83 Da), and $CH_3N(C_2H_3)_2CH_2$ and/or C_7H_{13} (97 Da). The high mass intense peaks at 269 Da and 297 Da are tentatively assigned to $C_{20}H_{29}$ and $C_{22}H_{33}$ respectively that may be stabilized by cyclic and/or resonance structures.

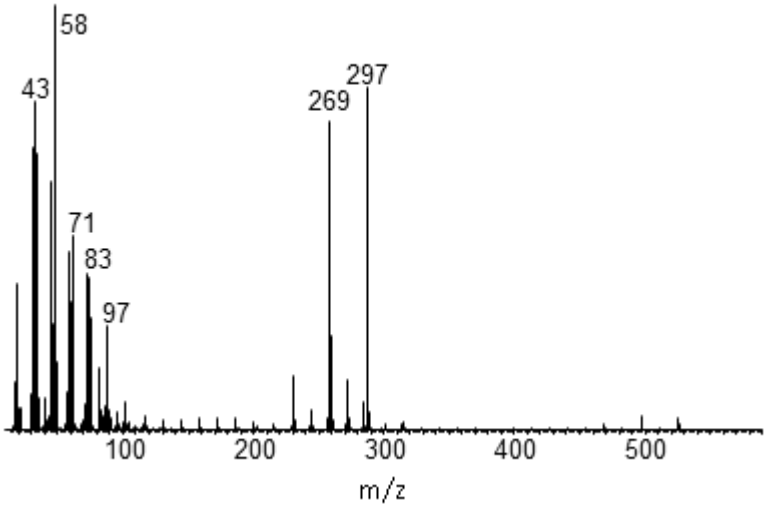

Figure 3-10 The pyrolysis mass spectrum of Cloisite 30B at 365.1°C

3.1.6. Polyamide 6/Melamine (PA6/Me)

The effect of melamine (Me) on LOI and vertical burning ratings (UL-94) of PA6 were studied by Doğan et al. Increase in LOI value from 22.5 to 31 and enhancement of vertical burning ratings from V2 to V0 were observed by addition of 20% of Me into PA6 [**38**]. Yet, improvement in thermal stability or char yield was not observed.

A broad weak peak at around 238°C and a strong peak with a maximum at around 465°C are detected in the TIC curve recorded during the direct pyrolysis mass spectrometry (DP-MS) analysis of PA6/Me (Figure 3-11). Mass spectra recorded at around 238°C and 465°C are also given in the figure. Changes in the relative intensities of diagnostic peaks of Me are determined in the pyrolysis mass spectrum recorded at around 238°C. The changes in the relative intensities indicate that some interactions between PA6 and Me are present. Characteristic peaks of PA6 are observed in the pyrolysis mass spectrum recorded at around 465°C [**20**].

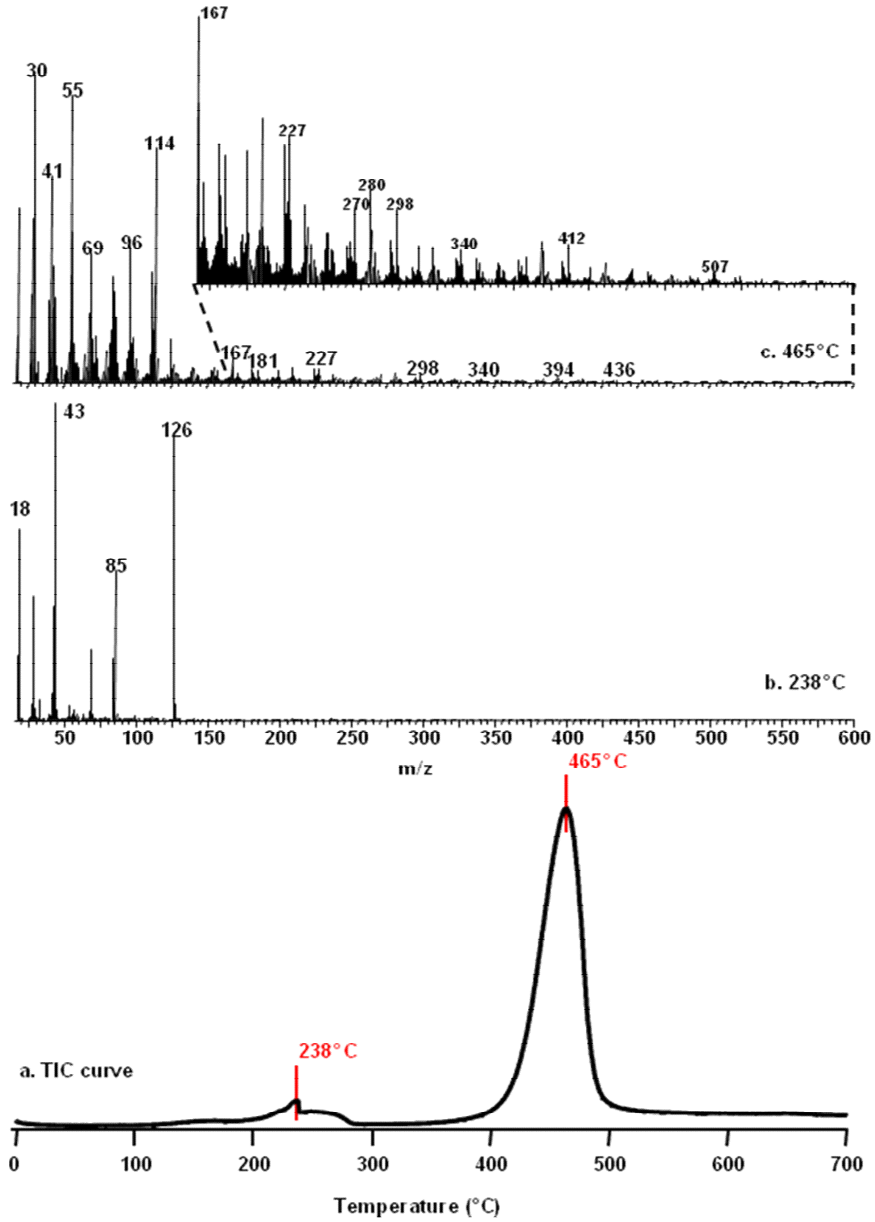

Figure 3-11 a) The TIC curve and the pyrolysis mass spectrum at b) 238°C and c) 465°C of PA6/Me

Mass spectral data and the assignments made for the characteristic and/or intense products are summarized in Table 3-5.

Table 3-5 Relative intensities, RI, of characteristic and/or intense peaks recorded in pyrolysis spectrum of PA6/Me at 238°C and 465°C

m/z (Da)	RI		Assignment
	238°C	465°C	
18	600.6	545.6	H_2O
30	9.6	1000.0	NH_2CH_2
42	355.2	368.4	N_2CH_2, C_3H_6, CH_2CO
43	1000.0	243.3	N_2CH_3, CONH, CH_2CHO
44	30.8	275.6	$CONH_2$, $NH_2C_2H_4$, CO_2
45	1.6	50.4	COOH
55	17.3	915.6	C_4H_7
85	468.6	284.6	$N_4C_2H_5$, C_3H_6CONH
111	1.0	353.9	$(CH_2)_5NHCN$
113	1.8	301.9	M
114	3.8	744.1	MH
126	896.6	54.7	$N_6C_3H_6$
130	4.8	12.5	$HN(CH_2)_5COOH$
139	0.5	46.3	MCN
167	0.2	79.9	$MC=NCH_2CH_2$
194	0.2	4.9	$C_4H_8NC(NCOC_5H_{10})$, $C_3H_7N=C(N_6C_3H_5)$
221	-	5.2	$C_5H_9NC(NCOC_5H_{10})CH_2$, $C_5H_{10}N=C(N_6C_3H_5)$
249	0.1	3.6	$COC_5H_9NC(NCOC_5H_{10})CH_2$, $COC_5H_{10}N=C(N_6C_3H_5)$
298	-	20.2	$NCNH(CH_2)_5MC(OH)(NH_2)NHCH_2$
566	-	1.4	M_5H
591	-	0.6	M_5CN
620	-	0.9	$M_5H(CH_2)_5C=NCH_2CH_2$

Single ion evolution profiles of most of the characteristic fragments observed during the pyrolysis of PA6/Me are similar to those of fragments formed during the pyrolysis of neat PA6 (Figure 3-12). According to the pyrolysis mass spectra, evolution of diagnostic thermal degradation products starts above 400°C and reaches to maximum yield at around 463°C. Evolution profiles of the products formed by aminolysis and dehydration reactions exhibit slight differences [**20**].

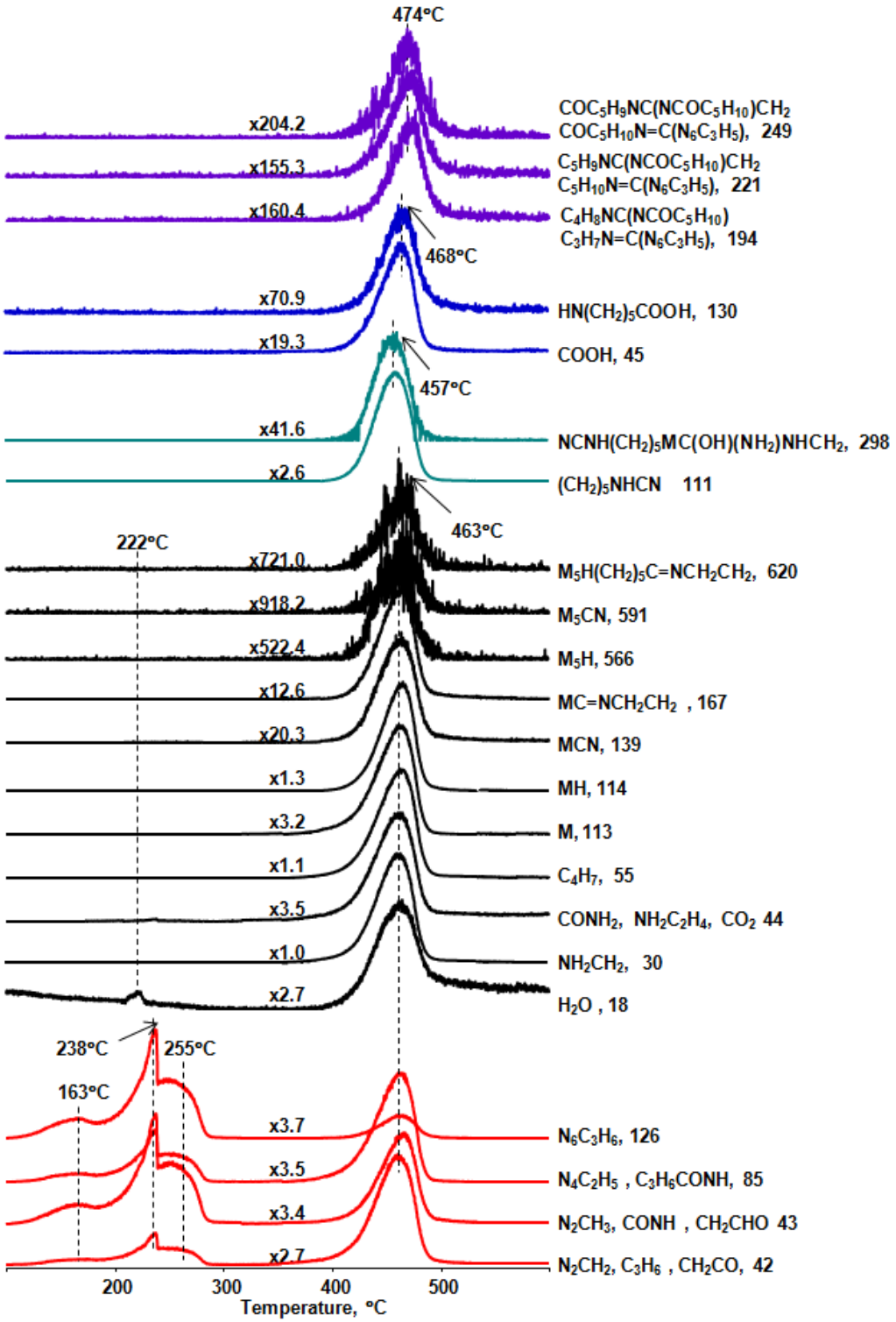

Figure 3-12 Single ion evolution profiles of some selected fragments recorded during pyrolysis of PA6/Me

Evaluation of Me based single ion pyrograms indicates that the evolution of Me begins slightly above 100°C and goes on over a broad temperature range indicating noticeable differences (Figure 3-12). As it is seen in the figure, there are overlapping peaks in the evolution profiles of Me based fragments. This overlapping may be considered as a direct evidence for several types of interactions between Me and PA6. The trends in the evolution profiles in the temperature range of 200-300°C may be associated with the degree of H-bonding, the number of amine groups of Me interacted with PA6 chains via H-bonding. Moreover, characteristic products of Me are detected at around 465°C, the temperature region at which degradation of neat PA6 takes place. Observation of these characteristic products in this temperature range indicates the presence of a strong interaction between Me and PA6. Contribution of decomposition products of PA6, with the same m/z value, may be the cause of high temperature peaks. As a matter of fact, these contributions may be crucial particularly for low mass products with m/z values of 42, 43, 68 and 85 Da. Nevertheless, the high temperature evolution of Me is quite clear, as the product with m/z 126 Da is not present in the pyrolysis mass spectra of PA6 [**20**]. Doğan et al. detected the evolution of Me during the analysis of PA6 containing 20% Me via TGA-FTIR [**38**]. The evolution of Me at high temperatures can only take place, if there is a chemical interaction between Me and PA6. Amine groups of Me may undergo an interaction with the carbonyl groups of PA6 as presented in Scheme 3-5. Dehydration of resultant products of this reaction yields imine units [**20**].

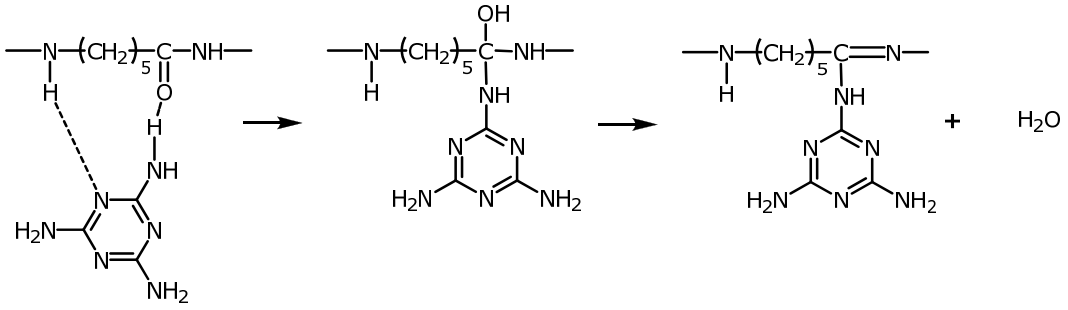

Scheme 3-5 Chemical interaction between amine group of Me and carbonyl group of PA6

It is seen that relative yields of fragments with m/z values 249, 221 and 194 Da are slightly increased with respect to the ones detected during the pyrolysis of pure PA6. Moreover, the temperature difference between the maxima of the evolution profiles of these fragments (m/z= 249, 221, 194 Da) and those of the major degradation products of PA6 is 7°C and 11°C for neat PA6 and PA6 containing Me, respectively. The generation of H_2O at around 222°C, where no other products are detected can be associated with the reactions between amine groups of Me and carbonyl groups of PA6 [**20**].

In the evolution profiles of products containing COOH end groups, a slight shift to higher temperature region is observed. One of the possible reasons may be the temperature rise in

the imine formation. Reactions of PA6 chains with H_2O may also form COOH end groups [**20**].

Conversely, in the evolution profiles of the fragments, for instance $NCNH(CH_2)_5MC(OH)(NH_2)NHCH_2$ (m/z= 298 Da) and $(CH_2)_5NHCN$ (m/z= 111 Da) are proposed to be formed by the reaction between NH_3 and carbonyl groups (Scheme 3-3), a slight shift to low temperatures is detected. A significant increase in the relative yields of these fragments, particularly in that of 298 Da fragment, is observed. It may be inferred that, NH_3 molecules, which are formed at the end of degradation of Me at relatively low temperatures, participate actively in the mentioned reactions. Therefore, increase in the yields of these fragments occurs [**20**].

3.1.6.1. Effect of Addition of Boron Compounds on PA6/Me

Addition of BPO_4

Doğan et al. determined that addition of BPO_4 has an effect on flame retardancy by physical means and diminishes the decomposition temperature of PA6. It was found that all BPO_4 containing samples at all tested compositions (1-5 wt%) have V0 ratings [**38**].

As in case of PA6/Me, the TIC curve of PA6/Me containing 3 wt% BPO_4 shows two peaks (Figure 3-13). A weak peak, which is due to evolution of Me based fragments, and a strong peak, which is associated with thermal degradation of PA6, are seen at around 247°C and 470°C, respectively. Characteristic peaks of thermal degradation products of PA6 are also detected in the presence of BPO_4. But, noticeable differences in the relative intensities of characteristic peaks of both Me and PA6 are detected in the presence of BPO_4 [**60**].

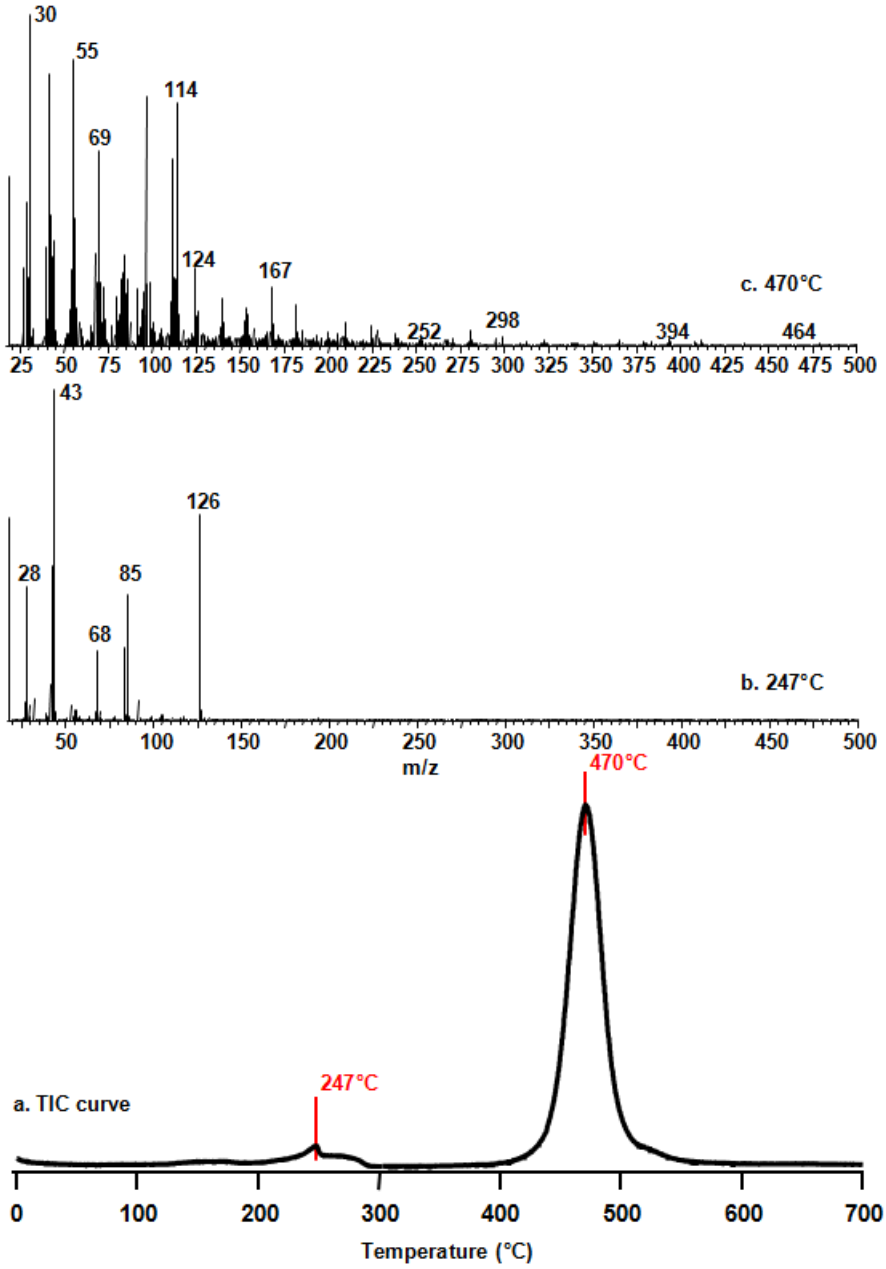

Figure 3-13 a) The TIC curve and the pyrolysis mass spectra at b) 247°C and c) 470°C of PA6/Me involving 3% BPO_4

Assignments made for selected peaks are collected in Table 3-6. In addition, relative intensities of these peaks are given in the table.

Table 3-6 Relative intensities, RI, of characteristic and/or intense peaks recorded in pyrolysis spectrum of PA6/Me involving BPO_4 at 247°C and 470°C

m/z (Da)	RI		Assignment
	247°C	470°C	
18	613.3	505.3	H_2O
30	11.3	1000.0	NH_2CH_2
42	467.3	386.3	N_2CH_2, C_3H_6, CH_2CO
43	1000.0	276.5	N_2CH_3, CONH, CH_2CHO
44	27.8	315.4	$CONH_2$, $NH_2C_2H_4$, CO_2
45	-	45.8	COOH
55	29.6	849.8	C_4H_7
111	0.4	573.5	$(CH_2)_5NHCN$
113	0.3	202.0	M
114	3.5	718.0	MH
126	625.0	96.3	$N_6C_3H_6$
130	1.0	15.3	$HN(CH_2)_5COOH$
139	0.3	142.8	MCN
167	1.2	162.1	$MC{=}NCH_2CH_2$
194	2.5	10.8	$C_4H_8NC(NCOC_5H_{10})$, $C_3H_7N{=}C(N_6C_3H_5)$
221	1.1	9.5	$C_5H_9NC(NCOC_5H_{10})CH_2$, $C_5H_{10}N{=}C(N_6C_3H_5)$
249	0.1	6.3	$COC_5H_9NC(NCOC_5H_{10})CH_2$, $COC_5H_{10}N{=}C(N_6C_3H_5)$
298	0.1	-	$NCNH(CH_2)_5MC(OH)(NH_2)NHCH_2$
566	-	0.9	M_5H
591	0.1	0.9	M_5CN
620	0.1	1.1	$M_5H(CH_2)_5C{=}NCH_2CH_2$

Single ion evolution profiles of characteristic products recorded during the pyrolysis of PA6/Me containing 3% BPO_4 are shown in Figure 3-14. In order to make comparison easily, single ion pyrograms of corresponding products recorded during the pyrolysis of PA6/Me are also placed in the figure. A slight shift to higher temperatures are determined in the overlapping peaks at around 238°C, which are due to the evolution of Me and Me H-bonded to PA6. As mentioned in Section 3.1.6; the structure, which is observed in the evolution profiles of Me and its decomposition fragments in temperature region from 200°C to 300°C, is related to the amount of H-bonding of Me with PA6 [**20**]. Moreover, the evolution of Me in the temperature range at around 470°C, at which degradation of PA6 occurs, is increased noticeably in the presence of BPO_4. The relative yields of fragments with m/z values 249 and 194 Da, which are apparently formed by reactions between Me and carbonyl groups (Scheme 3-5), are also enhanced when compared with PA6/Me. Maximum yields of these fragments are reached at slightly higher temperatures, at around 478°C. These observations indicate stronger interaction between Me and PA6 in the presence of BPO_4 [**60**].

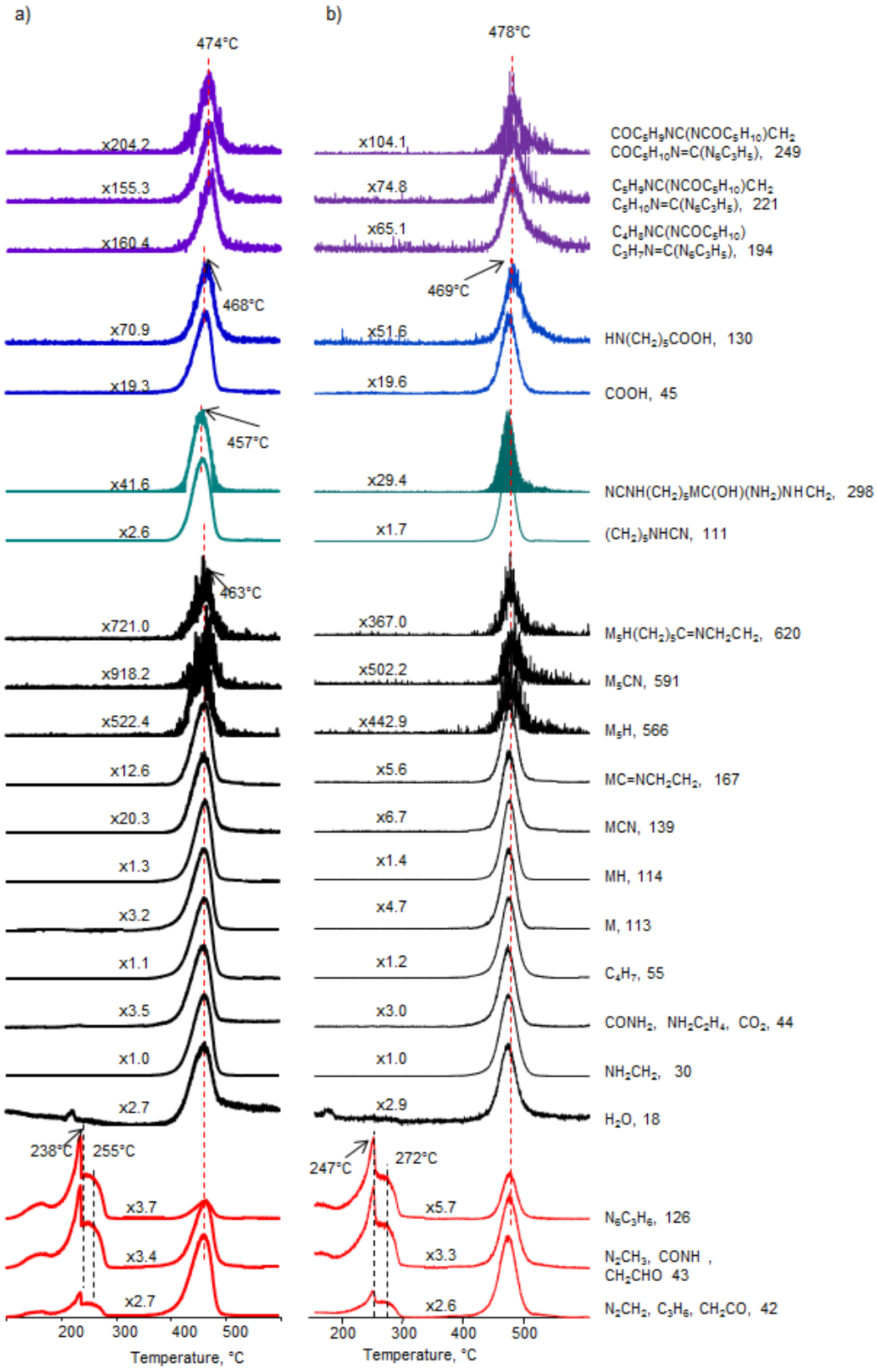

Figure 3-14 Single ion evolution profiles of characteristic and/or intense pyrolysis products of a) PA6/Me and b) PA6/Me involving 3% BPO_4

Relative yields of fragments with m/z values 298 and 111 Da, which may be formed by intermolecular interactions (Scheme 3-4), are observed to be slightly higher compared to PA6/Me. As suggested in Section 3.1.6; NH_3, which is released during the decomposition of Me at relatively low temperatures, also plays a role in the aminolysis reactions increasing the yields of these units at slightly lower temperatures (Scheme 3-3) [**20**]. These fragments show identical evolution profiles with those of almost all other thermal decomposition products of PA6 as in the case of neat PA6, while relative yields of these fragments are increased in the presence of BPO_4 indicating improvement of intermolecular interactions between PA6 chains [**60**].

In fact, as a result of increase in the extent of aminolysis reactions, relative yield of H_2O should also be increased. However, no enhancement in the evolution of H_2O is detected. Increase in the relative yields of products involving COOH end groups, such as fragment with m/z value 130 Da, which may also be formed by hydrolysis of PA6 chains, may be a possible reason [**60**].

Addition of ZnB

Doğan et al. determined that addition of ZnB has an effect on flame retardancy by physical means and diminishes the decomposition temperature of PA6 as in case of BPO_4 addition. It was found that ZnB containing samples up to 3 wt% compositions have V0 ratings [**38**].

Upon addition of ZnB, contrary to the results obtained for PA6/Me involving BPO_4, remarkable decrease in the thermal stability of PA6 chain is detected. The TIC curve and the mass spectra observed at the peak maxima recorded during the pyrolysis of PA6/Me containing ZnB are given in Figure 3-15. The yields of thermal degradation products of PA6 are maximized at around 444°C, indicating about 30°C shift to low temperatures compared to PA6/Me involving no boron compounds; though, the temperature region where the evolution of melamine occurs is almost similar. On the other hand, in the presence of ZnB, about 4 folds decrease in the relative yield of melamine is detected. In contrast, the yields of low mass products, which may be associated with decomposition of melamine such as N_2CH_2, (m/z= 42 Da) and N_2CH_3, (m/z= 43 Da), are increased. These fragments may also be produced during the ionization of melamine in the ion formation room. As the conditions of ionization were kept constant, it can be concluded that the amount of sublimation of melamine is suppressed while that of decomposition of melamine is enhanced in the presence of ZnB [**60**].

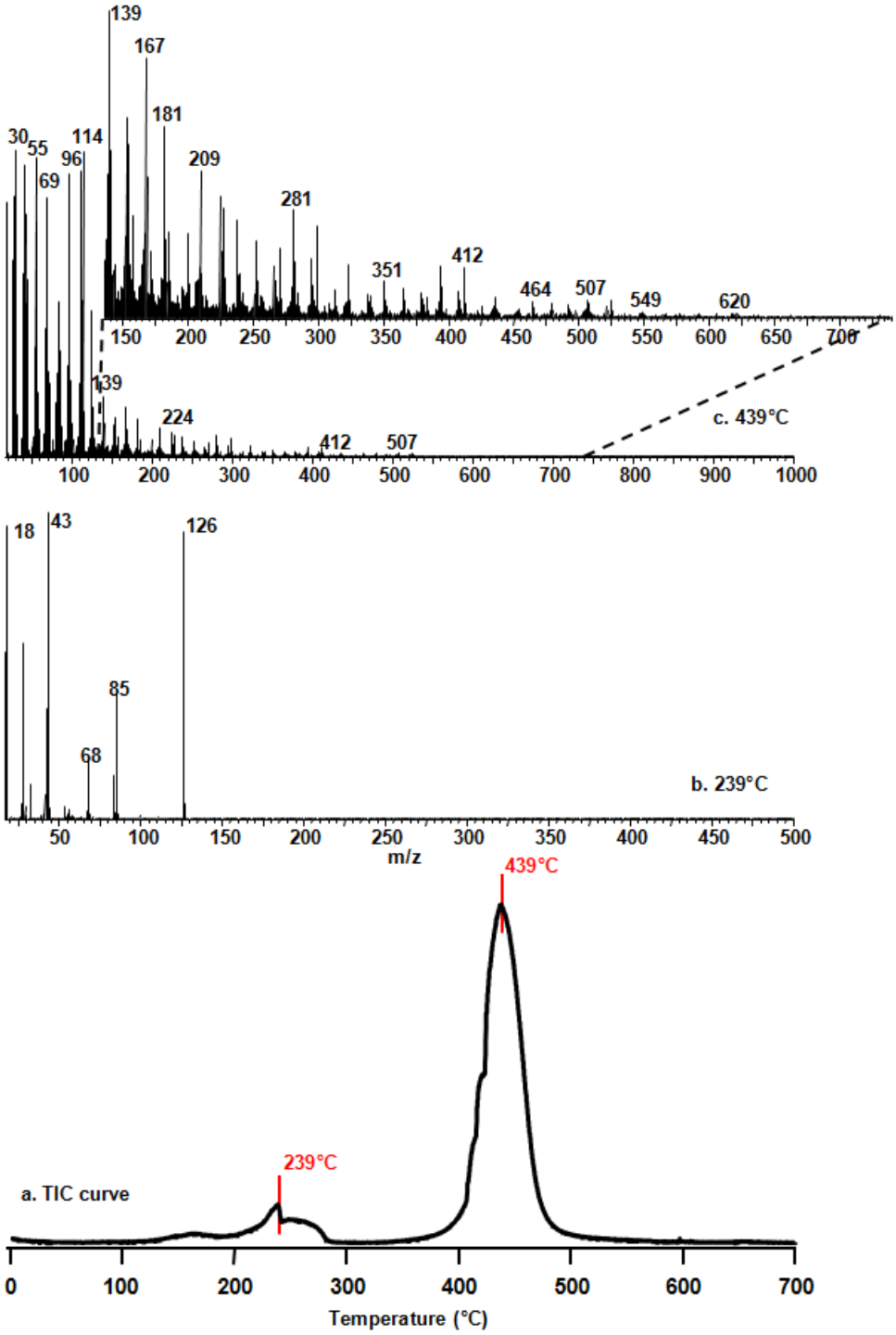

Figure 3-15 a) The TIC curve and the pyrolysis mass spectra at b) 239°C and c) 439°C of PA6/Me involving 3% ZnB

The relative intensities of the peaks and the assignments made for these peaks detected in the mass spectra of PA6 containing 17% Me and 3% ZnB recorded at 239°C and 439°C, are given in Table 3-7.

Table 3-7 Relative intensities, RI, of characteristic and/or intense peaks recorded in pyrolysis spectrum of PA6/Me involving ZnB at 239°C and 439°C

m/z (Da)	RI		Assignment
	239°C	439°C	
18	956.2	828.7	H_2O
30	13.4	1000.0	NH_2CH_2
42	361.2	791.9	N_2CH_2, C_3H_6, CH_2CO
43	1000.0	498.6	N_2CH_3, CONH, CH_2CHO
44	37.9	577.7	$CONH_2$, $NH_2C_2H_4$, CO_2
45	1.9	99.5	COOH
55	15.5	976.0	C_4H_7
111	1.4	930.9	$(CH_2)_5NHCN$
113	2.2	513.2	M
114	4.8	993.2	MH
126	936.8	162.0	$N_6C_3H_6$
130	0.4	18.5	$HN(CH_2)_5COOH$
139	0.2	193.1	MCN
167	0.2	163.3	$MC{=}NCH_2CH_2$
194	0.2	5.6	$C_4H_8NC(NCOC_5H_{10})$, $C_3H_7N{=}C(N_6C_3H_5)$
221	0.2	8.3	$C_5H_9NC(NCOC_5H_{10})CH_2$, $C_5H_{10}N{=}C(N_6C_3H_5)$
249	-	5.8	$COC_5H_9NC(NCOC_5H_{10})CH_2$, $COC_5H_{10}N{=}C(N_6C_3H_5)$
298	-	6.8	$NCNH(CH_2)_5MC(OH)(NH_2)NHCH_2$
566	-	1.2	M_5H
591	-	1.7	M_5CN
620	-	2.2	$M_5H(CH_2)_5C{=}NCH_2CH_2$

Single ion evolution profiles of characteristic fragments of PA6/Me involving 3% ZnB are shown in Figure 3-16. Broadening of the single ion evolution profiles of all PA6 based products is observed. Furthermore, increase in the relative intensities of high mass fragments, being more pronounced for those generated by intermolecular reactions are detected; the relative yields of M_5CN (m/z= 591 Da) and M_5H (m/z= 566 Da) are increased about 2.7 and 1.8 folds, respectively.

Again, increase in the yields of the products, which are related with the reactions of melamine and NH_3 with carbonyl groups of PA6 (Scheme 3-3 and Scheme 3-5), are noted. The yield of fragments, which may also be originated by the reactions of NH_3 such as $NCNH(CH_2)_5MC(OH)(NH_2)NHCH_2$ (m/z= 298 Da) and $(CH_2)_5NHCN$ (m/z= 111 Da), are maximized at slightly lower temperatures, at 436°C as in case of PA6/Me involving no boron compounds. Yet, contrary to expectations, significant reduction in the yield of H_2O is recorded. On the other hand, the yields of products of hydrolysis reactions, such as CO_2 (m/z= 44 Da), COOH (m/z= 45 Da) and $HN(CH_2)_5COOH$ (m/z= 130 Da), are enhanced more in the presence of ZnB, as compared to those that are in the presence of BPO_4, clarifying the decrease in the yield of H_2O [**60**].

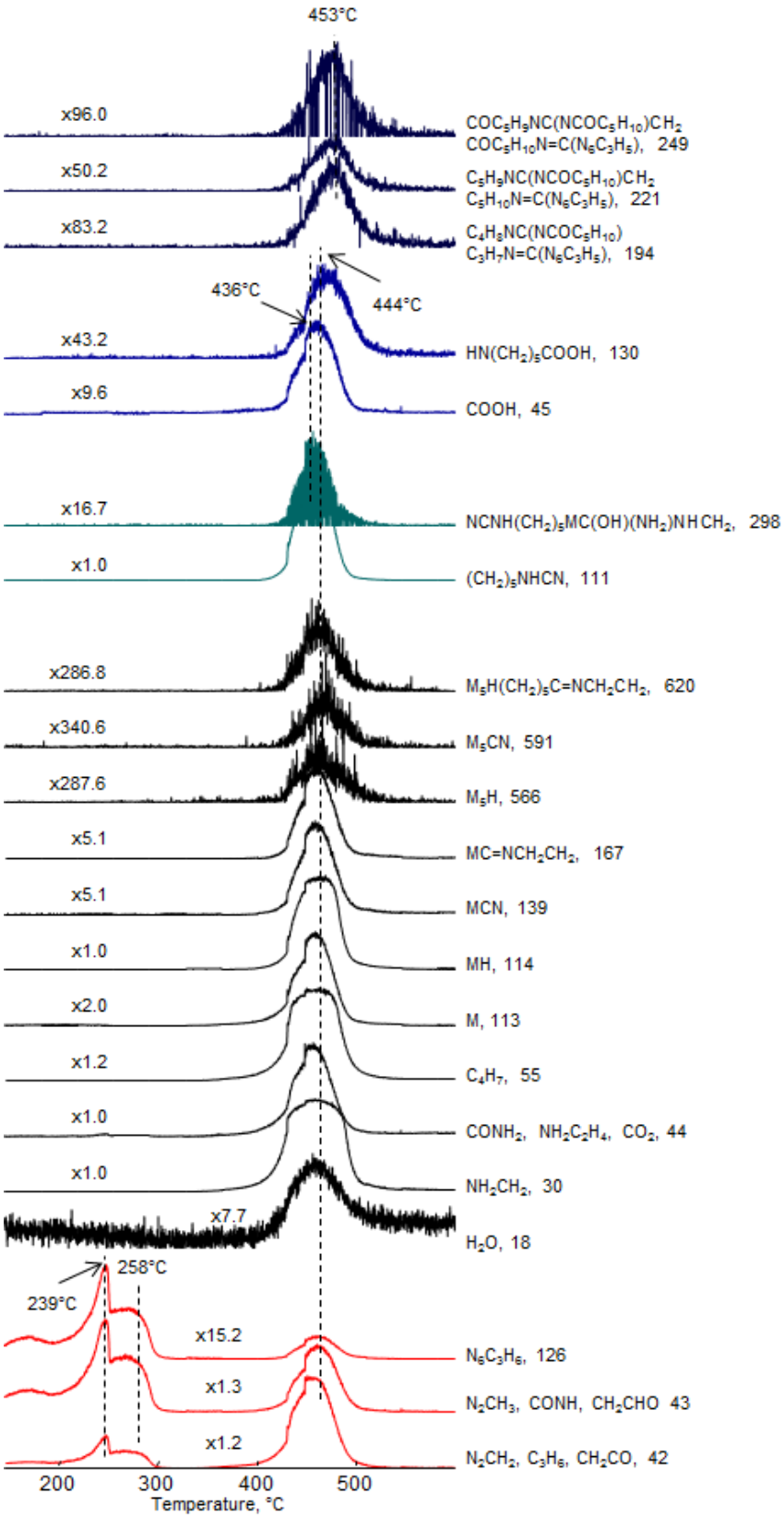

Figure 3-16 Single ion evolution profiles of characteristic and/or intense pyrolysis products of PA6/Me involving 3% ZnB

It has been determined that ZnB forms a glassy surface during combustion which significantly decreases the rate of sublimation and heat-sink action of Me and simultaneously, the LOI values for PA6/Me [**38**]. It may be concluded that this glassy structure, which is formed over the liquid combustion phase inhibiting the sublimation of Me, accelerates degradation of Me, which in turn increases the possibility of reactions between NH_3, Me and PA6, leading to a decrease in its thermal stability [**60**].

Addition of BSi

Doğan et al. determined that addition of BSi affects flame retardancy by physical means and diminishes the decomposition temperature of PA6 as in cases of BPO_4 and ZnB additions. It was found that all BSi containing samples have V2 ratings at all compositions (1-5 wt%) [**38**].

The TIC curve and the mass spectra at the peak maxima, recorded during the pyrolysis of PA6/Me containing 3% BSi, are presented in Figure 3-17. The relative intensity of low temperature peak, related with evolution of Me, again decreased noticeably. Moreover, the high temperature peak, due to degradation of PA6, shifts significantly to a much lower temperature, as compared to the amount of temperature shift observed in the case of ZnB involving sample, which shows peak maximum at 436°C. Another point, which can be noticed contrary to the results obtained for PA6/Me involving BPO_4 and ZnB, is the decrease in the relative yields of high mass degradation products of PA6 [**60**].

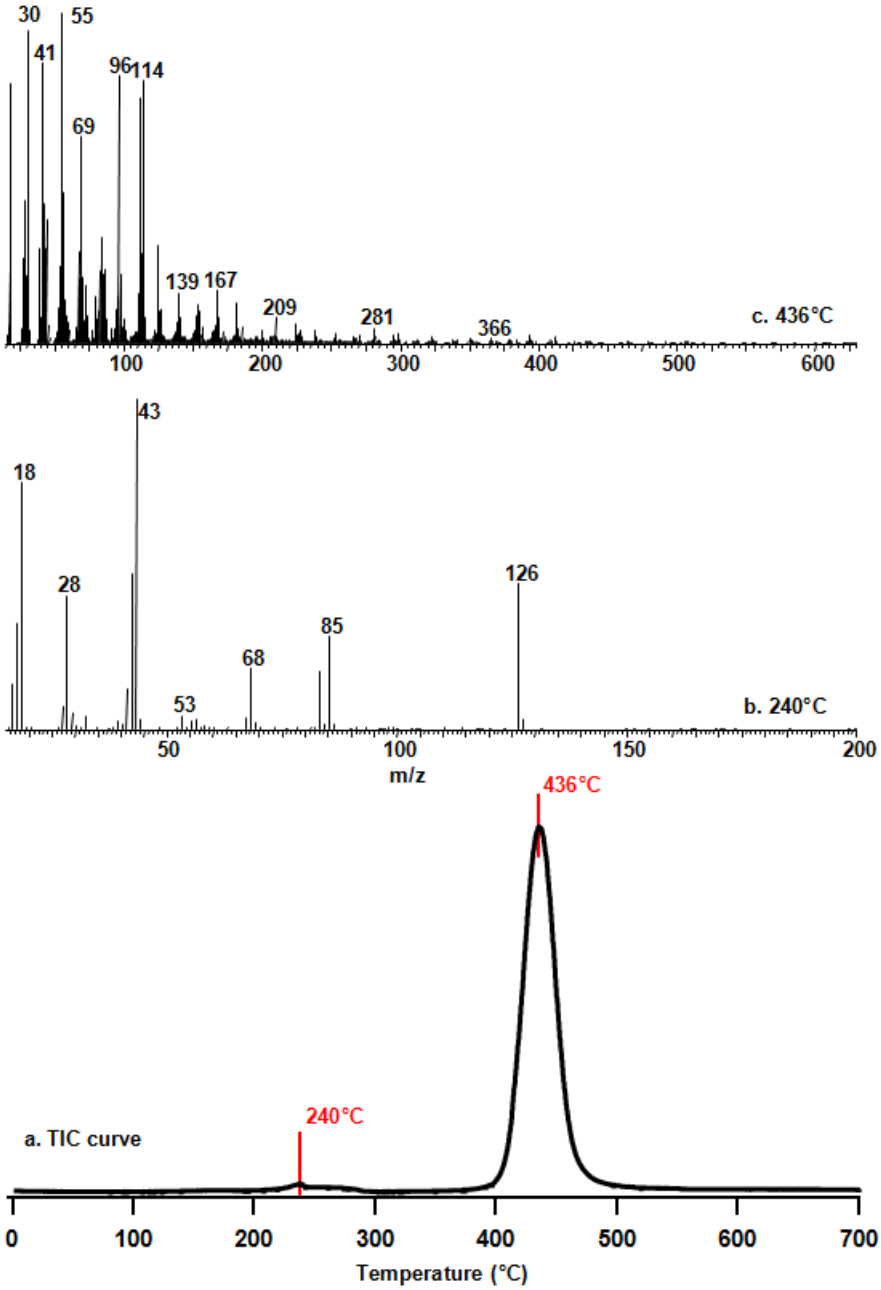

Figure 3-17 a) The TIC curve and the pyrolysis mass spectra at b) 240°C and c) 436°C of PA6/Me involving 3% BSi

Table 3-8 shows the relative intensities of characteristic and/or intense peaks present in the pyrolysis mass spectra of PA6 containing 17% Me and 3% BSi at 240°C and 436°C.

Table 3-8 Relative intensities, RI, of characteristic and/or intense peaks recorded in pyrolysis spectrum of PA6/Me involving BSi at 240°C and 436°C

m/z (Da)	RI		Assignment
	240°C	436°C	
18	746.9	783.5	H_2O
30	9.9	947.8	NH_2CH_2
42	471.8	424.0	N_2CH_2, C_3H_6, CH_2CO
43	1000.0	285.0	N_2CH_3, CONH, CH_2CHO
44	27.3	374.0	$CONH_2$, $NH_2C_2H_4$, CO_2
45	-	52.5	COOH
55	22.8	1000.0	C_4H_7
111	0.2	740.0	$(CH_2)_5NHCN$
113	1.1	271.2	M
114	2.4	794.2	MH
126	440.0	105.0	$N_6C_3H_6$
130	-	9.7	$HN(CH_2)_5COOH$
139	0.3	152.7	MCN
167	0.2	161.1	$MC{=}NCH_2CH_2$
194	-	6.4	$C_4H_8NC(NCOC_5H_{10})$, $C_3H_7N{=}C(N_6C_3H_5)$
221	0.1	6.8	$C_5H_9NC(NCOC_5H_{10})CH_2$, $C_5H_{10}N{=}C(N_6C_3H_5)$
249	-	-	$COC_5H_9NC(NCOC_5H_{10})CH_2$, $COC_5H_{10}N{=}C(N_6C_3H_5)$
298	-	3.1	$NCNH(CH_2)_5MC(OH)(NH_2)NHCH_2$
566	-	0.9	M_5H
591	-	0.6	M_5CN
620	0.1	1.2	$M_5H(CH_2)_5C{=}NCH_2CH_2$

Examination of single ion evolution profiles of Me and related fragments exhibits that, not only the evolution of melamine but also the loss of degradation products of melamine in the temperature region 200°C - 300°C are diminished significantly in the presence of BSi (Figure 3-18). Only for this composite, the relative yield of melamine released at high temperatures (in the temperature region where PA6 degradation takes place), is more than that is in the low temperature region. In addition, increase in the yield of H_2O and decrease in the yields of products generated by hydrolysis of PA6 are recorded contrary to what is observed for PA6/Me involving BPO_4 and ZnB. Significant enhancement in the yield of fragment with m/z value 111 Da is observed; although decrease in the yield of higher mass fragments with m/z value 298 Da, which are related with fragments generated by intermolecular aminolysis reactions, is observed. Therefore, it can be concluded that in the presence of BSi, the degradation products of melamine (mainly NH_3) which are trapped in the polymer matrix, react effectively with PA6 chains leading to its decomposition into relatively low mass fragments inhibiting also the hydrolysis reactions [**60**].

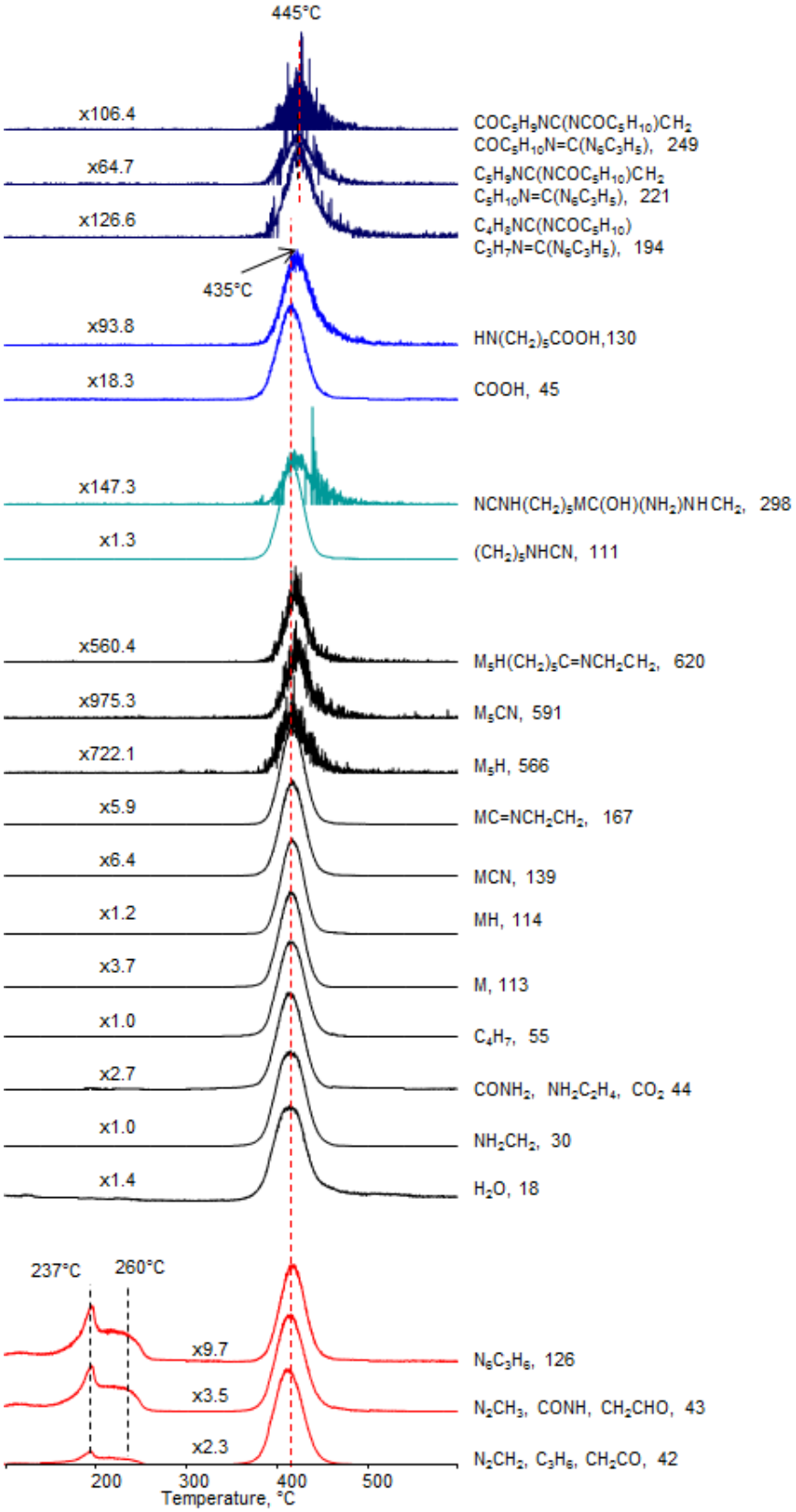

Figure 3-18 Single ion evolution profiles of characteristic and/or intense pyrolysis products of PA6/Me involving 3% BSi

As in case of ZnB addition, it has been determined that BSi forms a glassy surface during combustion which decreases the rate of sublimation and the heat-sink action of Me and simultaneously, the LOI values for PA6/Me significantly [**38**]. It may be concluded that this glassy structure, which is formed over the liquid combustion phase inhibiting the sublimation of Me, accelerates degradation of Me, which in turn increases the possibility of reactions between NH_3, Me and PA6, leading to a decrease in PA6/Me thermal stability [**60**].

In the light of these results, it can be concluded that in general, almost no change in sublimation temperature of Me is observed in the presence of ZnB and BSi. Yet, sublimation of Me is slightly shifted to high temperatures in the presence of BPO_4.

Relative intensities of the fragments generated by intermolecular reactions between Me and carbonyl group of PA6 or amine group and carbonyl group of two different PA6 chains (194, 221 and 249 Da) are increased upon addition of boron compounds.

As a result, thermal stability of PA6 decreases upon addition of ZnB and BSi, whereas, thermal stability of PA6 increases upon addition of BPO_4. The decrease is greatest for the sample involving BSi and smallest for the composite containing ZnB. Among the three boron compounds, the effect of BPO_4 on thermal degradation characteristics of PA6 is significantly different than those of BSi and ZnB.

3.1.7. Polyamide 6/Melamine Cyanurate (PA6/MC)

The effect of melamine cyanurate (MC) on LOI value of PA6 was studied by Doğan et al. A sharp increase in LOI value from 22.5 to 31.8 was observed by addition of 15% of MC into PA6 [**37**]. A slight increase in the char yield, from 0% to 0.6%, by the addition of MC is detected. According to the TGA, two weight loss steps exist resulting from the degradation of MC and PA6 [**37**]. Two peaks, which are consistent with the results in literature [**20**], are seen in the TIC curve as in the case of PA6/Me. A weak and broad peak and a strong peak are seen at around 311°C and 465°C, respectively. Figure 3-19 presents the TIC curve and the mass spectra, recorded at the peak maxima recorded during the pyrolysis of PA6/MC. The characteristic peaks of MC are observed mostly at around 311°C. Therefore, sublimation of MC shifts to higher temperatures as in case of Me during the pyrolysis of PA6/Me. On the other hand, noticeable differences in the fragmentation patterns are observed. The yield of cyanuric acid, which is formed via sublimation, shows a significant decrease in the relative intensity; however, the product with m/z value 43 Da, which is attributed to CONH, CH_2CHO and to CONH, N_2CH_3 in the pyrolysis mass spectra of PA6 and MC, respectively, shows a noticeable increase. Actually, the formation of the fragments with m/z value 43 Da in this temperature range should be due to the degradation of MC during pyrolysis and/or ionization, as thermal decomposition of PA6 occurs at higher temperature ranges. The fragment with m/z value 43 Da can also be attributed to cyanic acid (HOCN), which is isomer of isocyanic acid (HNCO) formed by the dissociation of cyanuric acid in the presence of PA6 [**20**].

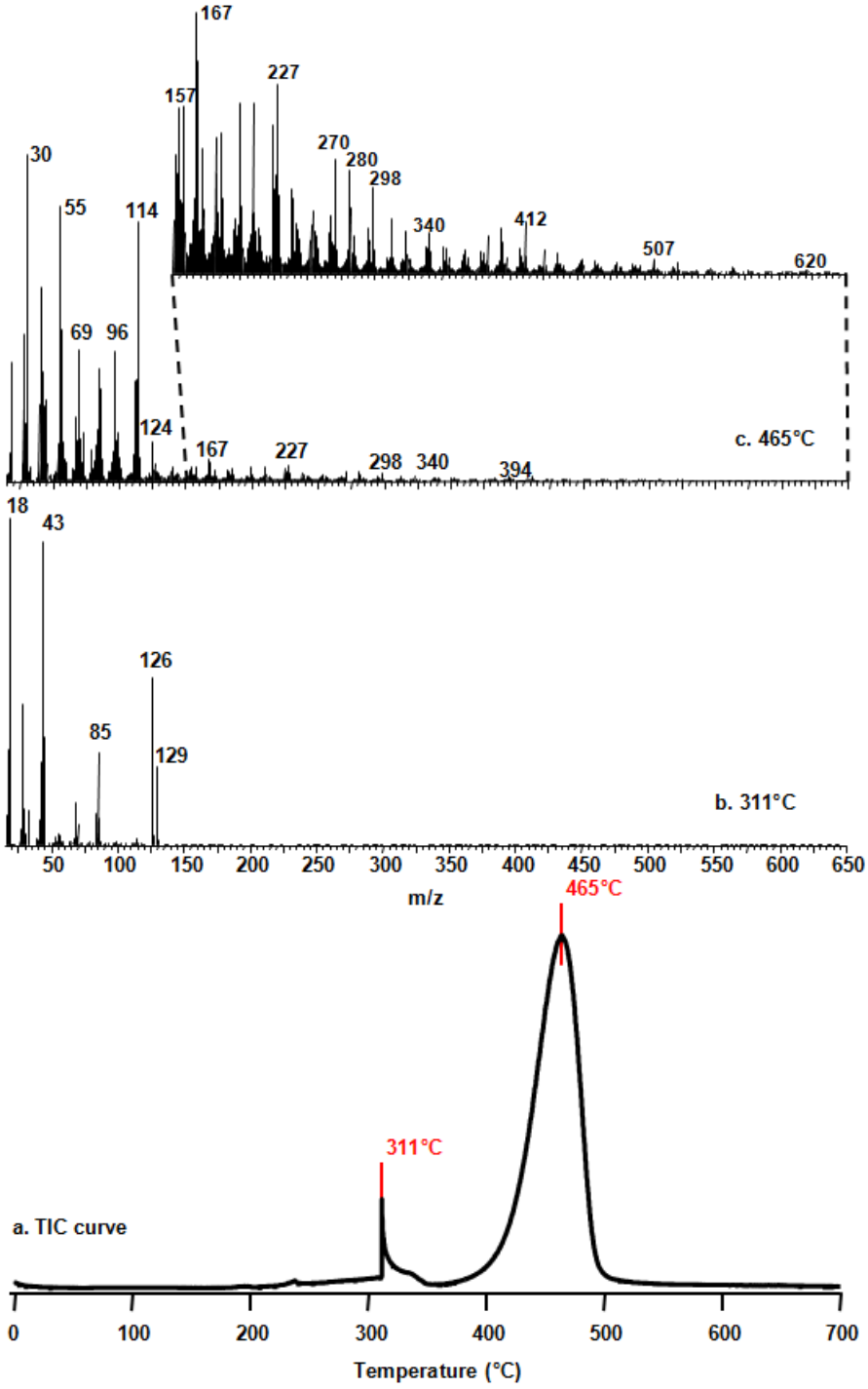

Figure 3-19 a) The TIC curve and the pyrolysis mass spectra at b) 311°C and c) 465°C of PA6/MC

Nagasawa et al. determined that cyanic acid was formed by the conversion of almost all cyanuric acid in the presence of polyamide 66 by the analysis with fast thermolysis/FTIR spectroscopy [**61**]. Doğan et al. reached similar result. They detected CN stretching modes of cyanic acid during TGA-FTIR analysis of PA6/MC; though there was no peak recorded due to cyanuric acid [**37**].

In opposition to the literature work; in the present study, peaks belonging to Me and cyanuric acid are also detected in the temperature region where degradation of PA6 occurs, although, decrease especially in the yield of cyanuric acid is observed in this temperature region [**37**]. Its detection may be achieved by mass spectrometry systems which are significantly much more sensitive than FTIR spectroscopy. Moreover, the yield of products belonging to Me substituted units, which diminish slightly, are detected. This may be related to the decrease in the amount of Me added [**20**].

Mass spectral data are summarized in Table 3-9.

Table 3-9 Relative intensities, RI, of characteristic and/or intense peaks recorded in pyrolysis spectrum of PA6/MC at 311°C and 465°C

m/z (Da)	RI		Assignment
	311°C	465°C	
18	203.5	359.3	H_2O
30	17.7	1000.0	NH_2CH_2
42	247.8	331.3	N_2CH_2, C_3H_6, CH_2CO
43	1000.0	238.4	N_2CH_3, CONH, CH_2CHO
44	320.8	248.6	$CONH_2$, $NH_2C_2H_4$, CO_2
45	6.6	50.4	COOH
55	10.1	856.0	C_4H_7
111	0.8	310.2	$(CH_2)_5NHCN$
113	2.1	306.6	M
114	3.3	800.6	MH
126	556.9	53.2	$N_6C_3H_6$
129	329.5	20.0	$N_3H_3C_3O_3$
130	14.1	12.8	$HN(CH_2)_5COOH$
139	0.3	39.5	MCN
167	0.2	66.2	$MC{=}NCH_2CH_2$
194	0.1	4.5	$C_4H_8NC(NCOC_5H_{10})$, $C_3H_7N{=}C(N_6C_3H_5)$
221	0.2	4.5	$C_5H_9NC(NCOC_5H_{10})CH_2$, $C_5H_{10}N{=}C(N_6C_3H_5)$
249	-	2.8	$COC_5H_9NC(NCOC_5H_{10})CH_2$, $COC_5H_{10}N{=}C(N_6C_3H_5)$
270	0.1	28.5	$M(CH_2)_5CONHCONH_2$
280	-	28.1	$M(CH_2)_5CON(CO)CHCH_2$
298	-	22.7	$NCNH(CH_2)_5MC(OH)(NH_2)NHCH_2$
412	-	14.8	$OHCM_2(CH_2)_5CONHCONH_2$
591	-	0.5	M_5CN
620	-	0.9	$M_5H(CH_2)_5C{=}NCH_2CH_2$

The single ion evolution profiles of some selected thermal degradation products of PA6, recorded during the pyrolysis of PA6/MC (Figure 3-20), demonstrate almost identical trends with those shown in single ion evolution profiles of PA6/Me. Yet, a slight decrease in the relative yields of high mass products is observed when compared to both neat PA6 and PA6/Me. It is proposed that thermal degradation of melamine salts yield acids which participate in the degradation of PA6 as catalyst. Therefore, it may be inferred that generation of cyanic acid results in decomposition of high mass products at least to a certain extent [**20**].

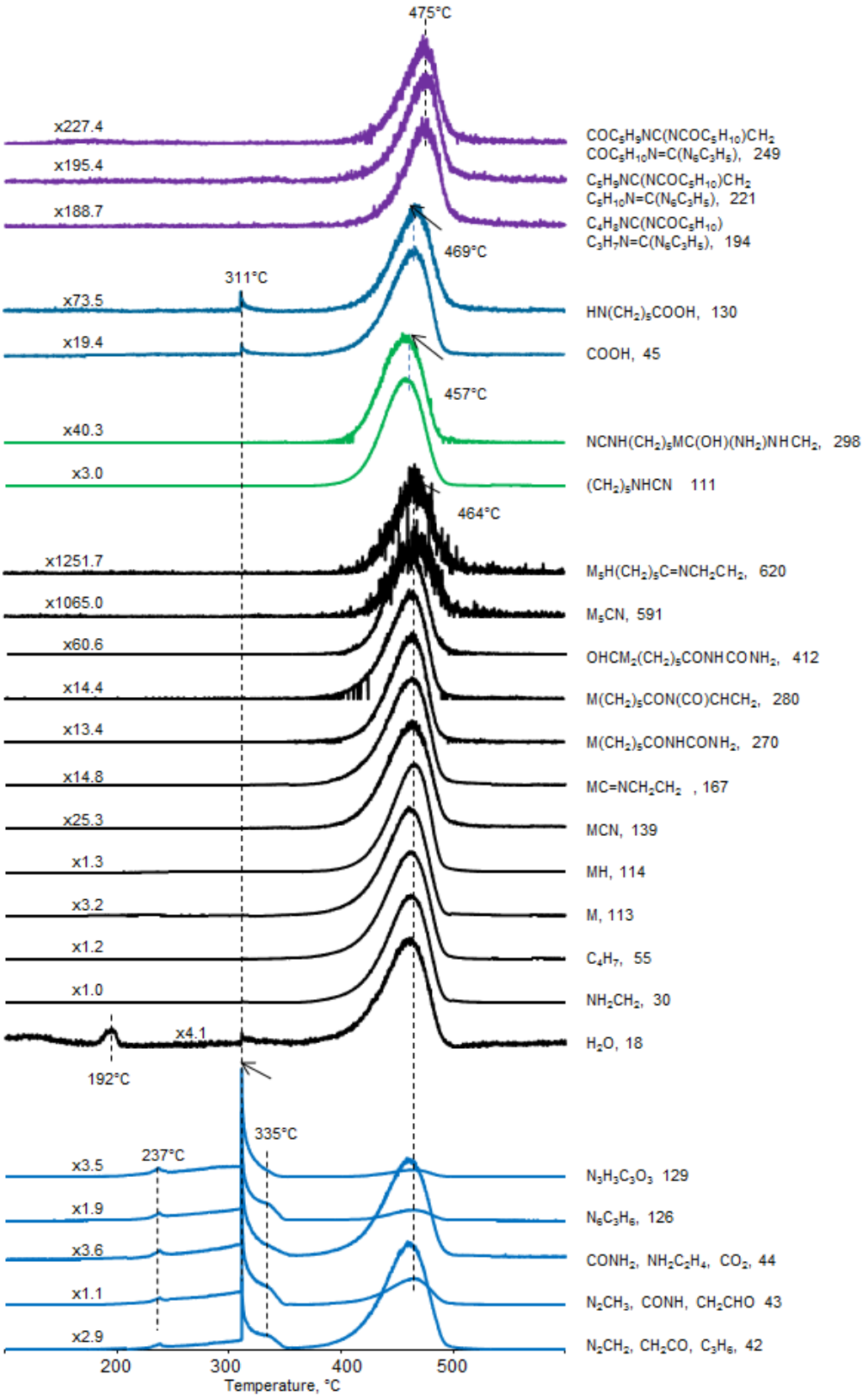

Figure 3-20 Single ion evolution profiles of some selected fragments recorded during pyrolysis of PA6/MC

The yield of products with m/z values 249, 221 and 194 Da, which are formed by addition of Me to carbonyl groups of PA6; reaches their maximum values at slightly higher temperatures, as in case of PA6/Me. In the low temperature ranges, evolution of H_2O, which maximizes at around 192°C and 311°C, is again detected. The products (m/z= 111 and 298 Da), which are generated by reactions of NH_3 and carbonyl groups of PA6, and products containing COOH end groups follow identical trends with those detected in analysis of PA6/Me above 400°C [**20**].

Yet, in the evolution profiles of the fragments with m/z values 18, 45 and 130 Da show weak peaks at around 311°C. These fragments may be generated by the reactions of cyanic acid with PA6 [**20**].

Cyanic acid may undergo interaction with amine groups of PA6 chains (Scheme 3-6). Peaks due to fragments with m/z values 412, 280 and 270 Da observed in the pyrolysis mass spectra of PA6/MC, show significant increase in their relative intensity when compared with those observed in the pyrolysis mass spectra of PA6 and PA6/Me [**20**].

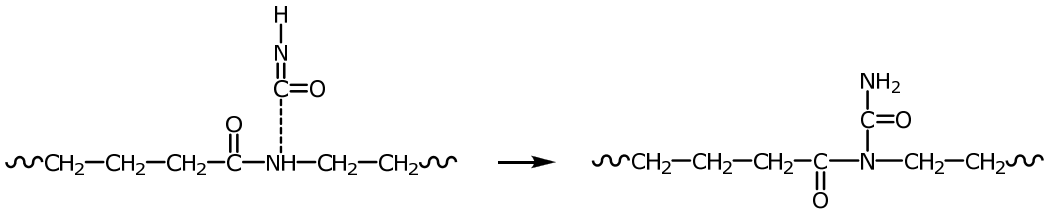

Scheme 3-6 Reaction between cyanic acid and amine groups of PA6 chains

The change in the relative intensities of peaks due to fragments with m/z values 17 and 18 Da should be mentioned. Relative intensity of m/z=17 Da peak increases about 9%. This increase may be related with the increase in the quantity of NH_3 evolution in this temperature region. As a result of the reactions of HNCO, amide units are formed, which can further eliminate NH_3 causing additional evolution of NH_3 [**20**].

3.1.7.1. Effect of Addition of Boron Compounds on PA6/MC

Addition of BPO_4

As mentioned in Section 3.1.5.1, Doğan et al. determined that addition of BPO_4 has an effect on flame retardancy by physical means and decreases the decomposition temperature of PA6. It was noted that BPO_4 enhances the drop density as the drop becomes heavier. Therefore the dripping rate is increased and the increase in the dripping rate causes the removal of flame source from the burning location, and as a consequence,

V0 ratings in UL-94 testing were obtained. It was found that all BPO_4 containing samples at all tested compositions (1-5 wt%) have V0 ratings [**37**, **51**].

As in case of PA6/MC, the TIC curve of PA6/MC containing 3 wt% BPO_4 shows two peaks (Figure 3-21). A strong narrow peak due to evolution of MC based fragments, and a strong, relatively broad peak associated with thermal degradation of PA6 are seen at around 325°C and 436°C, respectively. The maximum of the peak associated with thermal degradation of PA6 is shifted from 465°C to 436°C. Same product peaks are detected, yet, their relative intensities are changed.

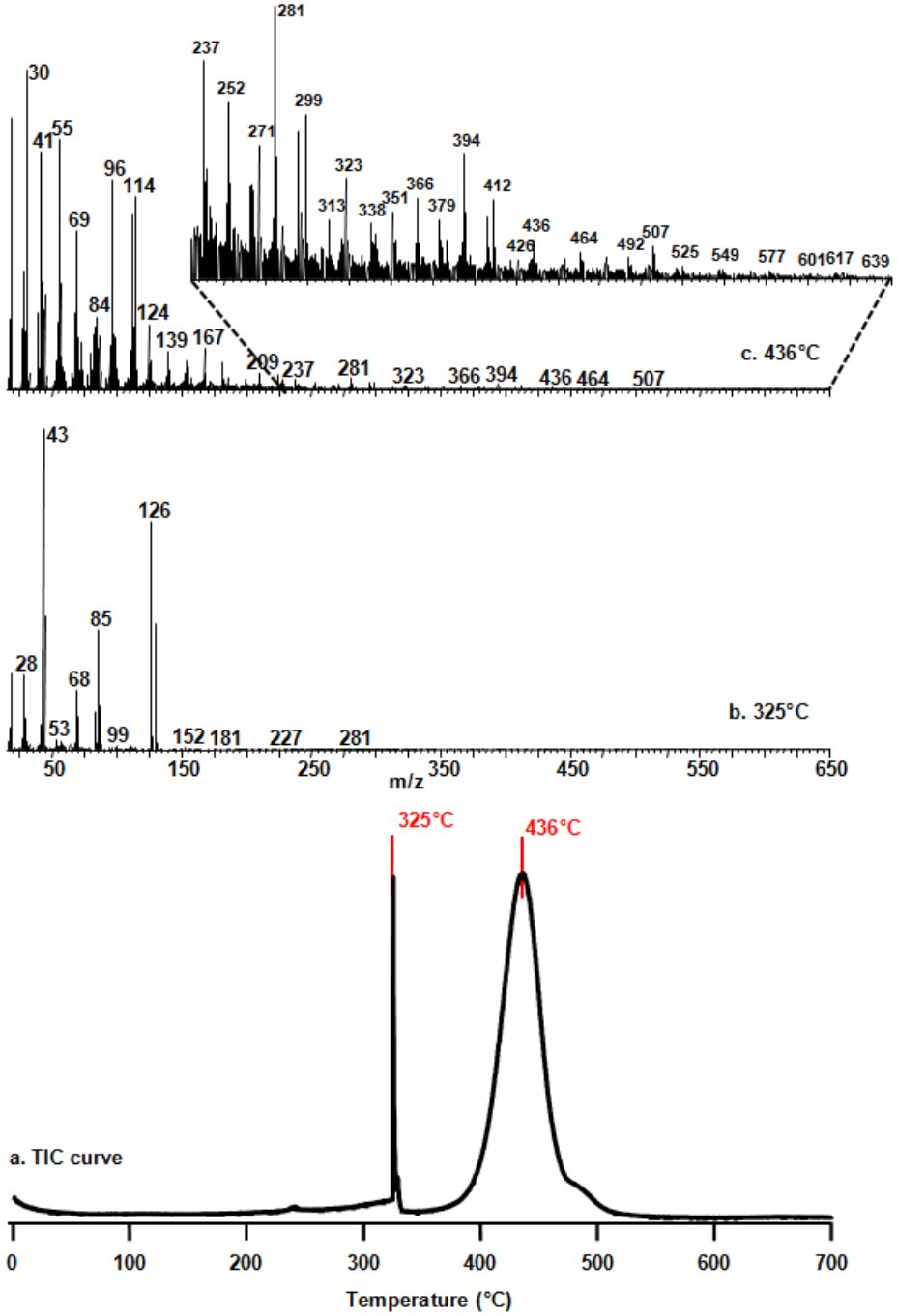

Figure 3-21 a) The TIC curve and the pyrolysis mass spectra at b) 325°C and c) 436°C of PA6/MC involving 3% BPO_4

The relative intensities of characteristic and/or intense peaks present in the pyrolysis mass spectra of PA6/MC involving 3% BPO_4 at 325 and 465°C and the related assignments are given in Table 3-10.

Table 3-10 Relative intensities, RI, of characteristic and/or intense peaks recorded in pyrolysis spectrum of PA6/MC involving 3% BPO_4 at 325°C and 436°C

m/z (Da)	RI		Assignment
	325°C	436°C	
18	238.2	878.5	H_2O
30	20.6	1000.0	NH_2CH_2
42	310.1	338.4	N_2CH_2, C_3H_6, CH_2CO
43	1000.0	242.7	N_2CH_3, CONH, CH_2CHO
44	414.3	297.8	$CONH_2$, $NH_2C_2H_4$, CO_2
45	7.8	42.2	COOH
55	7.8	769.8	C_4H_7
111	1.0	542.7	$(CH_2)_5NHCN$
113	1.4	203.3	M
114	1.4	618.1	MH
126	712.3	86.9	$N_6C_3H_6$
129	389.7	16.6	$N_3H_3C_3O_3$
130	17.0	8.4	$HN(CH_2)_5COOH$
139	0.3	121.9	MCN
167	0.2	130.2	$MC{=}NCH_2CH_2$
194	-	5.4	$C_4H_8NC(NCOC_5H_{10})$, $C_3H_7N{=}C(N_6C_3H_5)$
221	-	5.9	$C_5H_9NC(NCOC_5H_{10})CH_2$, $C_5H_{10}N{=}C(N_6C_3H_5)$
249	-	4.2	$COC_5H_9NC(NCOC_5H_{10})CH_2$, $COC_5H_{10}N{=}C(N_6C_3H_5)$
270	-	17.7	$M(CH_2)_5CONHCONH_2$
280	-	8.5	$M(CH_2)_5CON(CO)CHCH_2$
298	-	20.9	$NCNH(CH_2)_5MC(OH)(NH_2)NHCH_2$
412	-	12.1	$OHCM_2(CH_2)_5CONHCONH_2$
591	-	0.4	M_5CN
620	-	0.8	$M_5H(CH_2)_5C{=}NCH_2CH_2$

Diagnostic peaks of thermal degradation products of PA6, such as caprolactam, cyclic and protonated oligomers, and products involving C=N linkages and CN end groups, are also detected in the presence of BPO_4. But, the relative yields of these peaks are noticeably decreased. On the other hand, the relative yields of melamine cyanurate, MC, based products are increased. The peaks at 311°C, associated with evolution of MC products, are sharpened and are shifted to higher temperature regions, at around 325°C. The decrease of peak widths may be explained by the decrease in the extent of H-bonding between melamine and cyanuric acid and PA6 in the presence of BPO_4. Therefore, it can be concluded that the sublimation of MC is shifted to higher temperatures. Contrary to the trends recorded at around 325°C, the relative intensities of diagnostic peaks of MC at around 434°C, where the thermal degradation of PA6 takes place are decreased.

Single ion pyrograms of some characteristic products detected during the pyrolysis of PA6/MC involving 3% BPO_4 are shown in Figure 3-22. The corresponding ones recorded during the pyrolysis of PA6/MC composite involving no boron compounds are also included in the figure for comparison. Relative intensity of the peak due to cyanuric acid (m/z=129 Da), which is generated upon sublimation of MC, is increased significantly. Furthermore, relative intensity of the fragment with m/z value 43 Da, which is attributed to CONH and/or CH_2CHO in the pyrolysis mass spectra of PA6 and to CONH and/or N_2CH_3 in those of MC, is increased noticeably. The 43 Da peak is almost totally absent in the pyrolysis mass spectra recorded at around 434°C, where thermal degradation of PA6 takes place. Therefore, it can be concluded that the peak at 43 Da is mainly due to CONH and/or N_2CH_3 fragments generated by the decomposition of MC.

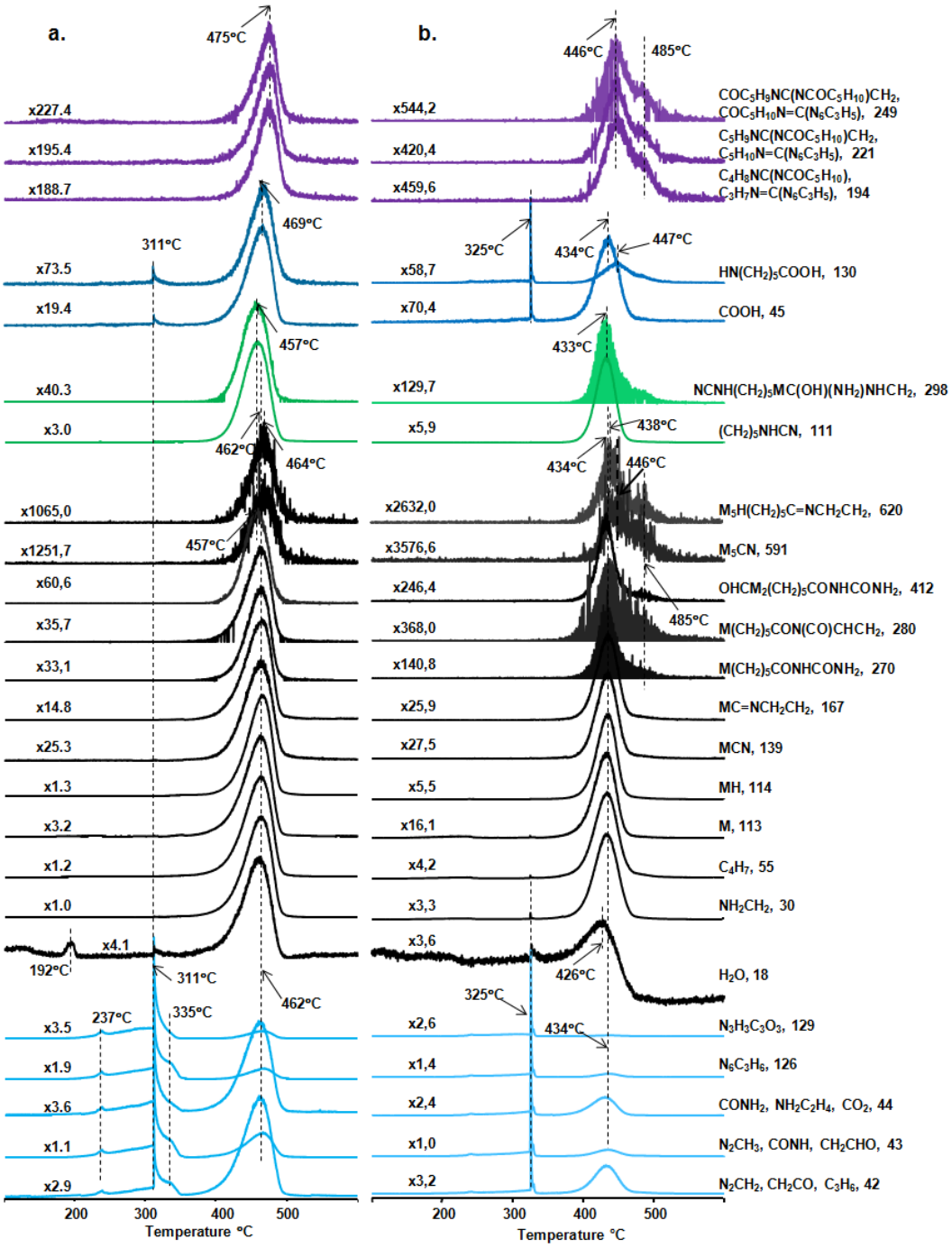

Figure 3-22 Single ion evolution profiles of characteristic and/or intense pyrolysis products of a) PA6/MC and b) PA6/MC involving 3% BPO_4

The relative yields of monomer and protonated monomer are decreased almost 5 folds. Similarly, the relative yields of the products involving unsaturated parts in their structure with the formula M_xCN and $M_xC{=}NCH_2CH_2$, such as those with m/z values 139 and 167 Da for x=1, the first component of each series respectively, are also decreased. The decrease is more pronounced for the M_xCN fragments.

In addition, evolution of H_2O occurred at around 192°C diminishes thoroughly in the presence of BPO_4. This decrease may be due to the hydrolysis of PA6 chains. Actually, the relative yield of $HN(CH_2)_5COOH$ (130 Da), at around 325°C, that may be generated by the interactions with cyanuric acid, is increased about 1.3 folds compared to the pendant composite, which means that its intensity is increased more than 4 folds compared to the most of the PA6 based products. Another point that should be noticed is the significant increase in the yield of fragments with COOH end groups at around 325°C, where MC is lost. Thus, it can be concluded that in the presence of BPO_4, the reactions between cyanuric acid and PA6 are enhanced significantly even at moderate temperatures.

Decrease in the relative intensities of peaks associated with fragments generated by reactions of NH_3 and melamine with carbonyls groups of PA6 are also detected. However, the decrease in the relative yield of the fragment with m/z value 111 Da generated by the reaction of NH_3 with carbonyl groups of PA6 is only about 2.5 folds. Similarly, the relative yields of the products (194, 221 and 249 Da) associated with the reactions due to attack of melamine to carbonyl groups (Scheme 3-5) is about 2.4 folds. Thus, it may be concluded that the relative yields of these fragments are increased approximately 2 folds compared to the monomer and protonated monomer.

The single ion evolution profiles of the fragments with m/z values 194, 221 and 249 Da show a peak at 446°C and also a side lobe at a slightly higher temperature region (at around 485°C). Actually, two different products with the same m/z values but with different structures formed through different processes (one of which is the reaction between amine groups of melamine and carbonyl groups of PA6 and the other is the degradation of PA6 itself) may be generated at slightly different temperatures. As a result, such a single ion evolution profile with a side lobe may be produced.

The decrease in the relative yields of fragments with m/z values 270, 280 and 412 Da, which are generated by the reactions of cyanuric acid with amine groups of PA6, are also decreased during the pyrolysis of PA6/MC involving BPO_4 compared to the corresponding values recorded for PA6/MC. But, again, an increase in their relative yields with respect to other PA6 based products is recorded.

Thus, in summary DP-MS results indicated that, in the presence of BPO_4, the reactions between H_2O, NH_3, melamine and cyanuric acid with PA6 are enhanced. As a consequence, the yield of fragments generated by classical thermal degradation pathways of PA6 is decreased. These behaviors may be associated with the increase in the dripping rate that may activate intermolecular interactions.

Addition of ZnB

Addition of ZnB affects flame retardancy by physical means and diminishes the decomposition temperature of both PA6 and MC, as in case of addition of BPO_4 [**37**, **51**]. However, in contrast, ZnB has a negative effect on drop density. And thus, no increase in dripping rate occurs. On the other hand, decomposition of ZnB increases the surface tension of the drop, therefore, decreases the dripping rate causing V2 rating. It was found that among the composites involving variable amounts of ZnB, only 1% ZnB containing sample has V0 rating, whereas 3% and 5% ZnB containing samples have V2 ratings. Furthermore, it was also noted that ZnB has the ability of forming glassy surface, slowing down MC sublimation [**37**, **51**].

As in case of PA6/MC, the TIC curve of PA6/MC containing 3 wt% ZnB shows two peaks (Figure 3-23). A strong narrow peak due to evolution of MC based fragments, and a strong, relatively broad peak associated with thermal degradation of PA6 are detected at around 321°C and 449°C, respectively. Although, the diagnostic peaks of MC and thermal degradation products of PA6 are detected in the pyrolysis mass spectra of PA6/MC, their relative intensities are changed significantly as in case of BPO_4 containing composite.

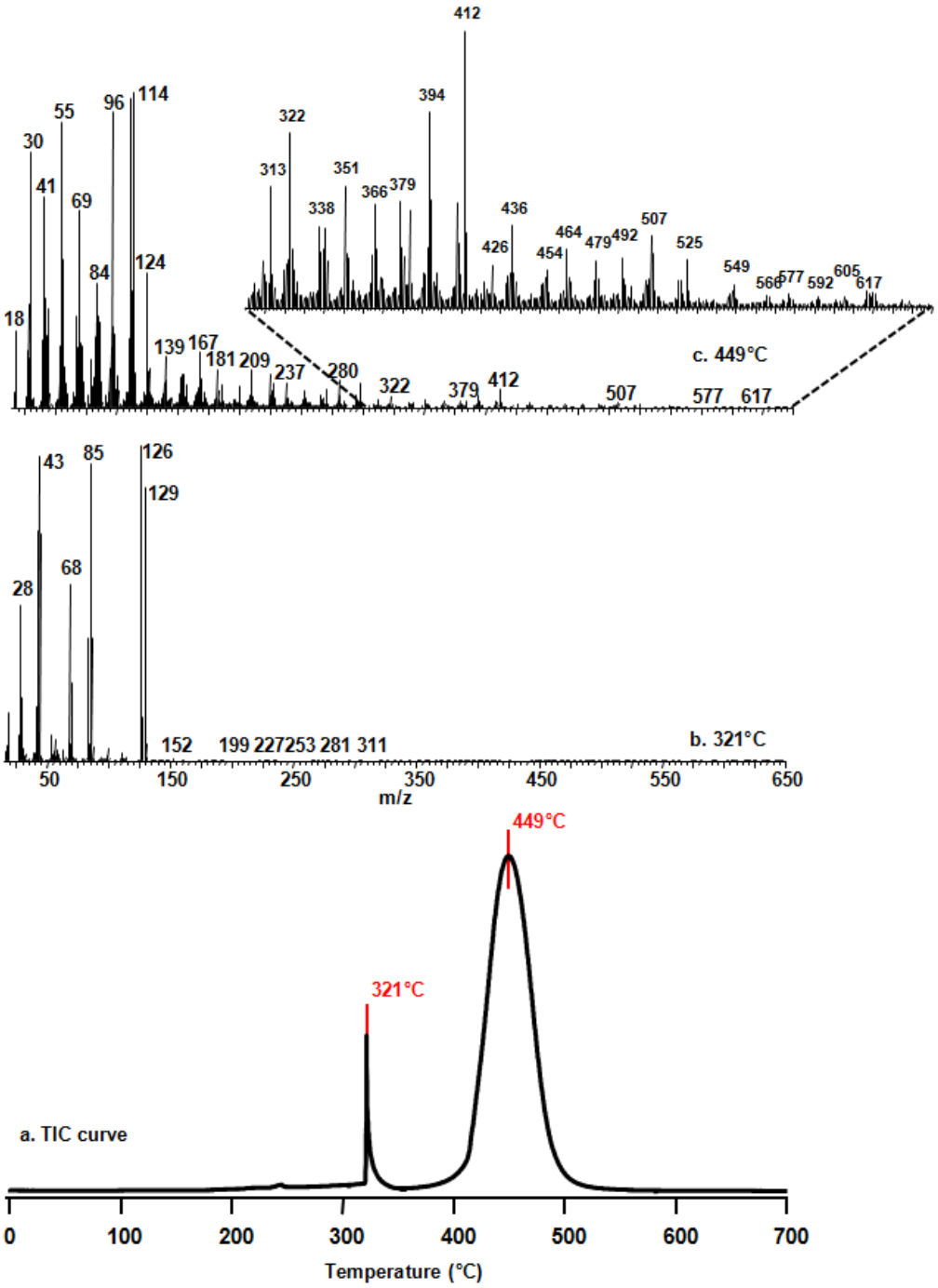

Figure 3-23 a) The TIC curve and the pyrolysis mass spectra at b) 321°C and c) 449°C of PA6/MC involving 3% ZnB

In the presence of 3 wt% ZnB, the thermal stability of PA6 is decreased as in case of BPO_4 involving composite. The maximum of the peak related to the degradation products PA6 is shifted from 465°C to 449°C. The diagnostic peaks of MC are recorded mainly at around 321°C. Therefore, it can be concluded that for PA6/MC composite involving 3 % ZnB, the sublimation of MC is shifted to higher temperatures compared to PA6/MC composite in parallel to BPO_4 involving sample. However, in contrast, the relative yields of PA6 based products are increased noticeably in the presence of ZnB.

The relative intensities of the peaks and the assignments made for these peaks detected in the mass spectra of PA6 containing 12% MC and 3% ZnB recorded at 321°C and 449°C, are given in Table 3-11.

Table 3-11 Relative intensities, RI, of characteristic and/or intense peaks recorded in pyrolysis spectrum of PA6/MC involving 3% ZnB at 321°C and 449°C

m/z (Da)	RI		Assignment
	321°C	449°C	
18	150.7	242.7	H_2O
30	38.3	819.7	NH_2CH_2
42	729.8	351.9	N_2CH_2, C_3H_6, CH_2CO
43	964.8	233.4	N_2CH_3, CONH, CH_2CHO
44	721.0	314.0	$CONH_2$, $NH_2C_2H_4$, CO_2
45	15.2	42.1	COOH
55	25.8	917.0	C_4H_7
111	4.6	987.4	$(CH_2)_5NHCN$
113	5.3	457.0	M
114	10.3	1000.0	MH
126	1000.0	126.4	$N_6C_3H_6$
129	869.5	28.0	$N_3H_3C_3O_3$
130	49.2	11.0	$HN(CH_2)_5COOH$
139	0.9	162.4	MCN
167	0.8	174.5	$MC{=}NCH_2CH_2$
194	0.2	6.5	$C_4H_8NC(NCOC_5H_{10})$, $C_3H_7N{=}C(N_6C_3H_5)$
221	0.2	8.1	$C_5H_9NC(NCOC_5H_{10})CH_2$, $C_5H_{10}N{=}C(N_6C_3H_5)$
249	-	6.6	$COC_5H_9NC(NCOC_5H_{10})CH_2$, $COC_5H_{10}N{=}C(N_6C_3H_5)$
270	0.2	59.1	$M(CH_2)_5CONHCONH_2$
280	0.1	86.9	$M(CH_2)_5CON(CO)CHCH_2$
298	0.1	75.2	$NCNH(CH_2)_5MC(OH)(NH_2)NHCH_2$
412	0	57.7	$OHCM_2(CH_2)_5CONHCONH_2$
591	-	1.1	M_5CN
620	-	3.1	$M_5H(CH_2)_5C{=}NCH_2CH_2$

Single ion pyrograms of some selected and characteristic products detected during the pyrolysis of PA6/MC involving 3% ZnB are shown in Figure 3-24. The corresponding ones recorded during the pyrolysis of PA6/MC composite involving no boron compounds are also included in the figure for comparison.

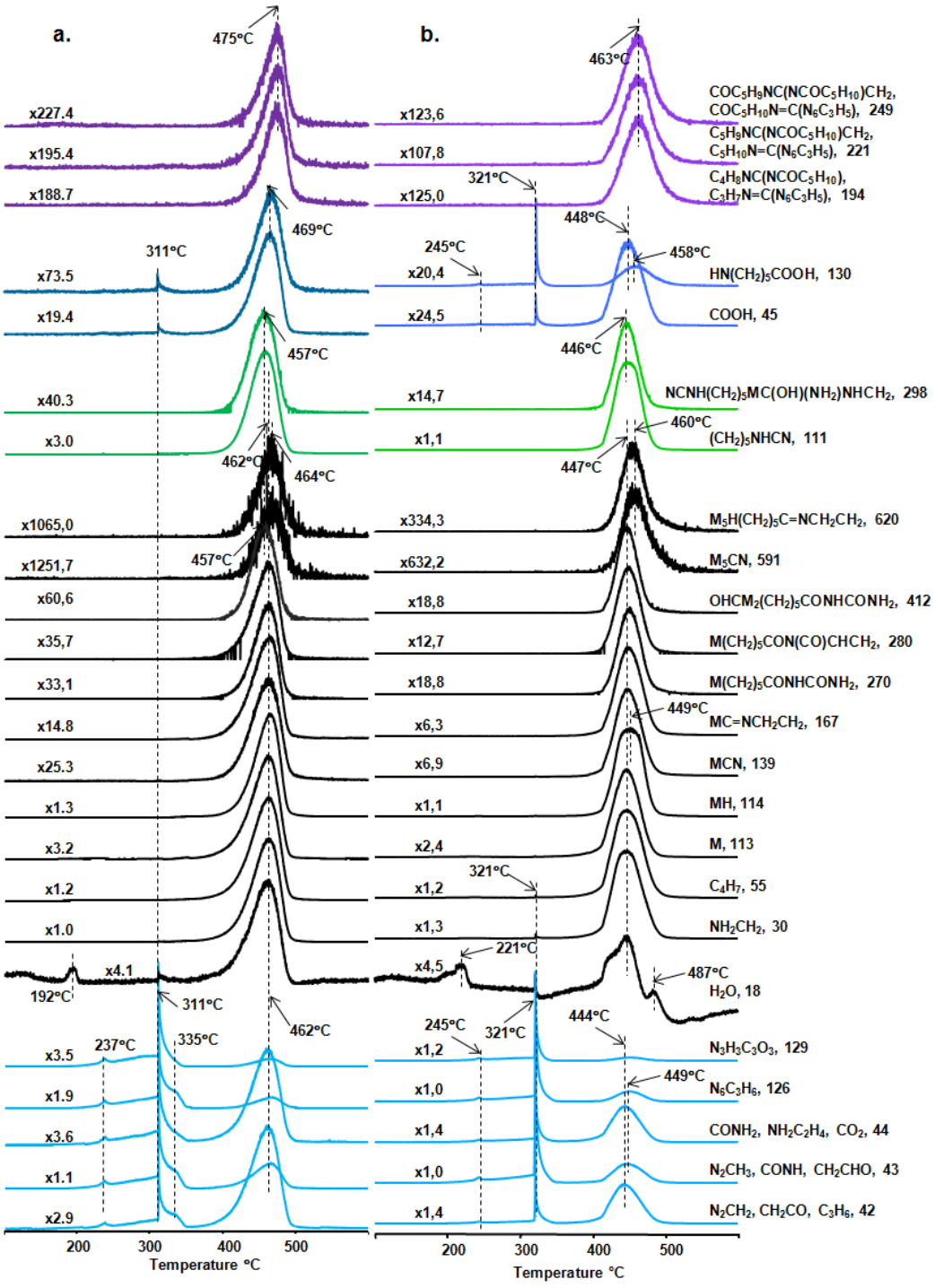

Figure 3-24 Single ion evolution profiles of characteristic and/or intense pyrolysis products of a) PA6/MC and b) PA6/MC involving 3% ZnB

The relative intensities of the peaks due to cyanuric acid (m/z=129 Da) and melamine (m/z=126 Da) generated upon sublimation, are increased significantly. Furthermore, the relative intensity of the peak at 43 Da, attributed to CONH and CH_2CHO in the pyrolysis mass spectra of PA6 and to CONH and N_2CH_3 in those of MC, is increased slightly. Only a small decrease in the relative yields of molecular ion of $N_3H_3C_3O_3$ and $N_6C_3H_6$, is recorded at around 449°C, where thermal degradation of PA6 takes place. However, the shoulder at 335°C present in the evolution profiles of MC based products is almost totally disappeared.

The relative yields of high mass thermal degradation products of PA6 generated through classical thermal degradation pathways increase noticeably. The relative yields of $(CH_2)_5NHCN$ (111 Da) and $NCNH(CH_2)_5MC(OH)(NH_2)NHCH_2)$ $(CH_2)_5NHCN$ (298 Da) generated by the reactions of NH_3 with carbonyl groups of PA6 are increased 2.7 folds. On the other hand, the relative yields of the products involving unsaturated parts in their structure with the formula M_xCN and $M_xC{=}NCH_2CH_2$, such as those with m/z values 139 and 167 Da, respectively, are increased more than 3 folds. The increase is more pronounced for the M_xCN, almost 5 folds.

Less than 2 folds increase in the relative yields of products with m/z values 194, 221 and 249 Da associated with reactions due to reactions of melamine with carbonyl groups of PA6 (Scheme 3-5) are detected. Increases in the relative yields of fragments with m/z values 270 (more than 2 folds), 280 (more than 3 folds) and 412 (more than 4 folds) Da, generated by the reactions of cyanuric acid with amine groups of PA6, are also observed.

The evolution of H_2O, detected at around 192°C during the pyrolysis of PA6/MC, is shifted 29°C to higher temperature region, to 221°C, in the presence of ZnB. But, contrary to BPO_4 involving composite, its relative intensity is not decreased. Thus, it may be concluded that the glassy surface formed by ZnB over the polymer matrix does not restrict evolution of H_2O. Although, the relative yield of the fragment with m/z value 130 Da associated with $HN(CH_2)_5COOH$ is increased more than 4 folds, the relative yield of COOH fragment is decreased about 1.3 folds. Actually, the increase in the yield of fragment with m/z value 130 Da is noted at around 321°C, in the region where MC is lost. Thus, it may be concluded that the extent of hydrolysis reactions is not enhanced. On the other hand, the interactions between cyanuric acid and PA6 in the region where sublimation of MC occurs are enhanced drastically. The increase in the relative yields of fragments due to reactions between cyanuric acid and PA6 such as $OHCM_2(CH_2)_5CONHCONH_2$ also supports enhancement of these reactions.

It is clear that the increase in the relative intensities of the fragments due to decomposition of PA6 chains is more pronounced than those generated by the reactions of H_2O, NH_3, melamine, cyanuric acid with carbonyl groups of PA6.

These behaviors may be associated with the decrease in the drop density. As the fragments may evolve more readily from the hot zone during pyrolysis, the possibility of detection of high mass fragments increases which in turn decreases the possibility of secondary reactions.

Addition of BSi

Doğan et al. determined that, as in the case of addition of ZnB, BSi also affects flame retardancy by physical means. The decomposition temperature of both PA6 and MC are diminished in the presence of BSi. BSi has reverse influence on drop density, as ZnB does. Thus, dripping rate does not increase. Similarly, the decomposition of BSi increases the drop surface tension; which consequently, decreases the dripping rate causing V2 rating. It was found that 1% BSi containing sample has V0 rating, whereas 3% and 5% BSi containing samples have V2 ratings. Furthermore, it was also noted that BSi has the ability of forming a glassy surface making MC sublimation slow down [**37**, **51**]. Thus, the effect of addition of ZnB and BSi are almost identical.

The TIC curve of PA6/MC containing 3 wt% BSi shows two peaks (Figure 3-25). A relatively weak and narrow peak due to evolution of MC based fragments, and a strong broad peak associated with thermal degradation of PA6 are detected at around 328°C and 435°C, respectively. Same products observed in Section 3.1.7 are detected; yet, their relative yields are changed.

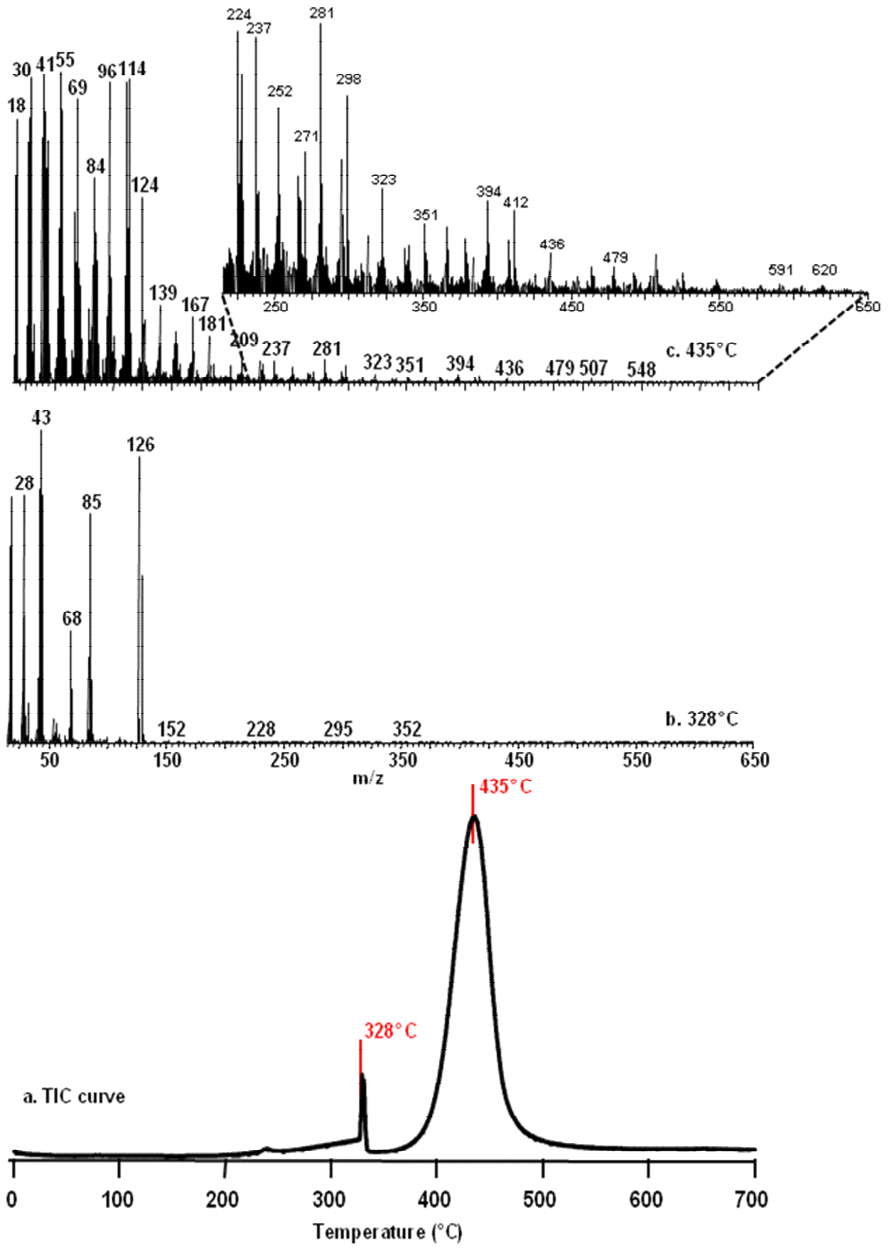

Figure 3-25 a) The TIC curve and the pyrolysis mass spectra at b) 328°C and c) 435°C of PA6/MC involving 3% BSi

In the presence of 3 wt% BSi, the trends in the TIC curve indicated that the thermal stability of PA6 is decreased; the maximum of the peak related to the degradation products PA6 is shifted from 465 to 435°C and the relative intensities of the characteristic peaks due to the thermal degradation products of PA6 are increased. On the other hand, the diagnostic peaks of MC are recorded mainly at around 328°C. Therefore, it can be concluded that for the PA6/MC involving 3% BSi, the sublimation of MC is shifted slightly to higher temperatures compared to PA6/MC, as in case of BPO_4 and ZnB. In addition, the relative yields of MC based products are increased.

Table 3-12 shows the relative intensities of characteristic and/or intense peaks present in the pyrolysis mass spectra of PA6 containing 12% MC and 3% BSi at 328°C and 435°C.

Table 3-12 Relative intensities, RI, of characteristic and/or intense peaks recorded in pyrolysis spectrum of PA6/MC involving 3% BSi at 328°C and 435°C

m/z (Da)	RI		Assignment
	328°C	435°C	
18	785.6	446.8	H_2O
30	79.3	979.4	NH_2CH_2
42	810.4	870.7	N_2CH_2, C_3H_6, CH_2CO
43	1000.0	691.2	N_2CH_3, CONH, CH_2CHO
44	788.5	782.2	$CONH_2$, $NH_2C_2H_4$, CO_2
45	20.5	123.4	COOH
55	26.8	1000.0	C_4H_7
111	3.6	966.5	$(CH_2)_5NHCN$
113	4.8	658.9	M
114	5.5	971.3	MH
126	914.9	200.4	$N_6C_3H_6$
129	535.7	38.7	$N_3H_3C_3O_3$
130	24.6	17.0	$HN(CH_2)_5COOH$
139	0.5	251.0	MCN
167	0.5	209.6	$MC{=}NCH_2CH_2$
194	0.2	8.1	$C_4H_8NC(NCOC_5H_{10})$, $C_3H_7N{=}C(N_6C_3H_5)$
221	0.1	7.5	$C_5H_9NC(NCOC_5H_{10})CH_2$, $C_5H_{10}N{=}C(N_6C_3H_5)$
249	0.1	7.7	$COC_5H_9NC(NCOC_5H_{10})CH_2$, $COC_5H_{10}N{=}C(N_6C_3H_5)$
270	0.1	-	$M(CH_2)_5CONHCONH_2$
280	-	18.5	$M(CH_2)_5CON(CO)CHCH_2$
298	-	52.7	$NCNH(CH_2)_5MC(OH)(NH_2)NHCH_2$
412	0.1	22.1	$OHCM_2(CH_2)_5CONHCONH_2$
591	0.1	2.1	M_5CN
620	-	2.0	$M_5H(CH_2)_5C{=}NCH_2CH_2$

Single ion pyrograms of some selected and characteristic products detected during the pyrolysis of PA6/MC involving 3% BSi are shown in Figure 3-26 together with the corresponding ones recorded during the pyrolysis of PA6/MC composite involving no boron compounds for comparison.

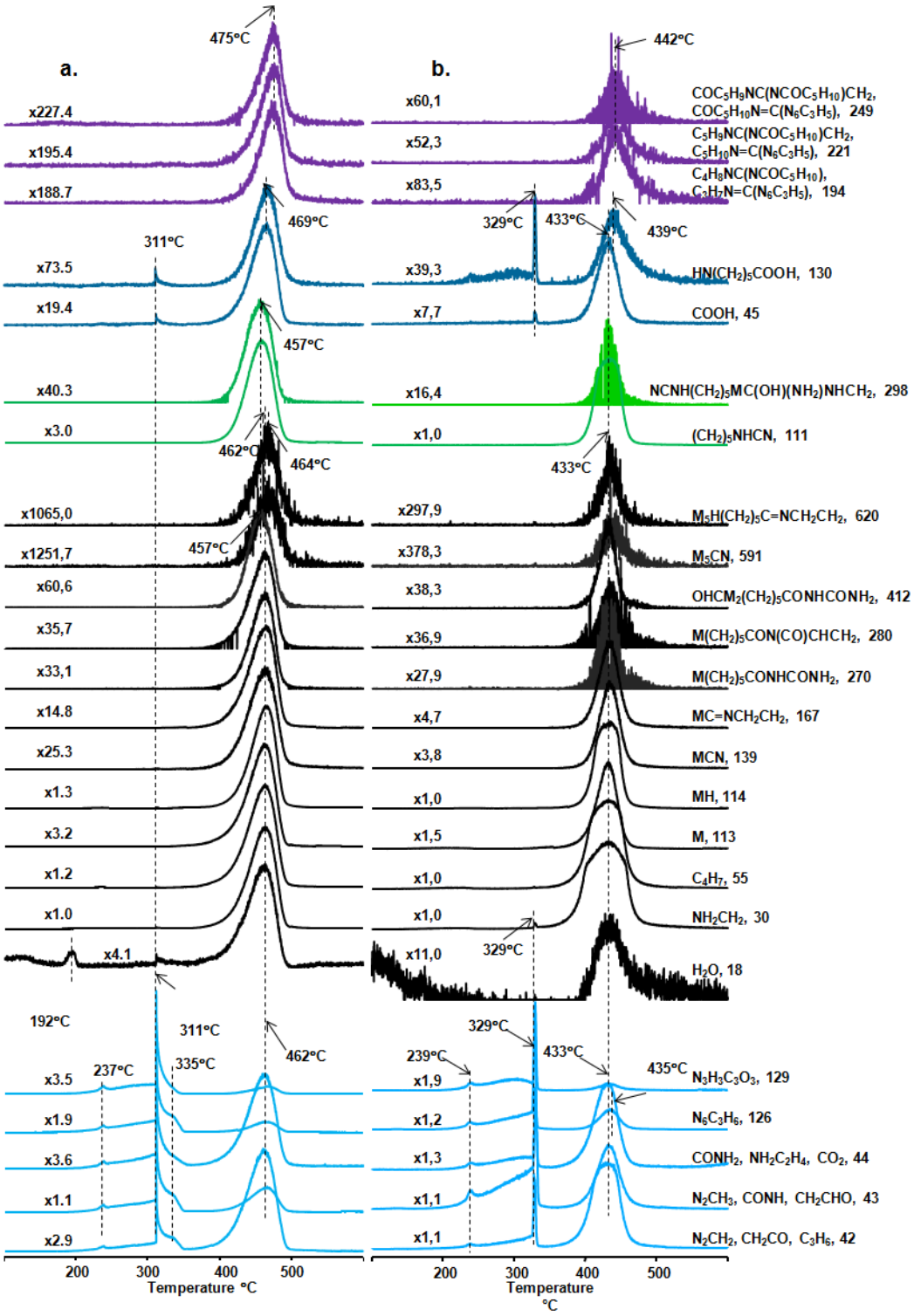

Figure 3-26 a) Single ion evolution profiles of characteristic and/or intense pyrolysis products of PA6/MC and b) PA6/MC involving 3% BSi

The single ion evolution profiles of diagnostic products of MC are slightly shifted to high temperature regions; evolution of these fragments starts at around 250°C and continues up to 329°C, where a sharp main peak is observed. This slight increase may be attributed to the increase in the extent of H-bonding between MC and PA6 chains.

The relative intensity of the peak due to cyanuric acid (m/z=129 Da), generated upon sublimation of MC, is increased approximately 2 folds. However, this peak is almost absent in the pyrolysis mass spectra recorded at 435°C, where thermal degradation of PA6 takes place. Similarly, the relative intensity of fragment with m/z value 126 Da, attributed to Me, is also increased in the presence of BSi. Contrary to PA6/MC involving ZnB, for which, the peak at 126 Da is also observed in the pyrolysis mass spectra recorded at around 449°C, where thermal degradation of PA6 takes place.

The evolution profiles of PA6 based fragments show noticeable differences compared to those recorded during the pyrolysis of PA6/MC involving BPO4 and ZnB. Firstly, significant increase in the relative yields of PA6 based products are detected during the pyrolysis of PA6/MC composite involving 3% BSi, as in case of ZnB involving sample, contrary to the results obtained for BPO_4 containing composite. Secondly, unlike ZnB containing composite, noticeable increase in the relative yields of low mass PA6 based fragments are observed. Furthermore, their evolution profiles are broadened. In addition, the relative yields of the products involving unsaturated parts in their structure with the formula M_xCN and $M_xC{=}NCH_2CH_2$, such as MCN and $MC{=}NCH_2CH_2$, are increased more than 3 folds. For the M_xCN, the increase is even more pronounced, more than 6 folds.

The relative yields of the products with m/z values 194, 221 and 249 Da, due to $C_4H_8NC(NCOC_5H_{10})$ and/or $C_3H_7N{=}C(N_6C_3H_5)$, $C_5H_9NC(NCOC_5H_{10})CH_2$ and/or $C_5H_{10}N{=}C(N_6C_3H_5)$) and $COC_5H_9NC(NCOC_5H_{10})CH_2$ and/or $COC_5H_{10}N{=}C(N_6C_3H_5)$ respectively, associated with the reactions of melamine with carbonyl groups (Scheme 3-5) are also increased; for the product with m/z value 194 Da, the increase is more than 2 folds and for those with m/z values 221 and 249 Da, the increase is more than 3 folds.

Evolution of H_2O is diminished thoroughly in the presence of BSi as in the case of BPO_4. This may be due to the consumption of evolved H_2O by the hydrolysis reactions of PA6. The noticeable increase in the relative yield of COOH at around 433°C confirms the enhancement of hydrolysis reactions. On the other hand, the increase in the relative intensities of 45 and 130 Da fragments involving COOH end groups is noticeably low in the region where MC sublimation takes place compared to the DP-MS results of the samples involving BPO_4 and ZnB.

The relative yields of the fragments $(CH_2)_5NHCN$ (111 Da) and $NCNH(CH_2)_5MC(OH)(NH_2)NHCH_2$ (298 Da) generated by the reactions of NH_3 with carbonyl groups of PA6 are also increased more than 2 folds.

On the other hand, almost no change in the relative intensities of the peaks with m/z values 270 and 280 Da and a slight increase in that of the peak at 412 Da, due to the

fragments generated by the reactions of cyanuric acid with amine groups of PA6, are observed compared to the corresponding values for PA6/MC.

These behaviors indicate that the intermolecular interactions between cyanuric acid and PA6 are depressed in the presence of BSi.

In the light of these results, it can be concluded that in general, sublimation of MC is slightly shifted to high temperatures in the presence of boron compounds. In addition, thermal stability of PA6 decreases. The decrease is greatest for the sample involving BSi and smallest for the composite containing ZnB. Among the three boron compounds, the effect of BPO_4 on thermal degradation characteristics of PA6 is significantly different than those of BSi and ZnB. For PA6/MC involving 3 wt% BPO_4 the relative yields of thermal degradation products of PA6 are decreased more than those of the fragments generated by the reactions between melamine, cyanuric acid and carbonyl groups of PA6. It may be thought that the increase in the dripping rate in the presence of 3 wt% BPO_4 may increase the possibility of occurrence of these reactions. On the other hand, for the samples involving ZnB and BSi, contrary to the effect of BPO_4, the relative yields of thermal degradation products of PA6 are enhanced more than those due to intermolecular interactions. It may be thought that the decrease in drop density increases the rate of evolution of thermal degradation products of PA6; thus, inhibiting intermolecular reactions in the temperature region where sublimation of MC takes place. In general, the relative yields of fragments generated by reactions of isocyanic acid with PA6 increase in the presence of ZnB and BSi. The increase due to addition of ZnB is higher than that of BSi. In case of addition of BPO_4, relative yields of those fragments decrease. As the temperature range, where MC sublimation occurs, shifts to higher temperatures, the thermal stability of PA6 decreases.

Furthermore, in the presence of 3 wt% ZnB or BSi, the relative yields of products generated by the intermolecular reactions of melamine and cyanuric acid with PA6 are enhanced; whereas, in the presence of BPO_4, relative yields of those products decrease. It may be suggested that the glassy surface produced by ZnB or BSi encloses the these molecules to a certain extent which then readily undergo reactions with PA6 decreasing thermal stability of the polymer.

Relative intensities of thermal degradation products of PA6 such as M, MH, MCN, and MC=NCH2CH2 (113, 114, 139 and 167 Da) are decreased significantly upon inclusion of BPO_4 and increased moderately upon inclusion of ZnB and BSi.

As a consequence, addition of boron compounds enhances the thermal stability of MC, but decreases the thermal stability of PA6 via interaction between MC and PA6 chains. The strongest effect on temperature shift is observed due to addition of BSi, then BPO_4 and ZnB, in descending order.

3.1.8. PA6/Aluminum Diethylphosphinate (PA6/AlPi) without Cloisite 30B

The effect of aluminum diethylphosphinate (AlPi) on LOI and vertical burning ratings (UL-94) of PA6 were studied by Doğan et al. Increase in LOI value from 22.5 to 29.5, enhancement of vertical burning ratings from V2 to V0 and decrease in maximum heat release rate from 375 to 300 kW/m^2 were observed by addition of 15% of AlPi into PA6, all of which indicated increase in flame retardancy of PA6 [**51**].

A strong peak, with a shoulder at high temperature side, at around 430°C, and a maximum at around 417°C, is seen in the TIC curve of PA6/AlPi (Figure 3-27). Mass spectrum recorded at around 417°C (also given in the figure) is dominated by the diagnostic peaks of both AlPi and PA6.

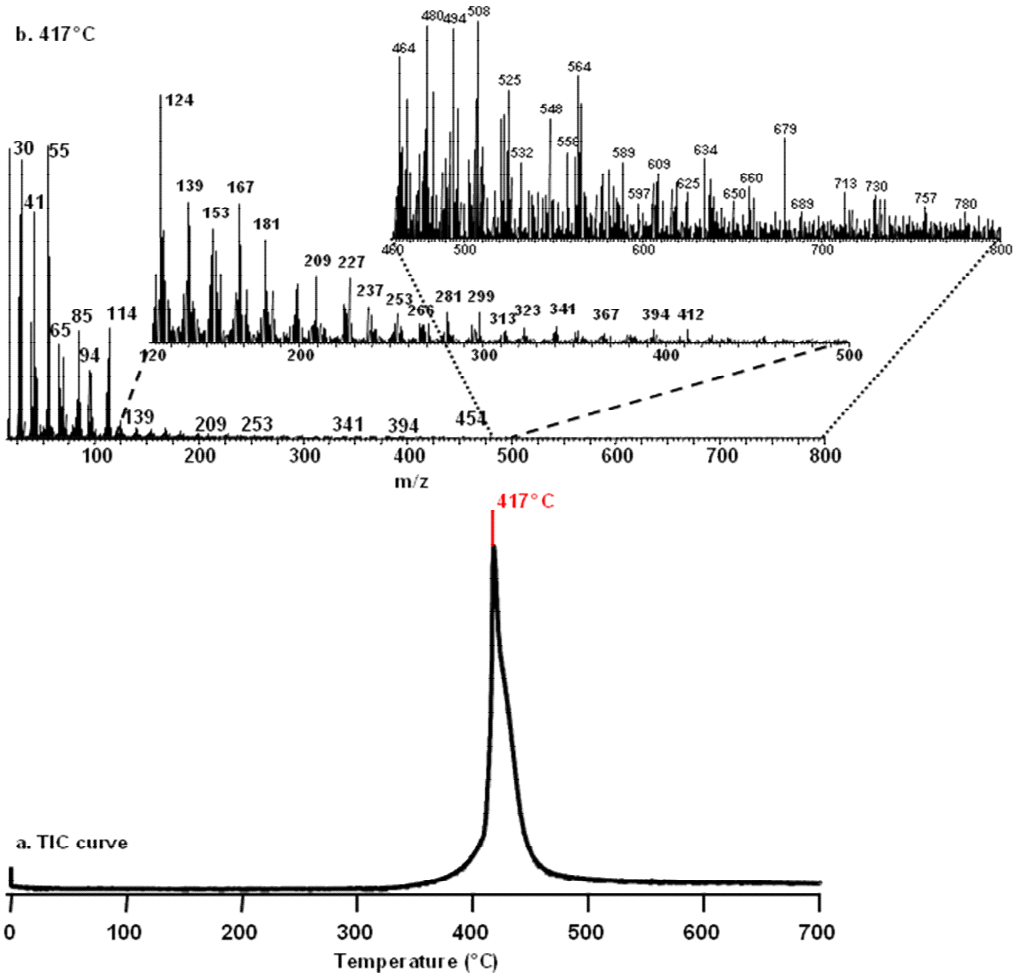

Figure 3-27 a) The TIC curve and b) the pyrolysis mass spectrum at 417°C of PA6 involving 15% AlPi

The relative intensities of some selected peaks detected in the mass spectrum of PA6 containing 15% AlPi at 417°C and the assignments made for these peaks, are given in Table 3-13.

Table 3-13 Relative intensities, RI, of characteristic and/or intense peaks recorded in pyrolysis spectrum of PA6/AlPi at 417°C

m/z (Da)	RI	Assignment
18	993.8	H_2O
29	320.3	C_2H_5, NCH_3, AlH_2
30	954.3	NH_2CH_2, AlH_3
44	202.6	NC_2H_6, AlH_2CH_3
45	32.6	HNC_2H_6
47	42.4	PO
55	1000.0	C_4H_7, $AlCH_2CH_2$
65	320.1	P_2H_3, HPO_2H
77	19.9	C_2H_5POH
79	42.1	$HPO(OCH_3)$
94	229.4	$C_2H_5P(OH)_2$
105	9.9	$(C_2H_5)_2PO$
107	3.7	$HPO(O(CH_2)_2CH_3)$
111	153.9	$(CH_2)_5C=NHCH_2$, $(POH)_2CH_3$, $(C_2H)_2(OCH_2)P$
113	269.3	M, $POH(C_2H)CH_3$
114	376.5	MH, $PHOH(C_2H)CH_3$
121	7.9	$HPO(O(CH_2)_3CH_3)$
122	15.4	$(C_2H_5)_2PO_2H$
123	9.8	$(CH_2)_4C=NHCH_2CN$, $(C_2H_5)_2P(OH)_2$
130	2.4	$HN(CH_2)_5COOH$
135	2.2	$HPO(O(CH_2)_4CH_3)$
136	5.3	$PO(C_2H_5)_2(OCH_3)$
139	32.0	MCN, $(C_2H_5)PHO_2PHO$
150	5.2	$PO(C_2H_5)_2(OCH_2CH_3)$
167	31.4	$MC=NCH_2CH_2$, $(C_2H_5)(C_2H_3)PO_2PHO$
169	6.1	$(C_2H_5)_2PO_2PHO$
194	0.9	$C_4H_8NC(NCO(CH_2)_5)$
211	4.2	$((C_2H_5)_2PO_2)_2H$
221	2.1	$C_4H_8NC(NCO(CH_2)_5)CH_2$
298	-	$NCNH(CH_2)_5MC(OH)(NH_2)NHCH_2$
566	0.4	M_5H
591	-	M_5CN
620	-	$M_5H(CH_2)_5C=NCH_2CH_2$
660	0.2	$(C_2H_5)(OP)AlO_2(P(C_2H_5)_2)_2O_2Al[(P(C_2H_5))_2O_2(P(C_2H_5))_2O]$

Single ion evolution profiles of characteristic products recorded during the pyrolysis of PA6/AlPi are shown in Figure 3-28.

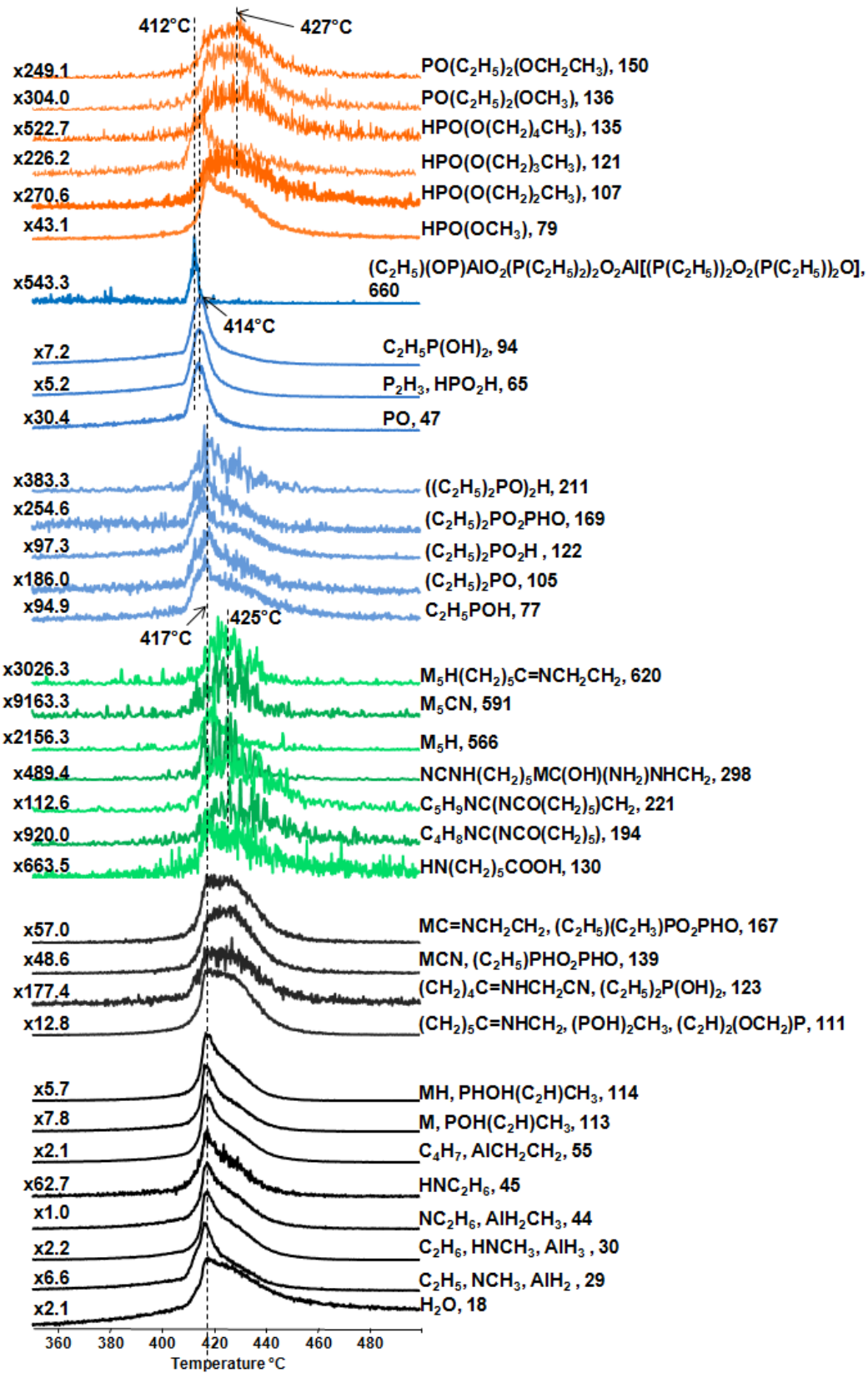

Figure 3-28 Single ion evolution profiles of some characteristic and/or intense pyrolysis products of PA6/AlPi

In the presence of AlPi, relative yields of PA6 based fragments with low mass remain almost unchanged; yet, those of the fragments with high mass are decreased significantly.

Evolution of AlPi based fragments are also detected during the pyrolysis of PA6/AlPi composite; yet, the relative intensities of these fragments differ from those of fragments detected in pyrolysis of pure AlPi. Actually, the decrease in the intensities of AlPi based fragments is expected due to low mass percentage of AlPi in the PA6/AlPi composite. In general, decrease in the relative yields is observed in accordance to expectations. However, the decrease in the relative yield of the high mass fragments is extremely drastic; for instance the decrease in the relative intensity the peak with m/z=660 Da is more than 500 folds whereas, the decrease in those of the peaks with m/z=65 and 47 Da is about 5 folds and that of the peak at m/z=94 Da is about 3 folds.

Larger decrease in the relative intensities of high mass fragments of both PA6 and AlPi may be regarded as an evidence of the existence of interactions between PA6 and AlPi related fragments. Trans-esterification type reactions between NH and ROP groups may increase the yield of phosphinic acid. Furthermore, the reactions between diethylphosphinic acid ($(C_2H_5)_2PO_2H$, 122 Da) and its low mass fragment HPO_2H, 65 Da, as shown in Scheme 3-7, may take place. As a result of such reactions, products such as $(C_2H_5)_2PO_2(CH_2)_xCH_3$ (m/z= 136, 150, 164, 178 and 192 Da for x=0 to 4) or $HPO_2(CH_2)_xCH_3$ (m/z= 79, 93, 107, 121 and 135 Da for x=0 to 4) may be formed.

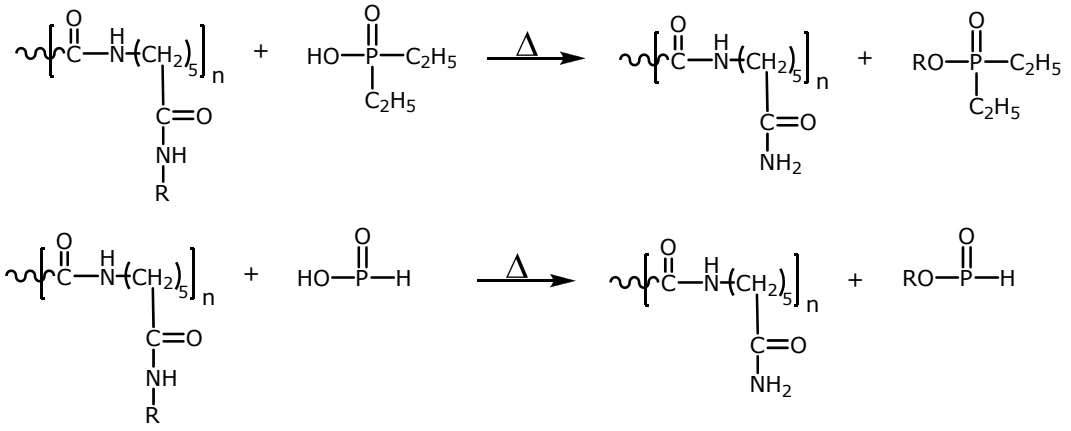

Scheme 3-7 Interaction between PA6 and diethylphosphinic acid or HPO_2H

In general, the significant increases in the relative intensities of characteristic peaks of related fragments such as those at 79 and 136 Da confirm the existence of these reactions, depressing the generation of Al-O-P linkages and inter and intra molecular interactions of PA6 chains.

3.1.8.1. Effect of Addition of Boron Compounds on PA6/AlPi

Addition of BPO_4

Doğan also investigated the effect of addition of BPO_4 on PA6/AlPi composite. According to his findings, the LOI value was slightly decreased from 29.5 to 29, UL-94 rating was remained V0 and the maximum heat release rate was increased from 300 to 345 kW/m^2 upon addition of BPO_4 [**51**]. Figure 3-29 presents the TIC curve of PA6/AlPi involving 1 wt% BPO_4 and the mass spectrum recorded at the peak maximum. The peak due to the thermal degradation of the composite has a maximum at 430°C, indicating increase in thermal stability upon addition of BPO_4. Another noticeable difference which is caused by the addition of BPO_4 is the broadening of the evolution profiles. It can be deduced that the degradation process takes place over a wider temperature range.

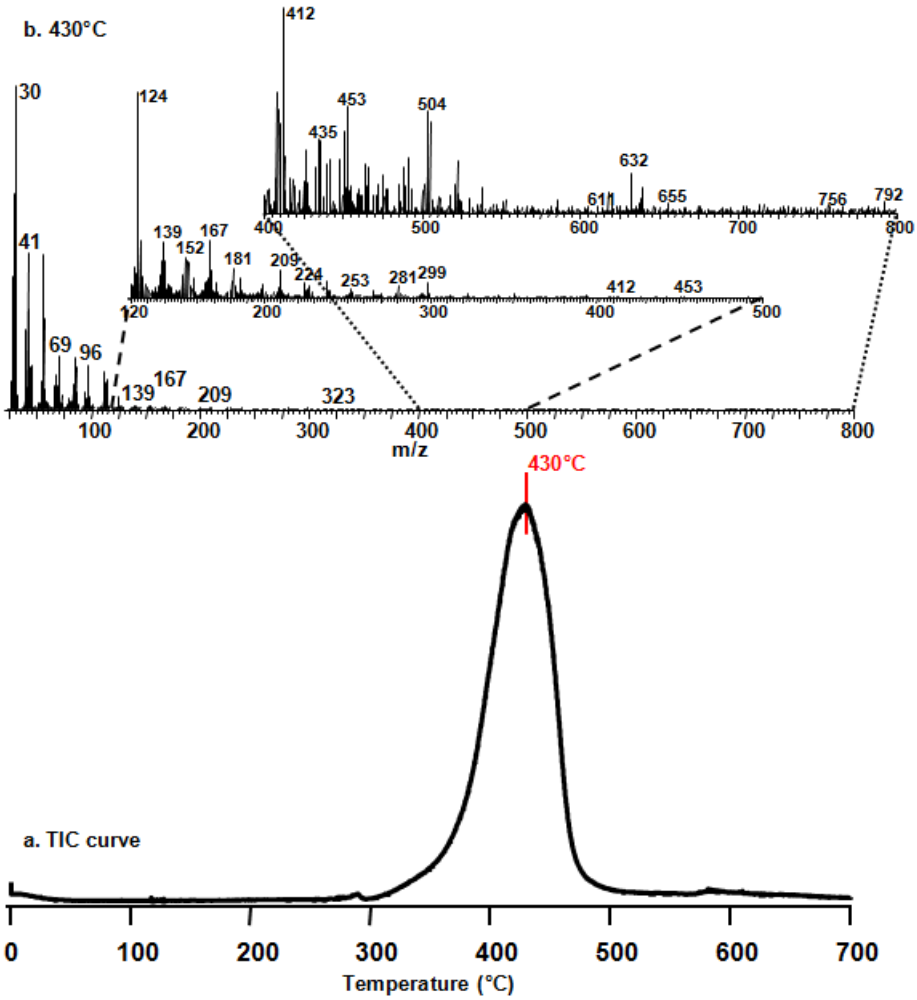

Figure 3-29 a) TIC curve and b) the pyrolysis mass spectrum at 430°C of PA6/AlPi involving 1% BPO_4

Mass spectral data and assignments made for the characteristic and/or intense peaks are summarized in Table 3-14.

Table 3-14 Relative intensities, RI, of characteristic and/or intense peaks recorded in the pyrolysis spectrum of PA6/AlPi involving 1% BPO_4 at 430°C

m/z (Da)	RI	Assignment
29	273.6	C_2H_5, NCH_3, AlH_2
30	1000.0	NH_2CH_2, AlH_3
44	135.0	NC_2H_6, AlH_2CH_3
45	17.2	HNC_2H_6
47	8.2	PO
55	477.1	C_4H_7, $AlCH_2CH_2$
65	72.7	P_2H_3, HPO_2H
77	13.6	C_2H_5POH
79	32.9	$HPO(OCH_3)$
94	50.1	$C_2H_5P(OH)_2$
105	3.5	$(C_2H_5)_2PO$
107	4.2	$HPO(O(CH_2)_2CH_3)$
111	116.7	$(CH_2)_5C=NHCH_2$, $(POH)_2CH_3$, $(C_2H)_2(OCH_2)P$
113	80.7	M, $POH(C_2H)CH_3$
114	91.6	MH, $PHOH(C_2H)CH_3$
121	2.3	$HPO(O(CH_2)_3CH_3)$
122	5.8	$(C_2H_5)_2PO_2H$
123	4.6	$(CH_2)_4C=NHCH_2CN$, $(C_2H_5)_2P(OH)_2$
130	1.2	$HN(CH_2)_5COOH$
135	1.1	$HPO(O(CH_2)_4CH_3)$
136	2.3	$PO(C_2H_5)_2(OCH_3)$
139	10.5	MCN, $(C_2H_5)PHO_2PHO$
150	2.9	$PO(C_2H_5)_2(OCH_2CH_3)$
167	10.9	$MC=NCH_2CH_2$, $(C_2H_5)(C_2H_3)PO_2PHO$
169	1.3	$(C_2H_5)_2PO_2PHO$
194	0.5	$C_4H_8NC(NCO(CH_2)_5)$
211	0.7	$((C_2H_5)_2PO_2)_2H$
221	0.8	$C_4H_8NC(NCO(CH_2)_5)CH_2$
298	0.3	$NCNH(CH_2)_5MC(OH)(NH_2)NHCH_2$
566	-	M_5H
591	-	M_5CN
620	-	$M_5H(CH_2)_5C=NCH_2CH_2$
660	-	$(C_2H_5)(OP)AlO_2(P(C_2H_5)_2)_2O_2Al[(P(C_2H_5))_2O_2(P(C_2H_5))_2O]$

Single ion pyrograms of some selected fragments detected during the pyrolysis of PA6/AlPi involving 1% BPO_4 are shown in Figure 3-30. The corresponding ones recorded during the pyrolysis of PA6/AlPi composite involving no boron compounds are also included in the figure for comparison.

As in the case of peak in TIC curve, single ion evolution profiles, as a result of addition of BPO_4, get broader indicating wider temperature range for thermal degradation.

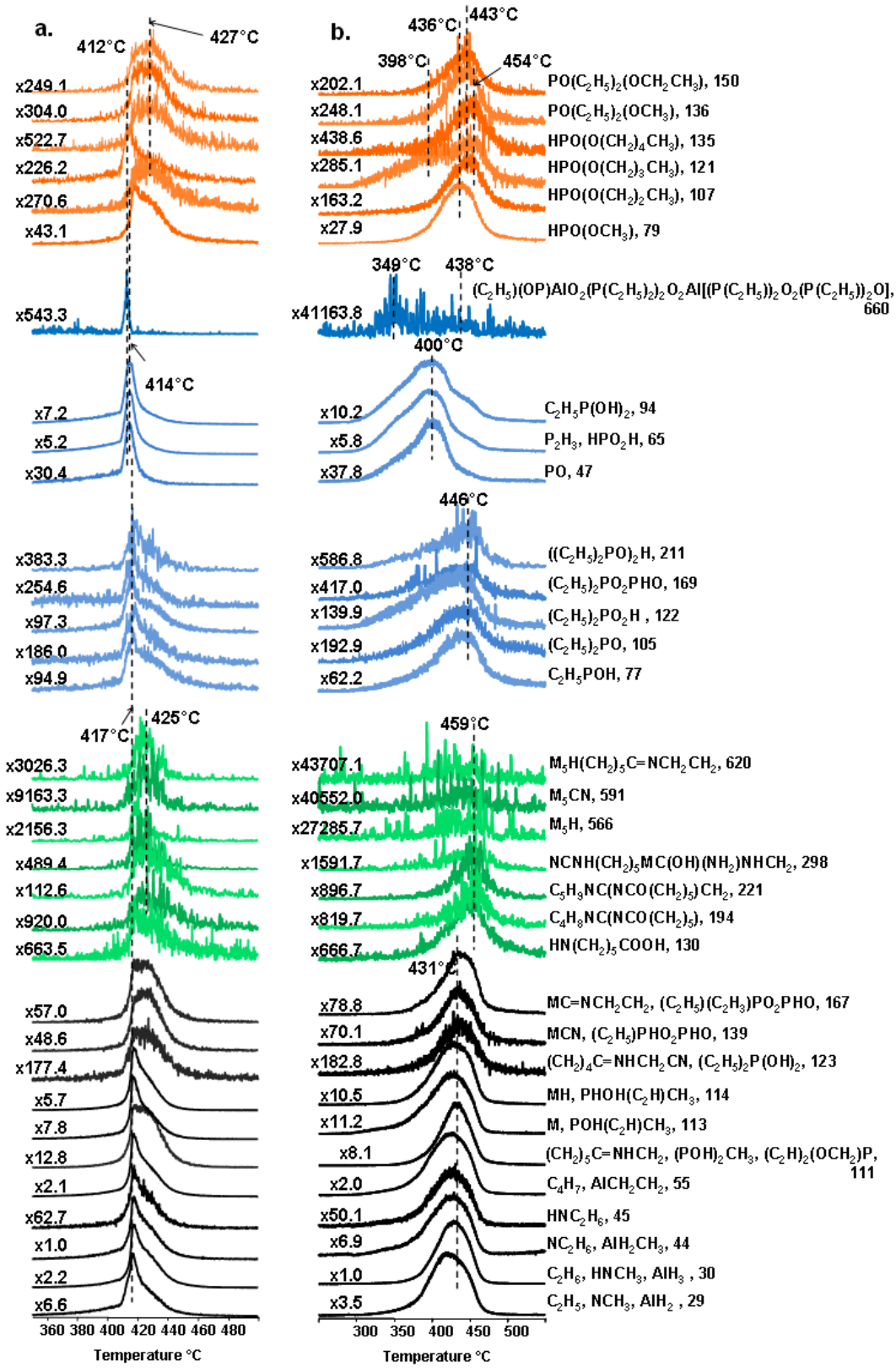

Figure 3-30 Single ion evolution profiles of characteristic and/or intense pyrolysis products of a) PA6/AlPi and b) PA6/ AlPi involving 1% BPO_4

Release of characteristic fragments of PA6 starts at around 350°C and continues up to 430°C, whereas evolution of those of AlPi starts at around 300°C and continues up to 396°C. Actually, almost all intense diagnostic peaks with high mass present in the pyrolysis mass spectra of AlPi are totally disappeared in the presence of 1% BPO_4. Only low mass fragments related to diethylphosphinate are recorded. The relative intensity of the peak m/z=660 Da is decreased about 75 folds whereas those of the peaks m/z=47, 65 and 94 Da are decreased not more than 1.5 folds.

In the evolution profiles of these fragments, a weak shoulder at high temperature regions is also observed. Release of PO (47 Da), HPO_2H (65 Da) and $C_2H_5P(OH)_2$ (94 Da) occurs over a significantly broad temperature range, compared to both PA6/AlPi and pure AlPi. Broadening of the temperature range due to the interactions between PA6 and AlPi is enhanced in the presence of BPO_4. In addition, decrease in the yields of the reaction products of PA6 with AlPi is observed, indicating that the interactions between PA6 and AlPi are inhibited. Consequently, thermal stability of the composite is increased to some extent.

Upon addition of BPO_4 to PA6/AlPi, relative yields of high mass fragments decrease significantly, whereas those of low mass fragments remain almost unchanged. The relative yields of characteristic fragments of AlPi are also decreased noticeably. The presence of BPO_4 partially eliminates the effect of AlPi, which causes decrease in thermal stability of PA6. It may be concluded that inclusion of BPO_4 prevents the interaction between PA6 and AlPi.

Addition of ZnB

By the addition of ZnB into PA6/AlPi composite, no change in the LOI value (29.5) and UL-94 rating (V0) but decrease in the maximum heat release rate (from 300 to 235 kW/m^2) were detected. [**51**].

The TIC curve of PA6/AlPi involving 1 wt% ZnB and the mass spectrum recorded at the peak maximum are given in Figure 3-31. Thermal degradation of PA6/AlPi/ZnB occurs at around 438°C at a higher temperature than that of PA6/AlPi composite. It can be said that thermal stability of PA6/AlPi composite was enhanced upon addition of ZnB. The amount of increase upon addition of ZnB is slightly higher than that of increase upon addition of BPO_4. Furthermore, increase in the width of the peak is also a prominent difference.

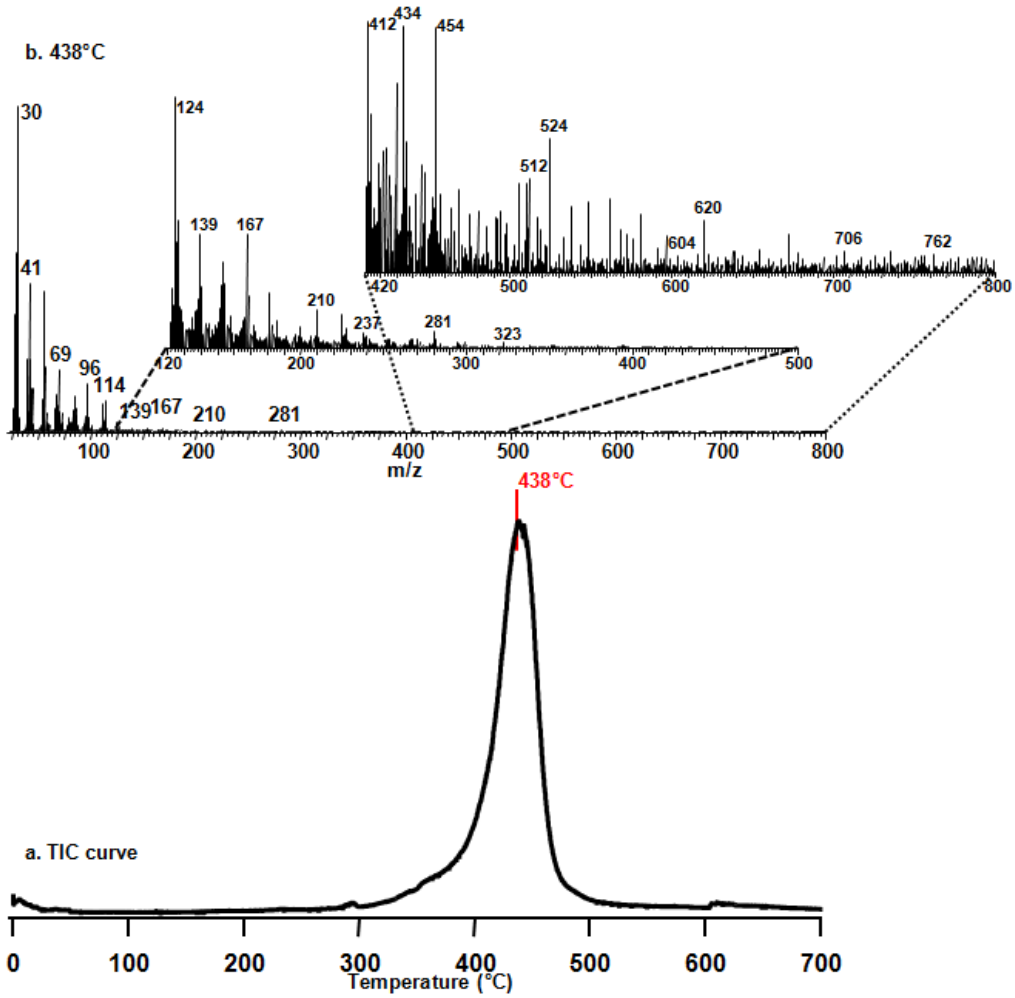

Figure 3-31 a) The TIC curve and b) the pyrolysis mass spectrum at 438°C of PA6/ AlPi involving 1% ZnB

Table 3-15 shows the relative intensities of characteristic and/or intense peaks present in the pyrolysis mass spectrum of PA6/AlPi containing 1% ZnB at 438°C.

Table 3-15 Relative intensities, RI, of characteristic and/or intense peaks recorded in pyrolysis spectrum of PA6/AlPi involving 1% ZnB at 438°C

m/z (Da)	RI	Assignment
29	264.5	C_2H_5, NCH_3, AlH_2
30	1000.0	NH_2CH_2, AlH_3
44	127.8	NC_2H_6, AlH_2CH_3
45	21.5	HNC_2H_6
47	8.0	PO
55	424.0	C_4H_7, $AlCH_2CH_2$
65	70.0	P_2H_3, HPO_2H
77	18.1	C_2H_5POH
79	37.7	$HPO(OCH_3)$
94	49.7	$C_2H_5P(OH)_2$
105	5.4	$(C_2H_5)_2PO$
107	6.0	$HPO(O(CH_2)_2CH_3)$
111	86.7	$(CH_2)_5C=NHCH_2$, $(POH)_2CH_3$, $(C_2H)_2(OCH_2)P$
113	54.6	M, $POH(C_2H)CH_3$
114	96.9	MH, $PHOH(C_2H)CH_3$
121	3.0	$HPO(O(CH_2)_3CH_3)$
122	6.5	$(C_2H_5)_2PO_2H$
123	4.3	$(CH_2)_4C=NHCH_2CN$, $(C_2H_5)_2P(OH)_2$
130	1.5	$HN(CH_2)_5COOH$
135	1.6	$HPO(O(CH_2)_4CH_3)$
136	3.1	$PO(C_2H_5)_2(OCH_3)$
139	14.2	MCN, $(C_2H_5)PHO_2PHO$
150	3.1	$PO(C_2H_5)_2(OCH_2CH_3)$
167	12.0	$MC=NCH_2CH_2$, $(C_2H_5)(C_2H_3)PO_2PHO$
169	1.1	$(C_2H_5)_2PO_2PHO$
194	0.4	$C_4H_8NC(NCO(CH_2)_5)$
211	0.8	$((C_2H_5)_2PO_2)_2H$
221	0.3	$C_4H_8NC(NCO(CH_2)_5)CH_2$
298	0.1	$NCNH(CH_2)_5MC(OH)(NH_2)NHCH_2$
566	-	M_5H
591	-	M_5CN
620	-	$M_5H(CH_2)_5C=NCH_2CH_2$
660	-	$(C_2H_5)(OP)AlO_2(P(C_2H_5)_2)_2O_2Al[(P(C_2H_5))_2O_2(P(C_2H_5))_2O]$

Figure 3-32 presents single ion evolution profiles of some selected and characteristic fragments detected during the pyrolysis of PA6/AlPi involving 1% ZnB. In order to make the comparison easier, the corresponding ones recorded during the pyrolysis of PA6/AlPi composite involving no boron compounds are also included in the figure.

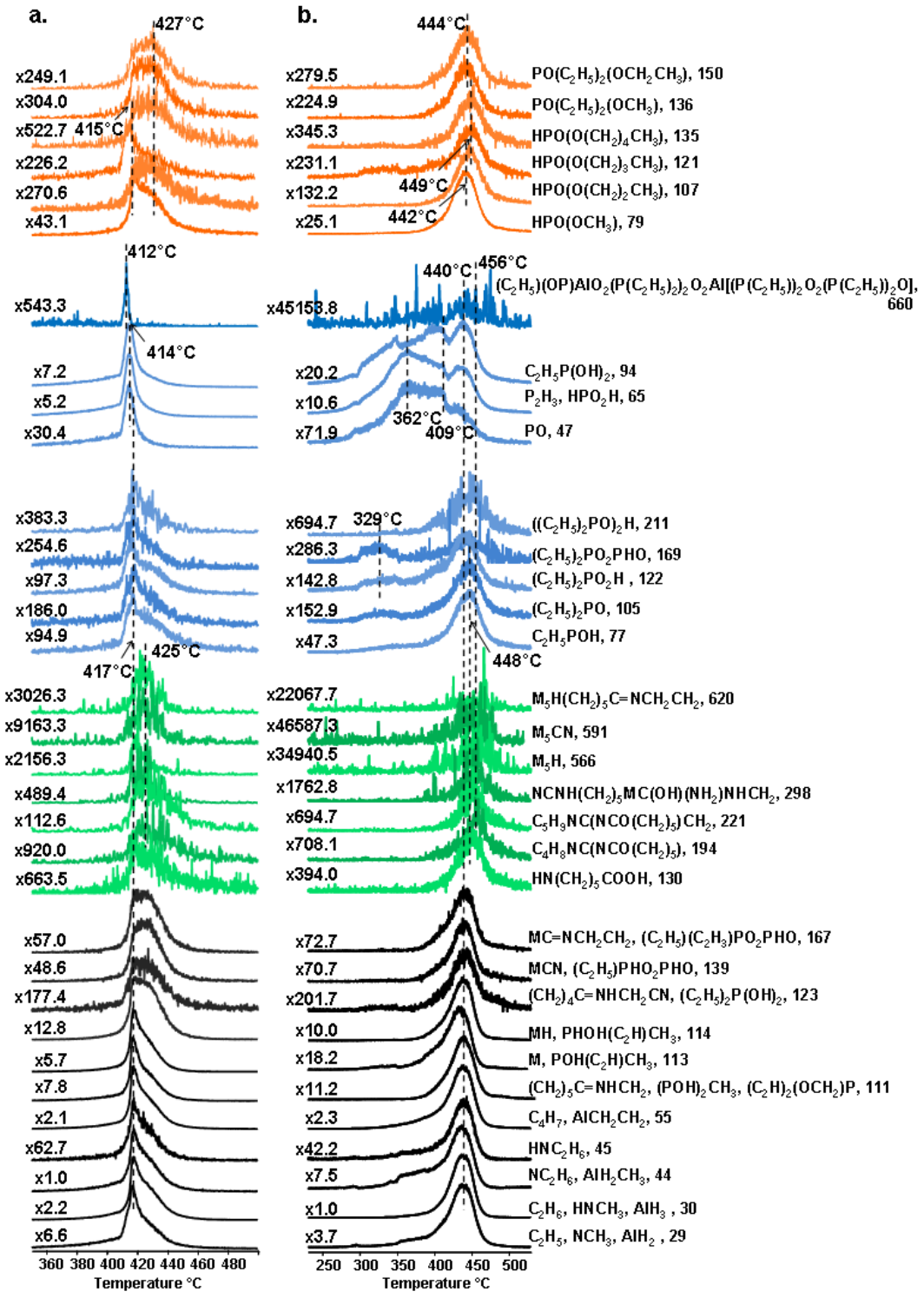

Figure 3-32 Single ion evolution profiles of characteristic and/or intense pyrolysis products of a) PA6/AlPi and b) PA6/AlPi involving 1% ZnB

By addition of ZnB, almost all diagnostic pyrolysis products of AlPi are again disappeared. The broadening in the single ion evolution profiles of HPO_2H and $C_2H_5P(OH)_2$ is even greater than that was observed in the presence of BPO_4. Upon addition of ZnB, decrease in the interaction between PA6 and AlPi may explain the broadening. It is observed that reduction effect of ZnB on interaction is more than that of BPO_4. This may cause increase in thermal stability. Moreover, inclusion of ZnB decreases the relative yields of products formed via reaction between PA6 and AlPi (Scheme 3-7). Release of these products is started just above 300°C. In addition, the trends observed in their evolution profiles are different, indicating degradation through different pathways.

Evolution of high mass fragments such as fragments with m/z= 660 Da has been maximized at around 440°C. Relative intensity of the peak with m/z= 660 Da, is decreased significantly, approximately 83 folds. Loss of low mass fragments, such as fragments with m/z= 47, 65, 94 Da, is decreased more than 2 folds.

Consequently, relative yields of diagnostic products of PA6 with low mass fragments are decreased slightly, whereas those of diagnostic products of PA6 with high mass fragments are diminished noticeably. The relative yields of characteristic fragments of AlPi are also decreased remarkably. The influence of addition of AlPi, which results in significant decrease in thermal stability of PA6, is partially eliminated by the addition of ZnB. As in case of addition of BPO_4, presence of ZnB may weaken the interaction between PA6 and AlPi. Upon addition of ZnB, larger decrease in relative intensities of the products formed by the reaction between PA6 and AlPi is more pronounced, as compared to that observed upon addition of BPO_4. Thus, it may be concluded that as the interaction weakens, the thermal stability is improved more.

3.1.9. PA6/Aluminum Diethylphosphinate (PA6/AlPi) with Cloisite 30B

Doğan investigated the effect of Cloisite 30B on flame retardancy properties of PA6/AlPi composite. It was determined that upon addition of Cloisite 30B to PA6/AlPi, LOI value (29.5) and UL-94 rating (V0) remained unchanged; whereas, a slight increase in the maximum heat release rate (from 300 to 315 kW/m^2) occurred [**51**].

Figure 3-33 shows the TIC curve of PA6/AlPi involving 1 wt% Cloisite 30B and the mass spectrum recorded at the peak maximum. The thermal degradation of PA6/AlPi/Cloisite 30B takes place at around 450°C, at a higher temperature region than that of PA6/AlPi composite. Addition of Cloisite 30B to PA6/AlPi composite helps to defeat the negative effect of addition of AlPi in terms of thermal stability of PA6.

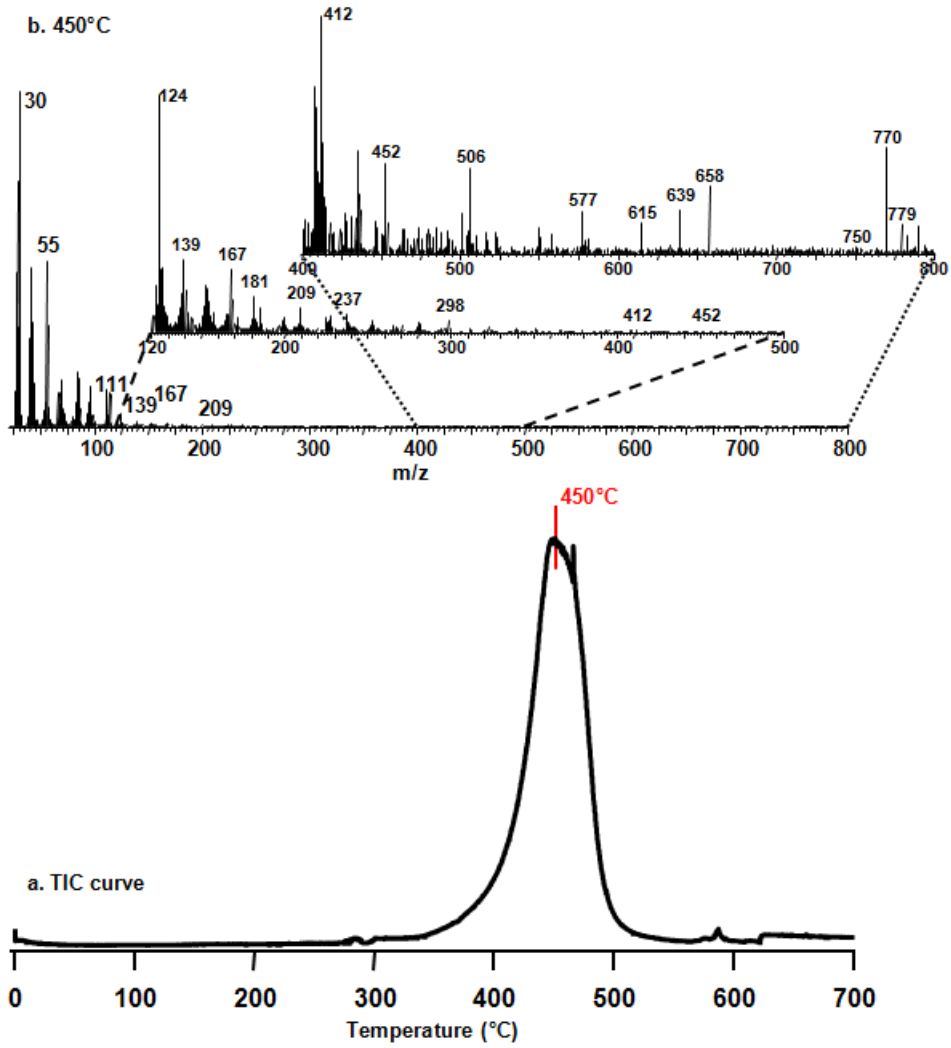

Figure 3-33 a) The TIC curve and b) the pyrolysis mass spectrum at 450°C of PA6/AlPi involving 1% Cloisite 30B

The relative intensities of some characteristic and/or intense peaks present in the pyrolysis mass spectrum of PA6/AlPi and 1% Cloisite 30B at 450°C are summarized in Table 3-16.

Table 3-16 Relative intensities, RI, of characteristic and/or intense peaks recorded in pyrolysis spectrum of PA6/AlPi involving 1% Cloisite 30B at 450°C

m/z (Da)	RI	Assignment
29	297.0	C_2H_5, NCH_3, AlH_2
30	1000.0	NH_2CH_2, AlH_3
44	129.5	NC_2H_6, AlH_2CH_3
45	16.3	HNC_2H_6
47	16.3	PO
55	493.1	C_4H_7, $AlCH_2CH_2$
65	101.7	P_2H_3, HPO_2H
77	13.2	C_2H_5POH
79	27.6	$HPO(OCH_3)$
94	69.5	$C_2H_5P(OH)_2$
105	3.1	$(C_2H_5)_2PO$
107	3.6	$HPO(O(CH_2)_2CH_3)$
111	107.9	$(CH_2)_5C=NHCH_2$, $(POH)_2CH_3$, $(C_2H)_2(OCH_2)P$
113	97.9	M, $POH(C_2H)CH_3$
114	92.5	MH, $PHOH(C_2H)CH_3$
121	2.4	$HPO(O(CH_2)_3CH_3)$
122	6.8	$(C_2H_5)_2PO_2H$
123	4.1	$(CH_2)_4C=NHCH_2CN$, $(C_2H_5)_2P(OH)_2$
130	1.0	$HN(CH_2)_5COOH$
135	1.2	$HPO(O(CH_2)_4CH_3)$
136	2.4	$PO(C_2H_5)_2(OCH_3)$
139	10.7	MCN, $(C_2H_5)PHO_2PHO$
150	2.5	$PO(C_2H_5)_2(OCH_2CH_3)$
167	9.3	$MC=NCH_2CH_2$, $(C_2H_5)(C_2H_3)PO_2PHO$
169	1.2	$(C_2H_5)_2PO_2PHO$
194	0.2	$C_4H_8NC(NCO(CH_2)_5)$
211	0.6	$((C_2H_5)_2PO_2)_2H$
221	0.3	$C_4H_8NC(NCO(CH_2)_5)CH_2$
298	1.7	$NCNH(CH_2)_5MC(OH)(NH_2)NHCH_2$
566	-	M_5H
591	-	M_5CN
620	-	$M_5H(CH_2)_5C=NCH_2CH_2$
660	-	$(C_2H_5)(OP)AlO_2(P(C_2H_5)_2)_2O_2Al[(P(C_2H_5))_2O_2(P(C_2H_5))_2O]$

Figure 3-34 presents single ion evolution profiles of some selected characteristic and/or intense fragments detected during the pyrolysis of PA6/AlPi involving 1% Cloisite 30B and pyrolysis of PA6/AlPi composite involving no boron compounds, side by side.

At the first glance, the difference in the evolution profiles of the fragments with m/z values of 65 and 94 Da draws attention. Additionally, similar to the cases of addition of both BPO_4 and ZnB, evolution of most of the characteristic fragments occurs over broader temperature ranges.

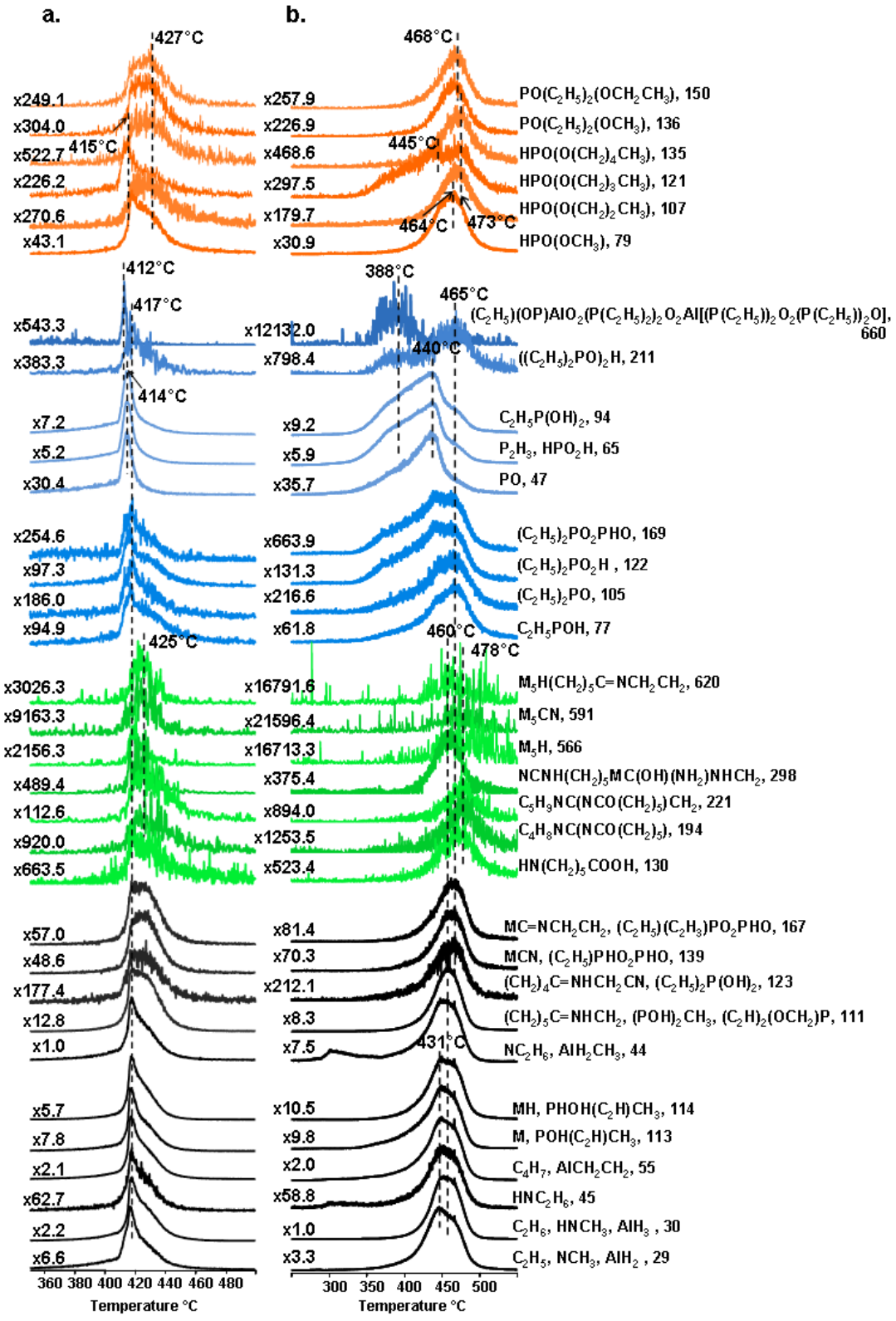

Figure 3-34 Single ion evolution profiles of some characteristic and/or intense pyrolysis products of a) PA6/AlPi and b) PA6/AlPi involving 1% Cloisite 30B

Due to the addition of Cloisite 30B, the relative yields of the high mass fragments decrease significantly; yet, only a slight amount of decrease in those of the low mass fragments is observed. For instance, relative intensity of the peak with m/z= 660 Da, is decreased noticeably, approximately 22 folds. Loss of low mass fragments, such as fragments with m/z= 47, 65, 94 Da, is decreased less than 1.5 folds.

The maximum of the single ion evolution profiles of PA6 based products shifts to noticeably higher values, from 417°C to 460°C. On the other hand, thermal degradation of AlPi shifts to higher temperature. Related products are maximized at around 440°C, indicating a shift of 26°C. Furthermore, a weak shoulder at around 465°C is appeared in the evolution profiles of AlPi based products. Thermal stability, which was decreased by addition of AlPi, is enhanced by addition of Cloisite 30B to PA6/AlPi composite. This may be explained by the decrease in the interactions between AlPi and PA6. Furthermore, evolution profiles get broader. Reduction of the interaction in the presence of Cloisite 30B may explain this broadening of the pyrograms.

Addition of AlPi to PA6 decreases thermal degradation temperature range of PA6. Whereas, when Cloisite 30B is added to this composite, influence of addition of AlPi is noticeably eliminated and thermal degradation temperature of PA6 shifts to a higher temperature regions (though, not to as high as that of pristine PA6).

The effect of Cloisite 30B is dominant, which may be due to the delamination of silicate layers within the polymer chains, which may cause much more decrease in interaction between PA6 and AlPi. Consequently, decrease in the relative yields of the products formed by the reaction between PA6 and AlPi is observed. In addition, thermal stability increases by addition of Cloisite 30B.

3.1.9.1. Effect of Addition of Boron Compounds on PA6/AlPi/Cloisite 30B

Addition of BPO_4

Doğan states in his Ph.D. study that, by the addition of BPO_4 to PA6/AlPi/Cloisite 30B composite, no change in the LOI value (29.5) and UL-94 rating (V0); reduction in the maximum heat release rate (from 300 to 288 kW/m^2) were observed [**51**]. Figure 3-35 presents the TIC curve of PA6/AlPi/Cloisite 30B involving 1 wt% BPO_4, and the mass spectrum recorded at the peak maximum. The thermal degradation temperature of BPO_4 containing composite shifts to higher temperature region (462°C), compared to that of PA6/AlPi/Cloisite 30B composite, indicating increase in thermal stability.

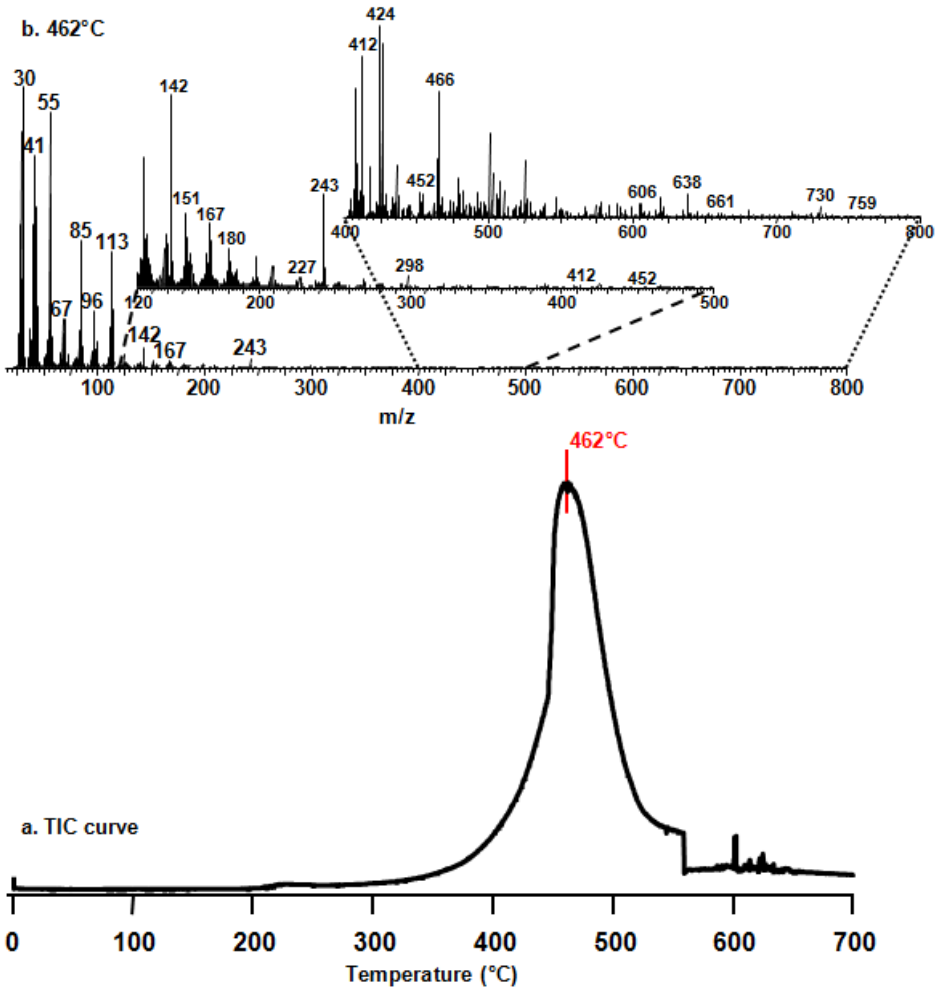

Figure 3-35 a) The TIC curve and b) the pyrolysis mass spectrum at 462°C of PA6/AlPi/Cloisite 30B involving 1% BPO_4

Table 3-17 shows the relative intensities of characteristic and/or intense peaks present in the pyrolysis mass spectrum of PA6/AlPi/Cloisite 30B involving 1% BPO_4 at 462°C.

Table 3-17 Relative intensities, RI, of characteristic and/or intense peaks recorded in pyrolysis spectrum of PA6/AlPi/Cloisite 30B involving 1% BPO_4 at 462°C

m/z (Da)	RI	Assignment
29	316.4	C_2H_5, NCH_3, AlH_2
30	1000.0	NH_2CH_2, AlH_3
44	225.0	NC_2H_6, AlH_2CH_3
45	16.3	HNC_2H_6
47	3.2	PO
55	911.3	C_4H_7, $AlCH_2CH_2$
65	53.4	P_2H_3, HPO_2H
77	21.2	C_2H_5POH
79	32.0	$HPO(OCH_3)$
94	51.2	$C_2H_5P(OH)_2$
105	9.8	$(C_2H_5)_2PO$
107	6.7	$HPO(O(CH_2)_2CH_3)$
111	146.6	$(CH_2)_5C{=}NHCH_2$, $(POH)_2CH_3$, $(C_2H)_2(OCH_2)P$
113	411.8	M, $POH(C_2H)CH_3$
114	202.9	MH, $PHOH(C_2H)CH_3$
121	3.8	$HPO(O(CH_2)_3CH_3)$
122	10.9	$(C_2H_5)_2PO_2H$
123	10.5	$(CH_2)_4C{=}NHCH_2CN$, $(C_2H_5)_2P(OH)_2$
130	2.5	$HN(CH_2)_5COOH$
135	3.0	$HPO(O(CH_2)_4CH_3)$
136	6.5	$PO(C_2H_5)_2(OCH_3)$
139	17.6	MCN, $(C_2H_5)PHO_2PHO$
150	6.5	$PO(C_2H_5)_2(OCH_2CH_3)$
167	21.5	$MC{=}NCH_2CH_2$, $(C_2H_5)(C_2H_3)PO_2PHO$
169	4.2	$(C_2H_5)_2PO_2PHO$
194	0.7	$C_4H_8NC(NCO(CH_2)_5)$
211	2.3	$((C_2H_5)_2PO_2)_2H$
221	0.2	$C_4H_8NC(NCO(CH_2)_5)CH_2$
298	4.4	$NCNH(CH_2)_5MC(OH)(NH_2)NHCH_2$
566	-	M_5H
591	-	M_5CN
620	-	$M_5H(CH_2)_5C{=}NCH_2CH_2$
660	-	$(C_2H_5)(OP)AlO_2(P(C_2H_5)_2)_2O_2Al[(P(C_2H_5))_2O_2(P(C_2H_5))_2O]$

Single ion pyrograms of some selected and characteristic fragments detected during the pyrolysis of PA6/AlPi/Cloisite 30B involving 1% BPO_4, and PA6/AlPi/Cloisite 30B composites are shown in Figure 3-36.

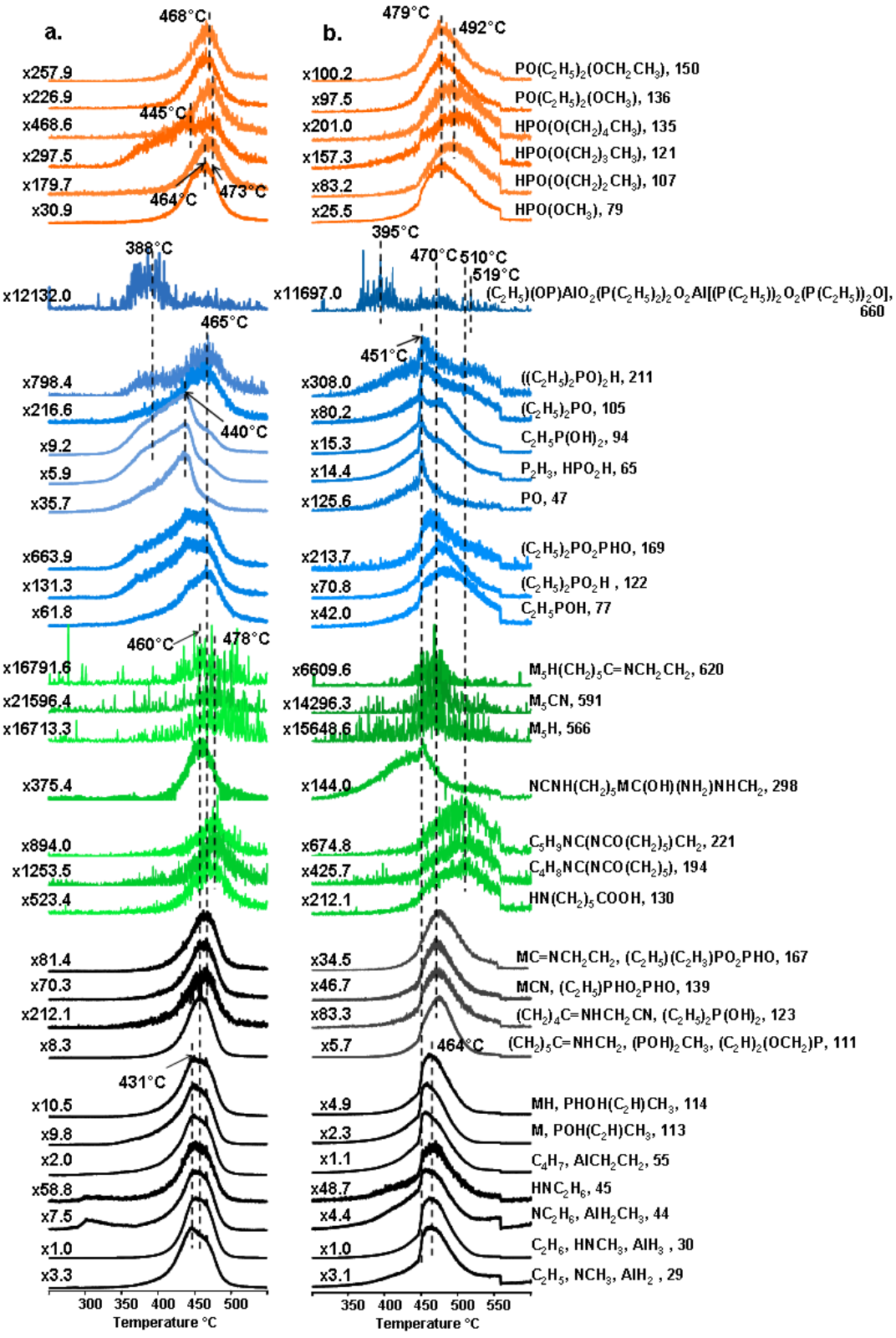

Figure 3-36 Single ion evolution profiles of characteristic and/or intense pyrolysis products of a) PA6/AlPi/Cloisite 30B and b) PA6/AlPi/Cloisite 30B involving 1% BPO_4

Evolution of all the fragments starts at around 400°C and continues up to 464°C. In the evolution profile of the fragment with m/z value of 211 Da, a weak shoulder at high temperature region (approximately 520°C) is detected.

The yield of products due to intermolecular interactions, such as products with m/z= 130, 194 and 211 Da, is decreased but their generation is shifted to significantly high temperatures by the addition of BPO_4 to PA6/AlPi/Cloisite 30B composite.

Upon addition of BPO_4 to PA6/AlPi/Cloisite 30B, relative intensities of all the fragments, except fragments with m/z values of 47, 65 and 94 Da, are increased by various amounts. Fragments with m/z values of 47, 65 and 94 Da have lower relative intensities. Moreover, by the inclusion of BPO_4, relative yields of products formed through the reaction between PA6 and AlPi are increased more than 2 folds. Yet, delamination of Cloisite 30B within the composite may retard the interaction between PA6 and AlPi, causing improvement in the thermal stability. On the other hand, in the presence of BPO_4, broadening of the evolution profiles is observed. It may be explained by the retardation of the interactions.

As mentioned in Section 3.1.8.1, addition of BPO_4 to PA6/AlPi results in increase in thermal stability of PA6/AlPi. Therefore, it may be concluded that, Cloisite 30B and BPO_4 act together so as to eliminate the negative influence of addition of AlPi to PA6; hence addition of BPO_4 improves thermal stability of PA6/AlPi/ Cloisite 30B.

Addition of ZnB

Investigation of the effect of addition of ZnB on PA6/AlPi/Cloisite 30B was also performed by Doğan. It was determined that, upon addition of ZnB to PA6/AlPi/Cloisite 30B, there was no change in UL-94 rating, slight increase in LOI value (from 29.5 to 31) and noticeable decrease in heat release rate (from 300 to 186 kW/m^2), all of which points to increase in flame retardancy [**51**].

The TIC curve of PA6/AlPi/Cloisite 30B containing ZnB, showing a broad peak with a maximum at around 452°C (Figure 3-37), indicates a significant increase in thermal stability compared to that of PA6/AlPi composite. On the other hand, as mentioned in the previous section, the presence of Cloisite 30B increases the thermal stability of PA6/AlPi composite already and the maximum of the evolution profiles is shifted to 450°C. Thus, it may be concluded that the addition of ZnB does not have any significant effect on thermal stability of PA6/AlPi/Cloisite 30B composite. In the mass spectrum (Figure 3-37), recorded at the peak maximum of TIC curve of PA6/AlPi/Cloisite 30B/ZnB, same fragments with the ones observed in mass spectrum of PA6/AlPi/Cloisite 30B composite are detected; however, changes in their relative intensities are determined.

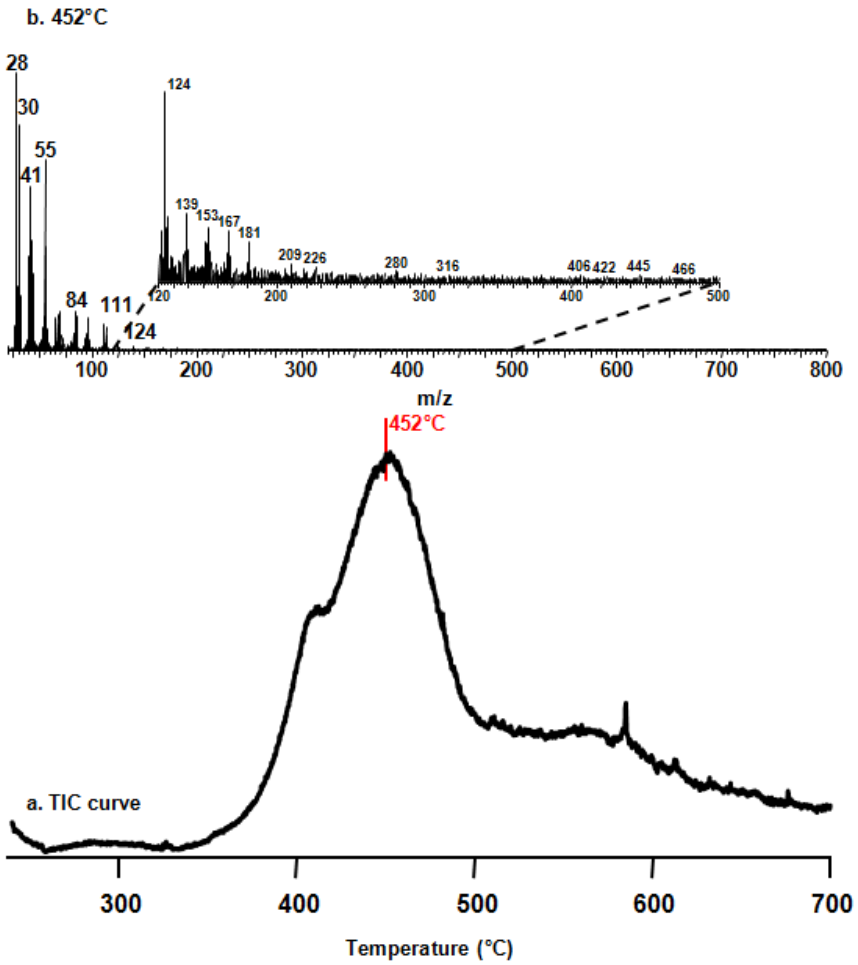

Figure 3-37 a) The TIC curve and b) the pyrolysis mass spectrum at 452°C of PA6/AlPi/Cloisite 30B involving 1% ZnB

Mass spectral data, such as relative intensities of characteristic and/or intense peaks and the assignments made, are summarized in Table 3-18.

Table 3-18 Relative intensities, RI, of characteristic and/or intense peaks recorded in the pyrolysis spectrum of PA6/AlPi/Cloisite 30B involving 1% ZnB at 452°C

m/z (Da)	RI	Assignment
29	306.9	C_2H_5, NCH_3, AlH_2
30	1000.0	NH_2CH_2, AlH_3
44	360.5	NC_2H_6, AlH_2CH_3
45	30.1	HNC_2H_6
47	17.2	PO
55	907.5	C_4H_7, $AlCH_2CH_2$
65	141.7	P_2H_3, HPO_2H
77	35.4	C_2H_5POH
79	39.2	$HPO(OCH_3)$
94	82.4	$C_2H_5P(OH)_2$
105	8.5	$(C_2H_5)_2PO$
107	7.5	$HPO(O(CH_2)_2CH_3)$
111	102.5	$(CH_2)_5C=NHCH_2$, $(POH)_2CH_3$, $(C_2H)_2(OCH_2)P$
113	97.8	M, $POH(C_2H)CH_3$
114	67.7	MH, $PHOH(C_2H)CH_3$
121	2.8	$HPO(O(CH_2)_3CH_3)$
122	8.5	$(C_2H_5)_2PO_2H$
123	5.3	$(CH_2)_4C=NHCH_2CN$, $(C_2H_5)_2P(OH)_2$
130	3.1	$HN(CH_2)_5COOH$
135	3.4	$HPO(O(CH_2)_4CH_3)$
136	5.3	$PO(C_2H_5)_2(OCH_3)$
139	11.6	MCN, $(C_2H_5)PHO_2PHO$
150	2.8	$PO(C_2H_5)_2(OCH_2CH_3)$
167	12.2	$MC=NCH_2CH_2$, $(C_2H_5)(C_2H_3)PO_2PHO$
169	1.3	$(C_2H_5)_2PO_2PHO$
194	1.3	$C_4H_8NC(NCO(CH_2)_5)$
211	1.3	$((C_2H_5)_2PO_2)_2H$
221	0.9	$C_4H_8NC(NCO(CH_2)_5)CH_2$
298	1.9	$NCNH(CH_2)_5MC(OH)(NH_2)NHCH_2$
566	0.3	M_5H
591	0.9	M_5CN
620	0.3	$M_5H(CH_2)_5C=NCH_2CH_2$
660	-	$(C_2H_5)(OP)AlO_2(P(C_2H_5)_2)_2O_2Al[(P(C_2H_5))_2O_2(P(C_2H_5))_2O]$

The trends in the single ion evolution profiles of PA6/AlPi/Cloisite 30B involving ZnB significantly differ from those of PA6/AlPi/Cloisite 30B (Figure 3-38). Addition of ZnB slightly affects the relative yields of fragments.

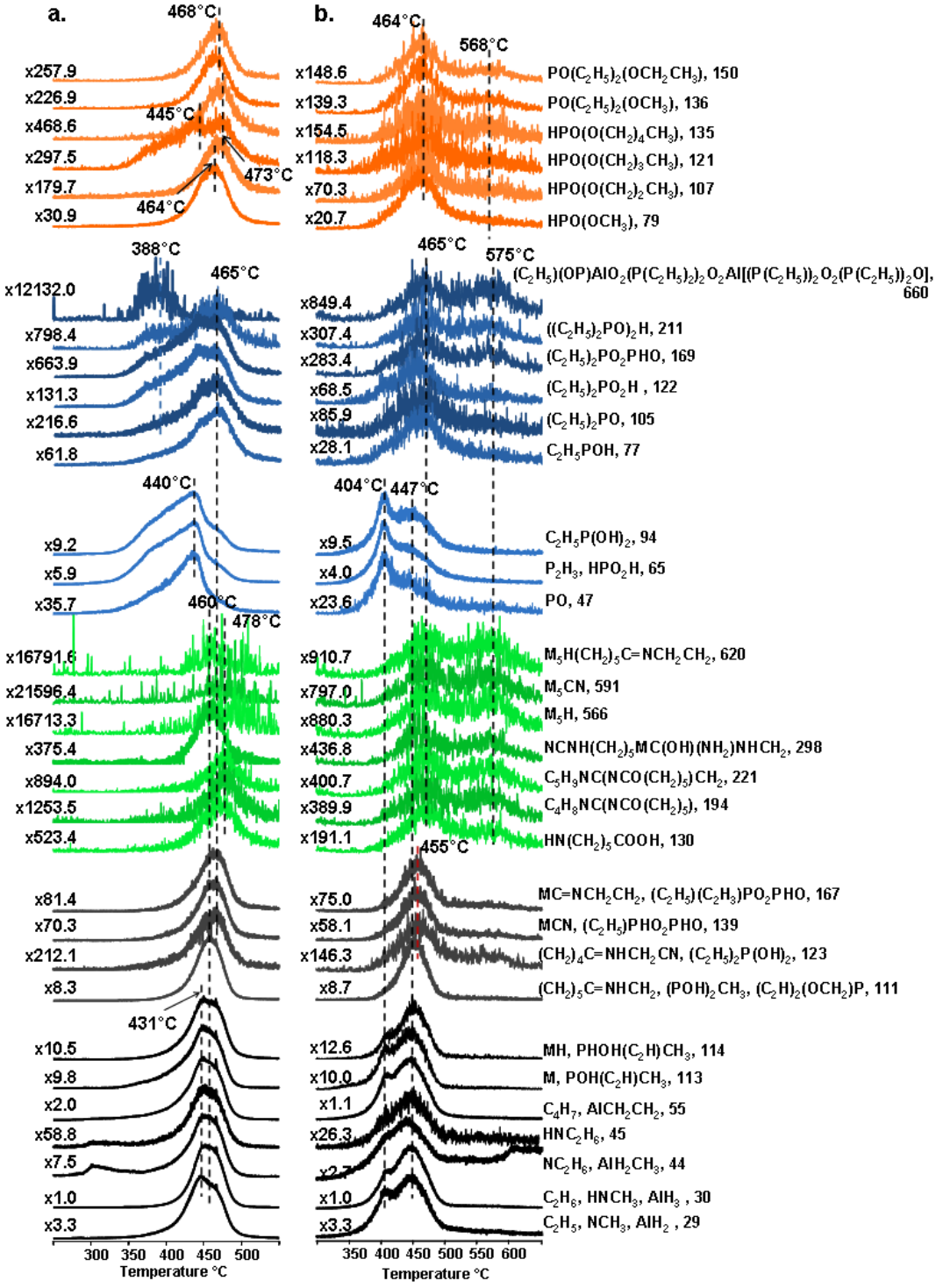

Figure 3-38 Single ion evolution profiles of some characteristic and/or intense pyrolysis products of a) PA6/AlPi/Cloisite 30B and b) PA6/AlPi/Cloisite 30B involving 1% ZnB

The trends in single ion evolution profiles (Figure 3-38) reveal that generation of some of the characteristic thermal degradation fragments of PA6/AlPi/Cloisite 30B involving ZnB occurs in two distinct temperature regions.

Evolution of products due to intermolecular interactions, such as products with m/z= 130, 194 and 211 Da, are also maximized at two different temperatures, one of which is observed at noticeably high temperature (around 575°C). On the other hand, the yield of these products is decreased, by the addition of ZnB to PA6/AlPi/Cloisite 30B composite.

Relative intensities of all the fragments are increased by various amounts. Additionally, relative yields of products with high mass formed through the reaction between PA6 and AlPi (Scheme 3-7) are increased more than 2.5 folds. This may be accepted as a direct evidence for the improvement of the interaction between PA6 and AlPi by the addition of ZnB. However, due to delamination of Cloisite 30B within the composite, the interaction between PA6 and AlPi may occur at higher temperature region, which results in improvement of the thermal stability.

Addition of ZnB results in broadening of the evolution profiles and occurrence of two peaks in the evolution profiles; because, contrary to BPO_4, formation of boron aluminum phosphate layer is occurred in the presence of ZnB [**51**]. Therefore, degradation of AlPi and PA6 takes place alternately. At higher temperatures, reactions between PA6 and AlPi occur. Therefore, variations in the trends of the evolution profiles are observed.

Upon addition of BPO_4 and ZnB, increase in the relative yields of products generated by the reaction mentioned in Scheme 3-7 is observed. In the presence of ZnB, the amount of increase is slightly greater than that of BPO_4. Two broad peaks are observed in the evolution profiles of PA6/AlPi/Cloisite 30B in the presence of ZnB, whereas a single broad peak is observed in the presence of BPO_4.

The amount of improvement in thermal stability detected due to addition of BPO_4 is greater than that detected due to addition of ZnB.

Among the PA6 based samples analyzed, the most thermally stable composite is obtained via addition of Me and BPO_4 into PA6. Contrarily, addition of AlPi into PA6 yields the least thermally stable composite. Addition of boron compounds into PA6/AlPi composite increases the thermal stability to some extent; still the resultant thermal stability is lower than that of pristine PA6.

3.2. The Effects of Boron Compounds on Thermal Degradation Characteristics of PP Composites

In order to investigate the effects of boron compounds on thermal degradation characteristics of PP composites, thermal degradation behaviors of each component of the composites, mixtures of different components and pristine polymer have to be known. Thus, DP-MS analyses of PP, PP-g-MA, Cloisite 15A and IFR (APP:PER=3:1) and PP

involving 5% PP-g-MA and 2% Cloisite 15A, PP involving 5% PP-g-MA, 2% Cloisite 15A and 20% IFR are performed and analyzed for comparison.

3.2.1. Polypropylene (PP)

Investigation of thermal degradation properties of PP is a widely studied topic in the literature [**45**-**48**, **50**]. It has been determined that thermal degradation of PP proceeds predominately by random chain breakages and the fragments generated are stabilized by H-transfer reactions. Burning characteristics of PP and the effects of various flame retardants on these have also been investigated by several scientists [**26**, **44**, **48**-**50**]. Recently, Dogan et al. stated that PP has LOI value of 17.5 and BC (Burn to Clamp) rating in UL-94 testing [**25**].

Pyrolysis of polypropylene yielded a TIC curve showing a single peak with a maximum at 469°C in accordance with the single step thermal decomposition mechanism for PP (Figure 3-39). The peaks due to low mass fragments are more intense due to the further dissociation of high mass pyrolysis products during dissociative ionization process. As a consequence, series of products with M_x, M_x-H, M_xH, M_xCH_3, $M_xCH_2CH_3$, and $M_xCH{=}CH_2$ (where M is the monomer, CH_3CHCH_2 and x= 1 to 6) are produced. Among these, the series with formula M_x-H and $M_xCH{=}CH_2$ are the most abundant. Furthermore, peaks due to HM_xH, (for x=1 to 6) and fragments involving extensive unsaturation, such as, C_6H_7 (79 Da) and C_6H_9 (81 Da) are detected.

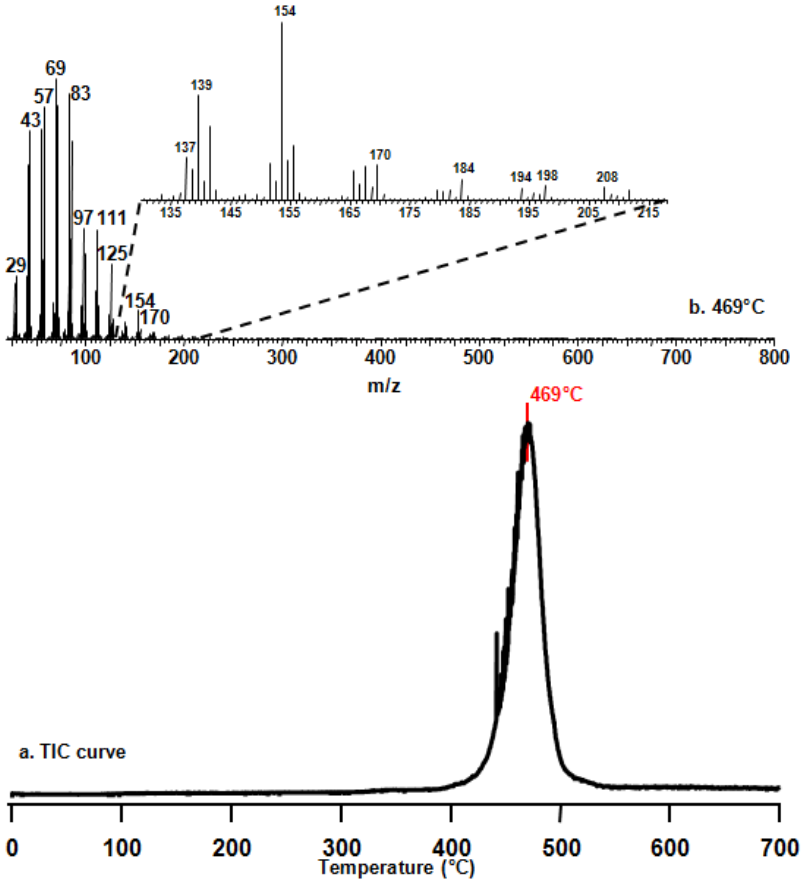

Figure 3-39 a) The TIC curve and b) the pyrolysis mass spectrum at 469°C of PP

The relative intensities of the characteristic and/or intense peaks detected in the mass spectrum of PP recorded at 469°C, and the assignments made for these peaks are given in Table 3-19.

Table 3-19 Relative intensities, RI, of characteristic and/or intense peaks recorded in pyrolysis spectrum of PP at 469°C

m/z (Da)	RI	Assignment
41	732.7	M(-H)
42	2336.1	M
43	822.4	MH
44	44.0	C_3H_8
57	877.5	MCH_3
69	1000.0	$MCH=CH_2$
71	886.5	MCH_2CH_3
79	35.7	C_6H_7
81	102.1	C_6H_9
83	937.4	M_2(-H)
85	831.2	M_2H
99	260.5	M_2CH_3
111	417.7	$M_2CH=CH_2$
113	124.7	$M_2CH_2CH_3$
125	290.9	M_3(-H)
168	18.3	M_4

Single ion pyrograms of some selected characteristic fragments detected during the pyrolysis of PP are shown in Figure 3-40.

Inspection of the trends in the single ion evolution profiles reveals that as the number of repeating unit increases the evolution profile sharpens. In other words, evolution profiles become broader as the number of repeating unit decreases. This behavior can directly be related to further dissociation of high mass fragments during the ionization process.

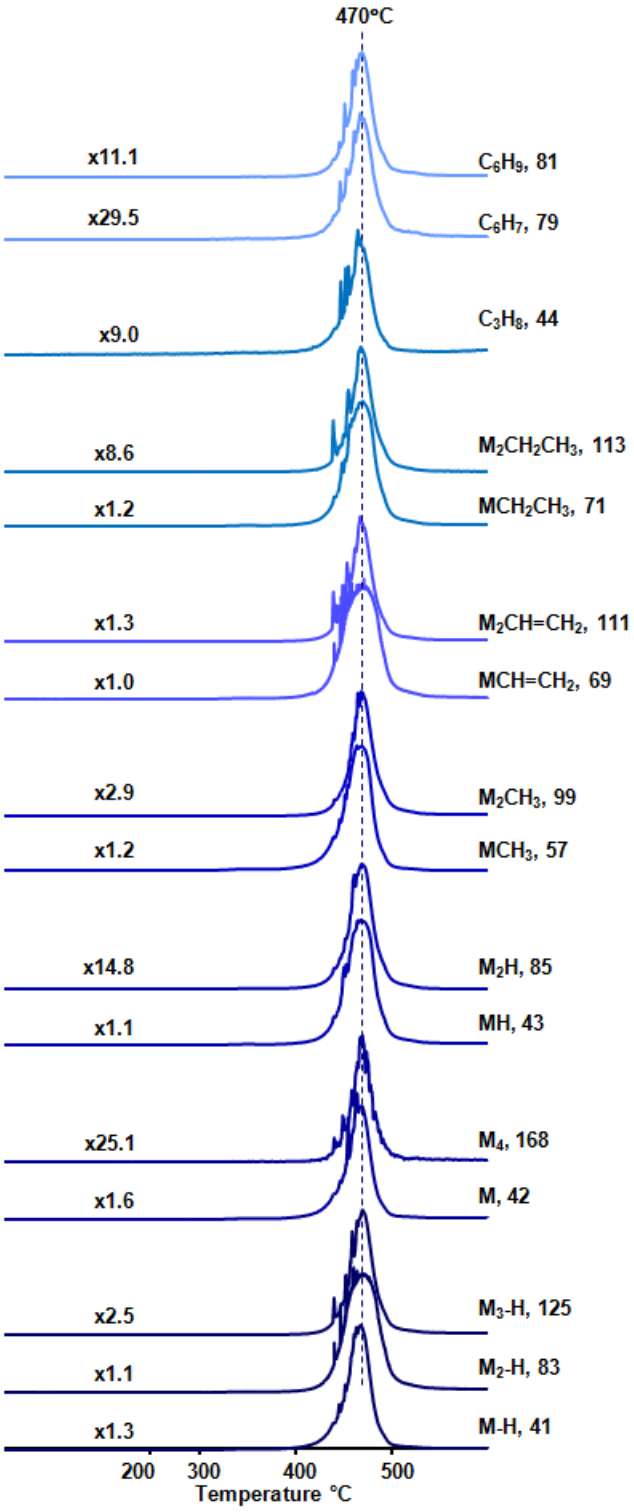

Figure 3-40 Single ion evolution profiles of characteristic and/or intense pyrolysis products of PP

3.2.2. Maleic Anhydride Grafted Polypropylene (PP-g-MA)

As mentioned in Section 2.1, PP-g-MA is used as compatibilizing agent in small amounts to delaminate the clay layers within the polymer matrix. The thermal stability of maleic anhydride grafted polypropylene is slightly higher than that of PP. The TIC curve and the mass spectrum of PP-g-MA recorded at the peak maximum of the TIC curve at around 481°C are shown in Figure 3-41. The diagnostic peaks detected in the mass spectrum of PP in Section 3.2.1 are also identified for this sample, as expected. Furthermore, no additional peaks are detected in the mass spectrum of PP-g-MA. However, it is observed that the relative intensities of most of the peaks, especially those of high mass fragments, are decreased in case of PP-g-MA.

Although, their relative intensities changed noticeably, 69 Da peak is the base peak in the pyrolysis mass spectra of both PP and PP-g-MA. Yet, its relative intensity is significantly enhanced in the mass spectra of PP-g-MA. It may be thought that the fragment, $CH_2CH(CH_3)CHCH_2$ that can be generated upon loss of CO_2 and CO from the units grafted to maleic anhydride, with the same m/z value of 69 Da, contributes to the intensity of this peak.

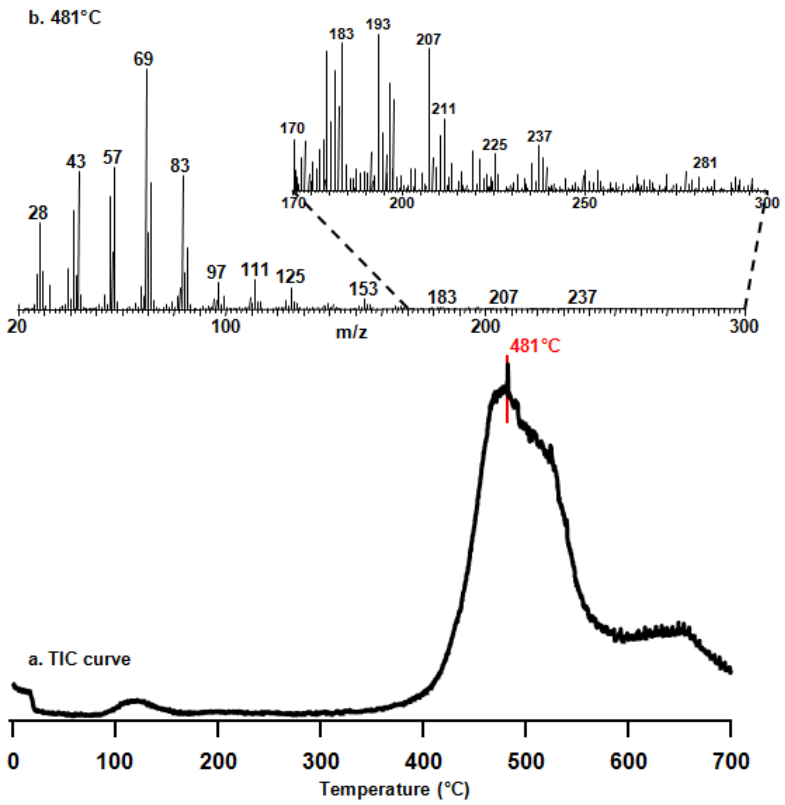

Figure 3-41 a) The TIC curve and b) the pyrolysis mass spectrum at 481°C of PP-g-MA

3.2.3. Cloisite 15A

Cloisite 15A, as mentioned in Section 1.2.2.7, is montmorillonite organically modified by dimethyl, dehydrogenated tallow, quaternary ammonium (Figure 1-8). Figure 3-42 presents the mass spectrum recorded at peak maximum, at 427°C. Dominant peaks detected in the spectrum, are due to fragments such as C_2H_5 (29 Da), C_3H_5 (41 Da), C_4H_7 and/or C_3H_5N (55 Da) and C_5H_7 (67 Da), generated by the decomposition of the organic modifier during pyrolysis and/or ionization processes.

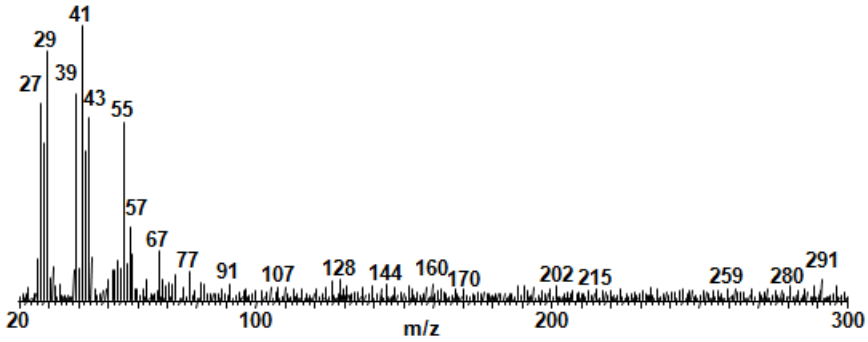

Figure 3-42 The pyrolysis mass spectrum of Cloisite 15A at 427°C

3.2.4. Intumescent Flame Retardant (IFR=APP:PER=3:1)

Intumescent flame retardant is a mixture of ammonium polyphosphate (APP) and pentaerythritol (PER) in the ratio of 3:1. APP and PER were analyzed by direct pyrolysis mass spectrometry, separately.

3.2.4.1. Ammonium Polyphosphate (APP)

The role of ammonium polyphosphate (Figure 1-5), as mentioned in Section 1.2.2.4, in the APP-PER mixture is to act as acid source and spumific agent. The TIC curve of APP, shown in Figure 3-43, presents a single peak with a maximum at 335°C. The mass spectrum of APP recorded at the peak maximum of the TIC curve is dominated by the peaks that can directly be associated with segments of polyphosphate chains, such as $(PO_3)_3PO$ (284 Da), $(PO_3)_2PO$ (205 Da), PO_2 (63 Da) and PO (47 Da) indicating rupture of P-O bonds during pyrolysis and dissociative ionization processes.

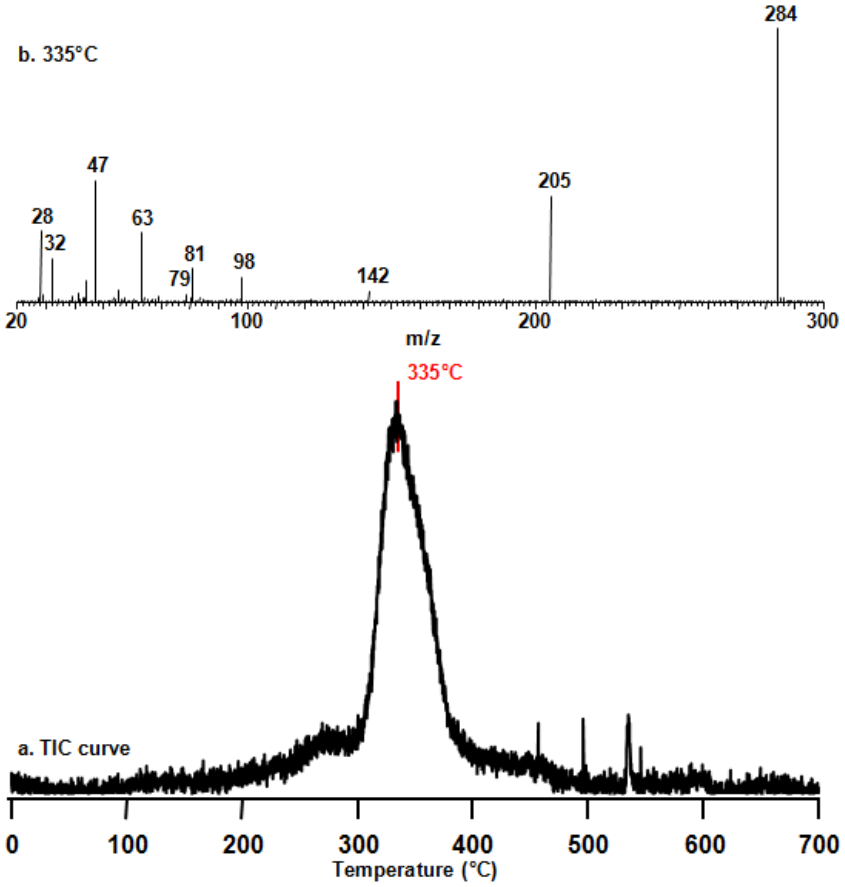

Figure 3-43 a) The TIC curve and b) the pyrolysis mass spectrum at 335°C of APP

Assignments made for some selected peaks are collected in Table 3-20. In addition, relative intensities of these peaks are given in the table.

Table 3-20 Relative intensities, RI, of characteristic and/or intense peaks recorded in the pyrolysis spectrum of APP at 335°C

m/z (Da)	RI	Assignment
47	443.3	PO
63	269.5	PO_2
79	18.4	PO_3
81	116.7	H_2PO_3
98	74.1	H_3PO_4
205	346.7	$(PO_3)_2PO$
284	1000.0	$(PO_3)_3PO$

Single ion evolution profiles of some characteristic products recorded during the pyrolysis of PP are shown in Figure 3-44. Fragments produced by rupture of P-O bonds of polyphosphate chains show identical evolution profiles reaching maximum yield at around 334°C. Evolution of phosphoric acid is detected at around 275°C and 361°C. On the other hand, evolution of NH_3 cannot be differentiated due to the high yield of OH fragments.

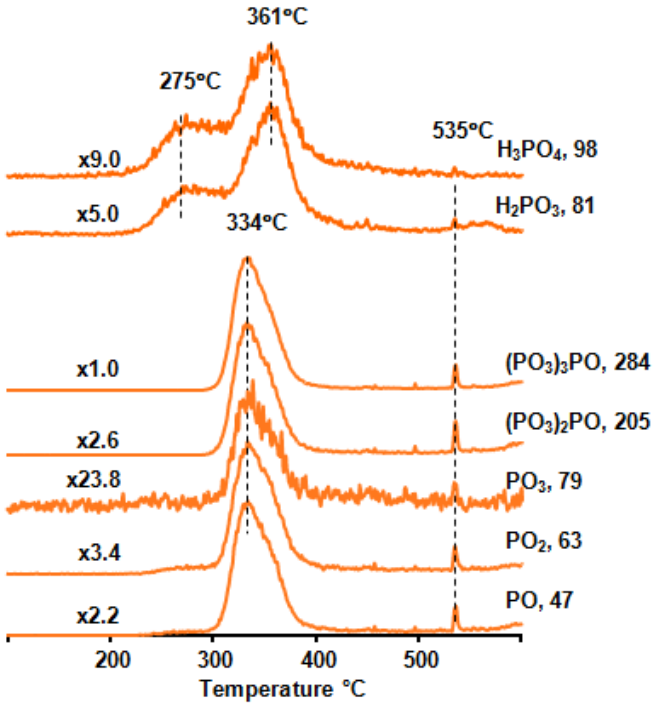

Figure 3-44 Single ion evolution profiles of characteristic and/or intense pyrolysis products of APP

3.2.4.2. Pentaerythritol (PER)

The duty of PER (Figure 1-5), as mention in Section 1.2.2.4, in IFR system is to act as char forming compound. The TIC curve and the mass spectra of PER recorded at the peak maxima are shown in Figure 3-45. The TIC curve shows two overlapping peaks, a strong peak with a maximum at 160°C and a weaker one with a maximum at 201°C.

The boiling point of pentaerythritol is given as 276°C at 30 mmHg. Evolution of pentaerythritol is started just above 100°C under the high vacuum conditions of the mass spectrometer (~10^{-7} mbar) and is maximized at around 160°C. The mass spectrum of pentaerythritol is dominated by peaks due to fragments CH_2OH (31 Da), $CH(CH_2)_2$ (41 Da), CCH_2O (42 Da), $CH_2{=}CCH_2OH$ (57 Da), $C(CH_2)_2CH_2O$ or $CH{=}C(CH_2)CH_2OH$ (70 Da) and $C(CH_2)_2(CH_2O)_2$ (88 Da) generated by successive loses of OH, H_2O and CH_2OH groups from the molecular ion as expected for alcohols.

Weak peaks due to $(CH_2)_2C(CH_2OH)CH_2O$ (101 Da), $CH_2C(CH_2OH)_3$ (119 Da) and protonated molecule $[C(CH_2OH)_4]H$ (137 Da) reach maximum abundance at around 200°C and are attributed to evaporation of molecules involving higher extent of crosslinking.

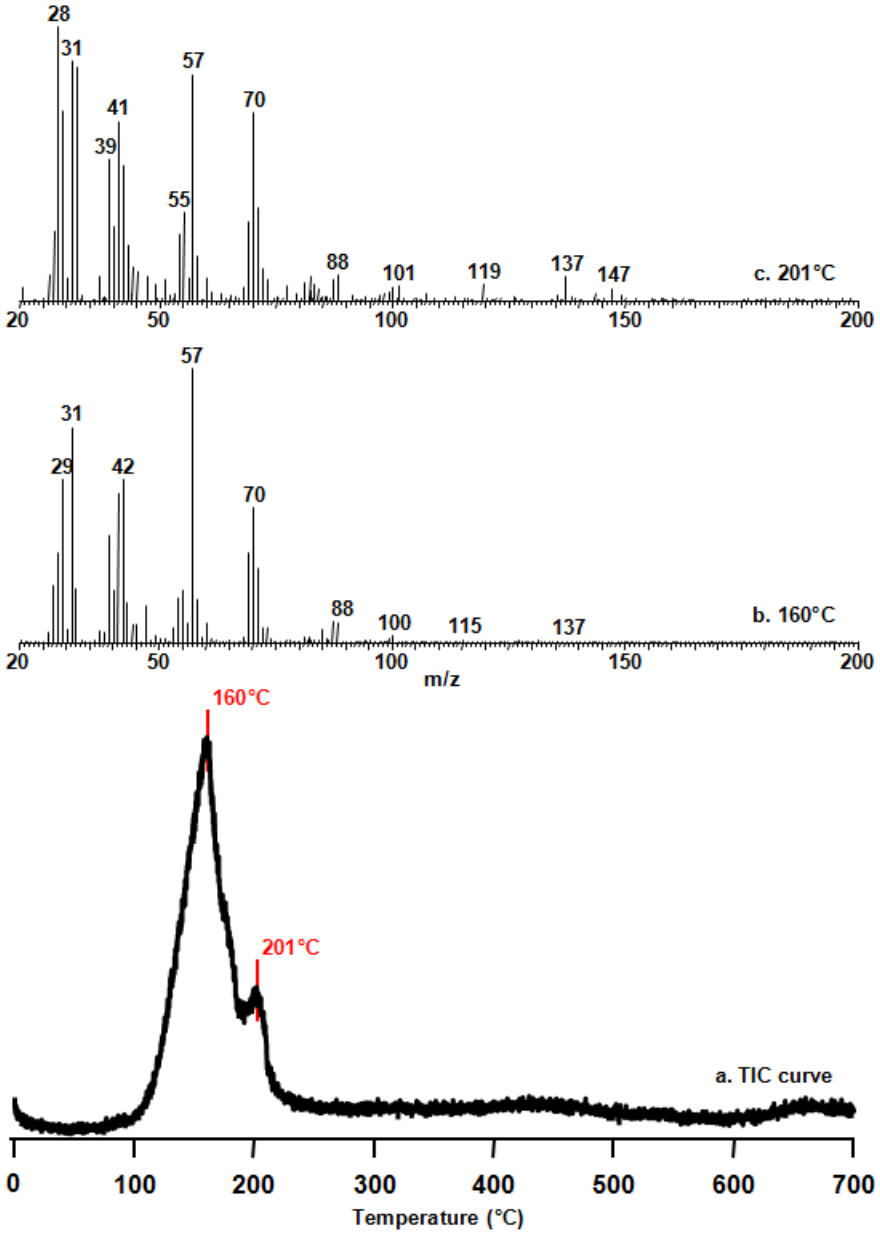

Figure 3-45 a) The TIC curve and the pyrolysis mass spectra at b) 160°C and c) 201°C of PER

The relative intensities of the peaks and the assignments made for these peaks detected in the mass spectra of PER recorded at 160 and 201°C, are given in Table 3-21.

Table 3-21 Relative intensities, RI, of characteristic and/or intense peaks recorded in the pyrolysis spectra of PER at 160°C and 201°C

m/z (Da)	RI		Assignment
	160°C	201°C	
28	330.4	1000.0	CO, C_2H_4
31	787.2	871.8	CH_2OH
41	544.9	654.4	C_3H_5
42	595.2	492.6	C_3H_6, C_2H_2O
57	1000.0	825.1	C_3H_5O
70	491.8	685.2	C_4H_6O
88	72.5	93.3	$C_4H_8O_2$
101	3.8	59.7	$C_5H_9O_2$
119	3.1	55.5	$C_5H_{11}O_3$
137	2.7	85.3	$C_5H_{13}O_4$

Single ion pyrograms of some selected and/or characteristic fragments detected during the pyrolysis of PER are shown in Figure 3-46.

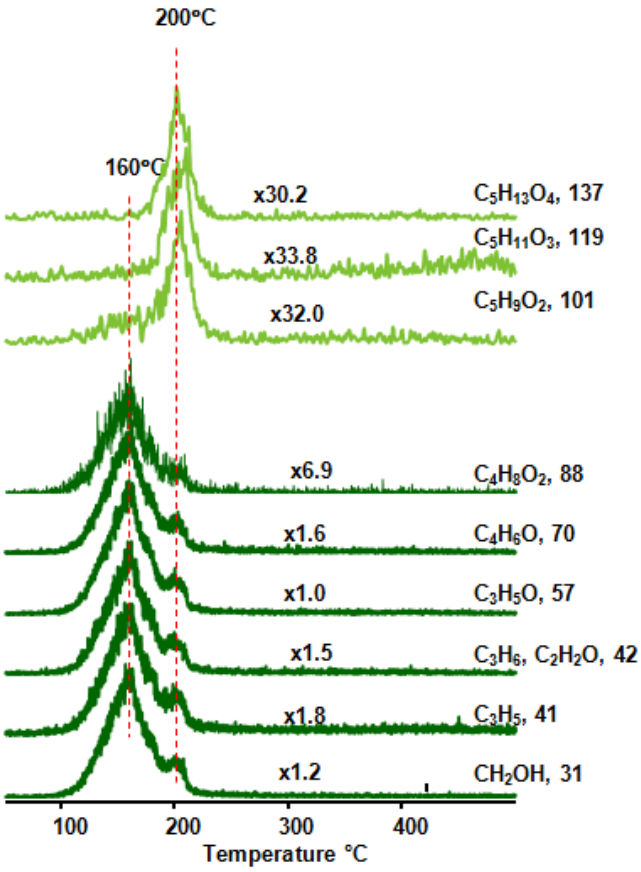

Figure 3-46 Single ion evolution profiles of characteristic and/or intense fragments detected during the pyrolysis of PER

3.2.5. Polypropylene Composites without Cloisite 15A

3.2.5.1. Effect of Addition of Boron Compounds on PP/IFR

Addition of BPO_4

In a study performed by Doğan, the effect of BPO_4 on flame retardant characteristics of PP/IFR composite was investigated. The parent composite PP/IFR had LOI value of 23 and BC rating at UL-94 test. By addition of BPO_4 to PP/IFR composite, LOI value was enhanced to 30 and UL-94 rating changed to V0. Moreover, it was stated that the maximum heat release was decreased from 305 to 226 kW/m^2, meaning increase in flame retardancy [**25**]. The TIC curve and the mass spectra observed at peak maxima recorded during pyrolysis of PP/IFR containing BPO_4 are given in Figure 3-47. Upon magnification of low temperature region of the TIC curve very weak peaks with maxima at around 174°C and 354°C, due to loss of APP and PER based fragments respectively, are observed. The strong peak in TIC curve at 484°C indicates that thermal stability of PP is enhanced significantly. Diagnostic peaks of PP are also recorded in the pyrolysis mass spectra PP/IFR, and relative yields of most of the fragments remain almost unchanged, however, those of high mass fragments are reduced. The reduction is more pronounced for the tetramer (M_4).

The base peak in the mass spectrum of pure PER, which is associated with C_3H_5O (57 Da), coincides with one of the intense and characteristic peaks in the mass spectrum of polymer associated with MCH_3 (57 Da). Therefore, being among dominant fragments, CH_2OH (31 Da) is chosen as a representative of PER based fragments.

Relative intensities of diagnostic peaks of APP and PER are expected to be low due to the fact that their mass percentages (15 and 5 wt%, respectively) within the composite is low. The reaction between H_3PO_4 (evolved from polyphosphate) and PER yields unstable phosphate ester which forms a carbon foam on the surface. This carbon foam acts as a barrier which prevents further degradation of the polymer.

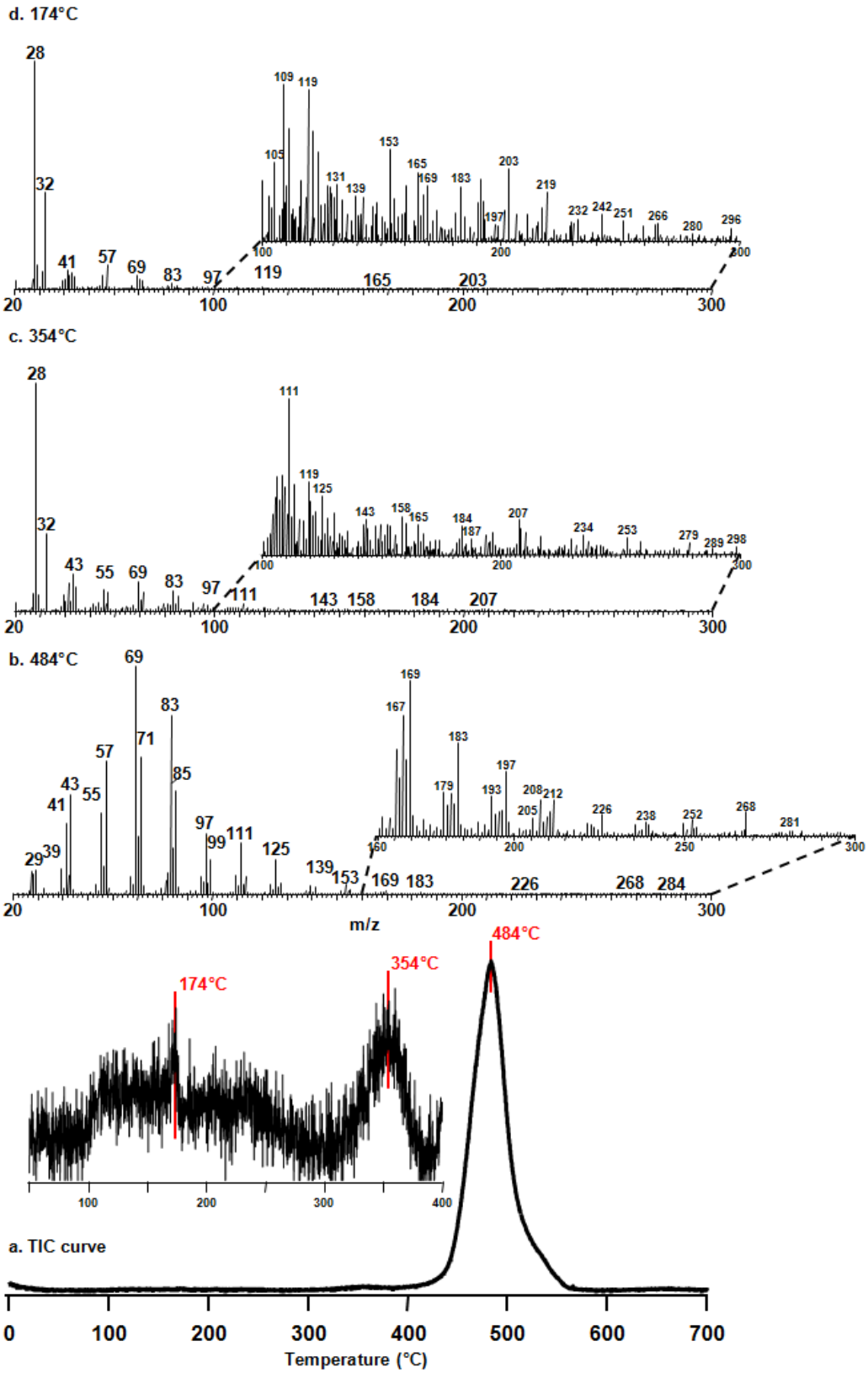

Figure 3-47 a) The TIC curve and the pyrolysis mass spectra at b) 484°C, c) 354°C and d) 174°C of PP/IFR involving 1% BPO_4

Assignments made for selected peaks are collected in Table 3-22. In addition, relative intensities of these peaks are also given in the table.

Table 3-22 Relative intensities, RI, of characteristic and/or intense peaks recorded in pyrolysis spectrum of PP/IFR involving 1% BPO_4 at 174, 354 and 484°C

m/z (Da)	RI			Assignment
	174°C	354°C	484°C	
31	7.1	1.0	0.8	CH_2OH, P
41	8.4	9.4	313.3	M(-H)
42	6.1	5.7	81.0	M
43	7.1	15.5	437.4	MH
44	5.5	10.7	20.2	C_3H_8
57	10.4	9.2	583.5	MCH_3
69	6.1	12.3	1000.0	$MCH=CH_2$
71	3.6	10.1	604.5	MCH_2CH_3
79	0.6	1.4	25.4	C_6H_7, PO_3
81	1.3	1.9	59.3	C_6H_9, H_2PO_3
83	2.5	8.0	787.5	M_2(-H)
85	1.3	7.7	455.7	M_2H
99	0.7	1.6	152.2	M_2CH_3
111	0.5	2.7	224.5	$M_2CH=CH_2$
113	0.1	0.8	78.0	$M_2CH_2CH_3$
125	0.2	1.3	152.1	M_3(-H)
168	0.1	0.4	7.0	M_4

Single ion pyrograms of some selected and/or characteristic fragments detected during pyrolysis of PP/IFR involving 1% BPO_4 are shown in Figure 3-48. The corresponding ones, recorded during the pyrolysis of neat APP, PER and PP are also included in the figure for comparison. Evolution profiles of PP based fragments show a single peak, similar to those of pure PP fragments. The peak maxima of these profiles are observed at 482°C, at a noticeably high temperature, compared to that is observed for neat PP. The relative yields of high mass fragments and that of fragment with m/z value of 44 Da due to HMH, C_2H_4O and CO_2 are decreased significantly.

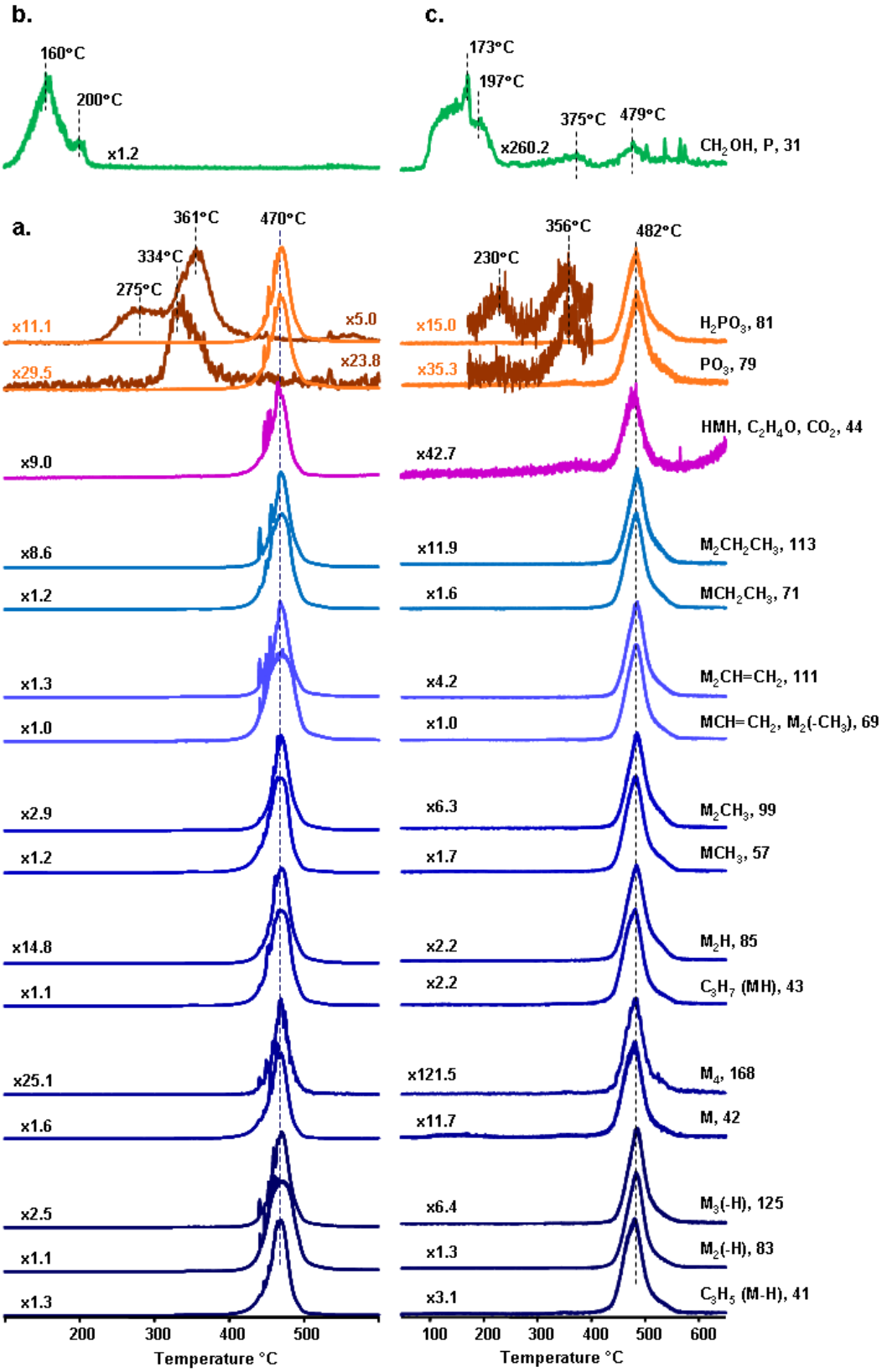

Figure 3-48 Single ion evolution profiles of characteristic and/or intense pyrolysis products of a) PP and (in brown) APP, b) PER and c) PP/IFR involving 1% BPO_4

Significant changes are detected in the evolution of APP and PER based fragments. Loss of PER takes place at higher temperatures (173°C) compared to that of the pure form It is also determined that the relative yields of PER based fragments are noticeably low. Moreover, a weak peak at around 375°C, where APP degradation is almost completed, may be acknowledged as an evidence of interaction of PER with APP. In addition, the weak peak at around 479°C may be due to an interaction between PER and PP.

In case of APP, evolution of fragment with m/z value of 79 Da occurs at higher temperatures (356°C) and that of fragment with m/z value of 81 Da occurs at two different temperatures, at moderately low temperature values compared to that of neat APP. It is also observed that relative yields of these fragments are significantly low. Therefore, it is difficult to differentiate evolution profiles of the APP based fragments from those of PP based fragments (both of which have the same m/z value) without zooming to the certain segment of corresponding evolution profile.

Addition of BSi

Doğan, in his Ph.D. study, found that the LOI value of PP was increased from 23 to 25.5 and the UL-94 rating was changed from BC to V0, upon addition of BSi to PP. Furthermore, decrease in the maximum heat release rate (from 305 to 255 kW/m^2) was measured [**25**]. The TIC curve of PP/IFR involving 1 wt% BSi and the mass spectra recorded at the peak maxima are given in Figure 3-49. The peak due to thermal degradation of PP has a maximum at 489°C indicating a shift to high temperature regions compared to neat PP and increase in thermal stability.

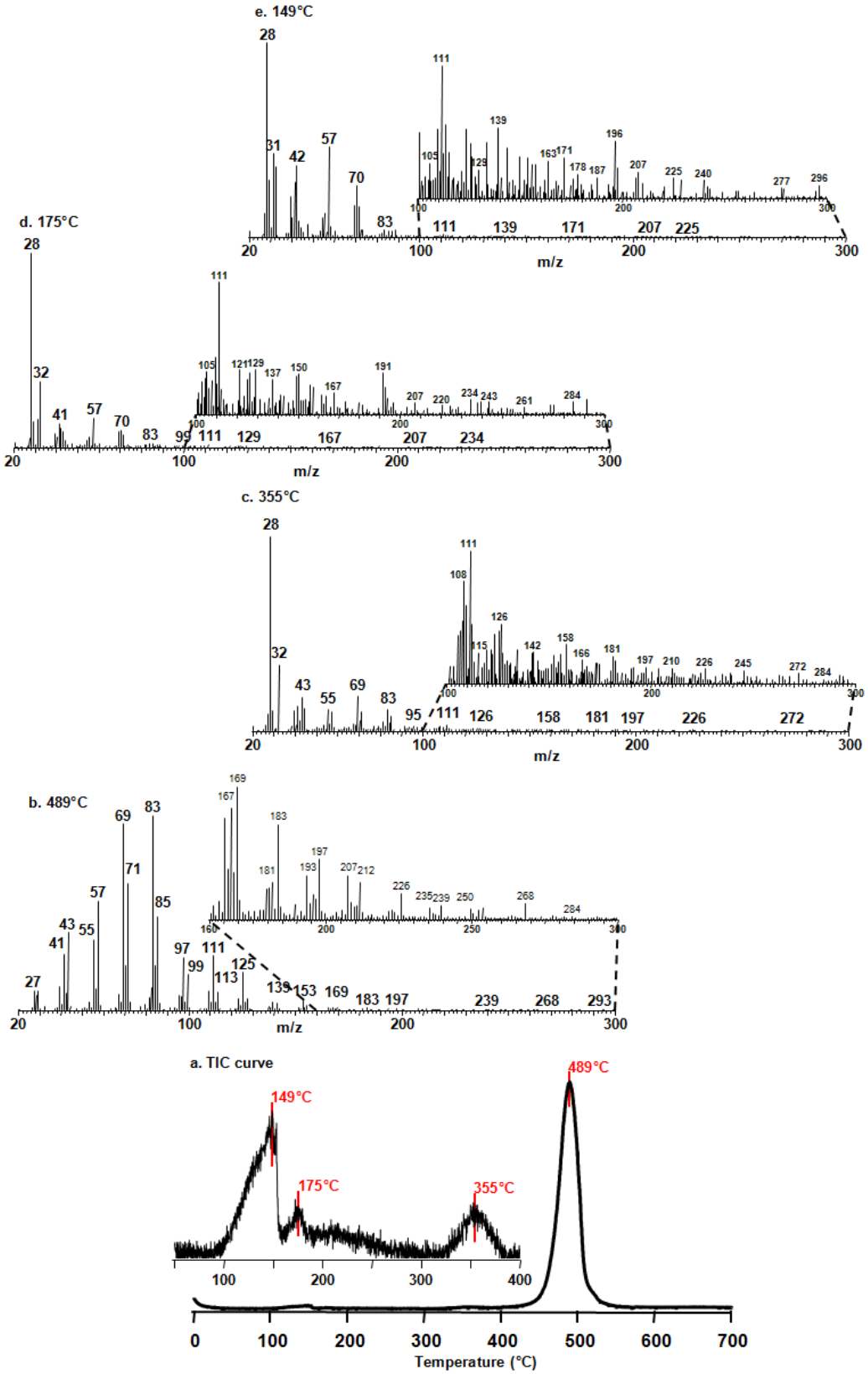

Figure 3-49 a) The TIC curve and the pyrolysis mass spectra at b) 489°C, c) 355°C, d) 175°C and e) 149°C of PP/IFR involving 1% BSi

Table 3-23 shows the relative intensities of characteristic and/or intense peaks present in the pyrolysis mass spectra of PP/ IFR containing 1% BSi at 149, 175, 355 and 489°C.

Table 3-23 Relative intensities, RI, of characteristic and/or intense peaks recorded in pyrolysis spectrum of PP/IFR involving 1% BSi at 149, 175, 355 and 489°C

m/z (Da)	RI				Assignment
	149°C	175°C	355°C	489°C	
31	59.1	18.7	1.4	0.8	CH_2OH, P
41	38.9	15.8	15.6	280.6	M(-H)
42	50.6	14.0	6.2	77.1	M
43	11.1	7.1	21.4	400.6	MH
44	6.3	6.3	14.4	18.5	C_3H_8
57	63.8	22.6	12.3	544.6	MCH_3
69	21.8	10.5	21.6	957.4	$MCH=CH_2$
71	21.3	7.6	12.2	648.2	MCH_2CH_3
79	0.5	1.0	2.9	25.4	C_6H_7, PO_3
81	1.8	2.5	5.5	60.3	C_6H_9, H_2PO_3
83	4.8	4.7	13.1	1000.0	$M_2(-H)$
85	3.7	3.9	9.2	484.2	M_2H
99	0.7	2.1	2.3	185.3	M_2CH_3
111	1.6	1.1	4.0	271.6	$M_2CH=CH_2$
113	0.8	0.5	0.6	91.7	$M_2CH_2CH_3$
125	0.6	0.5	1.7	208.5	$M_3(-H)$
168	0.1	-	0.5	4.5	M_4

Single ion pyrograms of some selected and characteristic fragments detected during the pyrolysis of PP/IFR involving 1% BSi are shown in Figure 3-50. In order to make the comparison easier, the related evolution profiles recorded during the pyrolysis of neat APP, PER and PP, are also included in the figure.

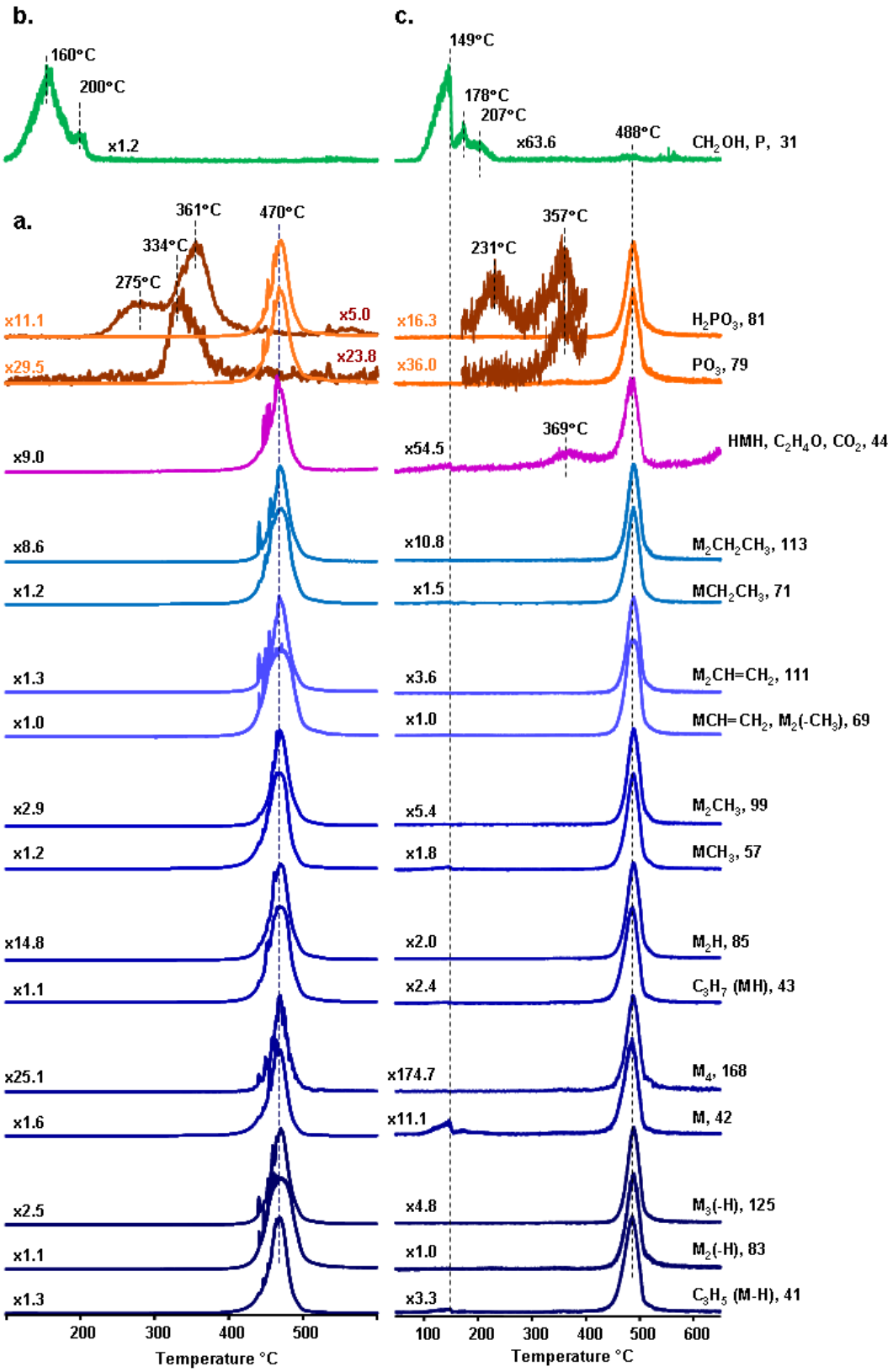

Figure 3-50 Single ion evolution profiles of characteristic and/or intense pyrolysis products of a) PP and (in brown) APP, b) PER and c) PP/IFR involving 1% BSi

Evolution profiles of PP based fragments present a single peak with a maximum at 488°C, being a higher temperature than those detected for the pure PP. The relative yields of high mass fragments and that of the fragment with m/z value of 44 Da due to HMH, C_2H_4O and CO_2 are decreased significantly.

Evolution of PER based fragments, such as m/z values of 41, 42 and 57 Da, occurs at lower temperature regions (149°C) compared to those detected for the pure PER. It is also determined that the relative yields of PER based fragments are again diminished but to a lower extent compared to the composite BPO_4. In the presence of BSi, significant changes are also detected in the evolution of APP. Evolution of 79 Da fragment shifts to higher temperatures (357°C). On the other hand, loss of 81 Da occurs at around two different temperatures at moderately low temperature values compared to those of neat APP. As in case of BPO_4, it is also observed that relative yields of these fragments are significantly low compared to those of pure APP; however, the effects of addition of both BPO_4 and BSi on relative yields of these fragments are similar.

Addition of LaB

According to the findings of Doğan et al., the LOI value was increased from 23 to 27, UL-94 rating was changed from BC to V0 and the maximum heat release rate was decreased from 305 to 260 kW/m^2 by addition of LaB to PP/IFR all of which indicated that the synergistic effect on flame retardancy was achieved [**25**].

Figure 3-51 presents the TIC curve of PP/IFR involving 1 wt% LaB and the mass spectra recorded at the peak maxima. The peak due to the thermal degradation of PP has a maximum at 483°C indicating again a shift to high temperature regions, as in the cases of BPO_4 and BSi involving composites, indicating increase in thermal stability.

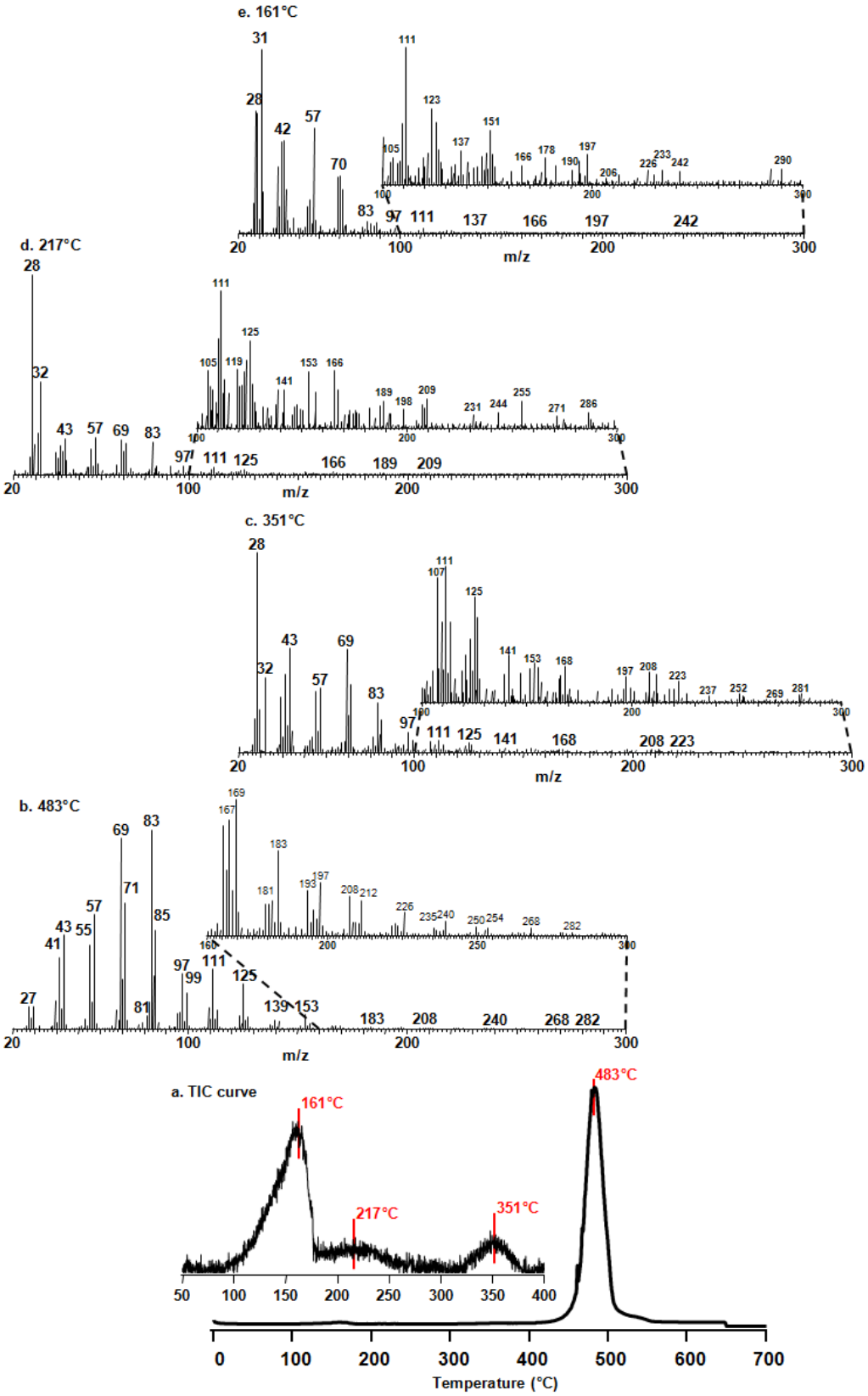

Figure 3-51 a) The TIC curve and the pyrolysis mass spectra at b) 483°C, c) 351°C, d) 217°C and e) 161°C of PP/IFR involving 1% LaB

Assignments made for selected peaks are collected in Table 3-24. In addition, relative intensities of these peaks are given in the table.

Table 3-24 Relative intensities, RI, of characteristic and/or intense peaks recorded in pyrolysis spectrum of PP/IFR involving 1% LaB at 161, 217, 351 and 483°C

m/z (Da)	RI				Assignment
	161°C	217°C	351°C	483°C	
31	250.2	30.0	0.1	0.3	CH_2OH, P
41	125.4	22.5	66.6	355.5	M(-H)
42	126.3	16.9	22.8	99.4	M
43	60.3	25.4	88.6	471.4	MH
44	17.6	10.1	17.7	20.1	C_3H_8
57	143.1	25.9	54.2	575.5	MCH_3
69	76.7	24.9	87.3	954.9	$MCH=CH_2$
71	59.7	22.6	58.0	633.9	MCH_2CH_3
79	4.0	0.9	4.7	29.8	C_6H_7, PO_3
81	7.8	2.2	12.8	66.0	C_6H_9, H_2PO_3
83	15.3	23.2	42.3	1000.0	M_2(-H)
85	13.0	5.7	27.7	494.4	M_2H
99	3.1	2.3	9.9	179.9	M_2CH_3
111	6.9	5.3	9.7	298.6	$M_2CH=CH_2$
113	0.4	2.7	5.7	92.7	$M_2CH_2CH_3$
125	3.1	3.4	7.5	222.7	M_3(-H)
168	0.1	-	2.5	5.3	M_4

Figure 3-52 shows the single ion pyrograms of some selected and/or characteristic fragments detected during the pyrolysis of PP/IFR involving 1% LaB. The related evolution profiles recorded during the pyrolysis of neat APP, PER and PP are also included in the figure for easier comparison.

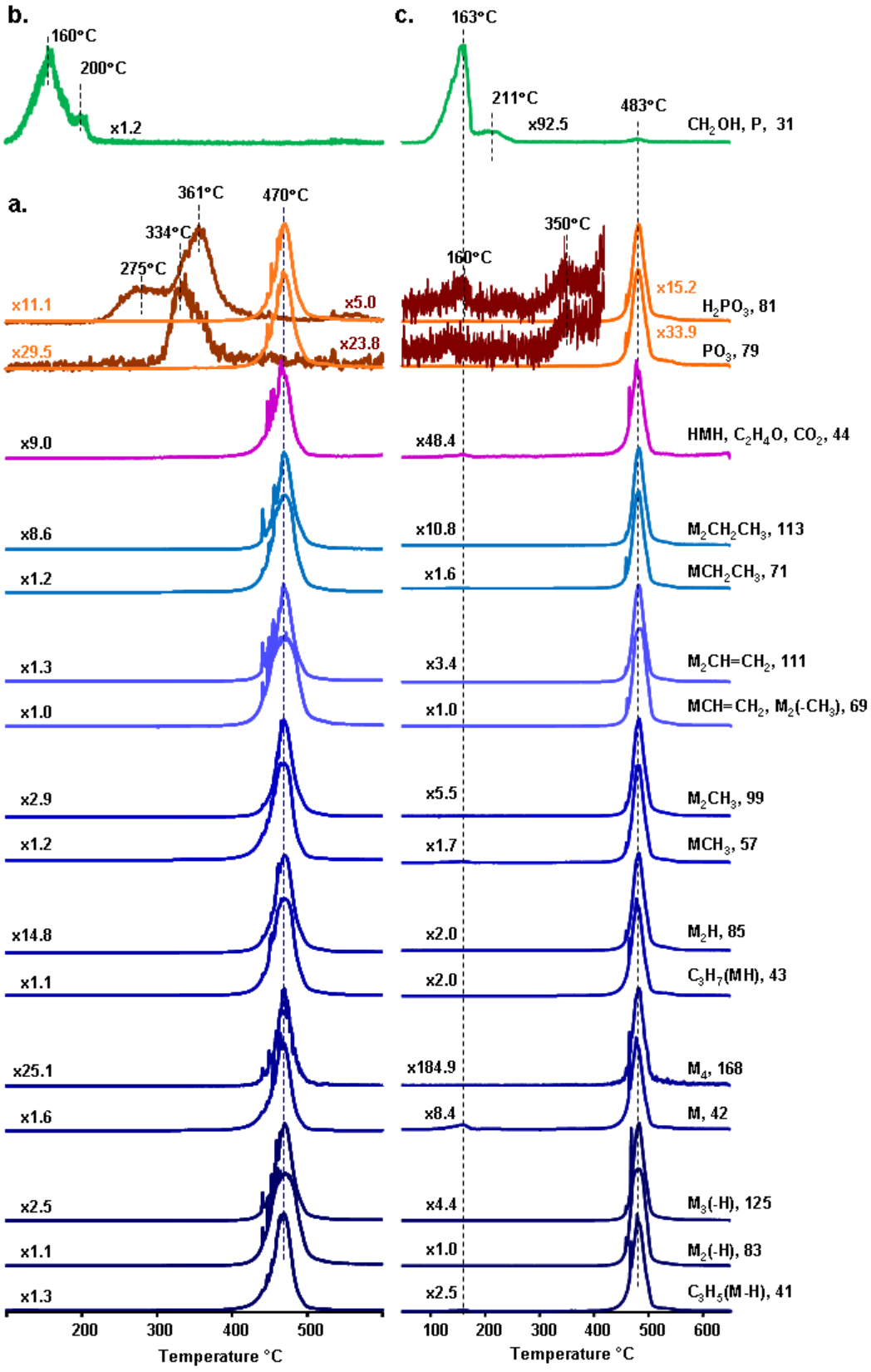

Figure 3-52 Single ion evolution profiles of characteristic and/or intense pyrolysis products of a) PP and (in brown) APP, b) PER and c) PP/IFR involving 1% LaB

Upon addition of LaB, evolution profiles of PP based fragments present a single peak with a maximum at 483°C, at a higher temperature than those of pure PP. The relative yields of high mass fragments and that of the fragment with m/z value of 44 Da due to HMH, C_2H_4O and CO_2 are decreased significantly. Evolution of PER based fragments occurs at almost the same temperature region (163°C) as in case of pure PER. It is also determined that the relative yields of PER based fragments are noticeably low; however, they are significantly higher than that are detected during the pyrolysis of PP/IFR involving BPO_4. Moreover, a weak peak at around 211°C is observed in the evolution profiles of pure PER. In addition, another weak peak at around 483°C is observed which may be due to the detection one of the fragments based on PP with same m/z value having very low relative yield.

By the addition of LaB, noticeable differences are also observed in the evolution of APP. As in the case of addition of both BPO_4 and BSi, evolution of fragment with m/z value of 79 Da occurs at higher temperatures (350°C) and that of the fragment with m/z value of 81 Da occurs at two different temperatures. As in case of both BPO_4 and BSi, it is also observed that relative yields of these fragments are significantly low compared to those of pure APP; however, the effects of addition of all boron compounds (BPO_4, BSi and LaB) on relative yields of these fragments are similar. In the light of these evaluations, the influences of three different boron compounds on thermal stability of PP/IFR show similarities. All of them work together with IFR and enhance the thermal stability. The amount of enhancement in thermal stability is almost similar for all the boron compounds.

3.2.6. Polypropylene Composites with Cloisite 15A

3.2.6.1. PP/PP-g-MA/Cloisite 15A

The effect of Cloisite 15A on LOI, vertical burning rating (UL-94) and heat release rate of PP were determined by Doğan [**52**]. They have determined that inclusion of clay causes a slight enhancement in LOI value from 17.5 to 18.2, but no change in UL-94 rating (BC). Furthermore, reduction in maximum heat release rate was obtained [**52**]. However, the TIC curve of the composite (Figure 3-53) shows a maximum at 457°C indicating a noticeable decrease in thermal stability. On the other hand, the relative yields of high mass fragments are increased noticeably. Fragments due to maleic anhydride cannot be differentiated due to its low concentration; yet, the decrease in thermal stability may be associated with its presence.

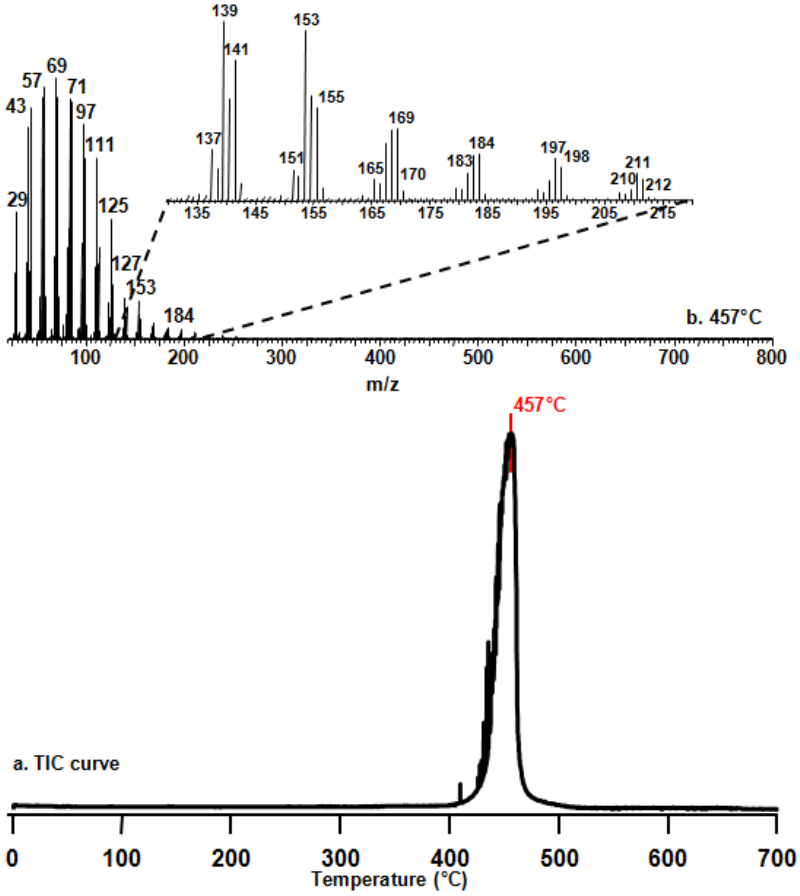

Figure 3-53 a) The TIC curve and b) the pyrolysis mass spectrum at 457°C of PP/PP-g-MA/Cloisite

Table 3-25 shows the relative intensities of some selected diagnostic peaks and the assignments made for the corresponding peaks.

Table 3-25 Relative intensities, RI, of characteristic and/or intense peaks recorded in pyrolysis spectrum of PP/PP-g-MA/Cloisite 15A at 457°C

m/z (Da)	RI	Assignment
41	811.8	M(-H)
42	259.1	M
43	888.3	MH
44	86.0	HMH, C_2H_4O, CO_2
57	967.5	MCH_3
69	1000.0	$MCH=CH_2$
71	925.3	MCH_2CH_3
79	93.8	C_6H_7
81	352.4	C_6H_9
83	924.3	M_2(-H)
85	912.6	M_2H
99	695.9	M_2CH_3
111	696.2	$M_2CH=CH_2$
113	348.3	$M_2CH_2CH_3$
125	462.2	M_3(-H)
168	60.2	M_4

Single ion evolution profiles of diagnostic fragments are presented in Figure 3-54. The corresponding ones recorded during the pyrolysis of pristine PP are also included for comparison. Sharpening of evolution profiles indicates that the thermal degradation process occurs within a narrower temperature range in the presence of Cloisite 15A. This situation may be explained by the delamination of clay layers into the PP chains which may cause increase in gaps between polymer chains, thus penetration of heat easily. The penetration of heat may result in faster and easier decomposition of the polymer chains even in the bulk region.

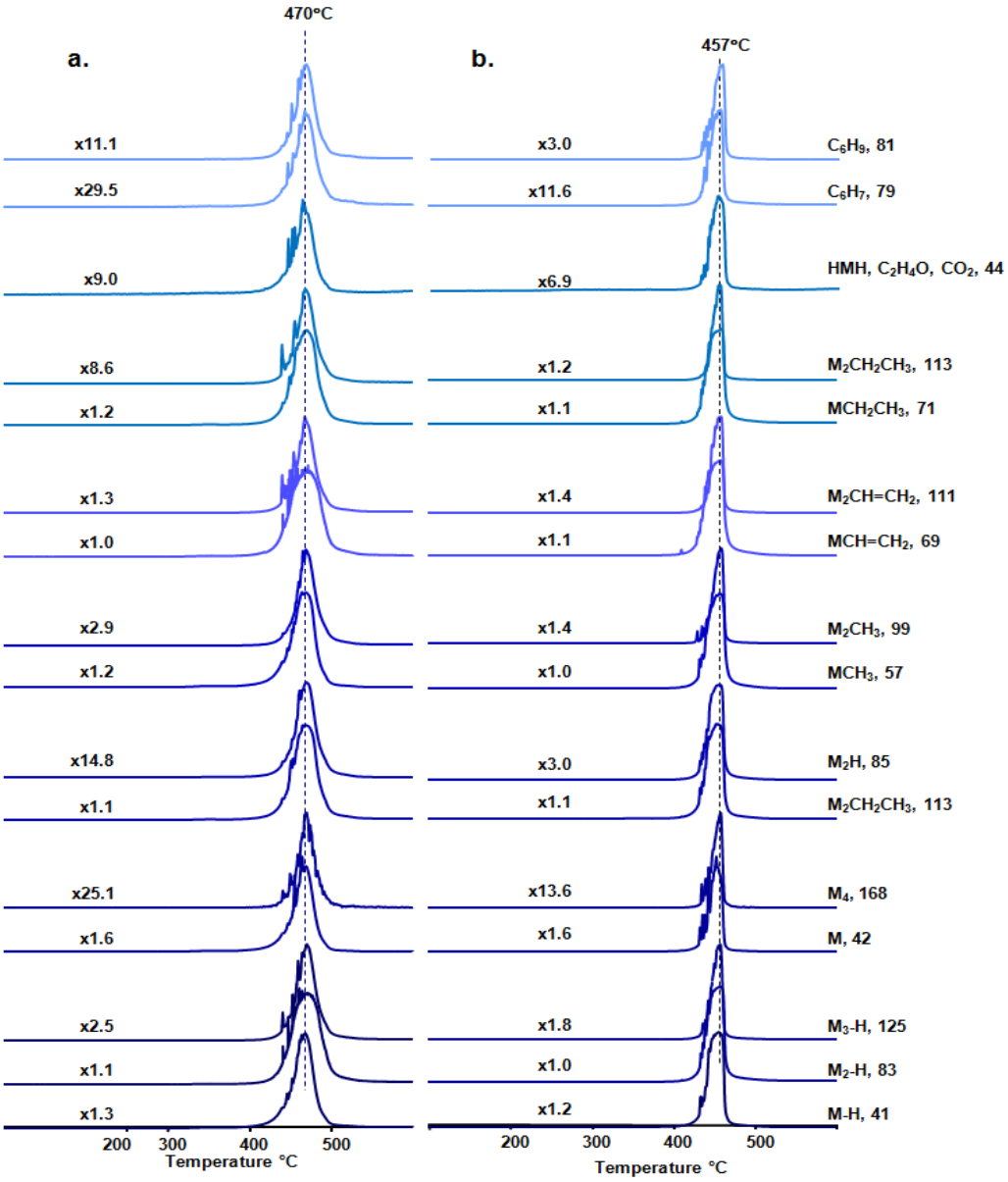

Figure 3-54 Single ion evolution profiles of characteristic and/or intense pyrolysis products of a) PP and b) PP/PP-g-MA/Cloisite 15A

3.2.6.2. PP/PP-g-MA/Cloisite 15A/IFR

Previous results of Doğan et al. showed that the addition of 20wt% intumescent flame retardant (IFR) to PP nanoclay composite increased the char formation, and thus improved flame retardancy. Moreover, it was determined that the LOI value enhanced from 18.2 to 23.5, yet, UL-94 rating was remained unchanged (BC) [**52**]. The broad peak with a tail at high temperature region and a maximum at 479°C in the TIC curve (Figure 3-55) points out an increase in thermal stability upon addition of IFR to the PP composite. The presence of IFR seems to overcome the negative effect of the PP-g-MA. Furthermore, in the presence of IFR, decrease in the relative abundances of high mass fragment peaks is noted. The decrease is more pronounced for the fragments with C_2H_5 end-groups.

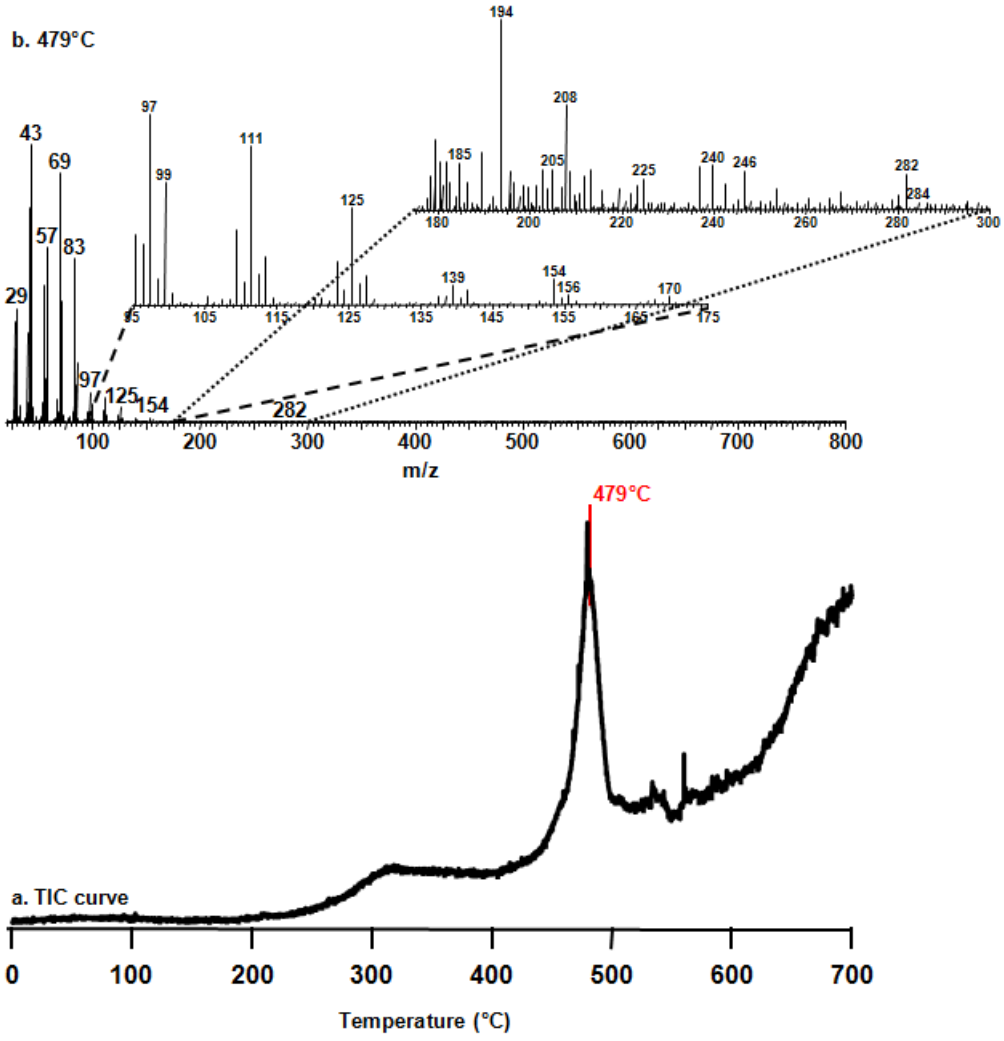

Figure 3-55 a) The TIC curve and b) the pyrolysis mass spectrum at 479°C of PP/PP-g-MA/Cloisite 15A/IFR

The relative intensities of some selected peaks present in the mass spectrum of PP/PP-g-MA/Cloisite 15A/IFR recorded at 479°C are given in Table 3-26.

Table 3-26 Relative intensities, RI, of characteristic and/or intense peaks recorded in pyrolysis spectrum of PP/PP-g-MA/Cloisite 15A/IFR at 479°C

m/z (Da)	RI	Assignment
31	4.2	CH_2OH, P
41	769.9	M(-H)
42	231.1	M
43	1000.0	MH
44	55.4	C_3H_8
57	627.5	MCH_3
69	895.3	$MCH=CH_2$
71	435.7	MCH_2CH_3
79	21.2	C_6H_7, PO_3
81	36.9	C_6H_9, H_2PO_3
83	590.1	$M_2(-H)$
85	212.4	M_2H
99	67.4	M_2CH_3
111	87.4	$M_2CH=CH_2$
113	26.3	$M_2CH_2CH_3$
125	53.4	$M_3(-H)$
168	2.5	M_4

Due to the similarities in the m/z values of diagnostic fragments of each component present in the composite, interpretation of the pyrolysis mass spectra of the composite is quite difficult. In addition, the relative intensities of characteristic peaks of pentaerythritol (PER) and ammonium polyphosphate (APP) are expected to be low due to the composition of the composite. It is known that the phosphoric acid generated reacts with pentaerythritol to form unstable phosphate ester which builds carbon foam on the surface. In general, the foam acts as an insulation layer preventing further decomposition of the polymer. Peaks due to pentaerythritol are easily differentiated as they appear in the early stages of pyrolysis. Loss of pentaerythritol occurs again in a broad temperature region but at slightly higher temperatures than the pure form. The maxima in the evolution profiles are at around 210°C as shown in Figure 3-56. The base peak in the mass spectrum of PER is at 57 Da due to C_3H_5O which coincides with one of the intense peaks in the pyrolysis mass spectra of PP due to MCH_3 (57 Da). Thus, as a representative example CH_2OH is chosen, which is also among quite abundant fragments of PER. Although, the sample contains 5% PER, the relative intensity of CH_2OH peak is decreased about 40 folds. Furthermore, a weak peak at around 363°C, where APP degradation occurs is detected.

These behavior may be regarded as a direct evidence of interactions of PER with phosphoric acid yielding unstable phosphate ester which may decompose immediately.

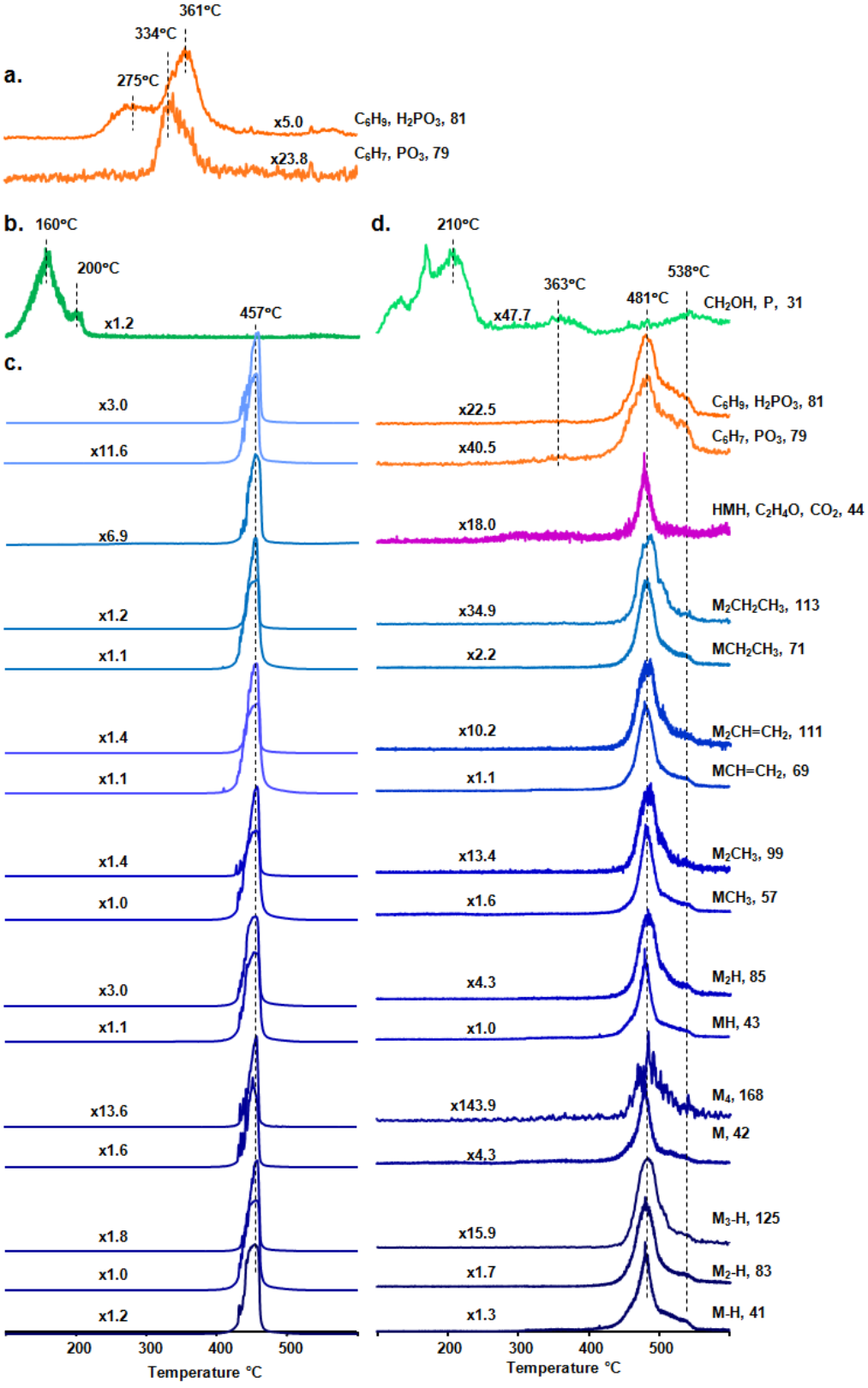

Figure 3-56 Single ion evolution profiles of some selected pyrolysis fragments of a) APP, b) PER, c) PP/PP-g-MA/Cloisite 15A and d) PP/PP-g-MA/Cloisite 15A/IFR

Fragments due to polyphosphate segments are totally absent in the spectra. On the other hand, diagnostic peaks of H_3PO_4, are detectable. However, most of the abundant thermal decomposition products of H_3PO_4 have the same m/z value with some of the thermal degradation products of PP; the H_2PO_3 and C_6H_9 have m/z value of 81 and PO_3 and C_6H_7 have m/z value of 81. Thus, it can be concluded that the intense peaks reaching maximum intensity at around 481°C are most likely due to C_6H_9 and C_6H_7 fragments. On the other hand, the significantly weak peaks, at around 363°C can be attributed to fragments generated by decomposition of APP. In addition, the relatively intense high temperature shoulders are present in the evolution profiles of these fragments at around 538°C. A weak peak is also present in the evolution profiles of diagnostic products of PER around this region.

The single ion evolution profiles of PP based products also show a high temperature tail (Figure 3-56) that may be regarded as an evidence for the interactions between PP chains, pentaerythritol (PER) and ammonium polyphosphate (APP).

3.2.6.2.1. Effect of Addition of Boron Compounds on PP/PP-g-MA/Cloisite 15A/IFR

Addition of BPO_4

Doğan determined that, the addition of BPO_4 resulted in enhancement of LOI value from 23.5 to 25.5 and having V2 rating from UL-94 testing. [**52**]. The TIC curve of the PP/PP-g-MA/Cloisite 15A composite involving BPO_4 (Figure 3-57) shows a broad peak with a maximum at 475°C indicating that thermal stability of PP is not affected by the presence of BPO_4. Mass spectrum of PP/PP-g-MA/Cloisite 15A/BPO_4 at peak maximum is also shown in Figure 3-57. The variations in the relative yields of PP based fragments are similar to those of PP/PP-g-MA/Cloisite 15A/IFR, contrary to the pyrolysis data of PP/PP-g-MA/Cloisite 15A.

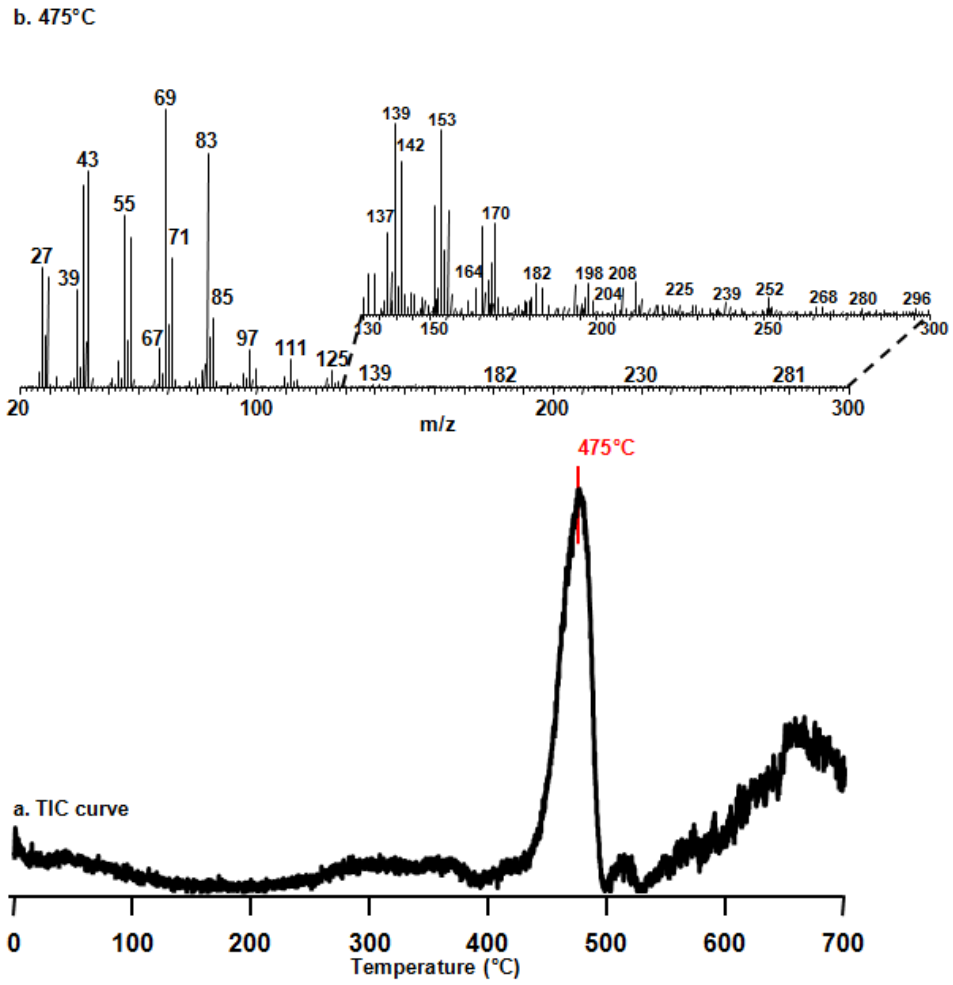

Figure 3-57 a) The TIC curve and b) the pyrolysis mass spectrum at 475°C of PP/PP-g-MA/Cloisite 15A/IFR involving 5% BPO_4

The relative intensities of some selected peaks in the pyrolysis mass spectrum of PP/PP-g-MA/Cloisite 15A/IFR involving 5% BPO_4 at 475°C and the assignments made are collected in Table 3-27.

Table 3-27 Relative intensities, RI, of some selected peaks recorded in pyrolysis spectrum of PP/PP-g-MA/Cloisite 15A/IFR involving 5% BPO_4 at 475°C

m/z (Da)	RI	Assignment
31	1.3	CH_2OH, P
41	730.7	M(-H)
42	161.4	M
43	779.3	MH
44	33.2	C_3H_8
57	538.3	MCH_3
69	1000.0	$MCH=CH_2$
71	464.9	MCH_2CH_3
79	34.0	C_6H_7, PO_3
81	59.9	C_6H_9, H_2PO_3
83	845.4	$M_2(-H)$
85	248.5	M_2H
99	66.9	M_2CH_3
111	97.1	$M_2CH=CH_2$
113	28.6	$M_2CH_2CH_3$
125	59.4	$M_3(-H)$
168	4.6	M_4

Single ion evolution profiles of some selected fragments of both PP/PP-g-MA/Cloisite 15A/BPO_4 and PP/PP-g-MA/Cloisite 15A are presented in Figure 3-58 for comparison. Although, no significant difference in the relative intensities of most of the PP based peak is detected, the relative yields of 79 and 81 Da fragments are increased about 1.7 and 1.4 folds respectively. Considering the region of evolution, this behavior may be associated with an increase in the yield of PP units involving unsaturation, and thus, the increase in the formation of crosslinked structure and the char yield. Increase in the char yield may result in more effective barrier between polymer and fire source, therefore enhancement of flame retardancy. Again, the high temperature shoulder at around 515°C is more intense in the evolution profiles of these fragments compared to those present in the evolution profiles of other PP based fragments.

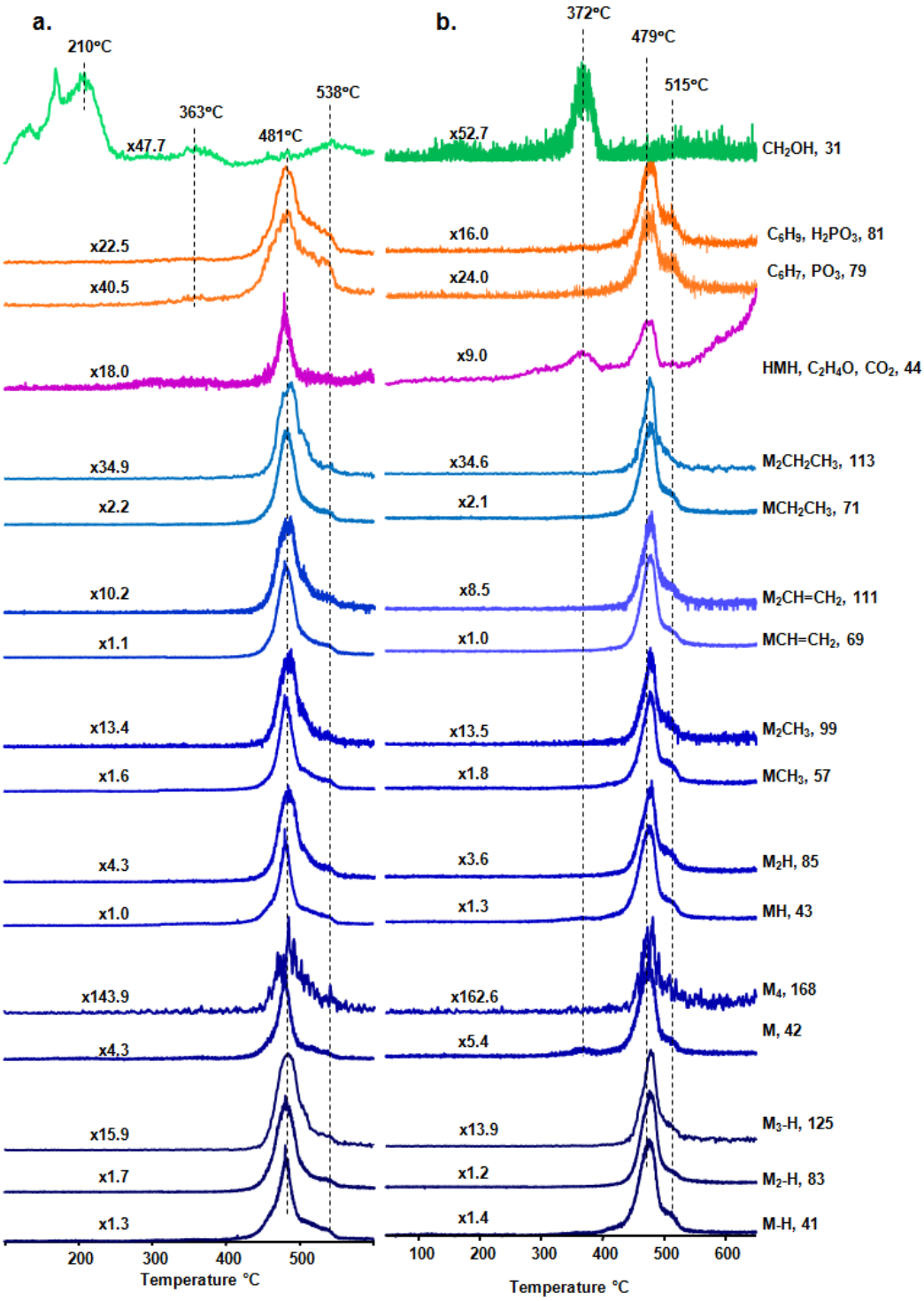

Figure 3-58 Single ion evolution profiles of characteristic and/or intense pyrolysis products of a) PP/PP-g-MA/Cloisite 15A/IFR and b) PP/PP-g-MA/Cloisite 15A/IFR involving 5% BPO_4

Significant changes are detected in the evolution profiles of PER and APP based fragments. Loss of pentaerythritol occurs only at drastically higher temperatures at around 372°C. In addition, the relative yields of related fragments decreases and their evolution profiles show a single peak. Evolution of 44 and 42 Da fragments, that may also be associated with C_2H_4O and C_2H_2O are also recorded at this temperature region. Thus, it can be concluded that in the presence of BPO_4, evaporation of PER is depressed and is shifted to high temperatures. As a consequence its interactions with H_3PO_4 increases and generates phosphate ester which in turn increases the flame retardant effect.

Addition of ZnB

It was detected by Doğan that, by addition of ZnB, LOI value of PP/PP-g-MA/Cloisite 15A/IFR was enhanced from 23.5 to 24.5. On the other hand, inclusion of ZnB had no effect on vertical burning rating [**52**]. The TIC curve of the composite containing ZnB shows a maximum at 457°C indicating a noticeable decrease in thermal stability (Figure 3-59). This noticeable decrease is supported by the significant increase in maximum heat release rate from 199 to 334 kW/m^2 [**52**].

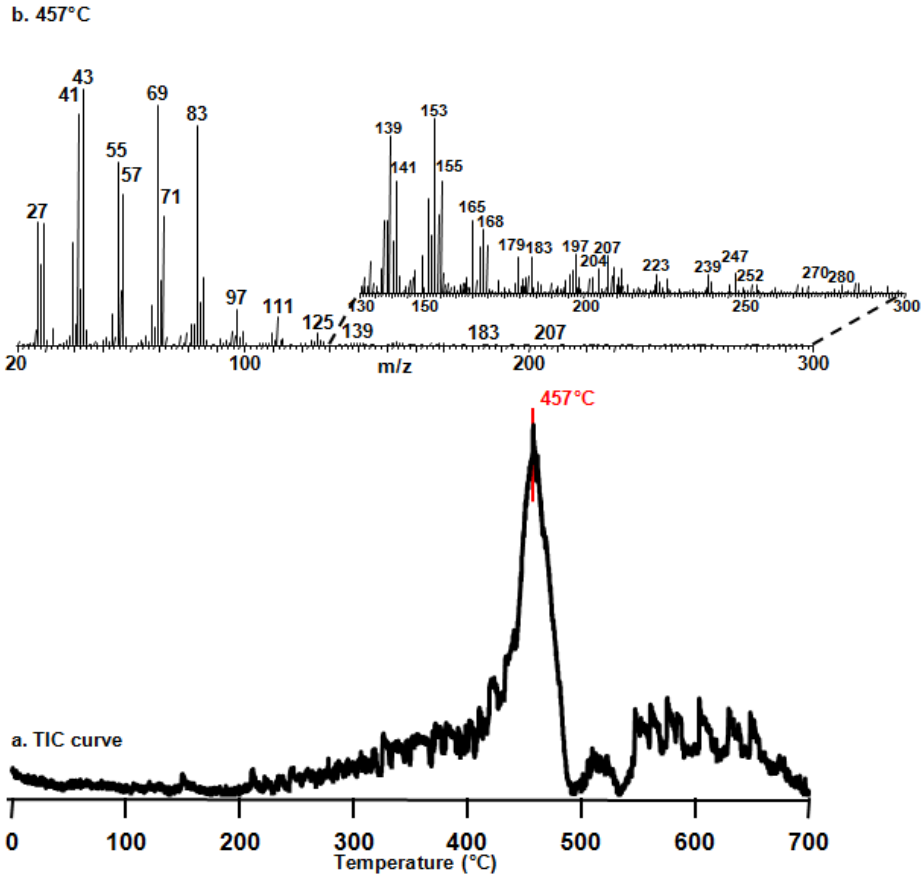

Figure 3-59 a) The TIC curve and b) the pyrolysis mass spectrum at 457°C of PP/PP-g-MA/Cloisite 15A/IFR involving 5% ZnB

Table 3-28 shows the relative intensities of some selected diagnostic peaks and the assignments made.

Table 3-28 Relative intensities, RI, of characteristic and/or intense peaks recorded in pyrolysis spectrum of PP/PP-g-MA/Cloisite 15A/IFR involving 5% ZnB at 457°C

m/z (Da)	RI	Assignment
31	1.3	CH_2OH, P
41	899.6	M(-H)
42	214.5	M
43	1000.0	MH
44	56.4	C_3H_8
57	587.2	MCH_3
69	937.6	$MCH=CH_2$
71	502.6	MCH_2CH_3
79	46.2	C_6H_7, PO_3
81	80.3	C_6H_9, H_2PO_3
83	857.3	M_2(-H)
85	259.0	M_2H
99	51.3	M_2CH_3
111	106.0	$M_2CH=CH_2$
113	20.9	$M_2CH_2CH_3$
125	44.4	M_3(-H)
168	2.6	M_4

Although inclusion of ZnB causes a decrease in thermal stability, the evolution profiles of PP based products get broader and show a shoulder at higher temperature region, at around 511°C (Figure 3-60). Furthermore, the relative yields of high mass products are slightly increased.

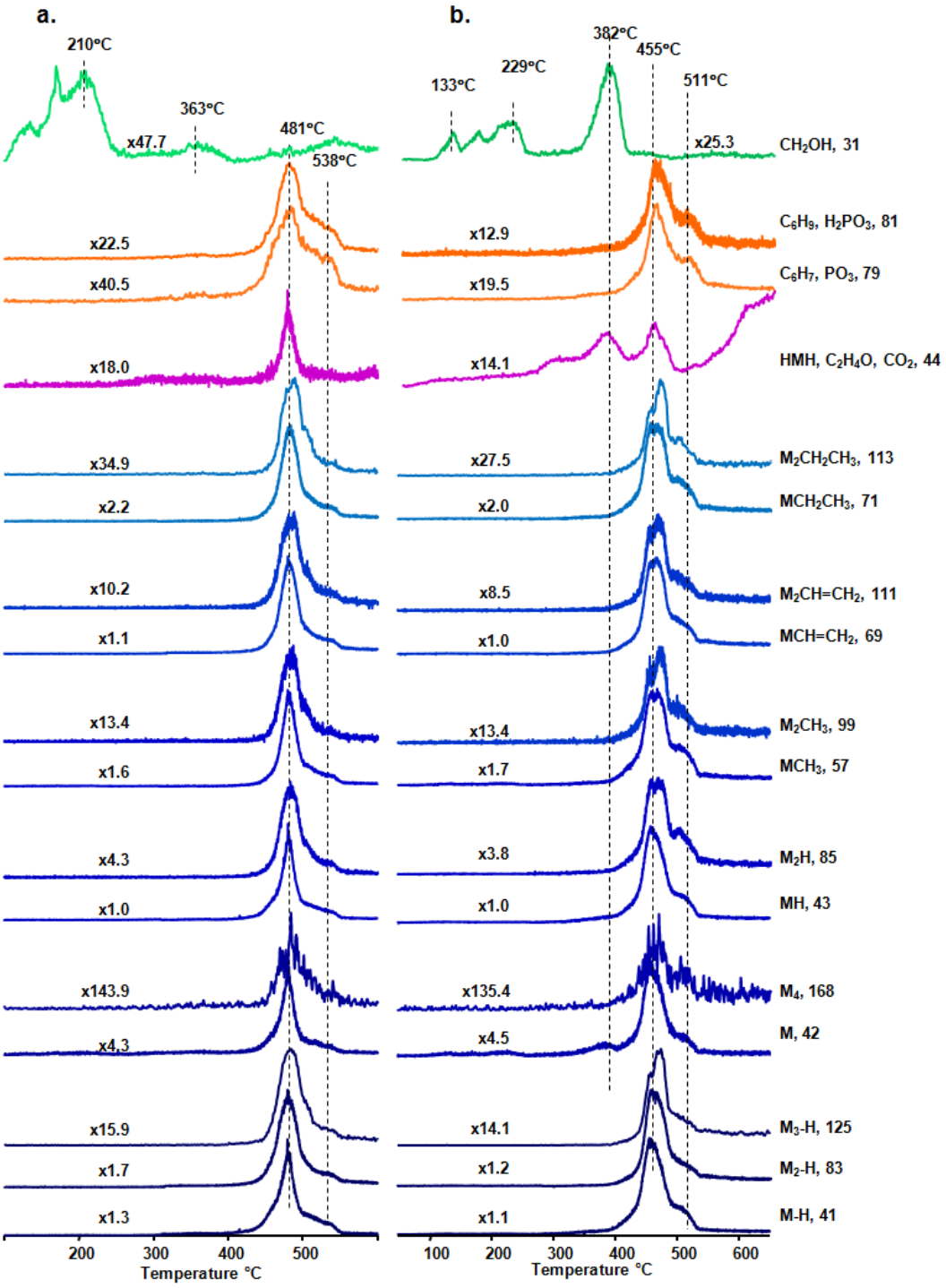

Figure 3-60 Single ion evolution profiles of characteristic and/or intense pyrolysis products of a) PP/PP-g-MA/Cloisite 15A/IFR and b) PP/PP-g-MA/Cloisite 15A/IFR involving 5% ZnB

The evolution profiles of PER based products show significant differences. It is observed that low temperature evaporations are slightly shifted to higher temperatures. In addition, instead of weak peak at around 363°C, a sharp and intense peak with a maximum at around 382°C is appeared in the evolution profiles of related fragments. Thus, it may be concluded that in the presence of ZnB, evaporation of PER occurs to a certain extent; yet, the interaction between PER and H_3PO_4 takes place at higher temperatures. The increases in the relative yields of 79 and 81 Da fragments are about 2.1 and 1.7 folds, respectively, which may be regarded as a support for the increase in extent of unsaturated units. Furthermore, the shoulder at higher temperature region is more pronounced.

Addition of BSi

In the presence of BSi the LOI value of PP/PP-g-MA/Cloisite 15A/IFR nanocomposite was increased from 23.5 to 24.2, whereas, the maximum heat release rate was slightly increased from 199 to 206, indicating a slight reduction in the flame retardancy. Furthermore, the UL-94 rating was changed from BC to V2 [**52**].

The TIC curve and the mass spectra observed at the peak maxima recorded during the pyrolysis of PP/PP-g-MA/Cloisite 15A/IFR containing 5% BSi are given in Figure 3-61. The TIC curve presents two peaks. The first one is a weak peak and appears at low temperature region and has a maximum at 134°C. The second one is a strong with a maximum at 467°C. Thus, upon addition of BSi, the high temperature peak associated with thermal degradation of PP shifts about 12°C to low temperature regions. The slight decrease in the thermal stability may indicate that the enhancement in thermal stability of PP in the presence of PER-APP is disappeared in the presence of BSi. However, the relative yields of PP based fragments are almost unchanged which may point out that thermal degradation mechanism is not affected by addition of BSi.

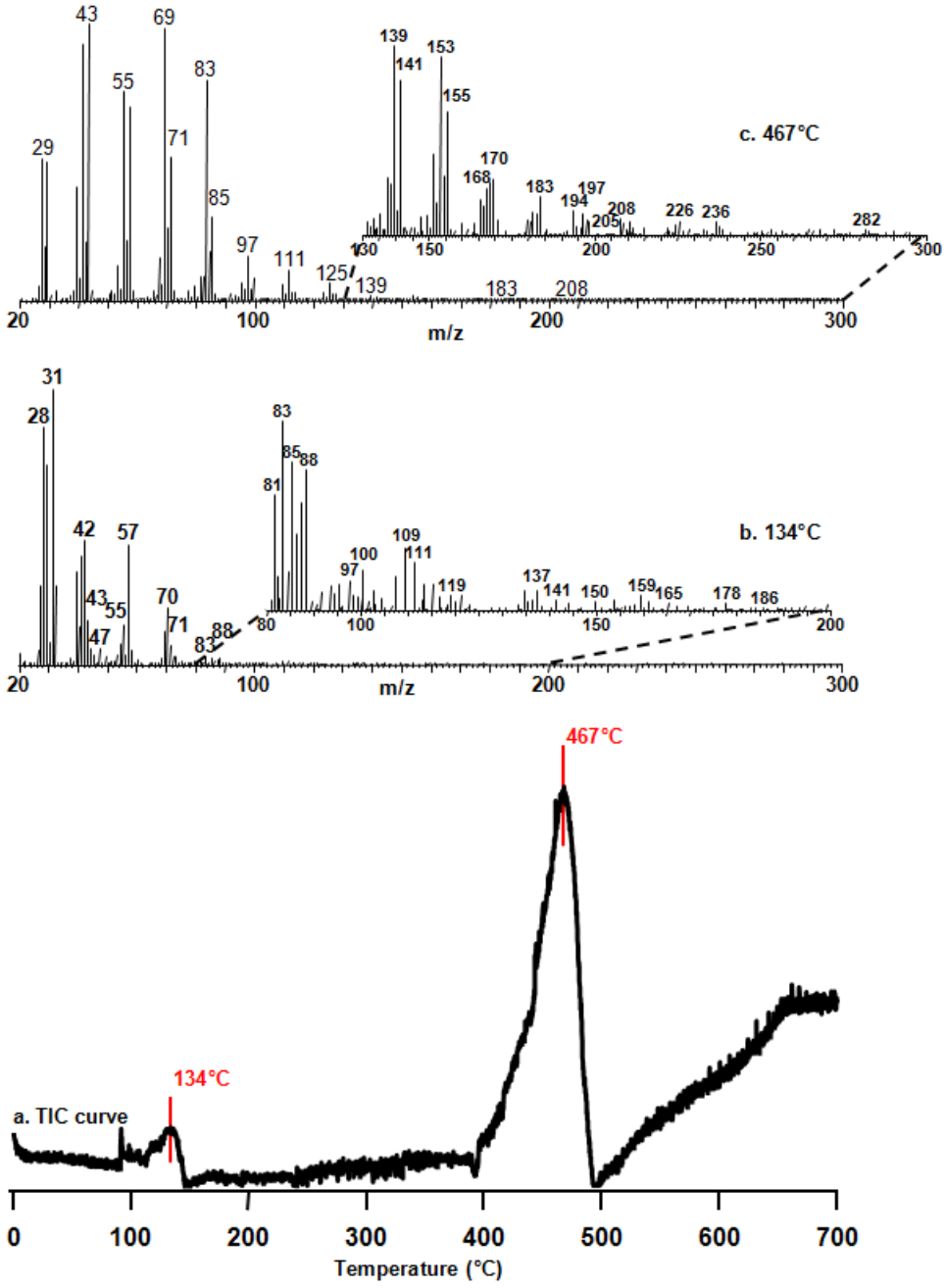

Figure 3-61 a) The TIC curve and the pyrolysis mass spectra at b) 134°C and c) 467°C of PP/PP-g-MA/Cloisite 15A/IFR involving 5% BSi

The mass spectra recorded at around 134°C (Figure 3-61) is dominated by diagnostic peaks of PER indicating that its evaporation occurs at relatively low and narrow temperature region in the presence of BSi.

Table 3-29 shows the relative intensities of characteristic and/or intense peaks present in the pyrolysis mass spectra of PP/PP-g-MA/Cloisite 15A/IFR containing 5% BSi at 134°C and 467°C, respectively.

Table 3-29 Relative intensities, RI, of characteristic and/or intense peaks recorded in pyrolysis spectrum of PP/PP-g-MA/Cloisite 15A/IFR involving 5% BSi at 134°C and 467°C

m/z (Da)	RI		Assignment
	134°C	467°C	
31	1000.0	0.4	CH_2OH, P
41	393.0	928.2	M(-H)
42	447.8	210.3	M
43	159.2	1000.0	MH
44	54.7	33.9	C_3H_8
57	435.3	701.6	MCH_3
69	116.9	987.2	$MCH=CH_2$
71	68.4	514.3	MCH_2CH_3
79	8.7	46.8	C_6H_7, PO_3
81	17.4	84.0	C_6H_9, H_2PO_3
83	26.1	796.8	$M_2(-H)$
85	19.9	300.4	M_2H
99	1.2	75.3	M_2CH_3
111	6.2	107.0	$M_2CH=CH_2$
113	5.0	26.5	$M_2CH_2CH_3$
125	-	59.4	$M_3(-H)$
168	-	3.7	M_4

The single ion evolution profiles of some selected thermal degradation fragments recorded during the pyrolysis of PP/PP-g-MA/Cloisite 15A/IFR/BSi nanocomposite is shown in Figure 3-62. Evolution profiles of PP based products follow similar trends with the nanocomposite involving no BSi. In addition, the relative yields of these products are not affected by the presence of BSi.

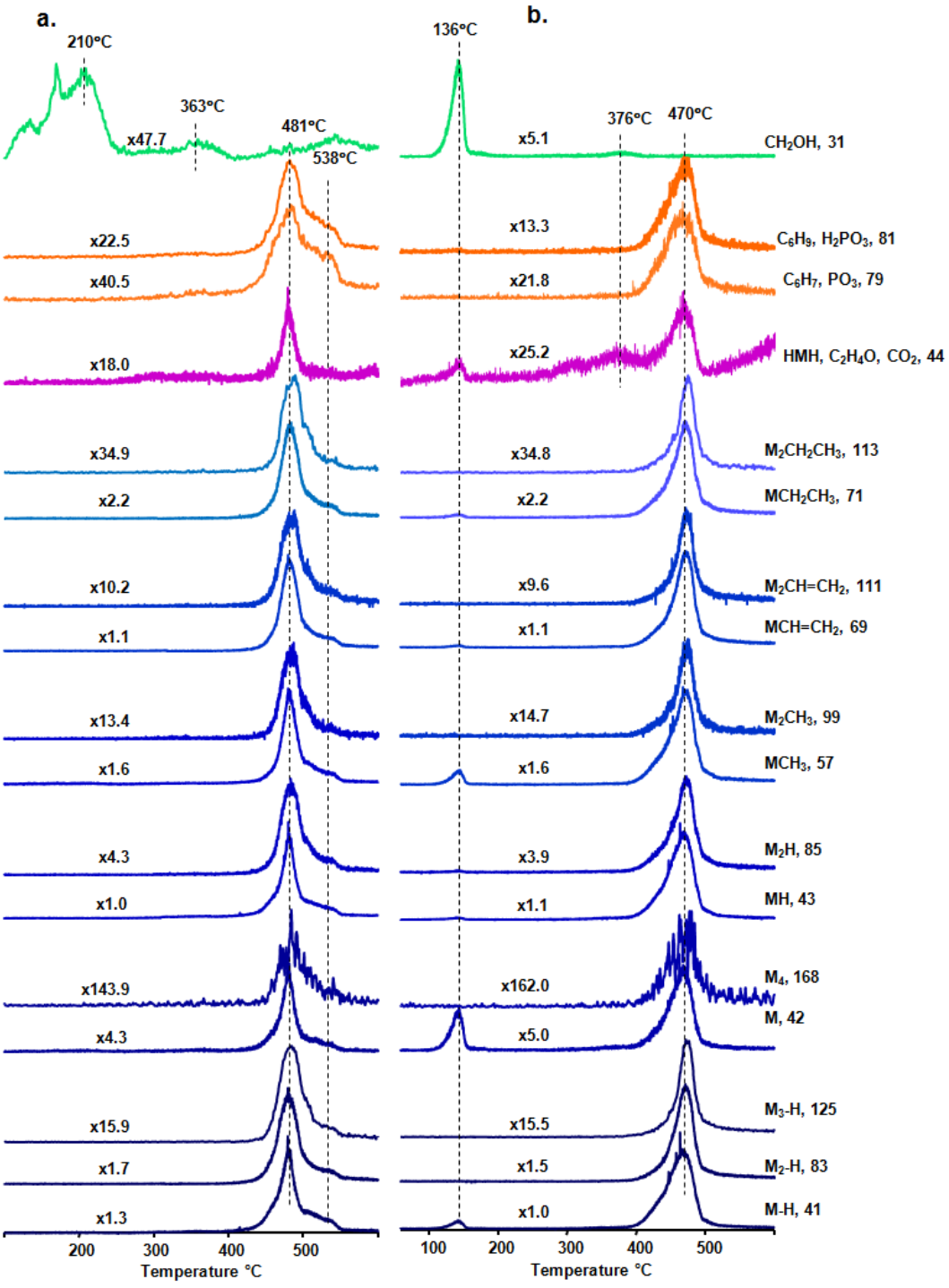

Figure 3-62 Single ion evolution profiles of characteristic and/or intense pyrolysis products of a) PP/PP-g-MA/Cloisite 15A/IFR and b) PP/PP-g-MA/Cloisite 15A/IFR involving 5% BSi

Unlike pure PER and PP/PP-g-MA/Cloisite 15A/IFR nanocomposite, only a sharp peak is present in single ion evolution profiles. In the presence of BSi, loss of PER based fragments at low temperature regions, may be due to decrease in extent of interactions between phosphoric acid and PER. This may be one of the basic reasons for the reduction in thermal stability of PP.

No direct evidence for decomposition of APP is recorded. Although no significant difference in the relative intensities of most of the PP based products is detected, the relative yields of 79 and 81 Da fragments are again increased, about 1.9 and 1.7 folds respectively. These fragments are also associated with segments with unsaturated structure, which may generate a crosslinked structure and cause an increase in the extent of char formation. However, in the evolution profiles, no shoulder in the high temperature region is detected, unlike PP/PP-g-MA/Cloisite 15A/IFR and BPO_4 or ZnB involving composites.

Thus, it can be concluded that in the presence of BSi, PER is lost more readily and its flame retardancy ability is diminished. However, segments involving unsaturation in their structure may generate crosslinked structures, which in turn increases enhancing char yield.

The findings indicate that loss of PER based fragments shifts to high temperature regions in the presence of both BPO_4 and ZnB; whereas it shifts to low temperature regions in the presence of BSi, compared to nanocomposite involving no boron compounds. The relative yield of PER based products, especially the fragment with m/z value 31 Da, slightly decreases by the addition of BPO_4; contrarily, it increases by the addition of other boron compounds, the increase is more pronounced upon BSi addition. Increase in the relative yield of this fragment may be explained by the decrease in phosphate ester formation (generated by the reaction between phosphoric acid and PER). Additionally, the intumescent flame retardancy effect of IFR may decrease, and so does its thermal stability. On the other hand, loss of PP based fragments shifts to lower temperatures in the presence of boron compounds; the temperature shift due to addition of ZnB is the greatest. The relative yields of thermal degradation products of PP remain almost unchanged; except those of the fragments having unsaturated structure, such as those with m/z values of 79 and 81 Da. The increase is greatest for the composite involving ZnB.

The lowest amount of decrease in thermal stability of PP/PP-g-MA/Cloisite 15A/IFR composite is observed upon addition of BPO_4; whereas the highest amount of decrease is observed upon addition of ZnB. Addition of BSi into this composite causes moderate amount of decrease in thermal stability.

Among the PP based samples analyzed, the most thermally stable composite is obtained by the addition of IFR and LaB into PP. On the other hand, the thermal stability of PP is also enhanced through inclusion of PP-g-MA, Cloisite 15A, IFR and BPO_4 together. Still, the amount of enhancement is not as high as that obtained by the addition of IFR and LaB.

CHAPTER 4

CONCLUSION

In this work, the effects of addition of boron compounds, namely boron phosphate (BPO_4) zinc borate (ZnB), borosilicate (BSi) and lanthanum borate (LaB) on thermal degradation characteristics of composites of polyamide 6 (PA6) and polypropylene (PP) are analyzed via direct pyrolysis mass spectrometry (DP-MS) technique. These composites contain organically modified layered silicate, nitrogen or phosphorus containing, or intumescent flame retardants. The organically modified layered silicate, nitrogen or phosphorus containing, or intumescent flame retardants used are Cloisite 15A, Cloisite 30B, melamine, (Me), melamine cyanurate, (MC), aluminum diethylphosphinate, (AlPi, OP1230) or ammonium polyphosphate (APP)/pentaerythritol (PER).

4.1. The Effects of Boron Compounds on Thermal Degradation Characteristics of PA6 Composites

The effect of addition of melamine (Me) to PA6 on thermal stability, degradation characteristics and thermal degradation mechanisms are investigated. As a consequence of the strong interaction between amine groups of Me and carbonyl groups of PA6, the thermal degradation mechanism of PA6 is changed. In the presence of boron compounds, significant changes in the release of Me and in the degradation products of Me and enhancements in the interactions between Me and PA6 are observed.

- Upon addition of BPO_4, the temperatures at which Me sublimes and degradation of PA6 occurs are shifted to slightly higher temperature region.

- ZnB and BSi have no effect on the temperature region where evolution of Me takes place. Yet, due to the glassy surface formed, a significant decrease in the amount of Me sublimation is detected. The glassy surface formed by ZnB during pyrolysis lets evolution of small species to a certain extent, whereas the glassy surface formed by BSi, traps almost all the degradation products of Me and causes release of thermal degradation products of PA6 at significantly lower temperatures.

The thermal degradation characteristics of PA6 are also affected by the presence of MC. Attack of amine groups of MC to carbonyl groups of PA6 and attack of cyanic acid to amine groups of PA6 result in generation of high mass fragments. In the presence of boron compounds, significant changes in the evolution of Me and cyanuric acid, and in their degradation products are detected.

- Upon addition of BPO_4, ZnB or BSi the temperature at which MC sublimes is shifted to slightly higher temperature regions and the temperature at which degradation of PA6 occurs is slightly shifted to lower temperature regions.

- For the composites involving ZnB or BSi, evolution of degradation products of MC is enhanced. Therefore, glassy surface formed by ZnB or BSi allows the release of thermal degradation products of MC at least to a certain extent. On the other hand, for the composite involving BSi, suppression of the intermolecular interactions between cyanuric acid and PA6 is observed.

The influences of aluminum diethylphosphinate (AlPi) on thermal stability of PA6 are examined. Characteristic thermal degradation fragments of both AlPi and PA6 are detected, though the relative intensities of PP base fragments with high mass are decreased. New products are generated in low yields via reactions between AlPi and PA6. As a result of these reactions, thermal stability of PA6 decreases significantly. By addition of boron compounds, improvement in the thermal stability of PA6/AlPi composite is recorded.

- Upon addition of BPO_4 or ZnB, only low mass fragments related to diethylphosphinate and change in its degradation pathways are detected.

- For all composites involving BPO_4 or ZnB, the interactions between AlPi and PA6 are weakened; as a consequence, the presence of additives partially eliminates the influence of AlPi which reduces the thermal stability of PA6.

The thermal degradation characteristics of PA6/AlPi are also affected by the presence of Cloisite 30B. The temperature, at which degradation of PA6/AlPi composite takes place, shifts to higher temperature regions. Inclusion of Cloisite 30B eliminates the interaction between PA6 and AlPi, thus thermal stability of the composite enhances, yet, significant decrease in the relative intensities of high mass fragments is detected. By addition of boron compounds improvement in the thermal stability of PA6/AlPi/Cloisite 30B composite is recorded.

- Only low mass fragments related to diethylphosphinate and change in thermal degradation pathways of diethylphosphinate are observed in the presence of BPO_4 or ZnB. Decrease in the relative intensities of these fragments is more pronounced for the composite involving BPO_4.

- Addition of BPO_4 or ZnB enhances the thermal stability, especially that of BPO_4. Both of them exhibit synergistic effect in terms of improvement of thermal stability of PA6/AlPi/Cloisite 30B composite.

- Upon addition of ZnB, contrary to BPO_4, evolution of most of the fragments yields two peaks at two distinct temperatures. Formation of boron aluminum phosphate layer may be a possible reason for the occurrence of such a trend in evolution profiles. Loss of AlPi and PA6 based fragments and loss of products formed by the reaction between PA6 and AlPi are observed separately.

4.2. The effects of boron compounds on Thermal Degradation Characteristics of PP composites

Addition of boron containing compounds to PP involving intumescent flame retardant system (IFR) improves the thermal stability of PP; yet, no significant differences in the thermal degradation pathways of PP based fragments are observed.

- For all the composites involving BPO_4, BSi or LaB, decrease in the relative intensities of PP based fragments with high mass and in those of both PER and APP based fragments are recorded.

- Upon addition of BPO_4 or LaB, release of PER is shifted to higher temperature regions and that of APP to lower temperature regions.

- In the presence of BSi, loss of both PER based fragments and APP based fragments are shifted to lower temperatures.

The influence of addition of Cloisite 15A and intumescent flame retardant (IFR) to PP on thermal stability and degradation characteristics are examined. The penetration of heat fastens in the presence of Cloisite 15A, thus, the thermal stability of PP is decreased. Inclusion of IFR to this composite (PA6/PP-g-MA/Cloisite15A) improves the thermal stability by forming carbon foam which acts as a barrier on the surface.

- Addition of BPO_4 to PP/PP-g-MA/Cloisite 15A/IFR composite does not noticeably affect the thermal stability; yet, yields of PP fragments with unsaturated units are increased. Thus, a more effective barrier is formed which causes the improvement of flame retardancy, but not thermal stability.

- For the composites involving ZnB and BSi, significant reductions in the thermal stability of PP chains are detected. Additionally, relative intensities of unsaturated PP fragments are increased more than those detected in the case of addition of BPO_4. On the other hand, in the presence of ZnB, release of PER occurs only to a certain extent. In contrast, evolution of PER based fragments is enhanced in the presence of BSi.

REFERENCES

1 Pielichowski, K.; Njuguna, J. Thermal Degradation of Polymeric Materials; Rapra Technology Limited: Shropshire, UK, 2005; pp 1, 10, 31, 32, 47.

2 Bamford, C. H.; Tipper, C. H. Comprehensive Chemical Kinetics, Volume 14; American Elsevier Publishing Company, Inc.: New York, NY, USA, 1975; p 1.

3 Wampler, T. P. Applied Pyrolysis Handbook, Second Edition; CRC Press: Boca Raton, FL, USA, 2007; pp 1, 2, 5, 34, 48, 71, 234.

4 Moldoveanu, S. C. Analytical Pyrolysis of Natural Organic Polymers; Elsevier Science B.V.: Amsterdam, The Netherlands, 1998; pp 3, 20, 36, 144, 145.

5 Moldoveanu, S. C. Analytical Pyrolysis of Synthetic Organic Polymers; Elsevier Science B.V.: Amsterdam, The Netherlands, 2005; pp 31-36, 210, 597.

6 Menczel, J. D.; Prime, R. B. Thermal Analysis of Polymers, Fundamentals and Applications; John Wiley & Sons Inc.: New Jersey, USA, 2009; pp 7, 58.

7 Sobeih, K. L.; Baron, M.; Gonzalez-Rodriguez, J. Recent Trends and Developments in Pyrolysis-Gas Chromatography. Journal of Chromatography A. 2008, 1186, 51-66.

8 Dass, C. Fundamentals of Contemporary Mass Spectrometry; John Wiley & Sons Inc.: New Jersey, USA, 2007; pp 3, 5, 6.

9 Downards, K. Mass Spectrometry, A Foundation Course; TJ International Ltd: Padstow, Cornwall, UK; p 22.

10 Montaudo, G.; Lattimer, R. P. Mass Spectrometry of Polymers; CRC Press LLC: Boca Raton, Florida, USA, 2002; Chapter 1.

11 Hacaloğlu, Jale. Pyrolysis Mass Spectrometry for Molecular Ionization Methods. The Encyclopedia of Mass Spectrometry: Ionization Methods, Volume 6, Edited by Michael L. Gross & Richard M. Caprioli. Elsevier Science Ltd 2007. pp 925-938.

12 Wilkie, C. A.; Morgan, A. B. Fire Retardancy of Polymeric Materials, Second Edition; CRC Press LLC: Boca Raton, Florida, USA, 2010; pp 2, 8, 91, 187, 216, 227, 228.

13 Hull, T. R.; Stec, A. A. Fire Retardancy of Polymers, New Strategies and Mechanisms; Royal Society of Chemistry: Cambridge, UK, 2009; pp 10-11.

14 Chen, Y.; Wang, Q.; Yan, W.; Tang, H. Preparation of Flame Retardant Polyamide 6 Composite with Melamine Cyanurate Nanoparticles In Situ Formed in Extrusion Process. Polymer Degradation and Stability. 2006, 91, 2632-2643.

15 Xanthos, M. Functional Fillers for Plastics; Viley-VCH Verlay GmbH & Co. KGaA: Weinheim, Germany, 2010; pp 329-330.

16 Liu, X.; Liu, J.; Cai, S. Comparative Study of Aluminum Diethylphosphinate and Aluminum Methylethylphosphinate-Filled Epoxy Flame-Retardant Composites. Polymer Composites. 2012, 33, 918-926.

17 Braun, U.; Schartel, B.; Fichera, M. A.; Jager, C. Flame Retardancy Mechanisms of Aluminium Phosphinate in Combination with Melamine Polyphosphate and Zinc Borate in Glass-Fibre Reinforced Polyamide 6,6. Polymer Degradation and Stability. 2007, 92, 1528-1545.

18 Yang, L.; Han, X. Y.; Tang, X. J.; Han, C., X.; Zhou, Y. X.; Zhang, B. G. A Novel Photo-Initiated Approach for Preparing Aluminum Diethylphosphinate under Atmospheric Pressure. Chinese Chemical Letters. 2011, 22, 385-388.

19 Lu, S.; Hamerton, I. Recent Developments in the Chemistry of Halogen-Free Flame Retardant Polymers. Prog. Polym. Sci. 2002, 27, 1661-1712.

20 Isbasar C.; Hacaloglu, J. Investigation of Thermal Degradation Characteristics of Polyamide-6 Containing Melamine or Melamine Cyanurate via Direct Pyrolysis Mass Spectrometry. Journal of Analytical and Applied Pyrolysis. 2012, 98, 221-230.

21 Bourbigot, S.; Bras, M. L.; Duquesne, S.; Rochery, M. Recent Advances for Intumescent Polymers. Macromolecular Material Engineering. 2004, 289, 499-511.

22 Bourbigot, S.; Bras, M. L. Zeolites: New Synergistic Agents for Intumescent Fire Retardant Thermoplastic Formulations - Criteria for the Choice of the Zeolite. Fire and Materials. 1996, 20, 145-154.

23 Mouritz, A. P.; Gibson, A. G. Fire Properties of Polymer Composite Materials; Springer: Dordrecht, The Netherlands, 2006; p 281.

24 Ambadas, G.; Packirisamy, S.; Ninan K. N. Synthesis, Characterization and Thermal Properties of Boron and Silicon Containing Preceramis Oligomers. Journal of Materials Science Letters. 2002, 21, 1003-1005.

25 Doğan, M.; Yılmaz, A.; Bayramlı, E. Snergistic Effect of Boron Containing Substances on Flame Retardancy and Thermal Stability of Intumescent Polypropylene Composites. Polymer Degradation and Stability. 2010, 95, 2584-2588.

26 Mittal, V. Polymer Layered Silicate Nanocomposites: A Review. Materials. 2009, 2, 992-1057.

27 Okamoto, M. Polymer/Layered Silicate Nanocomposites, Rapra Review Reports Volume 14; Rapra Technology Limited: Shropshire, UK, 2003; p 36.

28 Garg, P.; Singh, R. P.; Choudhary, V. Pervaporation Separation of Organic Azeotrope Using Poly(Dimethyl Siloxane)/Clay Nanocomposite Membranes. Separation and Purification Technology. 2011, 80, 435-444.

29 Cloisite® 15A Typical Physical Properties Bulletin. Southern Clay Products Inc., TX, USA.

30 Levchik, S. V.; Weil, E. D.; Lewin, M. Thermal Decomposition of Aliphatic Nylons. Polymer International. 1999, 48, 532-557.

31 Deopura, B. L.; Alagirusamy, R.; Joshi, M.; Gupta, B. Polyesters and Polyamides; Woodhead Publishing Limited: Cambridge, England, 2008; pp 44, 97f, 100f.

32 McKeen, L. W. The Effect of Temperature and Other Factors on Plastic and Elastomers, Second Edition; William Andrew Inc.: NY, USA, 2008; p 244f.

33 Liu, Y.; Wang, Q. The Investigation on the Flame Retardancy Mechanism of Nitrogen Flame Retardant Melamine Cyanurate in Polyamide 6. Journal of Polymer Research. 2009, 26, 583-589.

34 Gijsman, P.; Steenbakkers, R.; Fürst, C.; Kersjes, J. Differences in the Flame Retardant Mechanism of Melamine Cyanurate in Polyamide 6 and Polyamide 66. Polymer Degradation and Stability. 2002, 78, 219-224.

35 Wu, Z.; Xu, W.; Liu, Y.; Xia, J.; Wu, Q.; Xu, W. Preparation and Characterization of Flame-Retardant Melamine Cyanurate/Polyamide 6 Nanocomposites by In Situ Polymerization. Journal of Applied Polymer Science. 2009, 113, 2109-2116.

36 Li, Q.; Li, B.; Zhang, S.; Lin, M. Investigation on Effects of Aluminum and Magnesium Hypophosphites on Flame Retardancy and Thermal Degradation of Polyamide 6. Journal of Applied Polymer Science. 2012, 125, 1782-1789.

37 Doğan, M.; Yılmaz, A.; Bayramlı, E. Effect of Boron Containing Materials on Flammability and Thermal Degradation of Polyamide-6 Composites Containing Melamine Cyanurate. Polymers Advanced Technologies. 2011, 22, 560-566.

38 Doğan, M.; Bayramlı, E. Effect of Boron Containing Materials on the Flammability and Thermal Degradation of Polyamide 6 Composites Containing Melamine. Journal of Applied Polymer Science. 2010, 118, 2722-2727.

39 Bourbigot, S.; Devaux, E.; Flambard, X. Flammability of Polyamide-6/Clay Hybrid Nanocomposite Textiles. Polymer Degradation and Stability. 2002, 75, 397-402.

40 Dahiya, J. B.; Muller-Hagedorn, M.; Bockhom, H.; Kandola, B. K. Synthesis and Thermal Behaviour of Polyamide 6/Bentonite/Ammonium Polyphosphate Composites. Polymer Degradation and Stability. 2008, 93, 2038-2041.

41 Kiliaris, P.; Papaspyrides, C. D.; Xalter, R.; Pfaendner, R. Study on the Properties of Polyamide 6 Blended with Melamine Polyphosphate and Layered Silicates. Polymer Degradation and Stability. 2012, 97, 1215-1222.

42 Fang, K.; Li, J.; Ke, C.; Zhu, Q.; Tao, K.; Zhu, J.; Yan, Q. Intumescent Flame Retardation of Melamine-Modified Montmorillonite on Polyamide 6: Enhancement of Condense Phase and Flame Retardance. 2011, 51, 377-385.

43 Zhang, J.; Lewin, M.; Pearce, E.; Zammarano, M.; Gilman, J. W. Flame Retarding Polyamide 6 with Melamine Cyanurate and Layered Silicates. Polymers for Advanced Technologies. 2008, 19, 928-936.

44 Zhang, S.; Horrocks, R. A Review of Flame Retardant Polypropylene Fibres. Progress in Polymer Science. 2003, 28, 1517-1538.

45 Nakatani, H.; Kurniawan, D.; Taniike, T.; Terano, M. Degradation Behavior of Polymer Blend of Isotactic Polypropylenes with and without Unsaturated Chain End Group. Science and Technology of Advanced Materials. 2008, 9, 024401.

46 Qian, S.; Igarashi, T.; Nitta, K. Thermal Degradation Behavior of Polypropylene in the Melt State: Molecular Weight Distribution Changes and Chain Scission Mechanism. Polymer Bulletin. 2011, 67, 1661-1670.

47 Bertin, D.; Leblanc, M.; Marque, S. R. A.; Siri, D. Polypropylene Degradation: Theoretical and Experimental Investigations. Polymer Degradation and Stability. 2010, 95, 782-791.

48 Feng, C.; Zhang, Y.; Lang, D.; Liu, S.; Chi, Z.; Xu, J. Flame Retardant Mechanism of a Novel Intumescent Flame Retardant Polypropylene. Procedia Engineering. 2013, 52, 97-104.

49 Jiao, C.; Zhang, J.; Zhang, F. Combustion Behavior of Intumescent Flame Retardant Plypropylene Composites. Journal of Fire Sciences. 2008, 26, 455-469.

50 Li, B.; Xu, M. Effect of a Novel Charring-Foaming Agent on Flame Retardancy and Thermal Degradation of Intumescent Flame Retardant Polypropylene. Polymer Degradation and Stability. 2006, 91, 1380-1386.

51 Doğan, M. Production and Characterization of Boron Containing Flame Retardant Polyamide-6 and Polypropylene Composites and Fibers. Ph.D. Thesis, Middle East Technical University, Ankara, Türkiye, May 2011.

52 Doğan, M.; Bayramlı, E. Snergistic Effect of Boron Containing Substances on Flame Retardancy and Thermal Stability of Clay Containing Intumescent Polypropylene Nanoclay Composites. Polymers Advanced Technologies. 2011, 22, 1628-1632.

53 Sclavons, M.; Laurent, M.; Devaux, J.; Carlier, V. Maleic Anhydride-Grafted Polypropylene: FTIR Study of a Model Polymer Grafted by Ene-Reaction. Polymer 2005, 46, 8062-8067.

54 Rousseaux, D. D. J.; Sclavons, M.; Godard, P.; Marchand-Brynaert, J. Tuning the Functionalization Chemistry of Polypropylene for Polypropylene/Clay Nanocomposites. Reactive & Functional Polymers. 2012, 72, 17-24.

55 Kim, H. S.; Lee, B. H.; Choi, S. W.; Kim, S.; Kim, H. J. The Effect of Types of Maleic Anhydride-Grafted Polypropylene (MAPP) on the Interfacial Adhesion Properties of Bio-flour-filled Polypropylene Composites. Composites: Part A. 2007, 38, 1473-1482.

56 Zhou, X.; Zhang, P.; Jiang Z.; Rao, G. Influence of Maleic Anhydride Grafted Polypropylene on the Miscibility of Polypropylene/Polyamide-6 Blends Using ATR-FTIR Mapping. Vibrational Spectroscopy. 2009, 49, 17-21.

57 Wang, Y.; Parkin, S.; Atwood, D. Ligrand-Tetrahydrofuran Coupling in Chelated Aluminum Phosphinates. Inorganic Chemistry. 2002, 41, 558-565.

58 Mitra, A.; Parkin, S.; Atwood, D. A. Aluminum Phosphinate and Phosphates of Salen Ligands. Inorganic Chemistry. 2006, 45, 3970-3975.

59 Orhan, T.; Isitman N.A.,; Hacaloglu, J.; Kaynak, C. Thermal Degradation Mechanisms of Aluminium Phosphinate, Melamine Polyphosphate and Zinc Borate in Poly(Methyl Methacrylate). Polymer Degradation and Stability. 2011, 96, 1780-1787.

60 Isbasar, C.; Bayramlı, E.; Hacaloglu, J.; Direct Pyrolysis Mass Spectrometry Analyses of Polyamide-6 Containing Melamine and Boron Compounds. Polymer Composites. 2013, 34, 1389-1395.

61 Nagasawa, Y.; Yamamoto, M.; Ozawa, K. Study of Fire-Retardant Polymers Using Temperature Jump/Fourier Transform Infrared Spectroscopy. Thermochimica Acta. 1995, 267, 223-230.

CURRICULUM VITAE

Personal Details:

Name and Surname:	Güllü Ceyda İŞBAŞAR AFACAN
Address:	Çankaya / ANKARA
	ceyda.isbasar@titck.gov.tr
Place/Date of Birth:	Bilecik-Türkiye / 1983
Marital Status:	Married

Education:

TED Ankara College Ankara, Turkey	**High School** (1997-2000)
Middle East Technical University Ankara, Turkey	**B.Sc. in Chemistry** (2000-2005) Department of Chemistry
Middle East Technical University Ankara, Turkey	**M.Sc. in Organic Chemistry** (2005-2007) Department of Chemistry "Distyryl Boradiazaindacenes as Red and Near IR Switches" under the supervision of Prof. Dr. Engin Umut Akkaya
Middle East Technical University Ankara, Turkey	**Ph.D. in Department of Polymer Science and Technology** (2007-2013) "Thermal Characterization of Composites of Polyamide-6 and Polypropylene Involving Boron Compounds via Direct Pyrolysis Mass Spectrometry" under the supervision of Prof. Dr. Jale Hacaloğlu

Professional Experience:

Turkish Medicines and Medical Devices Agency Ankara, Turkey	**Chemist, M.Sc.** (2010-present) Department of Pharmaceutical, Biological and Medical Products Laboratory
Middle East Technical University Ankara, Turkey	**Research Assistant** (2005-2010) Department of Chemistry
TÜBİTAK-Ankara Test and Analysis Laboratory (ATAL) Ankara, Turkey	**Part-time Assistant** (Fall 2003) Instrumental Analysis Laboratory

Turkish Petroleum Corporation (TPAO) Ankara, Turkey	**Intern** (Summer 2003) Department of Research Center General Directorate of Production Technology
TÜBİTAK-Ankara Test and Analysis Laboratory (ATAL) Ankara, Turkey	**Intern** (Summer 2002) Instrumental Analysis Laboratory
Presidency of Refik Saydam Health Center Ankara, Turkey	**Intern** (January 2002) Biochemistry Analysis Laboratory

Special Skills:

Instrumental skills:	Analytical Methods: HPLC, AAS, UV-Vis, Py-MS
Language skills:	Turkish (native language) English (proficient in writing & speaking) German (elementary in speaking)
Computer skills:	Operating system: MS Windows Documentation: MS Office Scientific Tools: ChemOffice, MassLynx, IgorPro

Honors & Awards:

Middle East Technical University Ankara, Turkey	Graduate School of Natural and Applied Sciences Graduate Course Performance Award (2007-2008)
Middle East Technical University Ankara, Turkey	Chemistry Department High Honor Student (Fall 2002-2003)
Middle East Technical University Ankara, Turkey	Chemistry Department High Honor Student (Spring 2003-2004)

Publications:

Published Articles

1. Deniz, E.; Isbasar; G. C.; Bozdemir, O. A.; Yildirim, L. T.; Siemiarczuk, A.; Akkaya, E. U. Bidirectional Switching of Near IR Emitting Boradiazaindacene Fluorophores. Organic Letters. 2008, 10, 3401-3403.
2. Isbasar, C.; Hacaloglu, J. Investigation of Thermal Degradation Characteristics of Polyamide-6 Containing Melamine or Melamine Cyanurate via Direct Pyrolysis Mass Spectrometry. Journal of Analytical and Applied Pyrolysis. 2012, 98, 221-230.

3. Isbasar, C.; Bayramlı, E.; Hacaloglu, J. Direct Pyrolysis Mass Spectrometry Analysis of PA-6 Containing Melamine and Boron Compounds. Polymer Composites. 2013, 34, 1389-1395.

Articles in Preparation

1. Isbasar, C.; Doğan, M.; Hacaloglu, J. Direct Pyrolysis Mass Spectrometry Analysis of PA-6 Containing Melamine Cyanurate and Boron Compounds.
2. Isbasar, C.; Hacaloglu, J. Investigation of Thermal Degradation Characteristics of Polyamide-6 Containing Aluminum Diethylphosphinate and Boron Compounds via Direct Pyrolysis Mass Spectrometry.
3. Isbasar, C.; Doğan, M.; Bayramlı, E.; Hacaloglu, J. Thermal Degradation Characteristics of Polyamide-6 Containing Aluminum Diethylphosphinate and Organically Modified Layered Silicate via Direct Pyrolysis Mass Spectrometry.
4. Isbasar, C.; Hacaloglu, J. Direct Pyrolysis Mass Spectrometry Analysis of Polypropylene Containing Intumescent Flame Retardant and Boron Compounds.
5. Isbasar, C.; Doğan, M.; Bayramlı, E.; Hacaloglu, J. Investigation of Effects of Addition of Boron Compounds on Thermal Degradation Characteristics of Polypropylene Containing Intumescent Flame Retardant and Organically Modified Layered Silicate via Direct Pyrolysis Mass Spectrometry.